PREPARATION AND CHARACTERIZATION OF LUFFA CYLINDRICA FIBER REINFORCED POLYMER COMPOSITE

Dissertation submitted to the

National Institute of Technology Rourkela

in partial fulfillment of the requirements

of the degree of

Doctor of Philosophy

in

Mechanical Engineering

by

Niharika Mohanta

(Roll Number: **512ME125**)

Under the supervision of

Prof. Samir Kumar Acharya

January, 2016

Department of Mechanical Engineering

National Institute of Technology Rourkela

Mechanical Engineering
National Institute of Technology Rourkela

January 18, 2016

Certificate of Examination

Roll Number: 512ME125
Name: Niharika Mohanta
Title of Dissertation: Preparation and Characterization of Luffa Cylindrica Fiber Reinforced Polymer Composite

We the below signed, after checking the dissertation mentioned above and the official record book (s) of the student, hereby state our approval of the dissertation submitted in partial fulfillment of the requirements of the degree of Doctor of Philosophy in Mechanical Engineering at National Institute of Technology Rourkela. We are satisfied with the volume, quality, correctness, and originality of the work.

Samir Kumar Acharya
Principal Supervisor

Rabindra Kumar Behera
Member (DSC)

Sumit Kumar Pal
Member (DSC)

Prasanta Kumar Bhuyan
Member (DSC)

Examiner

Alok Satpathy
Chairman (DSC)

Mechanical Engineering
National Institute of Technology Rourkela

Prof. /Dr. Samir Kumar Acharya
Professor

January 18, 2016

Supervisor's Certificate

This is to certify that the work presented in this dissertation entitled “Preparation and Characterization of Luffa Cylindrica Fiber Reinforced Polymer Composite " by "*Niharika Mohanta*", Roll Number *512ME125*, is a record of original research carried out by her under my supervision and guidance in partial fulfillment of the requirements of the degree of *Doctor of Philosophy* in *Mechanical Engineering*. Neither this dissertation nor any part of it has been submitted for any degree or diploma to any institute or university in India or abroad.

Samir Kumar Acharya

.

Dedicated to
my parents

Declaration of Originality

I, *Niharika Mohanta*, Roll Number *512ME125* hereby declare that this dissertation entitled "Preparation and Characterization of Luffa Cylindrica Fiber Reinforced Polymer Composite" represents my original work carried out as a doctoral student of NIT Rourkela and, to the best of my knowledge, it contains no material previously published or written by another person, nor any material presented for the award of any other degree or diploma of NIT Rourkela or any other institution. Any contribution made to this research by others, with whom I have worked at NIT Rourkela or elsewhere, is explicitly acknowledged in the dissertation. Works of other authors cited in this dissertation have been duly acknowledged under the section "Bibliography". I have also submitted my original research records to the scrutiny committee for evaluation of my dissertation.

I am fully aware that in case of any non-compliance detected in future, the Senate of NIT Rourkela may withdraw the degree awarded to me on the basis of the present dissertation.

January 18, 2016

NIT Rourkela

Niharika Mohanta

Acknowledgement

I would like to express my special appreciation and thanks to my advisor **Dr. S.K. Acharya,** Professor, Department of Mechanical Engineering, NIT, Rourkela for suggesting the topic of my thesis and his ready and able guidance throughout the course of my work.

I express my sincere thanks to Director NIT Rourkela **Prof. Sunil Kumar Sarangi** and **Prof. S.S. Mohapatra,** Head of the Department of Mechanical Engineering for providing all academic and administrative help during the course of my work.

The guidance, review and critical suggestion of the Doctoral scrutiny Committee (DSC) during various presentations and review meeting comprising of **Prof. R.K. Behera**, **Prof. S.K. Pal** and **Prof. P.K Bhuyan** are acknowledged. I also express my thanks to **Prof. S. K. Pratihar** of Ceramic Engineering Department for his help during my experimental work in the laboratory.

I am also thankful to all the staff members of the Department of Mechanical Engineering, Metallurgical Engineering and Ceramics Engineering for their timely help in completing my thesis work. I am thankful to all **PhD and M-tech** Scholars of Tribology Lab for giving me support whenever I need realizing that they are traveling in the same boat.

Last but not least, I would like to pay high regards to my father **Mr.B.K. Mohanta** & my father-in-law **Mr. B. Mohanta**, my mother **Mrs. Padmini Mohanta** & my mother-in-law **Mrs. Promodini Mohanta** for their blessing, guidance and supports**.** This work could have been a distant dream if I did not get the moral encouragement and support from my spouse **Dr. Trinath Mohanta** throughout my research work and lifting me uphill this phase of life. My daughter **Adyasha** missed me a lot and sacrificed many of her pleasant dreams for me. This thesis is the outcome of the sincere prayers and dedicated support of my family.

Finally, I wish to acknowledge the support given to me by **Mr. M.P. Panigrahi**, Principal Government polytechnic, Balasore and all the staff members of the Department of Mechanical Engineering, GP Balasore.

January 18, 2016 *Niharika Mohanta*
NIT Rourkela **Roll Number: 512ME125**

Abstract

Environmental awareness today motivates the researchers, worldwide on the studies of natural fiber reinforced polymer composite and cost effective option to synthetic fiber reinforced composites. The availability of natural fibers and ease of manufacturing have tempted researchers to try locally available inexpensive fibers and to study their feasibility of reinforcement purposes and to what extent they satisfy the required specifications of good reinforced polymer composite for different applications. With low cost and high specific mechanical properties, natural fiber represents a good renewable and biodegradable alternative to the most common synthetic reinforcement, i.e. glass fiber. Despite the interest and environmental appeal of natural fibers, there use is limited to non-bearing applications, due to their lower strength compared with synthetic fiber reinforced polymer composite. The stiffness and strength shortcomings of bio composites can be overcome by structural configurations and better arrangement in a sense of placing the fibers in specific locations for highest strength performance. Accordingly extensive studies on preparation and properties of polymer matrix composite (PMC) replacing the synthetic fiber with natural fiber like Jute, Sisal, Pineapple, Bamboo, Kenaf and Bagasse were carried out. These plant fibers have many advantages over glass fiber or carbon fiber like renewable, environmental friendly, low cost, lightweight and high specific mechanical performance.

There are many potential natural resources, which India has in abundance. Most of it comes from the forest and agriculture. Luffa cylindrica (L.) synonym L. aegyptiaca Mill, a forest product commonly called sponge gourd, loofa, vegetable sponge, bath sponge or dish cloth gourd, is a member of cucurbitaceous family. The luffa cylindrica is a subtropical plant abundantly available in China, Japan, India and other countries in Asia as well as in Central and South America. The fruit luffa cylindrica can be eaten as a vegetable when it is young. But mature fruits can’t be eaten because of its bitter taste due to development of purgatives chemicals. Due to its purgative property, it is used as medicine for remedy of dropsy, nephritis, and chronic bronchitis and lung complaints. The Luffa fruit has a fibrous vascular system that forms a natural mat when dried. The natural luffa mat possesses remarkable strength, stiffness and energy absorption capacity comparable to metallic cellular material in a similar density range. This Luffa fiber contains cellulose 62%, hemicelluloses 20%, lignin 11.2%, extractives 3.2 % and ash 0.4%. This makes it

suitable for reinforcing material in polymer matrix. However, there is a limited amount of research has been conducted on the luffa sponge as a source of bio-fibers and bio-composites in the last ten to fifteen years. Those researchers indicated that it was a potential alternative material for packaging, water absorption and waste water treatment. The luffa fibers were also used as reinforcement fiber for other materials and cell immobilization for biotechnology. At the same time, sponge gourd (LC), the luffa sponge material, has not yet had their potentialities fully explored.

Against this back ground the present research work has been undertaken with an objective to explore the use of natural fiber luffa cylindrica, as a reinforcement material in epoxy base.

The work presented in this dissertation involves investigation of three distinct problems of natural fiber composites:

i. A study of favorable mechanical properties of luffa cylindrica fiber in thermosetting matrix composite.

ii. An experimental investigation of tribological properties of luffa cylindrica reinforced epoxy composite.

iii. An Experimental investigation in to mechanical and tribological properties of luffa-glass hybrid composite with different stacking sequence.

To study the mechanical properties of the composite, different Layer such as Single, Double and Triple layer of fiber have been taken. Usual hand-lay-up technique has been adopted for manufacturing the composite. To have a good compatibility between the fiber and matrix, chemical modification of fibers such as alkali, benzoyl-chloride and potassium permanganate treatments has been carried out. It was found that benzoyl-chloride treated fiber composite exhibits favorable strength and stiffness in comparison to other treatments. Moisture absorption behavior of both treated and untreated fiber composite was also carried out. The moisture sorption kinetics of the composite has also been studied. The study confirms that the Fickian's diffusion can be used to adequately describe the moisture absorption in the composite.

For studying the tribo-potential of luffa cylindrica fiber, solid particle erosion behavior by Air jet erosion test rig, have been carried out. All these tests have been carried

out as per ASTM standard. The solid particle erosion test clearly indicates that the composite behavior is semi-ductile in nature.

To study the mechanical and tribological properties of luffa-glass hybrid composite, five groups of samples were prepared with different stacking sequences of glass and Luffa layers. The tensile strength, flexural strength, ILSS and hardness of the Luffa-glass hybrid composite were studied as per ASTM standard. It is found that layering sequence significantly affects the tensile, flexural and interlaminar shear strength. The erosion wear response of the hybrid composite with different layering sequences is evaluated using a solid particle erosion test rig. The experiments results illustrate that under all impact velocities the erosive were response of all composites exhibit semi ductile behavior. It is observed that layering sequence and velocity of impact has significant influence on the erosion rate of the composite and the erosive strength of luffa fiber laminate increases by hybridization with synthetic fiber glass.

There are other fabrication techniques available like injection moulding, compression moulding and extrusion, where the volume fraction of reinforcement can be increased. In addition there are other chemical methods by which the fiber surface modification could be carried out. This work can be further extended to those techniques. However the results reported here can act as a starting point for both industrial designer and researchers to design and develop polymer matrix composite components using luffa cylindrica fiber as reinforcement.

The whole dissertation has been divided in to seven chapters to put the analysis independent of each other as far as possible. Major works on mechanical characterization, moisture absorption characteristics, and erosive wear characteristics of LC-epoxy composite and mechanical, tribological behavior of luffa glass hybrid composites is given in chapter 3, 4, 5, and 6 respectively.

Keywords*: *Luffa cylindrica Fiber*; *Fiber surface treatment*; *Mechanical Properties*; *Moisture absorption*; *Erosive wear*; *Luffa-Glass hybrid composite*; *SEM

TABLE OF CONTENTS

Chapter 2 Literature review

Chapter 3 Mechanical characterization of luffa cylindrica fiber epoxy composite

LIST OF TABLES

LIST OF FIGURES

LIST OF SYMBOLS

D_x	Diffusion coefficient
E_r	Erosion rate
EDX	Energy dispersive X-ray spectroscopy
FTIR	Fourier Transform Infrared
H (t)	Sample thickness at any time‘t’
H_∞	Sample thickness at equilibrium condition
I_c	Crystallinity index
K_{SR}	Thickness swelling parameter
L	Applied Normal Load
LCF	Luffa Cylindrica Fiber
M_m	Maximum percentage of moisture content
M_t	Moisture absorption
SEM	Scanning electron microscope
t	Time
T(s)	Thickness swelling
TGA	Termo gravimetric Analysis
V	Impact velocity
Vv	Voids content
W	Wear rate
W_0	Oven-dry weight
W_t	Weight after time‘t’

XRD	X-ray Diffraction
Δw	Wear loss/ Weight loss
w	Cumulative weight loss
α	Impingement / Impact angle
η	Erosion efficiency
ρ	Density

National Institute of Technology Rourkela
Rourkela, Odisha, India-769008

1. Title of the thesis

Preparation and Characterization of Luffa Cylindrica Fiber Reinforced Polymer composite

2. Name Designation and institution of the supervisor

Prof. Samir Kumar Acharya
Professor, Mechanical Engineering Department,
NIT Rourkela.

3. List of publication (Journal articles)

i. **Niharika Mohanta** and S. K. Acharya "Mechanical and Tribological Performance of Luffa cylindrica Fiber-Reinforced Epoxy Composite" Bio Resources 2015, Vol 10(4), 8364-8377.

ii. **Niharika Mohanta** and S. K. Acharya "Fiber-surface treatment: Its effect on structural, thermal and Mechanical properties of Luffa cylindrica Fiber and its composite". Journal of composite material 2015 doi: 10.1177/0021998315615204.

iii. **Niharika Mohanta** and S. K. Acharya. "Implementations of Taguchi Design for Erosive wear of Luffa Cylindrica Fiber-Reinforced Epoxy hybrid Composite". Journal of Polymer Engineering, 2015, Vol 35 (4), pp. 391-399.

iv. **Niharika Mohanta** and S.K.Acharya. "Tensile, flexural and interlaminar shear properties of Luffa Cylindrica fiber reinforced epoxy composites". International Journal of Macromolecular Science, 2013, Vol 3(2), pp. 6-10.

v. **Niharika Mohanta** and S. K. Acharya." Investigation of mechanical properties of luffa cylindrica fiber reinforced epoxy hybrid composite". International Journal of Engineering, Science and Technology 2015. Vol. 7, No. 1, 2015, pp. 1-10.

vi. **Niharika Mohanta** and S. K. Acharya. "Solid Particle Erosion of Luffa cylindrica Fiber Reinforced Polymer Composite." Proceeding of International Conference on Advances in Tribology and Engineering Systems. Lecture Notes in Mechanical Engineering, springer 2014, pp-411-420.

vii. **Niharika Mohanta** and S. K. Acharya. "Effect of Alkali treatment on the Flexural Properties of Luffa Cylindrica Reinforced Epoxy Composite." Science and Engineering of Composite Materials (accepted)

viii. **Niharika Mohanta** and S. K. Acharya," Moisture Absorption and Thickness Swelling Behavior and Its Effect on Tensile and Flexural Properties of Luffa Fiber Reinforced Epoxy Composite" Journal of industrial textile (under review).

ix. **Niharika Mohanta** and S. K. Acharya, "Moisture absorption, thickness swelling behavior and its effect on mechanical properties of chemically modified Luffa Cylindrica reinforced epoxy composite". Advances in polymer technology (under review)

4. List of presentation in national/international conferences

i. **Niharika Mohanta**, Dr S K Acharya "Solid Particle Erosion of Luffa cylindrica Fibre Reinforced Polymer Composite". International Conference on Advances in Tribology and Engineering Systems (ICATES), October 15-17,2013.L. D. College of Engineering, Gujarat, India

ii. **Niharika Mohanta**, Dr S K Acharya." Luffa cylindrica-A new class of natural fibre as reinforcement in composite material". 6^{TH} International Congress of Environmental Research (ICER), December 19-21, 2013 Aurangabad, India.

iii. **Niharika Mohanta**, Dr S K Acharya. "Effect of stacking sequence on mechanical Properties of luffa cylindrica fibre reinforced epoxy hybrid composite". International conference on metallurgical and material process, products and applications (ICMMPPA), January 8-10, 2014, OPJIT Raigarh.

iv. **Niharika Mohanta**, Dr S K Acharya. "A study on the potential of luffa cylindrical Fiber reinforced polymer composite for tribological applications". ASIATRIB-2014, International conference, February 17-20, 2014, at Jaypee palace Convention center &hotel Agra.

v. **Niharika Mohanta**, Dr S K Acharya. "Tribological behaviour of natural fibre (luffa cylindrica) reinforced hybrid epoxy composite" International conf. on Wood is good; current trends and future prospects in wood utilisation.21-23 Nov 2014, IWST Bangalore.

vi. **Niharika Mohanta**, Dr S K Acharya. “Tribo Performance Analysis of Luffa Cylindrica Fibre-Reinforced Epoxy Hybrid Composite Using Experimental Design”. National tribology conference (NTC), Dec.15th -18th, 2014, PES University, Bangalore.

Chapter 1

Introduction

1.1 OVERVIEW OF COMPOSITE MATERIALS

"Growth in quality of human life, protecting the environment" has been a buzz word of human civilization. The development of science and technology has created a need to develop engineering materials having light weight, high strength with specific properties as per service requirement at low cost and minimum energy consumption. That is how, the concept of composite materials has come into existence partially replacing existing metals, non-metals and alloys in various engineering applications. Many composites used today are at the leading edge of materials technology, establishing their use in advanced applications such as aircraft and aerospace structures. The idea of composite materials however is not a new or recent one but has been around thousands of years. The Ancient Egyptians used the chopped straw to reinforce with mud bricks, and Mongol warriors used a composite consisting of Bullock tendon, horn, bamboo strips, silk and pine resin to produce High-performance archery bows.

Since the early 1960s, there has been an increase in the demand for stronger, stiffer and more lightweight materials for use in the aerospace, transportation and construction industries. High-performance demands on engineering materials have led to the extensive research and development of new and improved materials, such as composites. Composite materials used for structural purposes often have low densities, resulting in high stiffness to weight and high strength to weight ratios when compared to traditional engineering materials. Besides, the high fatigue strength to weight ratio and fatigue damage tolerance of many composites also makes them an attractive option [1].

Basically, composites are materials consisting of two or more chemically distinct constituents, on a macro-scale, having a distinct interface separating them. One or more discontinuous phases are, therefore, embedded in a continuous phase to form a composite [2]. The discontinuous phase is usually harder and stronger than the continuous phase and is called the reinforcement, which provides strength to the composite. Whereas, the continuous phase is termed as the matrix which holds the fibre in desired shape and transfer the load from one fibre to other. The matrix material can be metallic, polymeric or can even be ceramic. When the matrix is a polymer, the

composite is called polymer matrix composite (PMC). The focus of this research is on the development of PMCs.

Polymeric materials have been finding great potentials in the industry as a class of important engineering materials. For centuries, the use of polymers in everyday life has become important part of human life. The growth of polymer starts in the early 19^{th} century with the development of celluloid, a hard plastic which is formed from nitrocellulose. The development of polymer technology was slow until 1930s, before the material such as phenol, vinyl, polystyrene and polyester were developed. After the development of these materials, the polymer research has taken an enormous growth that is still going on. Polymers are rapidly developing materials with the attractive advantages of low density and cost compared to metals and ceramics. Generally, polymers are very large molecules consisting of many small molecules called monomers or repeating units that can be linked together to form long chains and are known as macromolecules. A typical polymer may include tens of thousands of monomers. This specific long chain like structures is responsible for their fascinating properties with a wide range of the versatility of polymers for years in different fields of consumer durables, electrical and electronic equipment, aerospace, packaging, medical equipment, automobiles and other engineering applications.

However, polymer in its pure form alone could not satisfy the demands for various applications, where a combination of good mechanical; wear properties is required. Hence reinforcements are needed to provide additional strength for polymers. Upon the combination of this material, a material with properties different from the individual characteristics is produce. The constituent materials contain matrix and reinforcement. The primary phase of composite materials is the matrix phase which is usually more ductile and less hard phase as well as it holds the reinforcing phase normally stronger than the matrix and transfer stresses between the reinforcements.

An enormous number of polymeric materials, both thermosetting and thermoplastic, are used as matrix materials for the composites. Thermosets are plastics that cannot be melted once cured and include resins such as epoxies, polyesters and phenolic. Thermoplastics, on the other hand, are plastics that can be repeatedly melted, thus enabling them to be recycled. Commonly used thermoplastics include

polyethylene, polypropylene and polyvinyl chloride (PVC). Both thermoset and thermoplastic polymers have advantages and disadvantages when used as composite matrices, as can be seen in Table- 1.1.

Table- 1.1 Advantages and disadvantage of thermoset and thermoplastic matrix materials

Thermoset advantages	**Thermoset disadvantage**
▪ Low resin viscosity ▪ Good fiber wettability ▪ Low thermal conductivities ▪ Good corrosion resistance ▪ Creep resistant	▪ Composites are brittle and thus are more easily damageable ▪ Non-recyclable via standard techniques ▪ Not post-formable
Thermoplastic advantage	**Thermoplastic disadvantage**
▪ Unlimited shelf life ▪ Easy to handle (no tackiness) ▪ Recyclable ▪ Easy to repair by welding and solvent bonding ▪ Post formable ▪ High toughness	▪ Prone to creep ▪ Poor melt flow characteristics ▪ Thermoplastics need to be heated above the melting point to sufficiently wet the fibers

Some common thermoplastics polymer includes polypropylene, polyvinyl chloride (PVC), nylon, polyurethane, poly-ether-ether ketone (PEEK), polyphenylene sulfide (PPS), and polysulpone etc. They have higher toughness, high volume, low processing cost and used within temperature range $\geq 225^{o}$. Thermoplastics are increasingly used over thermosets. Their processing is faster than thermoset composites since no curing reaction is required. Thermoplastic composites require only heating, shaping and cooling. They have high toughness, low moisture absorption, chemical resistance and low toxic etc.

Thermosets resin includes polyesters, epoxies and polyamides. Polyesters have low cost, good mechanical strength, low viscosity and versatility, good electrical properties and excellent heat resistance. They can be used in cold and hot moulding with curing temperature is 120°C. Epoxy resins are widely used for most advanced composites. They have low shrinkage during curing, high strength and flexibility, adjustable curing range, better adhesion between fiber and matrix, better electrical properties and resistance to chemicals and solvents. However, epoxies are somewhat toxic in nature. They have limited temperature application range up to 175°C and moisture absorption affecting dimensional properties. They also have high thermal coefficient of expansion and slow curing. Polyamides have excellent mechanical strength, good strength retention for long-term temperature range of 260-315°C (500-600°F) and short term in 370°C (700°F) range. They also have excellent electrical properties, good fire resistance and low smoke emission. The composite can be hot mould under pressure, and the curing temperature is 175°C and 315°C.

Usually the resinous binders (polymer matrices) are selected on the basis of adhesive strength, fatigue resistance, heat resistance, chemical and moisture resistance, etc. The resin must have mechanical strength commensurate with that of the reinforcement. It must be easy to use in the fabrication process selected and also stand up to the service conditions. The resin matrix must also be capable of wetting and penetrating into the bundles of fibers that provide the reinforcement, replacing the dead air spaces within and offering those physical characteristics capable of enhancing the performance of fibers.

Shear, chemical and electrical properties of a composite depend primarily on the resin. Again, it is the nature of the resin that will determine the usefulness of the laminates in the presence of a corroding environment and service temperature. Rule of mixture is a tool to predict the properties like density, tensile strength and modulus etc. of the composite when the properties of matrix and fiber and their volume fraction are known.

Table-1.2 and 1.3 indicate the approximate service temperature ranges for the resins and composites [3, 4]. It should be remembered that there is no place for compromise as to the nature of the matrix material, particularly when it comes to the

application temperature of the composite. If the application temperature exceeds, 300-350°C metal matrix appears to be the only alternative, at least for the present.

Table- 1.2 Application temperatures of some matrix material [3]

Matrix material	**Limit of**	
	Long term exposure, ^{0}C	**Short term exposure, ^{0}C**
Unsaturated polyesters	70	100
Epoxies	125	200
Phenolics	250	1600
polyimide	315	400

Table - 1.3 Trends for temperature application of heat resistant composites [4]

Fiber reinforced Composite	**Maximum service temperature, ^{0}C**	**Specific weight g/cm3**
Carbon / Epoxy	180	1.4
Boron/Epoxy	180	2.1
Borsic / Aluminium	310	2.8
Carbon/Polyimide	310	1.4
Boron/Polyimide	310	2.1
Carbon/Polyaminoxaline	350	1.4
Carbon/Polybenzthiazole	400	14

1.2 TYPES OF COMPOSITE MATERIALS

The composite materials are broadly classified into the following categories as shown in figure-1.1 (a - e).

1.2.1 Fiber-reinforced composites

Reinforced-composites are popularly being used in many industrial applications because of their inherent high specific strength and stiffness. Due to their excellent structural performance, the composites are gaining potential also in tribological

applications. Fiber reinforced composites materials consists of fiber of high strength and modulus bonded in to a matrix with distinct interfaces (boundary) between them [5, 6]. In this form both fibers and matrix retain their physical and chemical identities. Yet they produce a combination of properties that cannot be achieved with either of the constituents acting alone. In general, fibers are the principal load carrying candidates, while the surrounding matrix keeps them in the desired location and orientation [2, 7]. A fibrous composite can be classified into two broad groups: continuous (long) fiber composite and discontinuous (short) fiber composite.

1.2.1.1 Continuous or long fiber composite

Continuous or long fiber composite consists of a matrix reinforced by a dispersed phase in the form of continuous fibers. A continuous fiber is geometrically characterized as having a very high length-to- diameter ratio which is known as the aspect ratio. If the aspect ratio is more than 12 it comes under the category of long fiber. They are generally stronger and stiffer than bulk material. Based on the manner in which fibers are packed within the matrix, it is again subdivided in to two categories: (a) unidirectional reinforcement and (b) bidirectional reinforcement. In unidirectional reinforcement, the fibers are oriented in one direction only where as in bidirectional reinforcement the fibers are oriented in two directions either at right angle to one another (cross-ply), or at some desired angle (angle-ply). When fibers are large and continuous, they impart certain degree of anisotropy to the properties of the composites particularly when they are oriented. Multi-axially oriented continuous fiber composites are also display near isotropic properties.

1.2.1.2 Discontinuous or short fiber composite

Short-fiber reinforced composites consist of a matrix reinforced by a dispersed phase in form of discontinuous fibers. As mentioned earlier these fibers are also characterized by the aspect ratio. If the aspect ratio comes within 8-12 they are categorized as short fiber. The low cost, ease of fabricating complex parts, and isotropic nature are enough to make the short fiber composites the material of choice for large-scale production. Consequently, the short-fiber reinforced composites have successfully established its place in lightly loaded component manufacturing. Further the discontinuous fiber reinforced composite divided into: (a) biased or preferred

oriented fiber composite and (b) random oriented fiber composite. In the former, the fibers are oriented in predetermined directions, whereas in the latter type, fibers remain randomly. The orientation of short fibers can be done by sprinkling of fiber on to given plane or addition of matrix in liquid or solid state before or after the fiber deposition.The discontinuities can produce a material response that is anisotropic, but the random reinforcement produces nearly isotropic properties.

1.2.2 Laminate Composites

Laminate Composites are composed of layers of materials held together by matrix. Generally, these layers are arranged alternatively for the better bonding between reinforcement and the matrix. These laminates can have uni-directional or bi-directional orientation of the fiber reinforcement according to the end use of the composite. The different types of composite laminates are: unidirectional, angle-ply, cross-ply and symmetric laminates. A hybrid laminate can also be fabricated by the use of different constituent materials or of the same material with different reinforcing pattern. In most of the applications of laminate composites, man-made fibers are used due to their good combination of physico-mechanical and thermal behavior.

1.2.3 Particulate Composite

Particulate composite consists of the composite material in which the filler materials are roughly round. An example of this type of composite would be the unreinforced concrete where the cement is the matrix and the sand serves as the filler. Lead particles in copper matrix are another example where both the matrix and the filler are metals. Cermet is a metal matrix with ceramic filler. Particulate composites offer isotropic properties of composite along with increase in toughness. Particulate composites are used with all three types of matrix materials – metals, polymers and ceramics.

1.2.4 Flake composites

Flakes are often used in place of fibers as can be densely packed. Metal flakes that are in close contact with each other in polymer matrices can conduct electricity or heat, while mica flakes and glass can resist both. Flakes are not expensive to produce and usually cost less than fibers. But they fall short of expectations in aspects like

control of size, shape and show defects in the end product. Glass flakes tend to have notches or cracks around the edges, which weaken the final product. They are also resistant to be lined up parallel to each other in a matrix, causing uneven strength.

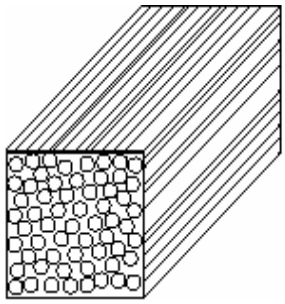

(a) Continuous fiber

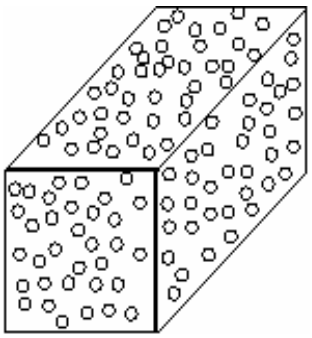

(b) Particulate composites composite

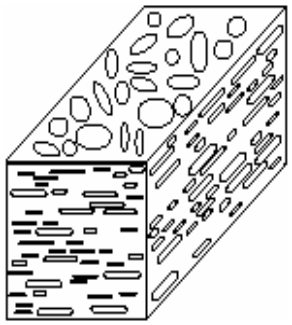

(c) Flake composites

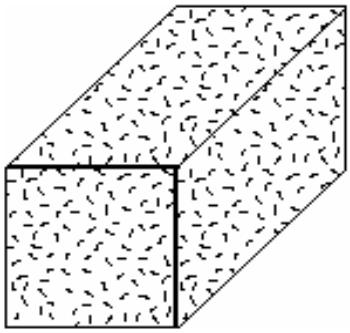

(d) Random fiber (short fiber) Composite

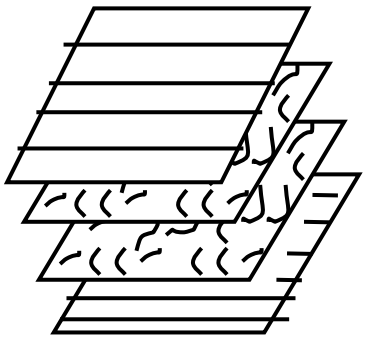

(e) Laminate Composite

Figure-1.1 (a-e) Schematic diagram of different types of Composite.

1.3 NATURAL FIBER COMPOSITES:

Synthetic fibre such as glass, carbon and aramid are being widely used in polymer composites because of their high stiffness and strength properties [8, 9]. But the charm of using synthetic fibers in polymer composites is fading day by day because of the following reasons: they are expensive, non-biodegradable, abrasive, thus making them dangerous to work with as well as increasing the wear on processing machinery. Environmental awareness on the other hand today motivates the researchers worldwide on the studies of natural fiber reinforced polymer composite as a cost effective option

to synthetic fiber reinforced composites. The availability of natural fibers and ease of manufacturing have tempted researchers to try locally available inexpensive fibers and to study their feasibility of reinforcement purposes and to what extent they satisfy the required specifications of a good reinforcement in polymer composite for different applications. With low cost and high specific mechanical properties, natural fiber represents a good renewable and biodegradable alternative to the most common synthetic reinforcement, i.e. glass fiber.

Natural fibers require very little energy to produce, and because they possess high calorific values, can be incinerated at the end of their lifetime for energy recovery. All plant-derived fibers utilize carbon dioxide when they are grown and can be considered CO_2 natural, meaning that they can be burned at the end of their lifetime without additional CO_2 being released into the atmosphere [10] . On the other hand, glass fibers are not CO_2 natural and require the burning of fossil fuels to provide the energy needed for production. The burning of fossil fuel-based products releases enormous amounts of CO_2 into the atmosphere and this phenomenon is believed to be the main cause of the greenhouse effect and the climatic changes that are being observed in the world today [11]. The geometry and properties of natural fibers depend, for example, on the species, growing conditions, cambium age, harvesting, defibration and processing conditions. Since cellulose fibers have the possibility to show a wide range with both poor and strong bonding to polymer matrix materials, depending on fiber-matrix modification and compatibility, the optimal interface is typically somewhere between the two extreme cases. For instance, if the interface is too strong, the composite material can become too brittle, resulting in a notch-sensitive material with low strength, since stress concentrating defects are inevitable [12].

The term "natural fiber" covers a broad range of vegetable, animal and mineral fibers. However in the composite industry, it is usually refers to wood fiber and agro based bast, leaf, seed, and stem fibers. These fibers often contribute greatly to the structural performance of plant and, when used in plastic composites, can provide significant reinforcement.

Despite the interest and environmental appeal of natural fibers, there use is limited to non-bearing applications due to their lower strength compared with synthetic fiber reinforced polymer composite. The stiffness and strength shortcomings of bio

composites can be overcome by structural configurations and better arrangement in a sense of placing the fibers in specific locations for highest strength performance. Accordingly extensive studies on preparation and properties of polymer matrix composite (PMC) replacing the synthetic fiber with natural fiber like jute, sisal, pineapple, bamboo, kenaf and bagasse were carried out [13-18]. As pointed out earlier these plant fibers have many advantages over glass fiber or carbon fiber like renewable, environmental friendly, low cost, lightweight, high specific mechanical performance.

1.4 OPPORTUNITIES FOR NATURAL FIBER COMPOSITES

In the present scenario, natural fibers have excellent potential to reduce not only CO_2 emissions but also save non-renewable resources by substituting glass fiber reinforcements in plastic composites. Traditionally, glass fibers/wool has been extensively used as building insulation material and reinforcement in auto sector thermoplastics. However, environmental performance of glass fiber mat thermoplastics (GMTs) has several drawbacks due to extensive energy consumption and potential health risks during production and handling. Glass fibers cause severe abrasion to process equipment and their composites may transform into sharp splints during collision causing extra injuries to passengers. Moreover GMTs are non-recyclable and their incineration generates clinker like mass that is hard to dispose off except land filling.

On the other hand, natural fibers are being explored more extensively by research institutions and automobile companies as environmental friendly alternative for the use of glass fibers. Most of the bast fibers being studied are obtained from naturally growing plants of flax, kenaf, sisal and hemp. Flax, sisal, and hemp are processed into door cladding, seatback linings, and floor panels. Coconut fiber is used to make seat bottoms, back cushions, and head restraints, while cotton is used to provide sound proofing, and wood fiber is used in seatback cushions [19]. Table-1.4 indicates some of the use of natural fiber in automobiles.

The use of natural fibre composites is not, however, limited only to the automotive industry. At least twenty manufacturers are producing wood fibre reinforced thermoplastic decking for the American markets [20]. Window and door profile manufacturers form another large industrial segment are also using wood as

reinforcing agent in polymers [21]. Other natural fibre composite applications that have been reported also include walls, flooring, louvers, and for indoor and outdoor furniture [20, 22].

Unfortunately, the current generation of natural fiber reinforced polymer composites do not offer sufficient mechanical properties to warrant their use in more demanding structural and load bearing applications. It is therefore necessary to improve the strength and stiffness of these composites, as well as other confronting issues such water absorption and thermal instability before they can be used to their full extent in industry.

Table-1.4 Example of interior and exterior automotive parts produced from natural materials [19]

Vehicle Part	**Material Used**
Glove Box	Wood/cotton fibers, flax/sisal
Door Panels	Flax/sisal with thermoset resin
Seat Coverings	Leather/wool backing
Seat Surface/Backrest	Coconut fiber/natural rubber
Trunk Panel	Cotton fiber
Trunk Floor	Cotton with PP/PET fibers
Insulation	Cotton fiber
Exterior Floor Panels	Flax mat with polypropylene

1.5 NATURAL FIBER: LUFFA CYLINDRICA

There are many potential natural resources, which India has in abundance. Most of it comes from agriculture or forest. The fruit of the Luffa cylindrica plant (genus: Luffa, species: Luffa aegyptiaca) a forest product which is of the Curcubitacea family [23] is shown in Figure-1.2 (a). The fruit shown in figure-1.2 (b) has a thick peel and the sponge gourd (figure-1.2(c)), which has a multidirectional array of fibers comprising a natural mat (figure-1.2 (d)), presents an inner fiber core (figure- 1.2(e)) and an outer mat core (figure- 1.2(f)). Common sponges vary in length from around 15–25 cm to 1.20–1.50 m [24]. The luffa cylindrica is a subtropical plant abundantly

available in China, Japan, India and other countries in Asia as well as in Central and South America [25]. The sponge guard are being used as component of shock absorbers, sound proof linings, utensils cleaning sponge, packing materials, for making crafts, filters in factories and part of soles of shoes [26]. Very limited scientific information available on this fruit in literature specially related to its structure and properties. The fruit is also of medicinal value. Immature fruit is used as vegetables, which is good for diabetes. The fruits are anthelmentic, carminative, laxative, depurative, emollient, expectorant, tonic and galactagogue and are useful in fever, syphilis, tumours, bronchitis, splenopathy and leprosy. Also it has purgative property and is used for dropsy, nephritis, chronic bronchitis and lung complaints [27]. The dried Luffa fruit fibres are used as abrasive sponges in skin care, to remove dead skin and to stimulate the circulation. The sponge gourd, fruit of Luffa cylindrica, has ligneous netting System in which the fibrous cords are disposed in a multidirectional array forming a natural mat. This fibrous vascular system is composed of fibrils glued together with natural resinous materials of plant tissue.

The importance of the luffa sponge material is growing in our society because of the search for sustainable solutions using new materials. In a recent study [28], the authors discovered that under quasi-static loading the luffa sponge material exhibits remarkable stiffness, strength and energy absorption capacities that are comparable to those of a variety of metallic cellular materials. It is interesting to note that this fiber contains cellulose 55-90%, hemicelluloses 8-22%, lignin 10-23%, and extractives 3.2 % and ash 0.4%. This makes it suitable for reinforcing material in polymer matrix [29-30]. Very limited research has been conducted in the past on this (luffa sponge) fibre as a potential reinforcement in bio composite. Those research findings indicate that it is a potential alternative material for packaging [23], water absorption [26, 31] and waste water treatment [32-33]. The luffa fibers were also used as reinforce-cement fiber for other materials [34-36] and cell immobilization for biotechnology [37-39]. From these findings it can be conclude that the full potential of luffa fiber is yet to be explored. Hence in the present work the main focus is to prepare a polymer matrix composite (PMC) using epoxy resin as matrix material and luffa cylindrica fiber as reinforcement material.

(a)

(b)

(c)

(d)

(e)

(f)

Figure-1.2 (a) The luffa cylindrica plant with fruit, (b) the fruit showing thick outer layer, (c) Luffa sponge with partial removed of outer skin (d) Luffa sponge (e) The inner fiber core. (f) The outer core opens as a mat.

Hence in the present work Single, double and triple layered composites are prepared by hand lay-up technique. The lignocellulosic fibers are hydrophilic and

absorb moisture. Removal of moisture from the fiber is an essential step to reduce its hydrophilic nature to make it suitable for outdoor application. Fiber surface modification by chemical have been carried out on the fibers to improve the strength, separation, crystallinity and removal of hydrophilic and thermally instability nature of luffa fiber. The morphological and surface chemistry of the untreated and treated fiber are studied by SEM, XRD, and FT-IR and correlated these studies to its thermal and some mechanical properties of the composite. Moisture absorption behavior of the developed composites was studied before and after modifying the fiber surface. To assess the suitability of the composites in tribological applications, solid particle erosion tests have been carried out under simulated laboratory conditions. It is known that mechanical properties of natural fiber composites are much lower than those of synthetic fiber. The use of natural fiber alone in polymer matrix is inadequate in satisfactorily tackling all the technical needs of a fiber reinforced composite. If natural fiber is combined with a synthetic fiber in the same matrix, the properties of natural fiber could be enhanced by taking the advantage of both the fibers. Hence luffa cylindrica-glass hybrid composites were prepared with varying stacking sequence. The effect of hybridization of glass and stacking sequence on mechanical properties and tribological behavior of the luffa cylindrica-glass fiber hybrid composites is also studied. The surface of fractured and worn out samples were studied using Scanning Electron Microscope (SEM) to have an idea about the fractured behavior of the composite.

1.6 STRUCTURE OF THE THESIS

The present thesis contains seven chapters. The first chapter introduces the polymer matrix composite and also discusses the benefits of natural fiber as a reinforcement material in polymer composite.

In the second chapter detail discussion of structure and chemical composition of natural fibers and work related to present investigation available in literature are discussed.

In the 3rd chapter characterization of both untreated and treated luffa fiber and mechanical properties of both untreated and treated luffa cylindrica reinforced composite.

The 4th chapter discusses the moisture absorption behavior and effect of moisture absorption on mechanical properties of both untreated and treated luffa cylindrica reinforced epoxy composite are discussed.

In the fifth chapter the erosive wear behavior of both untreated and treated luffa cylindrica reinforced epoxy composite.

In the sixth chapter the effect of stacking sequences on mechanical and tribological behavior of luffa- glass hybrid composite has been studied.

Finally, conclusions drawn from the present study mentioning the scope of future work are presented in chapter seven.

Chapter 2

Literature Review

2. LITERATURE REVIEW

The purpose of this literature review is to provide background information on the issues to be considered in this thesis and to emphasize the relevance of the present study. This treatise embraces various aspects of natural fiber polymer composites with a special reference to their mechanical and tribological behavior. This chapter includes reviews of available research reports.

- ✓ **On natural fibers and natural fiber reinforced composites**
- ✓ **On issues regarding the use of natural cellulose fibers in composites**
- ✓ **On chemical modification of fiber surface**
- ✓ **On hybrid composite**
- ✓ **On wear mechanism and its classification**

2.1 ON NATURAL FIBERS AND NATURAL FIBER REINFORCED COMPOSITE

Growing environmental awareness has triggered the researcher's worldwide to develop and utilize materials that are compatible with the environment. In the process natural fibers have become suitable alternatives to traditional synthetic or manmade fibers and have the potential to be used in cheaper, more sustainable and more environmentally friendly composite materials. Natural organic fibers can be derived from either animal or plant sources. The majority of useful natural textile fibers are plant derived, with the exceptions of wool and silk. All plant fibers are composed of cellulose, whereas fibers of animal origin consist of proteins. Natural fibers in general can be classified based on their origin, and the plant-based fibers can be further categorized based on part of the plant they are recovered from. An overview of natural fibers is presented in figure-2.1 [40].

Generally, plant or vegetable fibers are used to reinforce polymer matrices. Plant fibers are a renewable resource and have the ability to be recycled. The plant fibers leave little residue if they are burned for disposal, returning less carbon dioxide (CO2) to the atmosphere than is removed during the plant's growth.

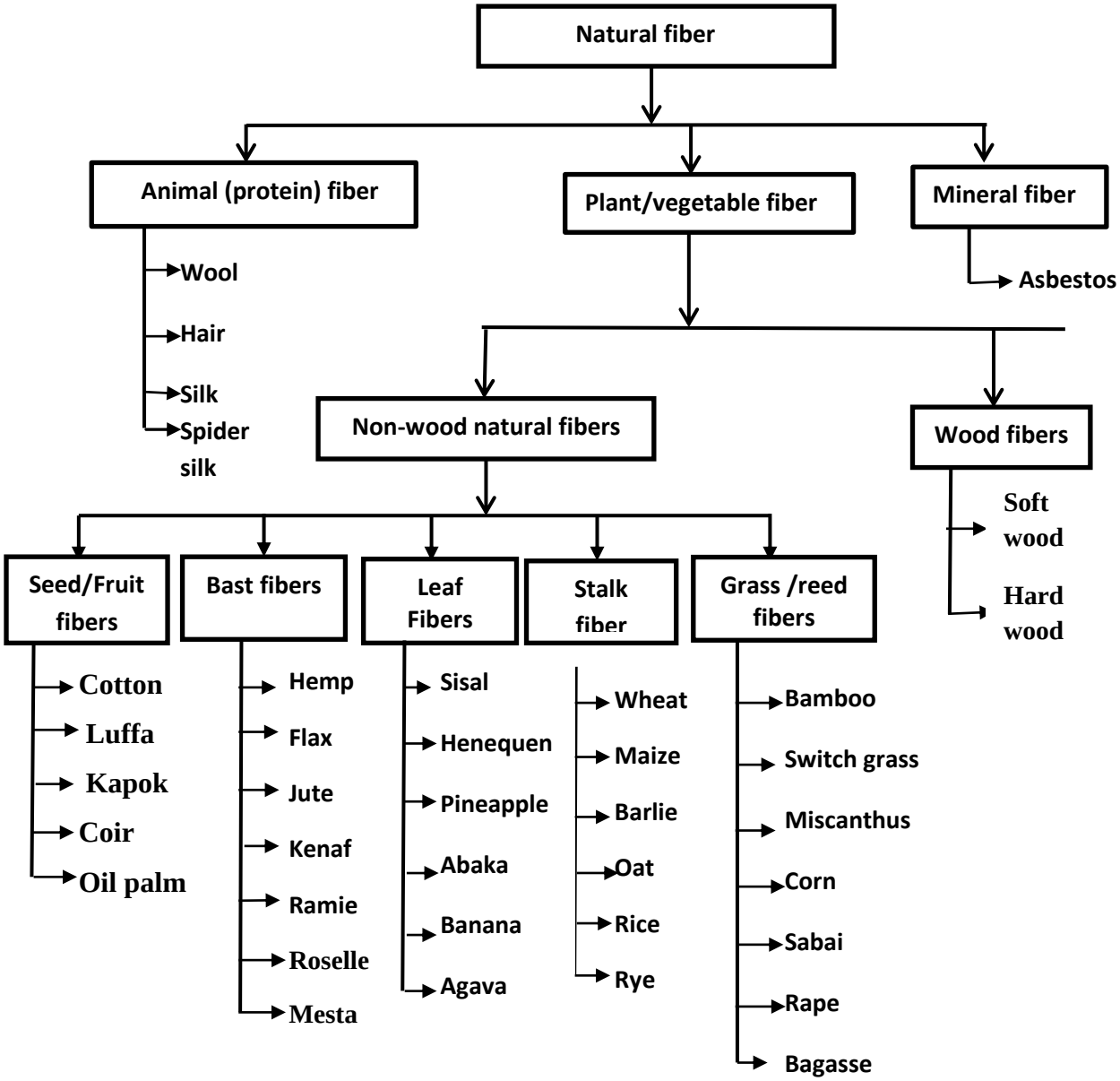

Figure-2.1 Overview of natural fibers

The leading driver for substituting natural fibers for glass is that they can be grown with lower cost than glass. The price of glass fiber is around Rs. 300.00/- per kg and has a density of 2.5 g/cc. On the other hand, natural fiber costs Rs. 15.00/- to 25.00/- per kg and has a density of 1.2-1.5 g/cc. As can be seen from Table-2.1 [40], the tensile strength of natural fibers is substantially lower than that of glass fibers though the modulus is of the same order of magnitude. However, when the specific modulus of natural fibers (modulus per unit specific gravity) is considered, the natural

fibers show values that are comparable to or even better than glass fibers. Material cost savings, due to the use of natural fibers and high fiber filling levels, coupled with the advantage of being non-abrasive to the mixing and moulding equipment make natural fibers an exciting prospect. These benefits mean natural fibers could be used in many applications, including building, automotive, household appliances, and other applications.

Table-2.1 Properties of glass and natural fibers [40]

Properties	**Fiber**						
	E-Glass	**Hemp**	**Flax**	**Jute**	**Sisal**	**Coir**	**Ramie**
Density (gm/cc)	2.25	1.48	1.4	1.46	1.33	1.25	1.5
Tensile strength (MPa)	2400	550-900	800-1500	400-800	600-700	220	500
Young's Modulus(GPa)	73	70	60-80	10-30	38	6	44
Specific Modulu (GPa)	29	-	26-46	7-21	29	5	2
Failure Strain (%)	3	1.6	1.2-1.6	1.8	2-3	15-25	2
Moisture absorption (%)	-	8	7	12	11	10	12-17

2.1.1 STRUCTURE OF PLANT FIBER

Natural plant fibers are constituents of cellulose fibers, consisting of helically wound cellulose micro fibrils, bound together by an amorphous lignin matrix. Lignin keeps the water in fibers; acts as a protection against biological attack and as a stiffener to give stem its resistance against gravity forces and wind. Hemicellulose found in the natural fibers is believed to be a compatibilizer between cellulose and lignin. The cell wall in a fiber (figure-2.2) is not a homogenous membrane [41]. The cell wall of each fiber is composed of several layers such as middle lamella, the thin primary wall, and the secondary wall, which is subdivided into external secondary wall (S1), middle secondary wall (S2) and internal secondary wall (S3) and a central called lumen, responsible for water and nutrients transportation. These secondary layers are composed of micro fibrils oriented into space in defined (angles) form [42, 43]. The thin primary wall which is the first layer deposited during cell growth, consists in a disordered arrangement of cellulose fibrils placed in a matrix of pectin, hemicellulose,

lignin, and protein [44, 45]. The secondary wall consists of crystalline cellulose micro fibrils organized in a spiral arrangement, where the middle layer (S2) determines the fiber mechanical properties. The middle layer consists of a series of helically wound cellular micro-fibrils formed from long chain cellulose molecules. These micro-fibrils have typically a diameter of about 10-30 nm and are made up of 30-100 cellulose molecules in extended chain conformation and provide mechanical strength to the fiber. The middle lamella, that is outer layer of cell, is composed predominantly by pectin that acts as cement between fibers [45]. The fiber strength can be an important factor in selecting a natural fiber for a specific application. A high aspect ratio (length/width) is very important in cellulose-based fiber composites as it gives an indication of possible strength properties.

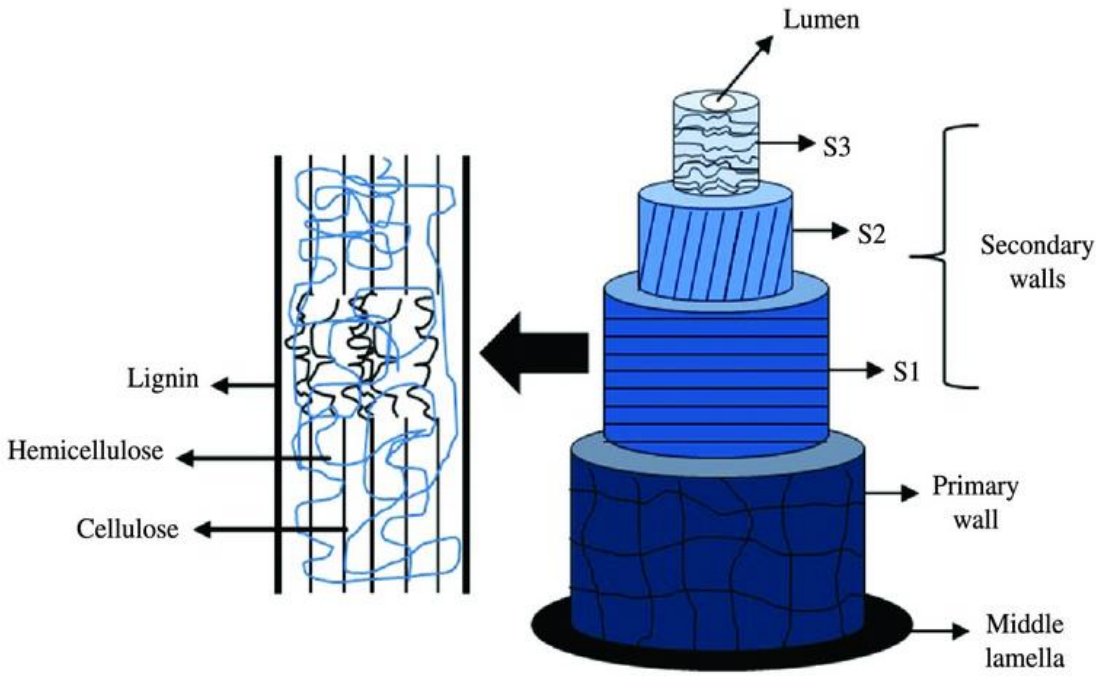

Figure-2.2 Structure of an elementary plant fiber (cell) [46].

2.1.2 CHEMICAL COMPOSITION OF NATURAL FIBERS

Cellulose, hemicellulose and lignin are the three main constituents of natural fibers. For this reason, they are also referred to as cellulosic or lignocellulosic fibers. The proportion of these components in a fiber depends on the area of production, variety, maturity of the plant (age) and the extraction conditions used to obtain the

fibers. Table-2.2 provides average values of chemical constituents of vegetable/plant fiber [46].

Table-2.2 Chemical constitution of wide variety of natural fiber [46]

Fiber type	Cellulose	Hemicellulose	Lignin	Ashes
Jute	60	22.1	15.9	1.0
Sisal	74-75	10-13.9	7.6-7.9	0.4
Banana	60-65	6-8	5-10	1.2
Hemp	72	10	3	2.3
Kenaf	72	20.3	9	4.0
Ramie	80-85	3-4	0.5	-
Pineapple	83	-	12	-
Curauá	70.7	21.1	7.5	
Luffa	62	20	11.2	0.40
Coir	43-53	14.7	38-40	
Rice straw	43.2	31.7	16.9	9.9
Barley	31-45	14-15	24-29	
Bamboo	33-45	30	20-25	
Bagasse	69.4	21	4.4	0.6

2.1.2.1 Cellulose

The major component of vegetal fibers is the cellulose which is a polymer of β-D-Glucose oriented in which -CH2OH group is alternating above and below the plane of the cellulose molecule thus producing long, unbranched chains (figure-2.3) presents in the secondary cell wall. It is responsible for the high mechanical strength of fibers and act as a reinforcing material. It consists of a linear polymer of D-anhydroglucose units where two adjacent glucose units are linked together by β-1, 4-glycosidic linkages with elimination of one water molecule between their -OH groups at carbon atoms 1 and 4. Chemically, cellulose is defined as a highly crystalline segment alternating with regions of non-crystalline or amorphous cellulose [47, 48].

The glucose monomers in cellulose form hydrogen bonds within its own chain (intramolecular) forming fibrils and with neighboring chains (intermolecular), forming micro-fibrils. These hydrogen bonds lead to formation of a linear crystalline structure with high rigidity and strength. The amorphous cellulose regions have a lower frequency of intermolecular hydrogen bonding, thus exposing reactive intermolecular -OH groups to be bonded with water molecules. Amorphous cellulose can therefore be considered as hydrophilic in nature due to their tendency to bond with water. On the other hand, very few accessible intermolecular –OH are available in crystalline cellulose and it is far less hydrophilic than amorphous cellulose. Crystalline micro-fibrils have tightly packed cellulose chains within the fibrils, with accessible –OH groups present on the surface of the structure. Only very strong acids and alkalis can penetrate and modify the crystalline lattice of cellulose.

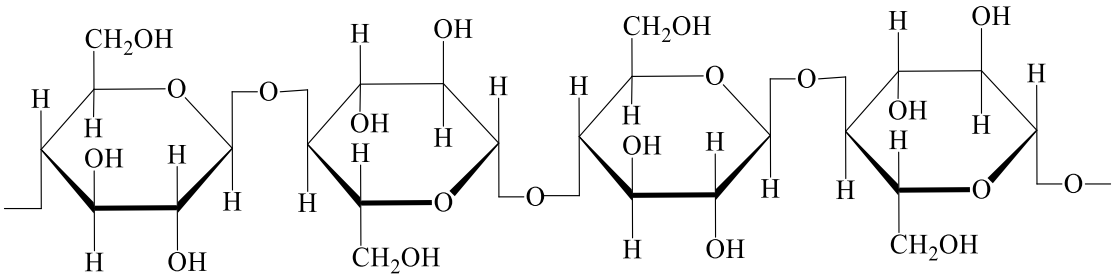

Figure-2.3 Structure of Cellulose

2.1.2.2 Hemicelluloses

Hemicellulose, any of a group of complex carbohydrates that, with other carbohydrates (*e.g.*, pectin's), surround the cellulose fibers of plant cells. The most common hemicelluloses contain xylans (many molecules of the five-carbon sugar xylose linked together), an uronic acid (*i.e.*, sugar acid), and arabinose (another five-carbon sugar). Xylan (figure-2.4) is an example of a pentosan consisting of D-xylose units with 1β→4 linkages. Hemicellulose is very hydrophilic, soluble in alkali, and easily hydrolyzed in acids.

Hemicelluloses differ from cellulose in three different ways. Firstly, unlike cellulose (containing only 1, 4-β-D-glucopyranose units) they contain several different sugar units. Secondly, they exhibit a considerable degree of chain branching, whereas cellulose is a linear polymer. Thirdly, the degree of polymerization of native cellulose is ten to hundred times higher than that of hemicelluloses. Unlike cellulose, the

constituents of hemicelluloses differ from plant to plant. Hemicelluloses contain substituents like acetyl (-COCH3) groups and glucoronic acid. By attaching ferulic acid and p-coumaric residues, hemicelluloses can form covalent bonds to lignin [49]. Due to this linking ability of hemicelluloses, degradation of it leads to disintegration of the fibers into cellulose micro-fibrils resulting in lower fiber bundle strength [50].

Mainly the acid residues attached to hemicelluloses make it highly hydrophilic and increase the fiber water uptake, which increases the risk of microbiological fiber degradation. It has been found that hemicelluloses thermally degrade more at lower temperatures (150-180°C) than cellulose (200-230°C) [51].

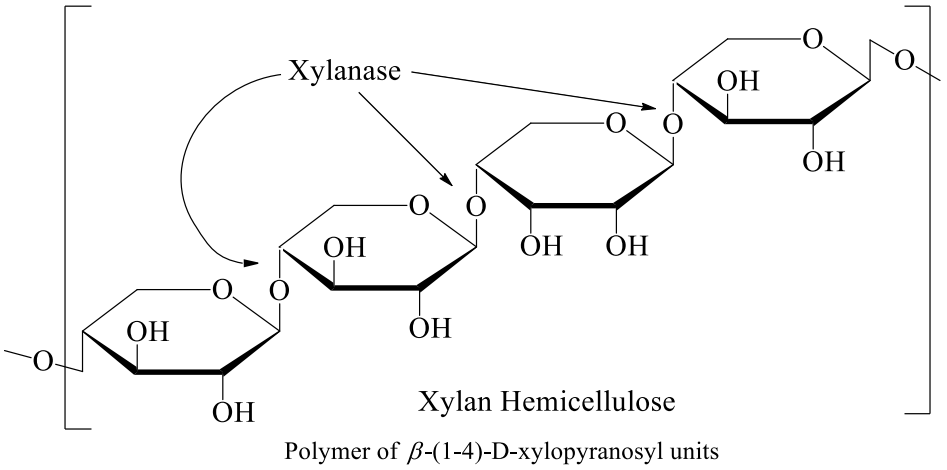

Figure-2.4 Structure of Hemi-Cellulose

2.1.2.3 Lignin

Lignin is a highly cross-linked molecular complex with amorphous structure and acts as a binder agent between individual fiber cells and the fibrils forming the cell wall [52]. Lignin increases the compression strength of plant fibers by gluing the fibers together to form a stiff structure, making it possible for trees of 100 meters to remain upright. Lignin is essentially a disordered, polyromatic, and cross-linked polymer arising from the free radical polymerizations of two or three monomers structurally related to phenyl-propane [53]. These three monomers make almost all lignin found in nature (figure-2.5 (a), (b)). Free radical coupling of the lignin monomers gives rise to a very condensed, reticulated, and cross-linked structure. The lignin matrix is therefore analogous to a thermoset polymer in conventional polymer terminology. The

dissolution of lignin using chemicals aids fiber separation. When exposed to ultraviolet light, lignin undergoes photochemical degradation [54]. The lignin seems to act like a matrix material within the fibers, making stress transfer on a micro-fibril scale and single fiber scale possible.

Lignin is the generic term for a large group of aromatic polymers resulting from the oxidative combinatorial coupling of 4-hydroxyphenylpropanoids [54a]. Lignin synthesis initiates through oxidative radical–radical coupling of monolignols and incorporates many more than the classical three monolignols p-coumaryl, coniferyl, and sinapyl alcohol, such as products from incomplete monolignol biosynthesis, which is 5-hydroxyconiferyl alcohol, hydroxycinnamaldehydes, and hydroxycinnamic acids [54b], or enzymatically made derivatives of the classical monolignols, such as sinapyl p-hydroxybenzoate, coniferyl and sinapyl p-coumarate, and coniferyl and sinapyl acetate all incorporate into the polymer at various levels. After lignin monomers are biosynthesized, they are translocated to the cell wall, where they are oxidized for polymerization.

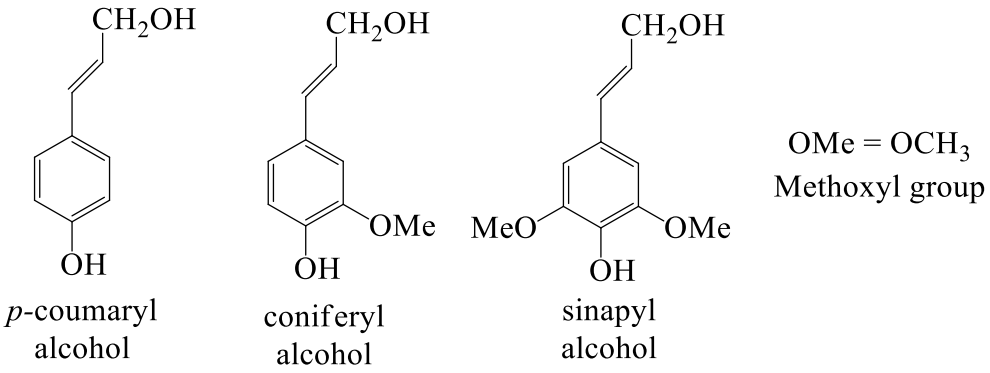

Figure-2.5 (a). Structure of lignin monomer

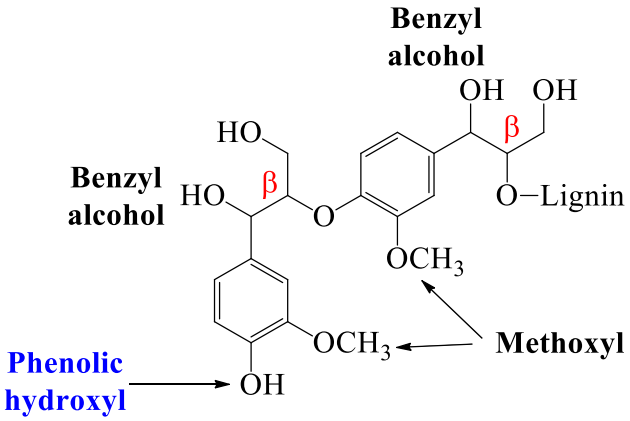

Figure-2.5 (b). Typical structure of Lignin

2.1.2.4 Pectin

Pectin is a complex branched structure of acidic structural polysaccharides, found in fruits and bast fibers. Figure-2.6 shows the typical structure of pectin. The majority of the structure consists of homopolymeric partially methylated poly-α-(1-4)-D-galacturonic acid residues, but there are substantial 'hairy' non-gelling areas of alternating α-(1-2)-L-rhamnosyl-α-(1-4)-Dgalacturonosyl sections containing branch-points with mostly neutral side chains (1-20 residues) of mainly L-arabinose and D-galactose (rhamnogalacturonan-I). Pectin is the most hydrophilic compound in plant fibers due to the carboxylic acid groups and is easily degraded by defibration with fungi [47]. Pectin along with lignin and hemicelluloses present in natural fibers can be hydrolysed at elevated temperatures.

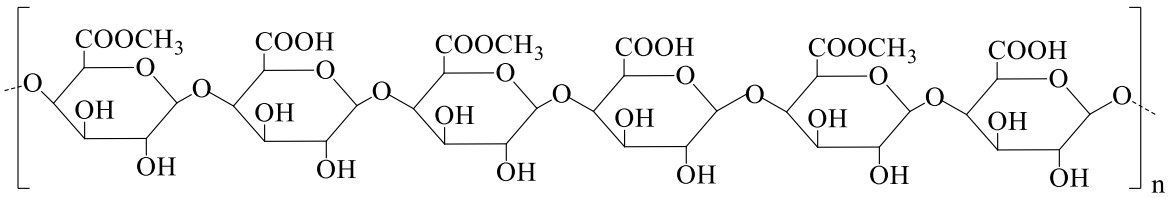

Figure-2.6 Typical structure of pectin

2.2. ISSUES REGARDING THE USE OF NATURAL CELLULOSE FIBRES IN COMPOSITES

Natural fibers possess several advantages compared to synthetic fibers, thus making them attractive reinforcements for composite materials. They are cheap, abundant and renewable, and have good specific properties such as tensile strength and stiffness. Despite these advantages, untreated natural fibre composites have performed much below their potential capabilities and have therefore not been used extensively in the polymer industry due the following reason.

The main reasons for this are as follows:

- Poor interfacial bonding between the cellulose fibers and the polymer matrix
- Limited thermal stability of the composite
- High moisture absorption of the cellulose fibers
- Biodegradability of the fibers

2.2.1 Interfacial Bonding

All plant derived cellulose fibers are polar and hydrophilic in nature, mainly as a consequence of their chemical structure. Plant fibers contain non-cellulosic components such as hemicelluloses, lignin and pectins, of which the hemicelluloses and pectins are the most hydrophilic. These components contain many accessible hydroxyl (OH) and carboxylic acid groups, which are active sites for the sorption of water [55]. The cellulose component also contains many OH groups, but little water can be accommodated within the highly ordered and highly crystalline micro fibrils. As a result of this, only un-bonded OH groups on the micro fibril surfaces are available for sorption. Polyolefins, such as polypropylene, are largely non-polar and hydrophobic in nature. The incompatibility of the polar cellulose fibers and non-polar thermoplastic matrix leads to poor adhesion, which then results in a composite material with poor mechanical properties [56]. To fully utilize the mechanical properties of the reinforcing fibers and thereby improve the composite properties, it is necessary to improve the adhesion between the fibers and matrix. This can be achieved by either modifying the surface of the fibers to make them more compatible with the matrix, or by modifying

the matrix with the addition of a coupling agent that adheres well to both the fibers and matrix. When the fibers and matrix have been brought into close proximity with one another, the Following interfacial bonding mechanisms may occur:

- Mechanical interlocking
- Electrostatic bonding
- Chemical bonding
- Reaction or Inter diffusion bonding.

2.2.2 Thermal Stability

Unlike many synthetic fibers, lignocellulosic fibers are inherently thermally unstable, and thermal degradation starts to occur at temperatures of around 200^{o}C. This results in the exclusion of some manufacturing processes, and also limits the use of the composites to low temperature applications. It is suggested by Yildiz et al. [57] that temperatures above 150^{o}C can lead to permanent alterations of the physical and chemical properties of lignocellulosic fibers such as wood. It is also stated that heat treatments at high temperatures can improve the biological durability of wood, but stiffness and strength are reduced. It has, however, been shown by several authors [58-60] that the thermal stability of lignocellulosic fibers can be improved to some extent by means of chemical modification of fiber surface.

2.2.3 Moisture Absorption

A further problem associated with using lignocellulosic fibers in composite materials is high moisture absorption [61]. A moisture build up in the fibre cell wall can lead to fibre swelling and dimensional changes in the composite, particularly in the direction of the fiber thickness [62]. Another problem associated with fibre swelling is a reduction in the adhesion between the fibre and the matrix, leading to a reduction in the mechanical properties of the composite. The debonding between the fibre and matrix may be initiated by the development of osmotic pressure pockets at the surface of the fibre, which is a result of the leaching of water-soluble substances. Besides dimensional stability; the hydrophilic nature of lignocellulosic fibers also influences the process ability of the composite. The tendency of lignocellulosic fibers to absorb moisture results in the release of water vapour in the composite during high

temperature compounding, leading to the formation of a highly porous material. Joseph et al. [63] have the opinion that these pores can act as stress concentration points, and can lead to premature failure of the composite during loading from the fiber surface. They also have the indicated that the water uptake of natural fibre composites can be reduced considerably by using coupling agents to assist with fibre-matrix adhesion.

2.2.4 Fiber Tensile Strength, Young's Modulus and Volume Fraction

Incorporation of natural fibers in to polymer is now a standard technology to improve the mechanical properties of polymer. The mechanical properties of the composite are strongly influenced by many factors such as strength of the fibers and matrix, fiber content, fiber aspect ratio, and the interfacial bonding between fibers and matrix [64-66]. Fibers act as carriers of load in the matrix. Good mechanical strength of composite depends more on effective and uniform stress distribution [65, 67]. By the rule of mixture adding high strength fibers to a matrix having low strength should result in increasing in tensile strength of the composite if interfacial bonding is good [66].

As reinforcing fibers are directly responsible for providing strength and stiffness to a composite, it is necessary to maximize the fiber tensile strength and Young's modulus to produce a composite material with enhanced properties. Fibre volume fraction (V_f) also plays an important role in determining the composite mechanical properties. For composites consisting of brittle fibers in a ductile polymer matrix, two possible failure regimes exist depending on whether the fibre volume fraction is above or below a minimum value (V_{min}). If a composite with $V_f < V_{min}$ is stressed, the polymer matrix will be able to carry the applied load after fibre fracture. Failure of the fibers does not lead to composite failure but results in a stress increase in the matrix. The failed fibers, which now carry no load, can be regarded as holes in the polymer matrix. If a composite with $Vf > V_{min}$ is stressed, brittle failure of the fibers leads to failure of the whole composite, since the polymer matrix in unable to support the additional load which is transferred into the matrix from the fibers [68]. When $V_f > V_{min}$, a point exists where the strength of the composite reaches its maximum value and

then surpasses the strength of the matrix alone, and this is known as the critical fibre volume fraction (V_{crit}) [69].

At very high fibre volume fractions, the strength of a composite starts to decrease due to insufficient wetting of the fibers with the polymer matrix. Recently El-Shekeil et al. [70] produced kenaf fiber reinforced thermoplastic polyurethane composites and found tensile strength of the composite increase with increase in fiber loading up to 30% and then dropped back due to insufficient wetting of fiber with the matrix and the increased population of fibers leads to agglomeration and stress transfer gets blocked. In an another work Nishino et al. [17] showed that tensile strengths of 40-mesh hardwood fibers reinforced HDPE composites increased gradually up to a maximum at 25% of fiber loading by volume, and then dropped back due to the poor fiber matrix adhesion .

2.3 ON CHEMICAL MODIFICATION OF FIBER SURFACE

As discussed in Art 2.2 it is certain that natural fiber reinforced polymer composites inherently have poor mechanical properties due to poor adhesion between the fibers and matrix. The interfacial adhesion can be improved by modifying the fibers, the matrix or both the fibers and the matrix by different physical and chemical methods. Matrix modifications generally involve the addition of chemical coupling agents and compatiblizers to polymer matrix, with the purpose of improving the polymer reactivity and wetting of the reinforcing fibers.

Fibre treatments may be biological, physical or chemical, and are performed to achieve one or more of the following objectives:

- Removal of undesirable fiber constituents
- Roughening of the fiber surface
- Separation of individual fibers from their fibre bundles
- Modification of the chemical nature of the fibre surface
- Reducing the hydrophilicity of the fibers

Fiber treatments involving the use of chemicals play an important role in improving the reinforcing capabilities of fibers. These treatments can either be

classified as fibre pre-treatments, coupling agents, compatibilizers or dispersing agents. Pre-treatments involve the use of chemicals that remove undesirable and non-strength contributing fibre constituents such as lignin, pectin and hemicelluloses. Compatibilizers are chemicals that lower the surface energy of fibers to make them more non-polar and therefore more compatible with polymer matrices. Dispersing agents are used to improve the dispersion of fibers in the matrix. Coupling agents are mainly responsible for improving the adhesion between reinforcing fibers and the matrix material, but can also reduce the water uptake of the fibers and assist with fibre dispersion as well. Due to this overlap in functions and to simplify matters, all bonding agents and surfactants have been grouped together as chemical treatments.

At present, over forty coupling agents have been used in the production and research of natural fiber composites [71]. The most popular treatments include the use of alkalis, anhydrides and anhydride-modified copolymers, benzoyl chloride, permanganate silanes and isocyanates.

2.3.1 Alkaline treatment

Alkaline treatment is one of the most used chemical treatments of natural fibers when used to reinforce thermoplastics and thermosets. The important modification done by alkaline treatment is the disruption of hydrogen bonding in the network structure, thereby increasing surface roughness. This treatment removes a certain amount of lignin, wax and oils covering the external surface of the fiber cell wall, depolymerizes cellulose and exposes the short length crystallites [72]. Addition of aqueous sodium hydroxide (NaOH) to natural fiber promotes the ionization of the hydroxyl group to the alkoxide [73].

$$\text{Fiber}\text{—}\text{OH} + \text{NaOH} \longrightarrow \text{Fibre}\text{—}\text{O}\text{—}\text{Na} + H_2O$$

Thus, alkaline processing directly influences the cellulosic fibril, the degree of polymerization and the extraction of lignin and hemicellulosic compounds [74]. It is reported that alkaline treatment has two effects on the fiber:

1) It increases surface roughness resulting in better mechanical interlocking, and
2) It increases the amount of cellulose exposed on the fiber surface, thus increasing the number of possible reaction sites [75].

Consequently, alkaline treatment has a lasting effect on the mechanical behavior of flax fiber, especially on fiber strength and stiffness.

2.3.2 Benzoyl chloride treatment

Benzoylation is an important transformation in organic synthesis [76]. Benzoyl chloride is most often used in fiber treatment. Benzoyl chloride includes benzoyl (C6H5C=O) which is attributed to the decreased hydrophilic nature of the treated fiber and improved interaction with the hydrophobic polymer matrix. The reaction between the cellulosic hydroxyl group of the fiber and benzoyl chloride is given as follows:

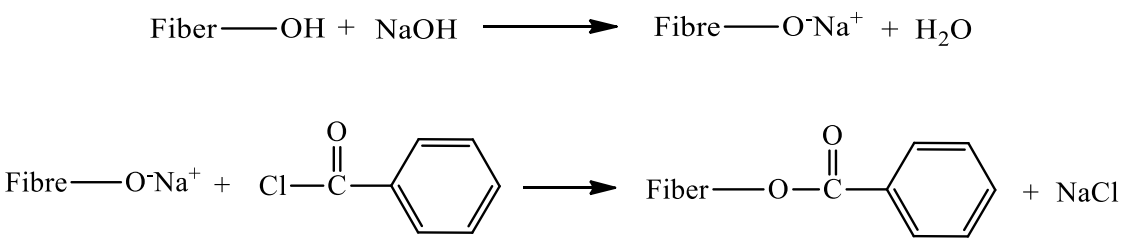

Benzoylation of fiber improves fiber matrix adhesion, thereby considerably increasing the strength of composite, decreasing its water absorption and improving its thermal stability [77, 78, and 79].

2.3.2 Permanganate treatment.

Permanganate treatment on natural fibres is generally conducted by potassium permanganate (KMnO4) in acetone solution. This treatment forms highly reactive permanganate (Mn3+) ions to reacts with the cellulose hydroxyl groups and forms cellulose–manganate for initiating graft copolymerization. This treatment enhances chemical interlocking at the interface and provides better adhesion with the matrix [80]. Formation of cellulose–manganate is responsible for higher thermal stability of the fibre. It also reacts with the lignin (hydrophilic -OH groups) constituents and separates from the fibre cell wall. It reduces the hydrophilic nature of the fibre. Higher concentrations of KMnO4 (more than 1%) cause excess delignification (removal of cementing materials) within the cellulosic structure and degrade fiber properties [81].

Paul et al. [81] reported that, during an oxidation reaction, KMnO4 etches the fiber surface and makes it physically rougher to improve mechanical interlocking with the matrix. Flexural strength and modulus properties were increased by 5% and 10% for the treated banana fiber polypropylene composites. Li et al. [82] applied 0.2% potassium permanganate (KMnO4) solution (in 2% acetone) on alkali (2% NaOH for 1 h) pre-treated flax fiber and reported treated fiber-LLDPE and HDPE composites had higher tensile strength properties compared to the untreated fiber composites. The reaction between fiber –OH group and potassium permanganate is given below:

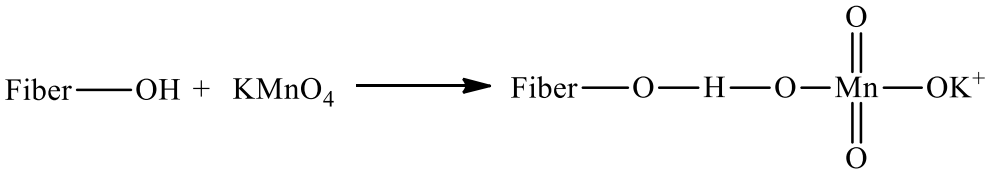

A number of investigations have been made on various chemical treatments of natural fibers such as kenaf, hemp, flax and jute to enhance mechanical properties of composite materials. Table-2.3 indicates some of the work done with different chemicals treatments for different natural fibers [41, 83-96].

2.4 ON HYBRID COMPOSITE

Composites can be broadly classified as synthetic fiber reinforced composites and natural fiber reinforced composites. Synthetic fiber reinforced composites have applications in various areas due to their favorable properties when compared with the conventional materials. In spite of all these advantages the synthetic fiber reinforced composites lack in various aspects like reusability, recycling and bio degradability after end of their life span. All the aforementioned issues are leading to the problems of environmental sensitivity; as a result we need to explore viable alternatives which could resolve our problems [97-101].

Table-2.3 Survey table for effect chemical modification of natural fiber on mechanical properties

Fiber matrix composites	**Applied treatment methods**	**Results**	**Ref**
Jute-Vinylester	5% NaOH for 4, 6 and 8hrs	4h NaOH treated composite accounted 20% and 19% increased in flexural strength and interlaminar shear strength properties.	2001 [83]
Sisal-epoxy	2% NaOH for 4 hours	Alkali treatment increases (i) fiber strength and (ii) The adhesion between the fiber bundles and the matrix.	2001 [41]
Sisal-Polycaprolactone	10% NaOH For 24 and 48hrs	Elastic modulus is increased with the increased with reaction time	2004[84]
Hemp fibre	8% NaOH treatment	Thermal stability of composite was increased by 4%.	2005[85]
Bagasse-polyester	1, 3, 5% NaOH	13% improvement in tensile strength, 14% in flexural strength and 30% in impact strength of composite was observed for 1% NaOH treatment.	2005[86]
Hemp-Euphorbia resin	0.16% NaOH for 48hrs	Tensile strength was increased by 30% and shear strength Properties of composite was doubled.	2007 [87]
Sisal-Polyester	0.5%, 1%, 2%, 4%, 10% NaOH treatment	Maximum tensile strength properties of composite were found for 4% NaOH treatment.	2007 [88]
Coir/polypropylene composite	2,4,6,8,10% NaOH	Higher alkali concentration (10%NaOH) deteriorates the fibre strength which decreased the mechanical properties of composite.	2009 [89]
Jute-epoxy	20% NaOH for 2 h	Alkali treatment enhanced mechanical properties of composite and	2012[90]

Sisal epoxy		treated jute composites give better results than treated sisal composites.	
Flax-PLA Polycarbonate	2,5,10% NaOH	Highest mechanical performance was observed for 2 % NaOH treated flax -PLA/PC composites.	2014 [91]
Durian skin fibre-PLA	4% sodium hydroxide (NaOH)	Treated DSF significantly enhanced the properties of PLA bio-composites as compared to untreated bio composite.	2014[92]
Jute-polypropylene	0.01%w KMnO4 in Oxalic acid Conc. of 1.0–10.0% w	Treatment of jute fabrics improved the thermal stability and mechanical of the composites	2012[93]
Sansevieria ehrenbergii polyester	6% BC in acetone ½ an hour,0.05 % KMnO4 in acetone for half an hour	The tensile strength was found to be highest for KMnO4-treated SE fiber-reinforced composite compared to other composites.	2014 [94]
Palmyra palm leaf stalk fiber–polyester	Pretreated with NaOH and agited benzoyl chloride for15 min	Tensile strength and modulus of the composite of the composite increased by 60% with the treated fiber.	2012 [95]
Areca fiber-epoxy	Pretreated with 6% NaOH and agitated with benzoyl chloride for 15 min	Treated fiber reinforced composite enhanced the impact properties of the composite.	2015 [96]

It is known that materials made of renewable resources like natural fibers reinforced in polymer matrix are called bio composites which is an interesting alternatives to synthetic fiber composites. Natural fibers such as jute, coir, sisal, pineapple, ramie, bamboo which have advantages of being economical to manufacture, ecofriendly, harmless to health, lightweight, high stiffness and specific strength provide a possible alternative to the synthetic fibers [102–104]. In due course of time it is thought that the natural fiber composites will replace synthetic fiber composites at least in some applications where a short life of the product is advantageous. In recent times the natural fiber composites have had huge growth in the automobile industry due to the advantages of renewability, reduced emission of pollutants and improved fuel efficiency because of reduced weight of the components [105, 11,106]. However besides the favorable properties natural fibers possess disadvantages like lack in thermal stability, strength degradation, water absorption and poor impact properties [106–108] .In order to improve their properties researchers turned their focus towards the study of effect on mechanical properties due to hybridization of natural fibers with synthetic fibers.

Hybrid composites consist of combination of two or more fibers reinforced in a single matrix. The possible combinations of hybrid composites include artificial–artificial, natural–artificial and natural–natural fiber types. Hybrid composite materials have wide applications in the field of engineering due to low cost, strength-to-weight ratio and ease of manufacturing, high specific modulus, and strength. Corrosion resistance and in many cases excellent thermal stability [109]. Research on various combinations of artificial fiber based hybrid composites revealed that they had certain advantages like high specific strength, high toughness, high impact resistance, etc. Owing to adverse effects on environment, high cost, etc. researchers started exploring natural fiber based hybrid composites. There are two possible varieties of natural fiber based hybrid composites which are obtained by combination of natural-natural fiber and natural- artificial fiber. Table-2.4 presents some natural fiber based hybrid composites studied by different researchers with different matrix material.

Table-2.4 Natural and artificial-natural hybrid composite.

SL no.	Natural fiber	Natural fiber	Artificial fiber	Matrix	Reference
1	Palmyra fiber waste		Glass	Polyester	[110]
2	Silk		Glass	Epoxy	[111]
3	Jute		Glass	Polyester	[112]
4	Wood flour	Kenaf		Polypropylene	[113]
5	Oil palm fiber (EFB)		Glass	Polyester	[114]
6	Kapok		Glass	Polyester	[115]
7	Sisal		Glass	Polypropylenes	[116]
8	Banana	Sisal		Polyester	[117]
9	Flax		Glass	Epoxy	[118]
10	Sisal	Silk		Polyester	[1]

2.5 ON WEAR MECHANISM AND ITS CLASSIFICATION

Wear is a process of removal of material from one or the other of two solid surfaces in the solid state contact, occurring when two solid surfaces are in sliding or rolling motion together according to Bhushan and Gupta [119]. The rate of removal is generally slow, but steady and continuous. Figure-2.7 shows the five main categories of wear and the specific wear mechanisms that occur in each category. Each specific mode of wear different from the next, and can be distinguished relatively easily.

Wear rate changes drastically in the range of 10^{-15} to $10^{-1}mm^3/Nm$, depending on operating conditions and material selections [120-126]. These results mean that design of operating conditions and selection of materials are the keys to controlling wear. As one way to meet these requirements, wear maps have been proposed for prediction of wear modes and wear rates [127-128]. Wear mechanisms are described by considering complex changes during friction. In general, wear does not take place

through a single wear mechanism, so understanding each wear mechanism in each mode of wear becomes important.

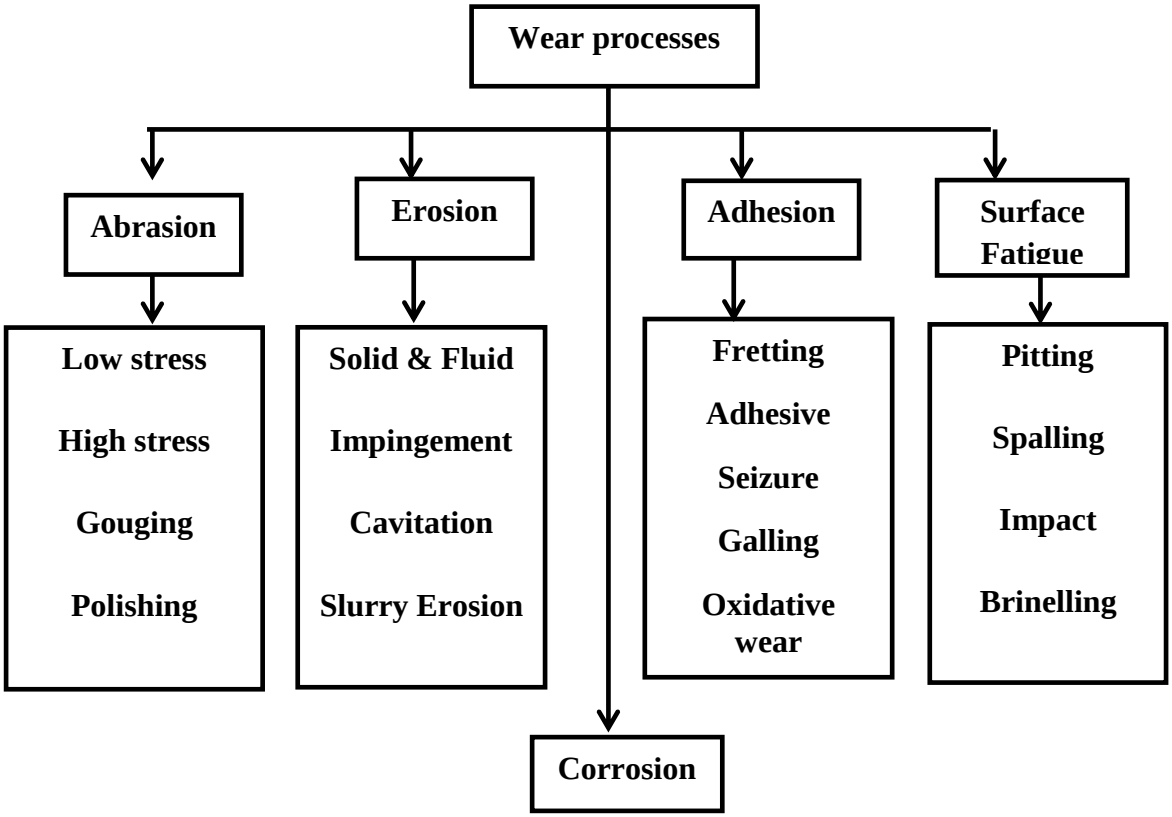

Figure-2.7 Flow chart of various wear mechanism

In order to focus on the wear mechanisms from the viewpoint of contact configurations, apparent and real contact conditions at the contact interface are introduced without particularizing about these contact configurations. Severity of contact, such as elastic contact or plastic contact, is the simplest and most direct way to think about wear mechanisms, and is a tribo system response determined by dynamic parameters, material parameters, and atmospheric parameters. The following four wear modes are generally recognized as fundamental and major ones [129].

2.5.1 Abrasive wear

If the contact interface between two surfaces has interlocking of an inclined or curved contact, ploughing takes place in sliding. As a result of ploughing, a certain volume of surface material is removed and an abrasive groove is formed on the weaker surface. This type of wear is called abrasive wear.

A common example of this problem is the wear of shovels on earth-moving machinery. It was originally thought that abrasive wear by grits or hard asperities closely resembled cutting by a series of machine tools or a file. It can be account for most failures in practice. Hard particles or asperities that cut or groove one of the rubbing surfaces produce abrasive wear. This hard material may be originated from one of the two rubbing surfaces. In sliding mechanisms, abrasion can arise from the existing asperities on one surface (if it is harder than the other), from the generation of wear fragments which are repeatedly deformed and hence get work hardened for oxidized until they became harder than either or both of the sliding surfaces, or from the adventitious entry of hard particles, such as dirt from outside the system. The way the grits pass over the worn surface determines the nature of abrasive wear.

The literature denotes two basic modes of abrasive wear such as two-body and three-body abrasive wear. In two-body abrasive condition; one surface is harder than the other rubbing surface. Hard asperities or rigidly held grits pass over the surface like a cutting tool is shown in figure-2.8(a). In three-body abrasive condition, generally a small particle of grit or abrasive, lodges between the two softer rubbing surfaces, abrades one or both of these surfaces is shown in figure-2.8(b). It was found that three body abrasive wear is ten times slower than two-body wear.

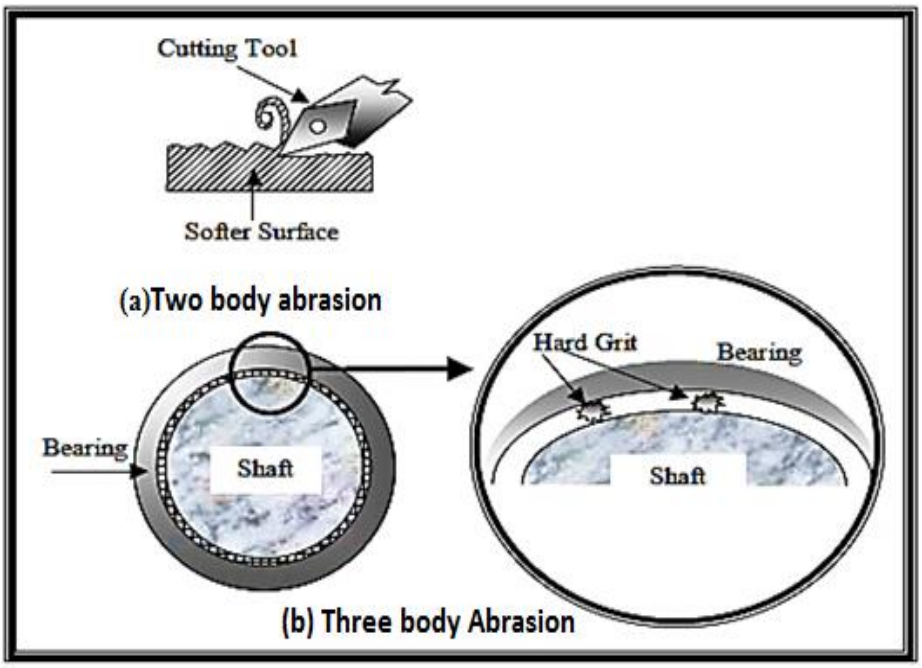

Figure-2.8 Schematic of abrasive wear phenomena [130]

2.5.2 Adhesive wear

Adhesive wear is a very serious form of wear characterized by high wear rates and a large unstable friction coefficient. It is also called galling and scuffing where interfacial adhesive junctions lock together as two surfaces slide across each other under pressure. Sliding contacts can rapidly be destroyed by adhesive wear and, in extreme cases, sliding motion may be prevented by very large coefficients of friction or seizure is shown in figure-2.9.

Most solids will adhere on contact with another solid to some extent provided certain conditions are satisfied. Adhesion between two objects casually placed together is not observed because intervening contaminant layers of oxygen, water and oil are generally present. The earth's atmosphere and terrestrial organic matter provide layers of surface contaminant on objects which suppress very effectively any adhesion between solids. Adhesion is also reduced with increasing surface roughness or hardness of the contacting bodies. Actual observation of adhesion became possible after the development of high vacuum systems which allowed surfaces free of contaminants to be prepared. Adhesion and sliding experiments performed under high vacuum showed a totally different tribological behavior of many common materials from that observed in open air.

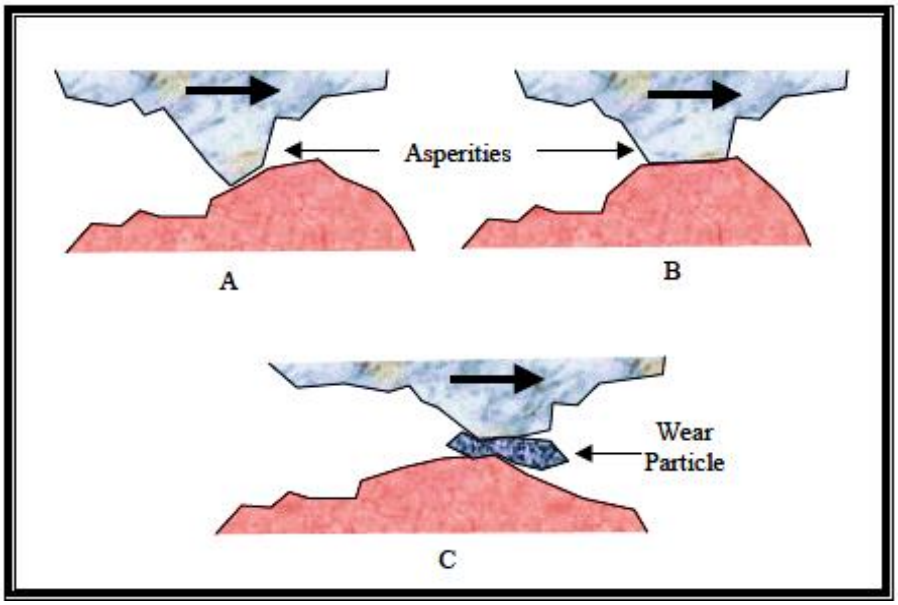

Figure-2.9 Schematic of generation of a wear particle as a result of adhesive wear process [130]

2.5.3 Erosive wear

The term 'erosive wear' refers to an unspecified number of wear mechanisms which occur when relative small particles impact against mechanical components. This definition is empirical by nature and relates more to practical considerations than to any fundamental understanding of wear.

Erosive wear is caused as a result of solid or small drops of liquid particles or gas impact against the surface of an object. The typical examples of solid particles erosive wear occurs in a wide variety of machinery and the damage to gas turbine blades when an aircraft flies through dust clouds, and the wear of pump impellers in mineral slurry processing systems. Examples include the ingestion of sand and erosion of jet engines and of helicopter blades.

Solid particle erosion is a result of the impact of a solid particle A, with the solid surface B, resulting in part of the surface B been removed is shown in Figure-2.10. The solid particles or liquid drops significantly contingent on the material properties and erosion process, such as impact velocity, impact angle and particle size. Angle of impingement and movement of particle stream have significantly effect on the rate of material removal. In common superior mechanical strength of a material does not guarantee better wear resistance, hence it is required a meticulous study of material characteristics for minimization of wear. The properties of the eroding particle are also recognized as a relevant parameter in the control of this type of wear.

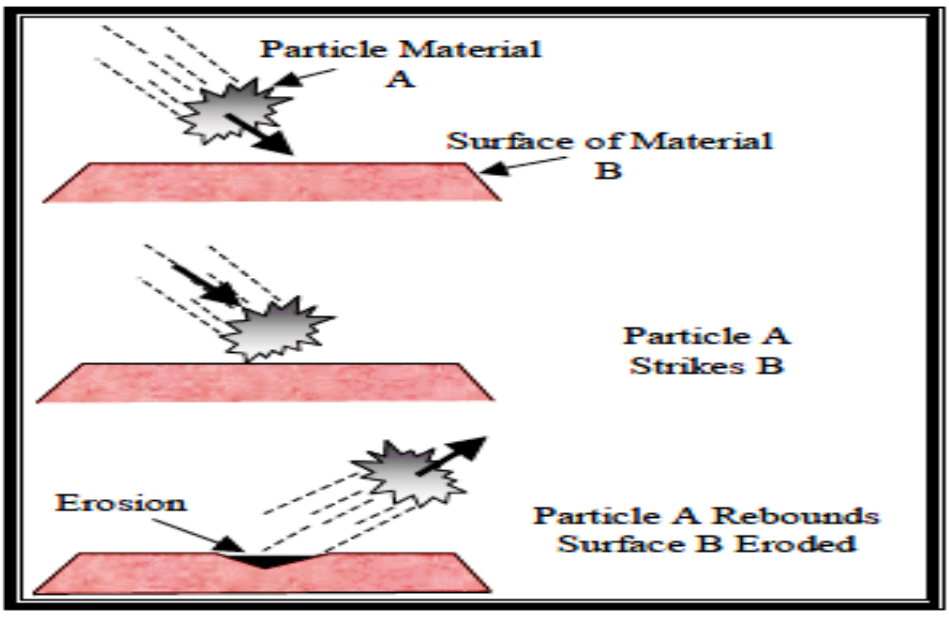

Figure-2.10 Schematic representations of the erosive wear mechanism [130]

2.5.4 Surface fatigue wear

When two surfaces slide across each other, the maximum shear stress lies some distance below the surface, causing micro cracks, which lead to failure of the component. These cracks initiate from the point where the shear stress is maximum and propagate to the surface as shown in Figure-2.11.

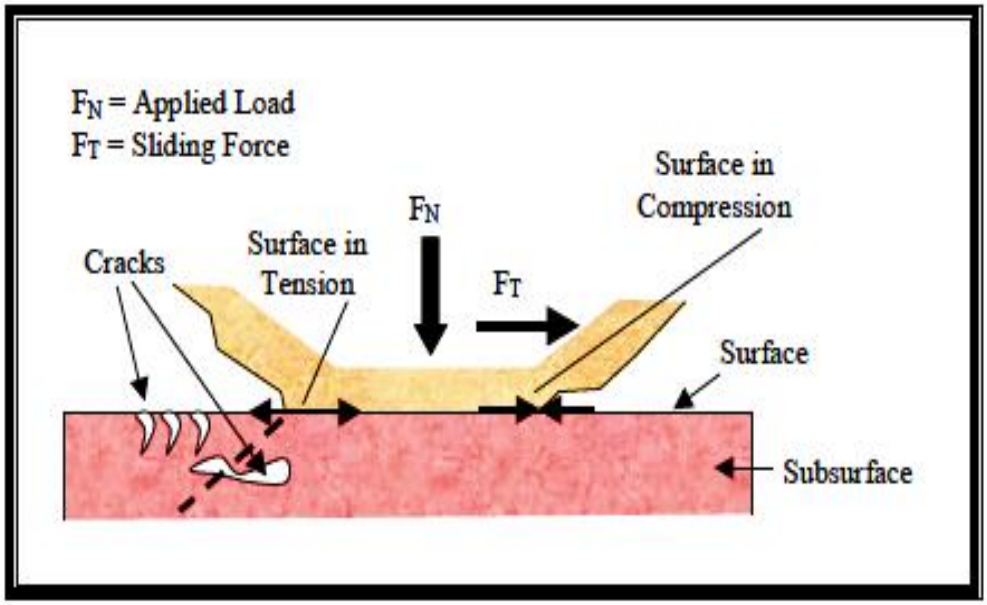

Figure-2.11 Schematic of fatigue wear, due to the formation of surface and subsurface cracks [130].

2.5.5 Corrosive wear

In corrosive wear, tribochemical reaction produces a reaction layer on the surface. At the same time, such layer is removed by friction is shown in figure-2.12. Therefore, relative growth rate and removal rate determine the wear rate of the reaction layers and, as a result, of the bulk material. Therefore, models of the reaction layer growth and those of the layer removal become very important.

Typical examples of corrosive wear can be found in situations when overly reactive E.P. additives are used in oil (condition sometimes dubbed as 'lubricated wear' [131] or when methanol, used as a fuel in engines, is contaminated with water and the engine experiences a rapid wear [132]. Another example of corrosive wear, extensively studied in laboratory conditions, is that of cast iron in the presence of

sulphuric acid [133]. The corrosivity of sulphuric acid is very sensitive to the water content and increases with acid strength until there is less water than acid. Pure or almost pure acid is only weakly corrosive and has been used as a lubricant for chlorine compressors where oils might cause an explosion [134].

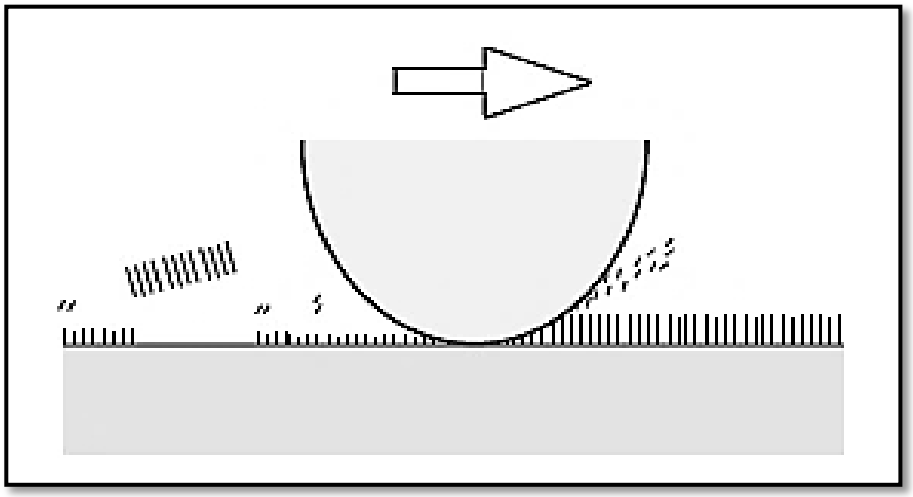

Figure-2.12 Schematic of corrosive wear, due to the formation of surface and subsurface cracks.

After reviewing the existing literature available on natural fiber composites, efforts are put to understand the basic needs of the growing composite industry. The conclusions drawn from this is that, the success of combining natural fiber with polymer matrices results in the improvement of mechanical properties of the composites compared with the matrix materials. These fillers are cheap and nontoxic, can be obtained from renewable sources, and are easily recyclable. Moreover, despite their low strength, they can lead to composites with high specific strengths because of their low density.

Thus the priority of this work is to prepare polymer matrix composites (PMCs) with luffa cylindrica fiber as reinforcement material. In the present work it is proposed to prepare luffa cylindrica reinforced epoxy composite. To improve the interfacial strength between the luffa cylindrica and the matrix, it is planned to modify the surface of the fiber by various chemical methods. The composite will then be subjected to different weathering condition like distilled, saline and subzero condition. The fiber characterization will be done by Fourier Transform Infrared (FTIR) spectroscopy, X-

Ray Diffraction (XRD), Energy-dispersive X-ray spectroscopy (EDX), Thermo gravimetric analysis (TGA) before and after the treatment of the fibers. The mechanical properties of the composite will be evaluated along with moisture absorption characteristics for both treated and untreated fiber reinforced composites. The potential of untreated and treated luffa cylindrica fiber reinforced composite for tribological application will be investigated by performing solid particle erosion test as per ASTM standards.

Also it is planned to prepare hybrid composite with luffa cylindrica and glass fiber with different stacking sequence. The mechanical and tribological properties of hybrid composite will be studied as per the ASTM standard.

Chapter 3

Mechanical Characterization of Luffa cylindrica fiber reinforced epoxy composite

3.1 INTRODUCTION

Recently studies on the use of natural fibres as replacement to man-made fibres in FRP composite are increasing rapidly and opening up new opportunities for various industrial applications. Natural fibre reinforced polymer composites are found to be effectively utilised for polymer composites in various application due their attractive features of light weight, high specific modulus, renewability, and biodegradability and potentially low cost over traditional glass fibers [135]. It is known that various elements that any natural fiber contains are cellulose, hemicelluloses, lignin, pectin, waxes and water soluble substances. Generally the elementary units of cellulose macromolecules are an hydro-d-glucose which contains three hydroxyls (–OH) [136]. These hydroxyls form the hydrogen bonds inside the macromolecule itself (intramolecular) and between the other cellulose macromolecules (intermolecular) as well. Therefore, all vegetable fibers are hydrophilic in nature. Hence the main bottle necks in the broad use of natural fibers in various polymer matrixes are poor compatibility with hydrophobic polymer matrix and the inherent high moisture absorption which brings about dimensional instability that leads to reduction in the mechanical properties of the composites [137]. However in order to overcome this problem, chemical treatment has been considered as a good technique to reduce the hydroxyl group in the natural fibres, improve cellulose exposure of the fiber, improve surface roughness of fibre for better fibre matrix adhesion and mechanical strength, improve thermal stability and improves crystallinity of fibre by delignification etc. Different chemical treatments such as alkali (NaOH), Peroxide, isocyanate, acrylation and acrylonitrile grafting, benzoylation, permanganate treatment, acetone treatment, acetylation, silane treatment etc. are reported by different researchers [14, 75,138-139].

Yan et al. [140] studied the effect alkali treatment on the mechanical properties of flax, linen and bamboo fabric reinforced epoxy composite. They observed that the fiber/epoxy interfacial adhesion was improved and the tensile and flexural strength of flax epoxy composite was increased by 21.9% and 16.1% compared to untreated one due to the surface modification of fiber by 5% cons alkali treatment for 30 min. In another paper, Yan et al.[141] reported that alkali treatment (5% NaOH for 30 min) enhances the compressive strength and compressive modulus, in-plane shear strength

and shear modulus, and specific impact strength of both flax-epoxy and linen-epoxy composites.

Ray et al. [142] studied the effect of alkali treated jute fibers on composite properties. They treated the jute fiber with 5% aqueous NaOH solution from 2 h. up to 8 h. and observed that the strength properties of the composite are enhanced significantly due to chemical modification of fiber surface.

Kushwaha et al. [143] investigated the mechanical of properties of alkali treated bamboo-fiber reinforced epoxy and polyester resin composite. They treated the bamboo fiber with 1, 2, 5, 10, 15, 20, and 25% concentration of NaOH in distilled water for 30 min at 20°C. They observed that the maximum improvement in mechanical properties of the composite is achieved with 5% NaOH treated fiber.

Paul et al. [81] treated sisal fibers in different concentration of permanganate (0.033, 0.0625 and 0.125%) in acetone for 1 min. They observed that as a result of permanganate treatment, the hydrophilic tendency of the fibers was reduced, and thus, the water absorption capacity of the composite decreases.

Zaman et al. [97] investigated the role of potassium permanganate and urea on the Improvement of the mechanical properties of jute polypropylene composites. They treated the jute fabric with potassium permanganate (KMnO4) solution in acetone of different concentrations (0.02, 0.03, 0.05, and 0.5 %) with different soaking times (1, 2, 3, and 5 min) before the composite fabrication. They observed that the maximum improvement in mechanical properties of the composite is achieved with jute fabrics treated with 0.03 % KMnO4. Again they treated 0.03 % KMnO4 treated jute fabrics with HEMA (15%) solution along with urea (1%) and observed promising improvement in mechanical properties of the composites.

Wang et al. [144] while working with flax fiber found that the interfacial adhesion of flax fiber and polyethylene (PE) matrix composite increases by treating the fiber with benzoyl chloride solution for 15 minutes.

Nair et al. [145] investigated the effects of fiber loading, fiber length, fiber orientation and fiber modification on the dynamic mechanical properties of the

polystyrene composites reinforced with short sisal fibers. They treated the fiber with benzoylation, polystyrene maleic anhydride coating and acetylation and observed that the treatments improve the fiber-matrix adhesion and subsequent increases in dynamic mechanical properties of the composite compared to untreated one.

It is clear from the above research findings that the chemical treatment of fiber aimed at improving the adhesion between the fiber surface and the polymer matrix by modifying the fiber surface and the fiber strength. It also reduces the water absorption capacity of the fiber and helps in improving the mechanical properties of the related composite. Out of the available chemical treatments, for the present case to have a good bonding between the fiber and the resin matrix luffa cylindrica have been treated with alkali, benzoyl-chloride and potassium permanganate (KMnO4). The subsequent section elaborates separately the treatment of the fiber surface by these chemical methods, Results of fiber modification were analyzed through XRD, FTIR, SEM,EDX and TGA and the effect of fiber treatment on mechanical properties of the composite were also studied and reported.

3.2 CHEMICAL MODIFICATION OF LUFFA FIBER

3.2.1 Methods of chemical modifications

Out of available methods for fiber modifications we have considered only alkaline, benzoyl chloride and permanganate treatment.

3.2.1.1 Alkaline treatment

For alkali treatment, the luffa cylindrica fiber were soaked in a 5% NaOH solution at room temperature maintaining a liquor ratio of 15:1. Prior to alkali treatment, the luffa fibers were washed thoroughly with fresh water to remove the any foreign matter/particle that adhere the fiber surface. The luffa cylindrica fiber mats were then dried in sun light. After complete drying the fibers were kept immersed in the alkali solution for 4 hours. Washing of fibers were then carried for several times with fresh water to remove any NaOH sticking to the fiber surface, neutralized with dilute acetic acid and finally washed again with distilled water. A final pH of 7 was maintained. The fibers were then allowed to dried at room temperature for 48 hours

followed by oven drying at 100°C for 6 hours. The alkali reaction between Luffa cylindrica fiber and NaOH is as follows:

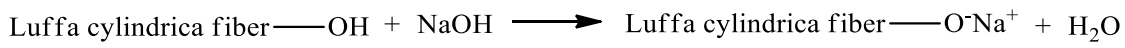

3.2.1.2 Benzoyl chloride treatment

In order to activate the hydroxyl groups of the cellulose and lignin, the fibers were treated with alkali initially, i.e., suspended in 10% NaOH for 1 hour and then with benzoyl chloride solution for 15 min with continuous stirring. Then the solution was drained out and the isolated fibers were soaked in ethanol for 1 hour in order to remove the benzoyl chloride. Finally, the fibers were washed properly with fresh water and dried in atmospheric air followed by oven drying at 70°C for 6 hours.

3.2.1.3 Permanganate treatment.

The pre-NaOH (5% cons) treated fibers were soaked in 0.05% concentration of the KMnO4 solution with acetone for 1 min. Then the KMnO4 solution was drained out, and the fibers were dried in atmospheric air.

3.3. PHYSICAL CHARACTERIZATION OF LUFFA CYLINDRICA FIBER

3.3.1 SEM analysis of untreated and treated fibers

The morphology of the untreated and treated fiber surfaces has been studied using Field emission scanning electron microscope (FESEM) Nova NANO SEM 450. The sample surfaces were gold coated to make them conductive prior to SEM observation. It is well established that the cellulose chains of natural fiber are strongly bounded by chemical constituents, lignin, and hemicellulose, resulting in the formation of multi-cellular fiber [146]. Figures-3.1-3.4 show the SEM micrographs of untreated, alkali, benzoyl chloride and KMnO4 treated fiber. The SEM micrographs of untreated luffa fiber shown in Figure-3.2 indicate the presence of amorphous waxy cuticle layer on the surface and packed fiber structure together. Presence of waxy/gummy substance contributed to poor fiber–matrix adhesion [147]. Figure-3.2-3.4 shows the micrographs

of the fiber surface treated with alkali, benzoyl chloride, and KMnO4 treated fiber. All the micrographs, indicates the removal of gummy and waxy substance and appearance of clean, smooth surface due to the chemical modification compared with untreated fiber (Figure-3.1). It is also seen that due to partial removal of gummy cementing substances, the packed structure splits and fibrillation of the fiber structure took places which increase the surface area of the fiber [86]. Similar types of observation are also reported by several researchers for other treated fibers such as sisal, flax, and etc. [41,148-150]. From the figures, it is also observed that the chemical treatment also reduces the fiber diameter.

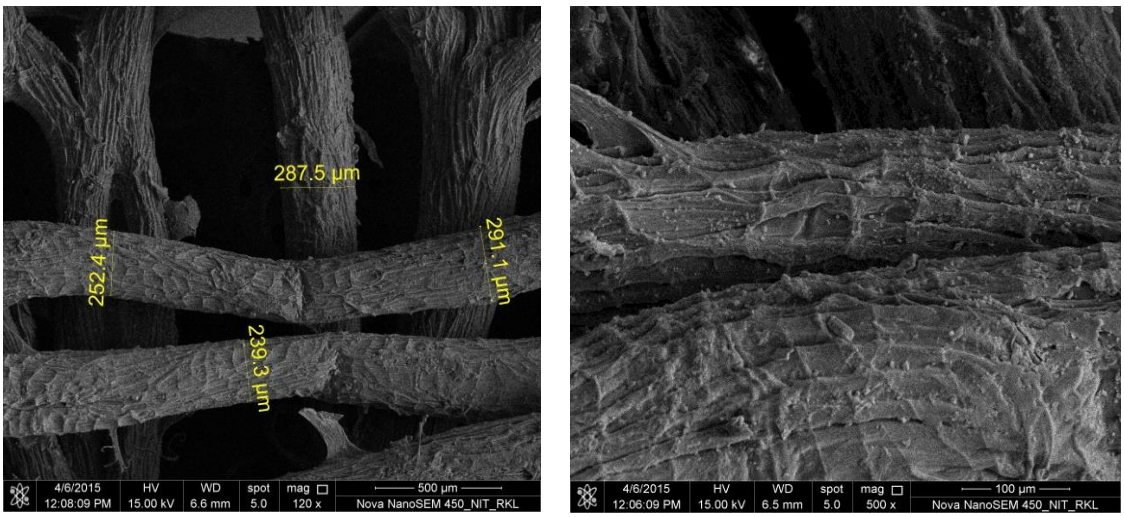

(a) (b)

Figure-3.1. SEM micrographs of untreated luffa cylindrica fiber at (a) 120X, (b) 500 X.

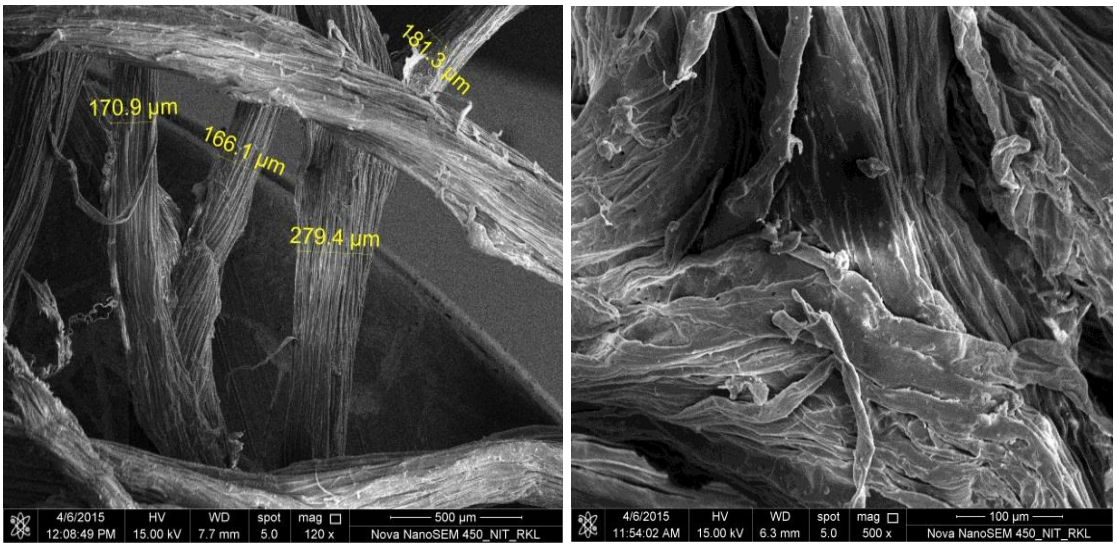

(a) (b)

Figure-3.2. SEM micrographs of alkali treated luffa cylindrica fiber at (a) 120X, (b) 500 X.

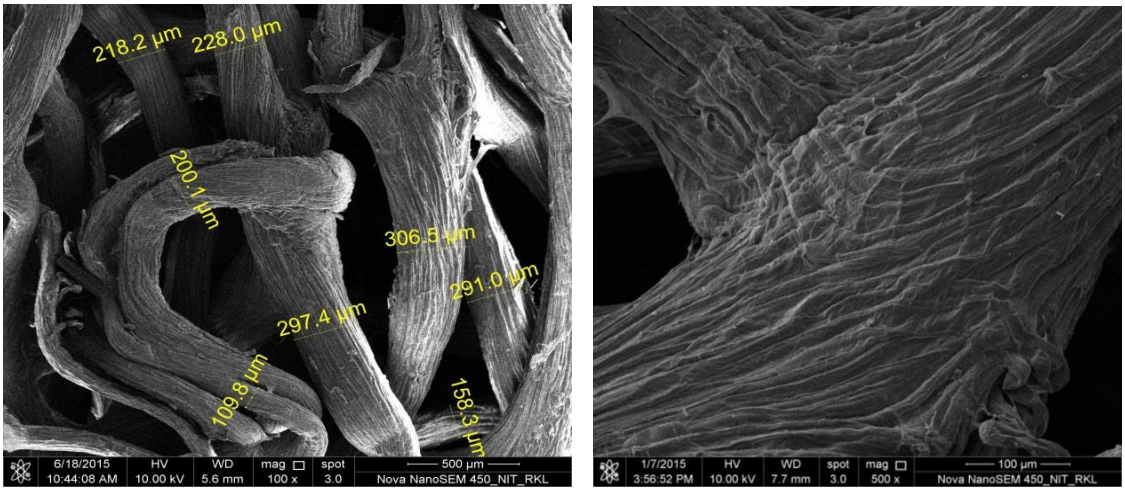

(a) **(b)**

Figure-3.3. SEM micrographs of benzoyl chloride treated luffa cylindrica fiber at (a) 120X, (b) 500 X.

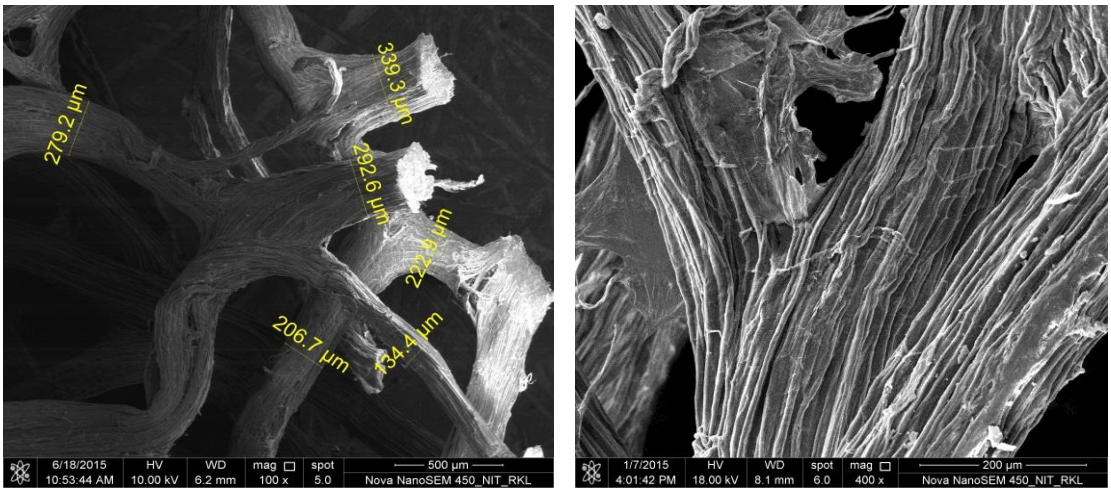

(a) (b)

Figure-3.4. SEM micrographs of KMnO4 treated luffa cylindrica fiber at (a) 120X, (b) 500 X.

3.3.2 EDX analysis

Energy dispersive spectrometer (EDX) analyser (NANO SEM 450) was used to determine the elemental analysis or chemical characterization of the luffa cylindrica fibres.

EDX spectrums of the untreated and treated luffa cylindrica fiber are shown in Figures-3.5 (a-d) and analyses are presented in Table-3.1. The EDX of the untreated fiber reveals that the surface contains C, O, N, Ca, Zr, Na, S, Cl, Cr, Ag, K, and Mg (Figure-3.5 a). Similar results were also reported by Dairo et al. [151]. EDX of treated fiber surfaces (Figure-3.5 (b-d)) reveals that some of the chemical elements were removed away due to treatments.

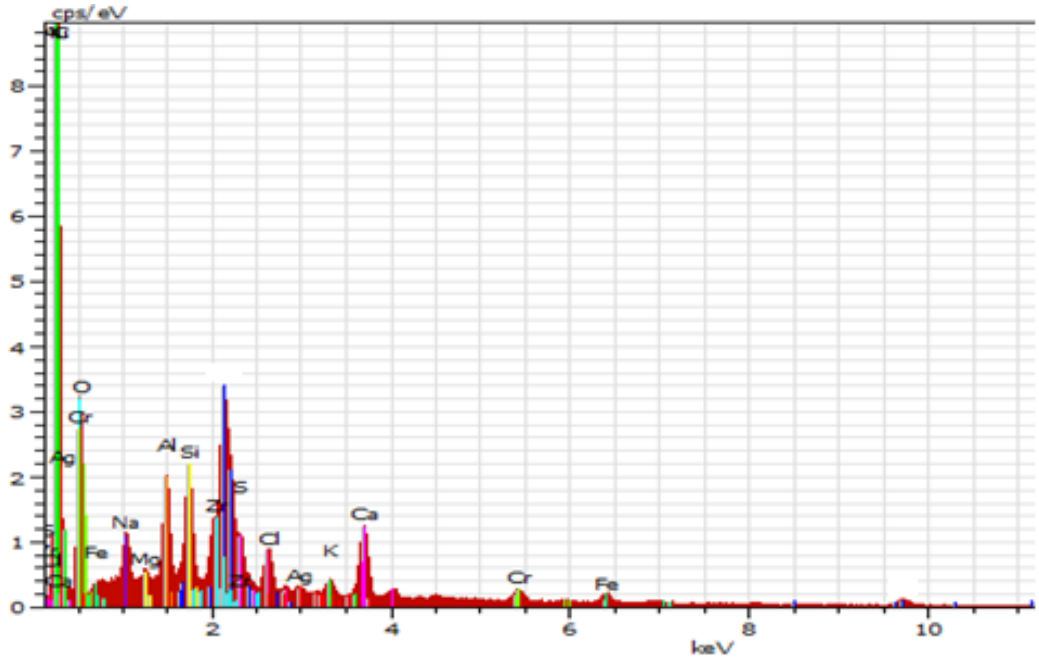

Figure-3.5 (a) EDX Spectra of untreated luffa cylindrica fiber.

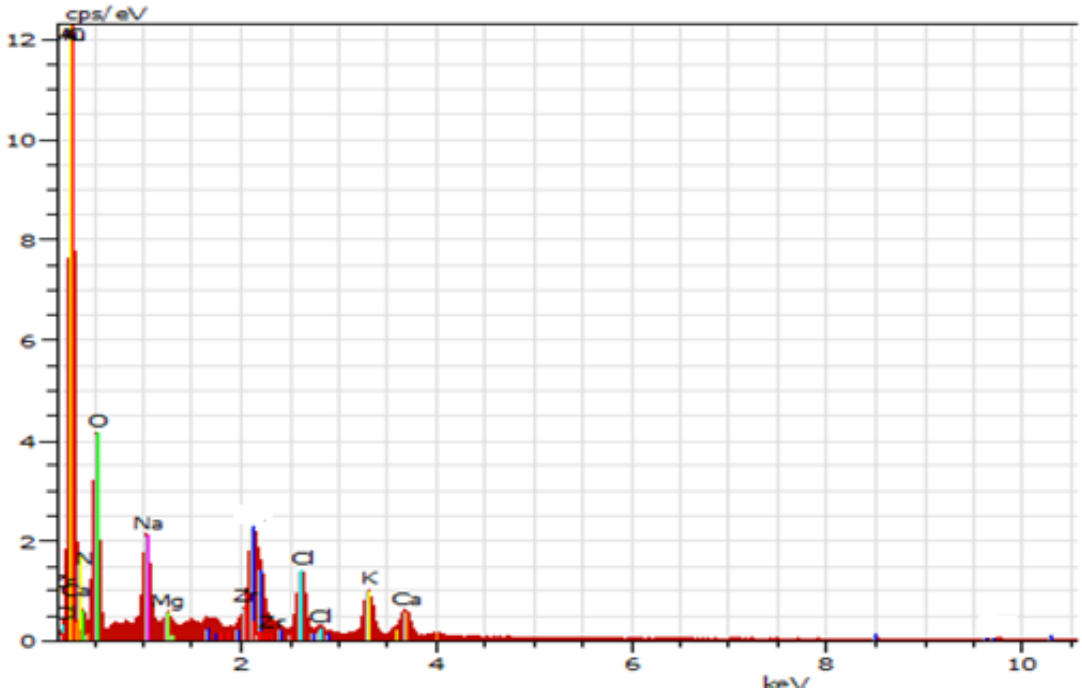

Figure-3.5 (b) EDX Spectra of alkali treated luffa cylindrica fiber.

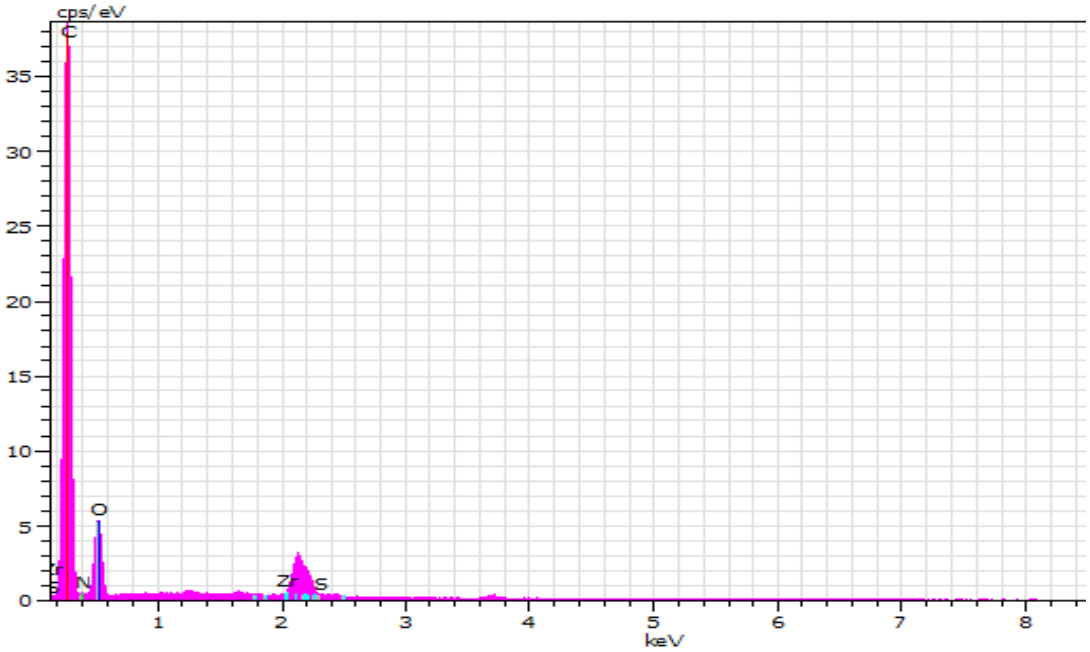

Figure-3.5(c) EDX Spectra of benzoyl chloride treated luffa cylindrica fiber.

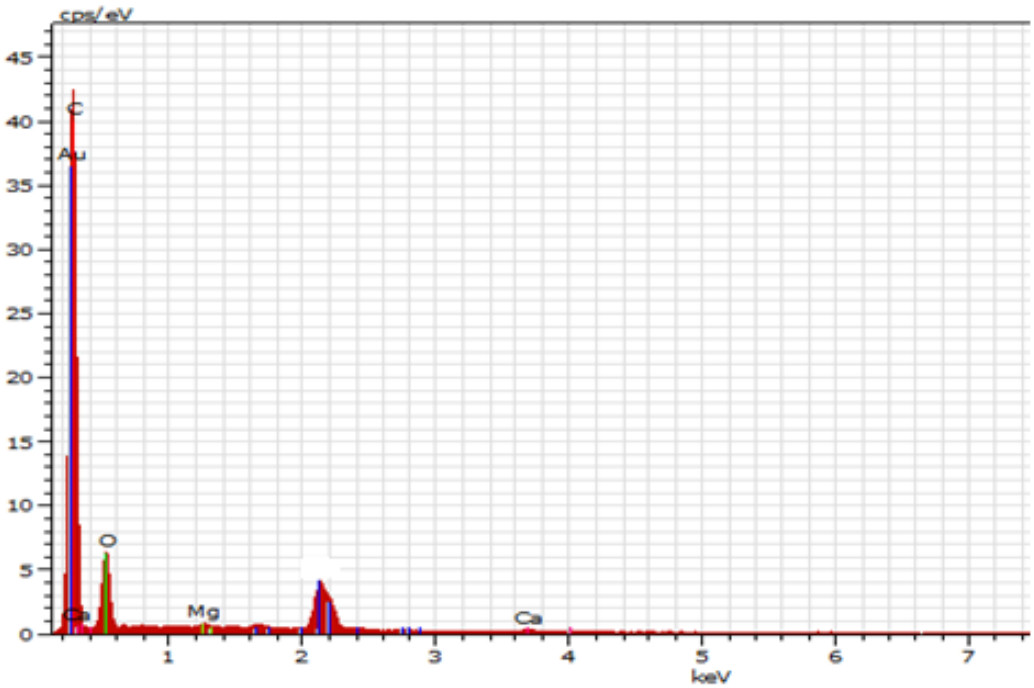

Figure-3.5 (d) EDX Spectra of KMnO4 treated luffa cylindrica fiber.

Table- 3.1 EDX Analysis of untreated and treated luffa cylindrica fiber.

Chemical element (Atomic %)	Untreated	Alkali treated	Benzolated	KMnO4 treated
C	66.51	57.33	65.73	60.94
O	25.20	27.16	30.79	26.59
N	0.00	10.02	2.47	7.43
Ca	2.29	0.72	0.61	0.00
Zr	0.70	0.08	0.00	2.54
Na	1.57	2.39	0.00	0.00
Fe	0.59	0.00	0.00	0.00
S	1.02	0.00	0.40	0.41
Cl	0.85	1.03	0.00	0.00
Cr	0.46	0.00	0.00	0.00
Ag	0.14	0.00	0.00	0.00
K	0.37	0.00	0.00	0.52
Mg	0.46	0.28	0.00	0.00
Mn	0.00	0.00	0.00	1.57

3.3.3 FTIR spectroscopy

FTIR spectroscopy was carried out to determine the functional group of both treated as well as untreated luffa fiber. FTIR measurement was performed using an IR-Prestige-21 spectrometer with scan rate 40 and range 4000 to 400 cm^{-1} wave number with a resolution of 0.5 cm^{-1}. KBr powder was used for making pallets for use in spectroscopic analysis.

The comparison graph of FTIR spectrum for luffa cylindrica fiber before and after chemical modification (alkali, benzoyl-chloride and KMnO4 treatment) is shown in figure-3.6 and possible band and assignments are presented in table-3.2. As pointed out by Khan et al. [152] the general characteristic features of the IR spectrum of the natural fiber are mainly due to α-cellulose, hemicelluloses and lignin. In comparison to the untreated luffa cylindrica, the alkali, benzoyl chloride and KMnO4 treated luffa cylindrica showed a reduction in absorption spectra due to dissolution of non-polar covalent compound like wax, fat etc. with the treated chemicals. The effect is more significant in case of Benzoyl Chloride treatment as this is a strong non-polar solvent which dissolves more non polar compound. The major functional group of luffa

cylindrica fiber remains same even after chemical modification. However reduction of peak intensity and small shifting is observed in many cases. The band 3464 cm-1 corresponds to H bonded O-H stretching [153] which is shifted to 3568 cm-1 for benzoyl chloride and KMnO4 treated fiber indicating participation of free hydroxyl group in these chemical reaction. The peak at 2922 cm-1 corresponds to saturated C-H stretching of methylene and methyl groups [153].The peak 2850.7cm-1 is present in untreated and chemical treated fibers corresponds to aldehyde C-H. Peak 2360cm-1 assigned to C-O stretching of acetyl or carboxylic acid which is shifted to 2358cm-1 for the case of benzoyl chloride and KMnO4 treated fiber. A peak at 1728 cm-1 is corresponding to the C=O stretching of carboxyl and acetyl group of hemicellulose shifted to 1732 for alkali, 1734 for both benzoyl chloride and KMnO4 treated fiber and reduction of peak intensity is observed may be due to removal of acetyl group present in hemicellulose. The peak at 1539 cm-1 is assigned to aromatic C=C is shifted to 1541 for both benzoyl chloride and KMnO4 Treated fiber. The peak around 1456 is assigned to CH3 deformation (asymmetric) in lignin. The band of medium intensity at 1192cm^{-1} Antisym bridge C-O stretching in acetyl xylene group present in untreated fiber shifted to 1193cm^{-1} for benzoyl chloride treatment, however it disappears in KMnO4 treated fiber. This may be due to removal of acetyl group present in hemicellulose [154]. The peak at 1047 cm-1 is assigned to aromatic C-H in plane deformation and C-O deformation [154] for primary alcohol in lignin are found higher intensity as compare to chemical treated fiber. The peak around 862 cm-1 represents as antisym out of phase ring which is shifted to 866, 862, 873cm-1 for alkali, benzolated, and KMnO4 treated fiber respectively.

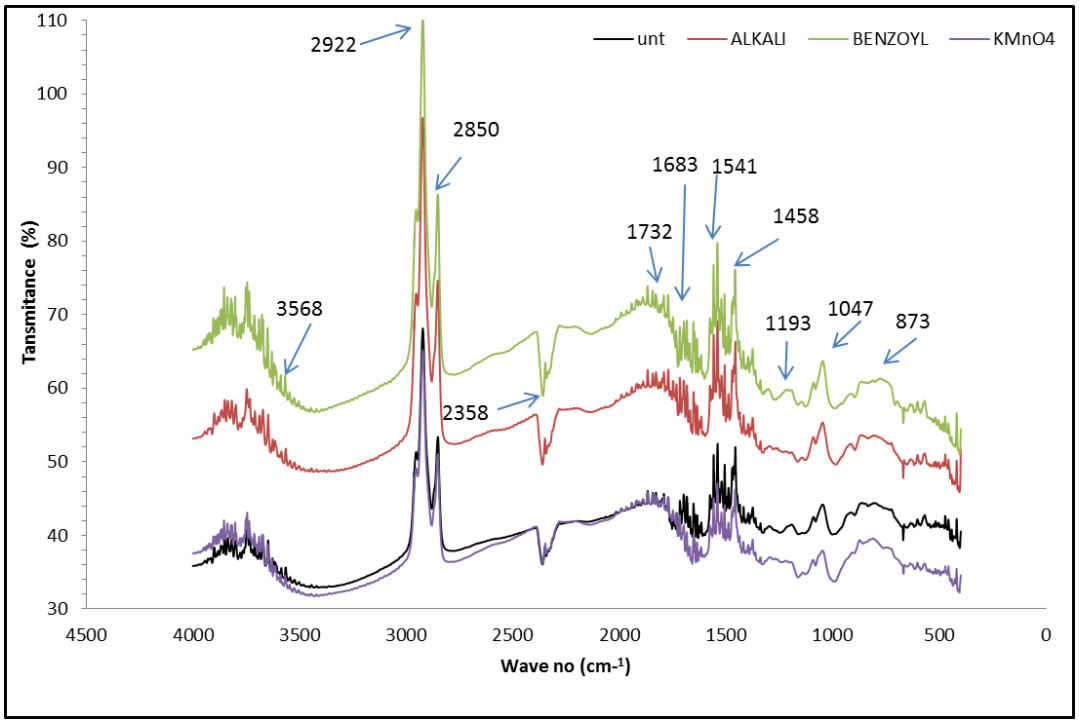

Figure-3.6 FTIR spectra of both treated and untreated LC fiber.

Table-3.2. FTIR Spectral data of untreated and treated luffa fiber

Wave no (cm-1)				**Possible assignments**
Untreated	Alkali	Benzoyl	KMnO4	
3564	3564	3568	3568	O-H stretching of α cellulose
2922	2922	2922	2922	Saturated C-H stretching
2850	2850	2850	2850	Aldehyde C-H
2360	2360	2358	2358	C-O stretching of acetyl or Carboxylic acid
1728	1732	1734	1734	Carboxylic acid C=O Stretching.
1681	1683	1683	1683	Amide C=O
1647	1652	1652	1652	Alkene C=C
1539	1539	1541	1541	aromatic C=C
1456	1456	1456	1456	CH3 deformation
1192	-	1193	-	Antisym bridge C-OR-C stretching
1047	1047	1047	1047	C-H ,C-O deformation
862	866	862	873	Antisym out of phage Ring

3.3.4 X-ray Diffraction

X-ray diffraction was carried out to evaluate the crystallographic structure of semi-crystalline materials such Luffa cylindrica fiber and to ascertain the change in crystalline character of material after chemical treatments. A Multipurpose X-ray diffraction Regaku Ultima IV employing CuKα (λ = 1.54) radiation and a graphite monochromator with a current of 40 mA and a voltage of 40 mV was used with a diffraction intensity in the range of 5 to 45^0 (2θ-angle range). The X-ray diffractograms of untreated, alkali treated, benzoyl-chloride treated and KMnO4 treated luffa cylindrica are present in figure-3.7. The cell walls of the plant fibers mainly consist of cellulose, hemicellulose, and lignin. Cellulose consists of both amorphous and crystalline regions, although lignin and hemicellulose are amorphous. It is observed that the major crystalline peak of each profile occurred at around 2θ value ranging from 22.5^0 to 22.75^0, which represents the cellulose crystallographic plane (002) [155] whereas the amorphous peak occurred at 2θ value ranging from 14.95^0 to 16.45^0 . The X-ray diffractograms show that the intensity of the (002) crystallographic plane and amorphous plane (am) were increased significantly with chemical modification of fiber and alkali treated fiber showing the maximum intensity.

The fiber Crystallinity indexes (I_c) of the treated and untreated fibers were calculated by Segal or peak height method [156-156a]:

$$I_c = \frac{I_{002} - I_{am}}{I_{002}} \tag{3.1}$$

Percentage Crystallinity (C_r %) (157) of the treated and untreated fibers were calculated by using equation:

$$Cr(\%) = \frac{I_{002}}{I_{002} + I_{am}} \times 100 \tag{3.2}$$

Where 'I_{002}' is the maximum intensity of diffraction of the (002) lattice peak at a 2θ angle of between 22.5^0 to 22.75^0, and 'I_{am}' is the intensity of diffraction of the amorphous material, which is taken at a 2θ angle between 14.95^0 to 16.45^0 where the intensity is at a minimum [158].

The results so obtained are summarized in Table-3.3. The crystallinity index and crystalline percentage of Luffa cylindrica fiber is found to increase upon chemical treatments. The highest crystallinity index was observed for the alkali treated fiber followed by benzoyl chloride and KMnO4 treated fiber. This might have happened due to better packing and stress relaxation of cellulose as a result of the removal of amorphous constituents and pectin from the fiber [85,159]. Ray et al. [83] also reported similar observation while they worked with NaOH treatment of jute fiber.

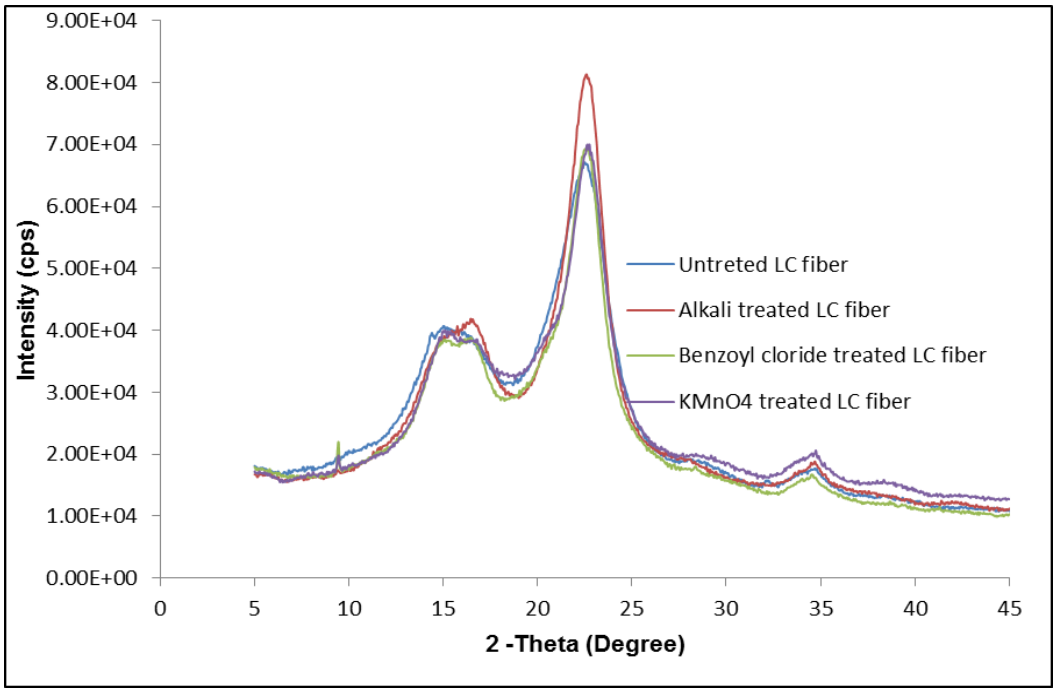

Figure-3.7 XRD analysis of untreated and treated LC fiber.

Table-3.3. Variation of crystalline index and crystalline percentage untreated and treated luffa fiber.

Fiber treatment	Maximum intensity Iam	Angle(2 Θ) at Iam	Maximum intensity I_{002}	Angle(2 Θ) at I_{002}	Crystallinity Index(CI)	Percentage of crystallinity
Untreated	40678	15	67120	22.5	0.39	62.26
Alkali	40985	16.05	81300	22.6	0.49	66.48
Benzoylated	38836	16.45	69312	22.55	0.44	64.08
KMnO4	39696	14.95	70003	22.75	0.43	63.81

3.3.5 Thermo Gravimetric Analysis (TGA)

Thermo gravimetric analysis was carried out on luffa cylindrica epoxy composites (both treated and untreated) using Netzsch, Germany, STA449C/4/MFC/G apparatus, applying heating rate of 100°C/min up to 600°C. Thermal stability of natural fiber reinforced composite depends upon the chemical constituents (cellulose, hemicellulose, and lignin) of fiber. The thermal degradation of lignin, hemicellulose, and cellulose take place over a range of temperature i.e.160–900°C, 220–315°C and 315–400°C respectively. The process is irreversible. Lignin decomposed at a slower rate compared to the other components of lignocellulose [160]. The TGA curve and weight loss at different temperatures of untreated and treated fibers are shown in figure-3.8 and table-3.4. It is evident from both the figure and table that thermal stability chemical treated fibers are higher than the untreated fiber. KMnO4 treated fiber shows the better thermal stability. The first step degradation was completed below 100° C with a weight loss of 7.32-9.7% for may be due to evaporation of moisture present in the fibers [145]. The next step of degradation starts at 264-278°C may be due to breakdown of hemicellulose, glycosidic linkage of cellulose [161]. The maximum rate of decomposition happens nearly about 313°C for untreated, however, it is shifted to 337,342, and 360°C for alkali, benzoyl chloride and KMnO4 treated fiber. The thermal decomposition of untreated and alkali treated fiber is completed at 417°C. However, it is shifted to 429 and 435°C for KMnO4 and benzoyl chloride treated fiber. Overall the decomposition of the cellulosic substances shifts slightly to higher temperatures for the treated fibers. The increase in thermal stability for cellulose material may be due to ordering of cellulose chains leading to higher thermal stability [162]. However, a study on sisal fiber has revealed reduction of thermal stability with alkali treatment (possibly due to high fibrillation) but increase with benzoyl peroxide treatment [163].

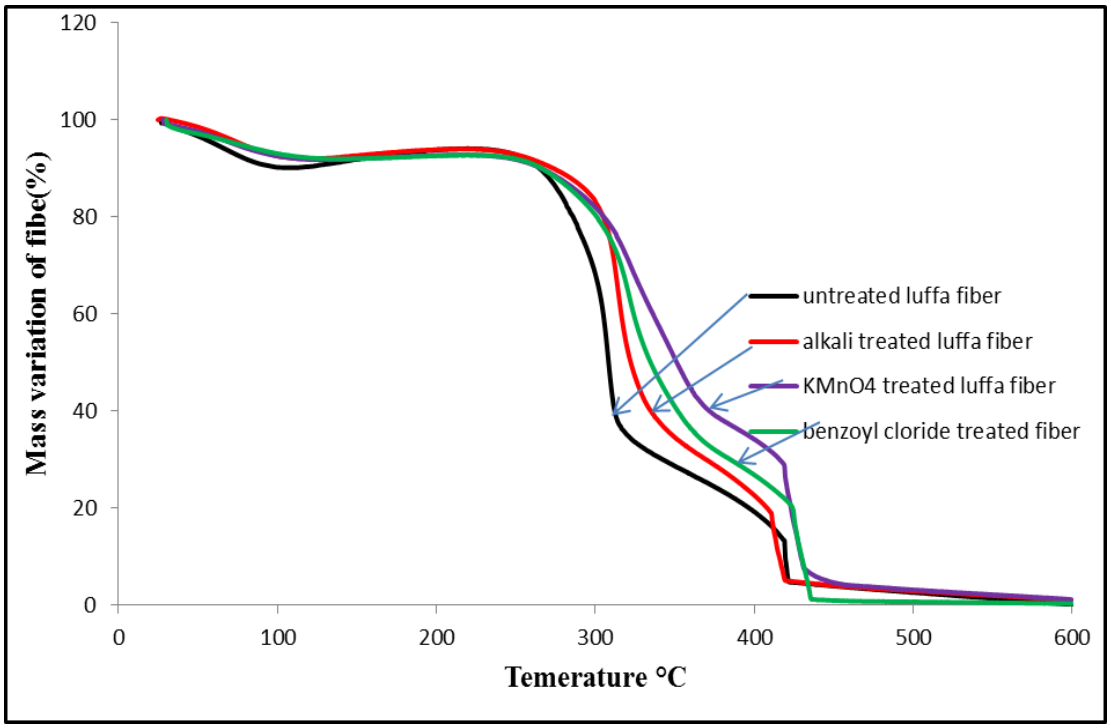

Figure-3.8 Thermo gravimetric analysis of both treated and untreated LC fiber.

Table-3.4. Percentage weight loss of both untreated and treated LC fiber at different temperatures.

Temperature(°C)	Untreated	Alkali treated	Benzoylated	KMnO4 treated
100	9.77	7.43	6.91	7.44
200	6.19	6.12	7.41	7.30
300	31.81	17.30	19.40	17.80
400	80.81	77.31	73.06	65.70
500	97.38	97.06	99.31	96.82

3.4 COMPOSITE FABRICATION

For preparation of composite the following materials have been used;

1. Epoxy

2. Hardener

3 Luffa cylindrica fiber

3.4.1 Preparation of Luffa Cylindrica

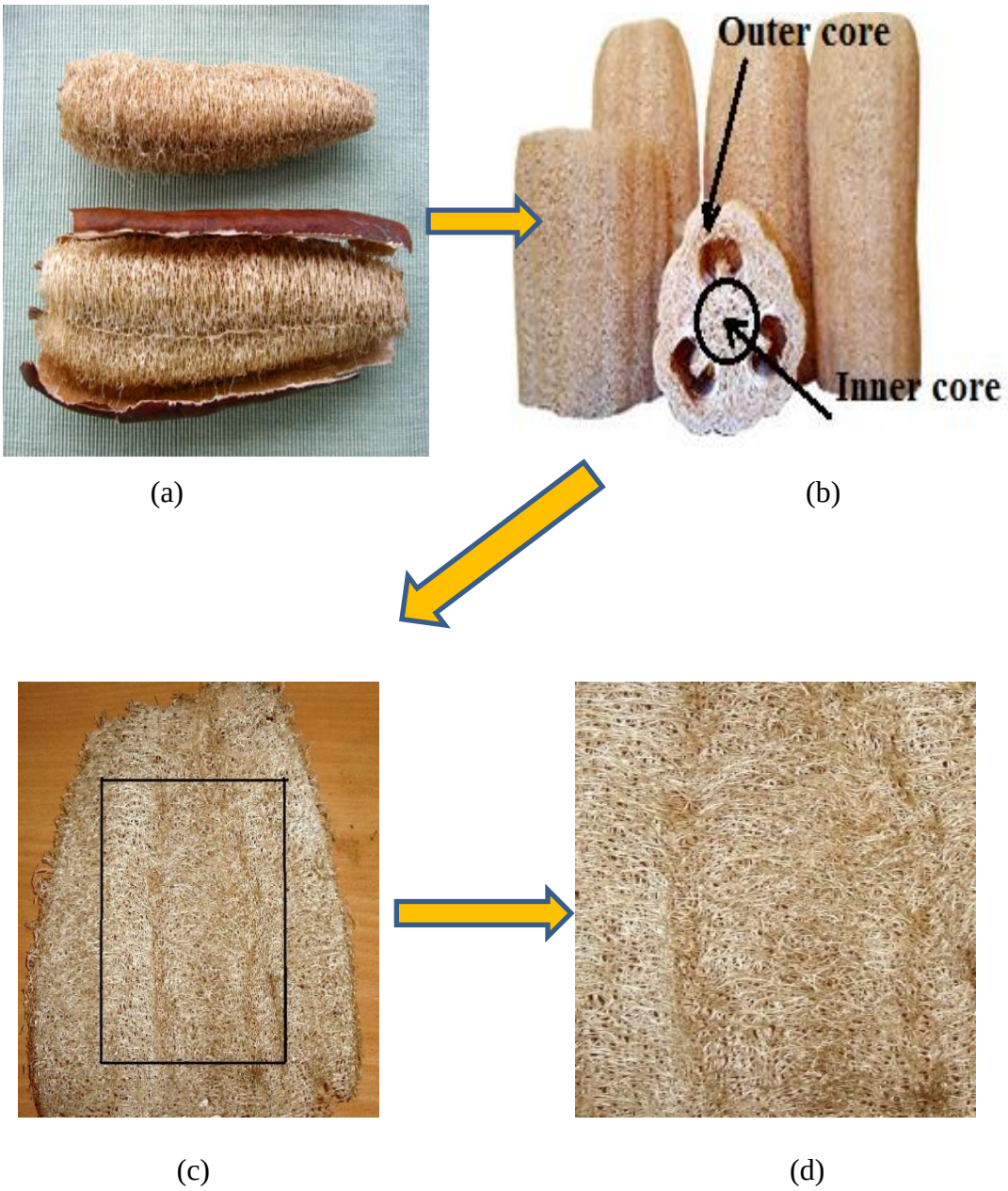

Figure-3.9. (a) Dried luffa fruit with partial removed of outer layer (b) Sponge guard with hollow micro channels (c) Outer core open as mat (d) The rectangular portion used for making composite.

Luffa cylindrica fiber used in this present study was collected locally in Rourkela, Odisha, India. The outer layer (bark) and seeds of luffa fruit were removed carefully as shown in figure-3.9 (a). Figure-3.9 (b) shows the sponge guard and the hollow micro channels. Then the luffa fibers were cut carefully to separate the outer core from inercore (central core). Only the outer core (figure-3.9 (c)) was used in this study. The outer core of luffa fibers were rolled to make mat like structure after washing them thoroughly with distilled water and air dried for 72h at room temperature. Then the outer core were cut to rectangular mat of size 140 mm x 100 mm as shown in figure-3.9 (d) by neglecting the end portion to keep the thickness same in all directions and have been used for manufacturing the layered composite.

3.4.2 Epoxy resin and hardener

Epoxy resins are relatively low molecular weight pre-polymers capable of being processed under a variety of conditions. Two important advantages of these over unsaturated polyester resins are: first, they can be partially cured and stored in that state, and second they exhibit low shrinkage during cure. However, the viscosity of conventional epoxy resins is higher and they are more expensive compared to polyester resins. It possesses outstanding mechanical and thermal properties such as high modulus and tensile strength, low creep, high glass transition temperature, high thermal stability, good moisture resistance, outstanding adhesion to a variety of substrates and good electrical properties. Approximately 45% of the total amount of epoxy resins produced is used in protective coatings while the remaining is used in structural applications such as laminates and composites, tooling, molding, casting, construction, adhesives, etc.Therefore it is widely used in composite industry.

The type of epoxy resin used in the present investigation is Araldite LY-556 which chemically belongs to epoxide family. Epoxy resins are characterized by the presence of a three-membered ring containing two carbons and an oxygen (epoxy group or epoxide or oxirane ring). Epoxy is the first liquid reaction product of bisphenol-A with excess of epichlorohydrin and this resin is known as Diglycidyl-Ether of Bisphenol-A (DGEBA). DGEBA is used extensively in industry due to its high fluidity, processing ease, and good physical properties of the cured of resin. Epoxy resin having density 1.2 g/cm^3 and viscosity is 11000-14000 MPa.s at 25°C.

The curing agent hardener HY-951 [NN0 (2-amineethylethane-1, 2- diamin)] is also used with epoxy resin with an amine value of 260–284 (mg KOH gm^{-1}). Both the epoxy resign and curing agent were obtained from supplier Ciba-Geigy of India Ltd.

3.4.3 Composite preparation

A wooden mold of dimension 150 mm×65mm×5mm was used for casting the composite sheet. Different groups of samples were manufactured with single (SL), double (DL) and triple (TL) layers of untreated luffa fiber and double (DL) layers of different treated luffa fiber as presented in Table-3.5. The weight percentage of the fiber is calculated by using the following formula.

$$Weight\ \%\ of\ fiber = \left(\frac{Weight\ of\ fiber}{Weight\ of\ fiber + Weight\ of\ epoxy\ resin}\right) \times 100 \qquad (3.3)$$

Table-3.5. Types of Luffa fiber used for preparation of composite.

Sl No	Type of fiber	Luffa fiber layers	Weight percentage of fiber (%)
Group 1	Untreated	Single layer (SL)	6.50
		Double layer (DL)	13.00
		Triple layer (TL)	19.00
Group 2	Alkali treated	Double layer (DL)	13.50
	Benzoylated	Double layer (DL)	13.90
	KMnO4 treated	Double layer (DL)	13.39

Usual hand lay-up technique was used for preparation of the samples. The schematic view of the layered composites is shown in figure-3.10. Figure-3.11 illustrates the mold used for preparation of the composite. For quick and easy removal of the composite a mold release sheet is placed on the bottom of the wooden mold. The mold release spray is also applied to the inner surface of the mold wall to facilitate easy removal of the composite specimen. For different layered composite a calculated amount of epoxy resin and hardener (ratio of 10:1 by weight) was thoroughly mixed in a container at room temperature (25°C). The mixture was then poured in to the

prepared mold. Then different layers of luffa fibres were kept in place in the mould. The remainder of the mixture was then poured into the mold. A roller was used to roll-

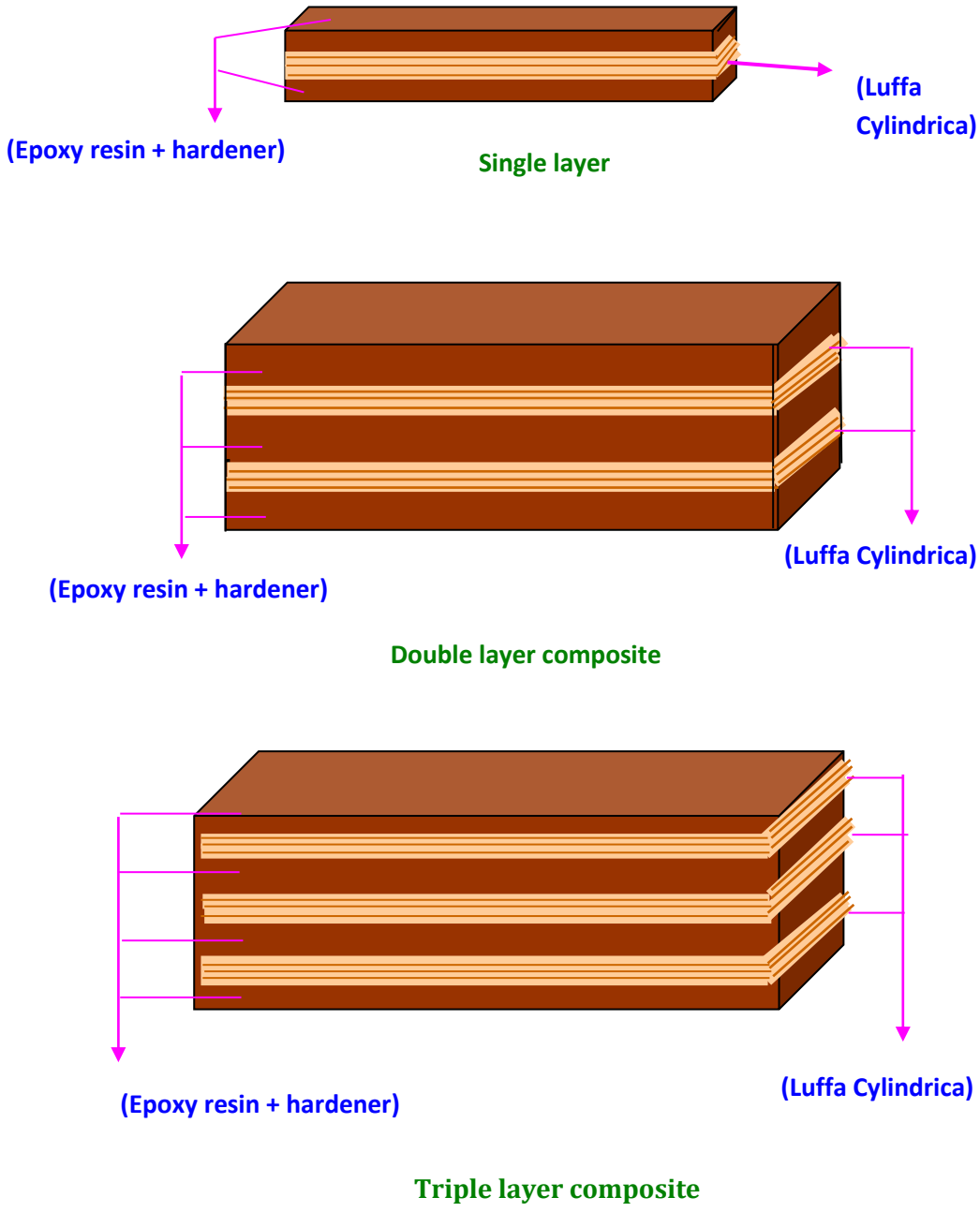

Figure-3.10. Schematic view of the composites.

over the mixture for even distribution and any air bubbles present in the mixture was also removed by this rolling. After 2 to 5min of rolling a mold release sheet was placed on the top of the mold. Before the reaction starts and mixture gets hardened a wooden board of required size was placed on the top of the mold and was loaded from the top with dead weights. The mold was kept with the load in that position for 48 h. Due to application of load some polymer may squeeze out from the mold. Care was taken during pouring for this squeezing out of the mix to get a uniform thickness specimen. After 48 hours the samples were taken out of the mold. Figure-3.12 shows the photograph of the composite and some of the specimen cut for flexural and tensile test. After cutting they were kept in airtight container for further experimentation.

Figure-3.11. Wooden mold for preparation of composite.

(a) (b)

Figure 3.12 (a) Photograph of composite slab and (b) Specimens for flexural and tensile test.

3.5 TESTING OF MECHANICAL PROPERTIES OF COMPOSITE

The study of mechanical properties such as density, tensile strength, flexural strength, impact strength and hardness of untreated and treated Luffa cylindrica reinforced epoxy composite have been conducted as per ASTM standard. The results are tabulated in table-3.6-3.7.

3.5.1 Density and void fraction

The theoretical density of the composite materials can be calculated in terms of weight fraction using Agarwal and Broutman [164] equation.

$$\rho_{ct} = \frac{1}{\frac{W_f}{\rho_f} + + \frac{W_m}{\rho m}} \qquad (3.\ 4)$$

Where 'w' and 'ρ' represent the weight fraction and density respectively. The suffix 'f', 'm' and 'ct' stand for the fiber, matrix and theoretical density of composite materials, respectively.

Actual density (experimental density) of the composite is determined by using Archimedes principle. The density of composites in terms of weight fraction is found out from the following equations 3.5.

$$S_m = \frac{w_0}{(w_0+(w_a-w_b))} \tag{3.5}$$

Where 'S_m' represents specific gravity of the composite, 'w_o' represents the weight of the sample; w_a represents the weight of the bottle + kerosene, w_b represents the weight of the bottle + kerosene + sample.

Density of composite = S_m ×Density of kerosine

The volume fraction of voids (V_v) in the composite is calculated by using equation.

$$V_v = \frac{\rho_{ct}-\rho_{ce}}{\rho_{ct}} \tag{3.6}$$

Where 'ρ' represents the density of the composite. The suffix 'ct' and 'ce' stand for the theoretical and experimental density of the composite materials.

For the present investigation the theoretical density, actual density and the void fraction so obtained for both untreated and treated fiber reinforced composites are presented in table-3.6.

Table -3.6. Measured and theoretical densities of the composite.

Fiber content	**Type of fiber**	**Theoretical density(g/cm^3)**	**Measured density(g/cm^3)**	**Volume fraction of void (%)**
Neat epoxy	-	1.2	1.18	1.66
SL	Untreated	1.045	1.0294	1.492
DL	Untreated	0.994	0.975	1.911
TL	Untreated	0.989	0.969	2.022
DL	Alkali	1.182	1.171	0.930
DL	Benzoylated	1.191	1.183	0.672
DL	KMnO4	1.190	1.178	1.008

3.5.2 Tensile strength

The tensile test is generally performed on flat specimens. The most commonly used specimen geometries are of dog-bone type and the straight side type with end tabs. The tensile test was conducted according to the ASTM D 3039-76 standard on a computerized Universal Testing Machine (INSTRON H10KS). The span length of the test specimen used was 42 mm. The tests were performed with a constant strain rate of 2 mm/min with 10 KN load cell. Five specimens of each sample were tested for accuracy. Figure-3.13 (a) shows, configuration of the sample. Few tested samples are shown in figure-3.13 (b). The results obtained from the tests are presented in table-3.7.

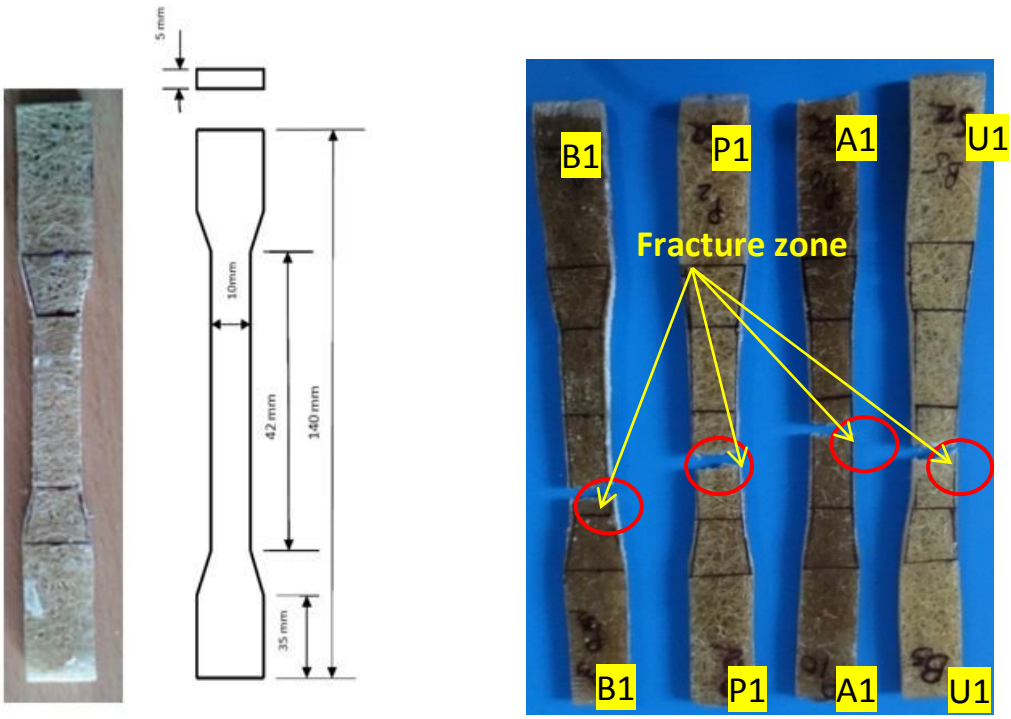

(a) (b)

Figure-3.13 Photographs of (a) Tensile test samples with configuration (b) Tensile tested sample.

3.5.3 Flexural and Interlaminar shear strength

The Flexural test was performed using 3-point bend test method according to the ASTM D790-03 standard on a computerized Universal Testing Machine (Hounsfield H10KS). Specimen of 140 mm length and 15 mm wide were cut and loaded in three points bending fixture with recommended span to depth ratio of 16:1. The specimens were tested at a crosshead speed of 2 mm/min with 10KN load cell. Five specimens for each sample were tested for accuracy. Figure-3.14 (a) configuration of the sample. Some of the flexural tested samples are shown in figure-3.14 (b) .The flexural strength can be found out by using the equation.

$$\sigma = \frac{3FL}{2bt^2} \tag{3.7}$$

Where F is the maximum load (N), L is the distance between the supports (mm), b and t are the width and thickness (mm) respectively. The data recorded during the 3-point

bend test can be used to evaluate the interlaminar shear strength (ILSS) by using equation.

$$ILSS = \frac{3F}{4bt} \tag{3.8}$$

Where F is the breaking load (N), *b* and *t* are the width and thickness of the specimen (mm)

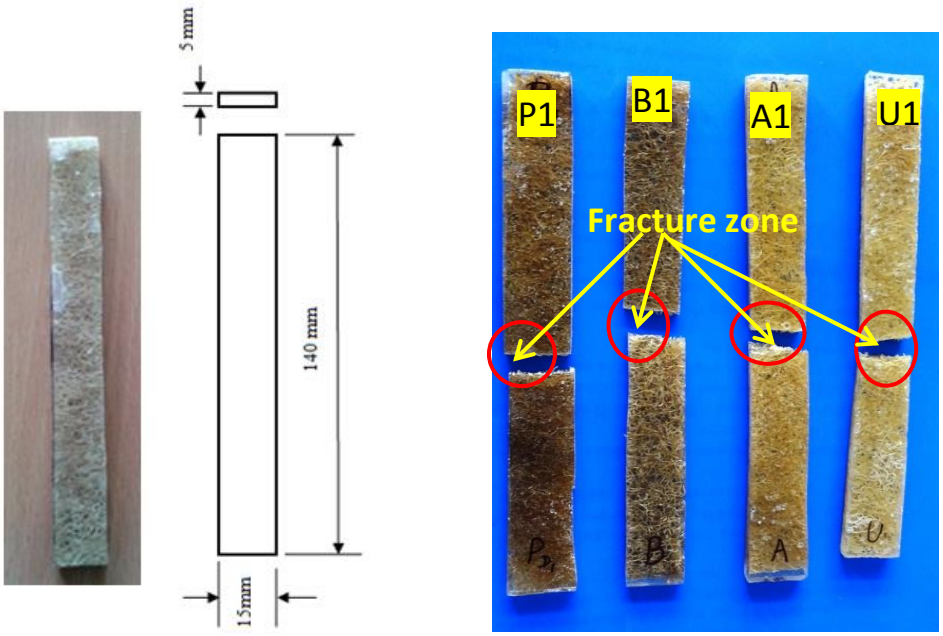

(a) (b)

Figure-3.14 Photographs of (a) Flexural test samples with configuration (b) Flexural tested sample.

3.5.4 Impact test

The impact test of the composite was performed by Izod impact tester (Veekay Test lab, Mumbai, Maharashtra, India) according to ASTM D 256. The size of the specimen is 63.5 long and 12.7mm width (figure-3.15). A 'V' notch (2.54 cm depth and 45° notch angle) is created at the center of the specimen. To perform the test hammer release angle of 150° with hammer range of 5.394 Joule was used. The impact energy of all composite samples was recoded directly from the dial indicator and is presented in table-3.7.

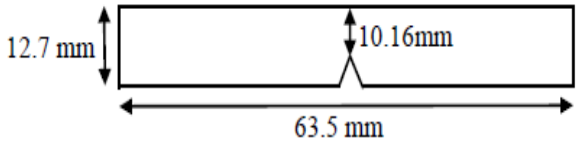

Figure-3.15 Configuration of impact test specimen.

Table-3.7. Mechanical properties of untreated and treated LC-epoxy composite

Fiber content	Type of fiber	Tensile strength (Mpa	Yong's Modulus (Mpa)	Flexural strength (MPa)	Flexural Modulus (MPa)	ILSS (Mpa)	Impact strength (KJ/m2)	Hardness (Hv)
NE	-	12.5	521	17	1425	0.6	2.5	17.9
SL	Untreated	16.5	650	28	2525	0.644	3.9	20.2
DL	Untreated	18	699	32	2064	1.01	4.9	22.15
TL	Untreated	16	725	27	1636	1.38	4	17.2
DL	Alkali	24	788	46.23	3097	1.97	6.5	21.96
DL	Benzoylated	27	890	53.8	3745	1.92	7.3	21.8
DL	KMnO4	25	900	50.1	3672	1.36	6.7	20.7

3.5.5 Micro-Hardness

Micro-hardness measurement is done using a Lecco Vickers Hardness (LV 700) tester. A diamond indenter, in the form of a right pyramid with a square base and an angle 136° between opposite faces, is forced into the material under a load. The two diagonals D_1 and D_2 of the indentation left on the surface of the material after removal of the load are measured and their arithmetic mean D is calculated. In the present study, the load considered F = 0.3KgF and Vickers hardness number is calculated using the following equation:

$$H_v = \frac{0.1889F}{D^2} \tag{3.9}$$

Where $D = \frac{D_1+D_2}{2}$

Where F is the applied load (KgF), L is the diagonal of square impression (mm), D_1 is the horizontal length (mm) and D_2 is the vertical length (mm).

3.5.6 Scanning Electron Microscopy

The fractured specimens are examined directly by Field emission scanning electron microscope (FESEM) Nova NANO SEM 450. The composite samples are mounted on the stubs with silver paste. To enhance the conductivity of the samples a thin film of gold is vacuum evaporated on to them before the photomicrographs are taken.

3.5.7 Results of mechanical tests

It is well known that fiber content and fiber strength are mainly responsible for strength properties of the composite. Therefore variation in strength properties of the composite with various fibers loading is obvious. This variation in tensile and flexural strength of the composites for untreated single, double and triple layer are presented in table-3.7 and are shown in figure-3.16. These figures clearly indicate that there is gradual increase in both tensile strength and flexural strength for single and double layer composite. However there is a decrease in both tensile and flexural strength for triple layer composite. It clearly indicates that inclusion of LC fiber up to double layer improves the load bearing capacity and ability to withstand the bending of the composite. Similar observations are reported by Shekeil et al. [70] and Acharya et al. [165] while they worked for cocoa pod husk fibers composite and jute fiber composites respectively.

Tensile and flexural moduli of the untreated luffa epoxy composites are presented in figure-3.17. From figure it is clearly observed that tensile modulus of the composite increases as the layer of luffa fiber increases. However flexural modulus increases up to double layer and decreases for triple layer composite.

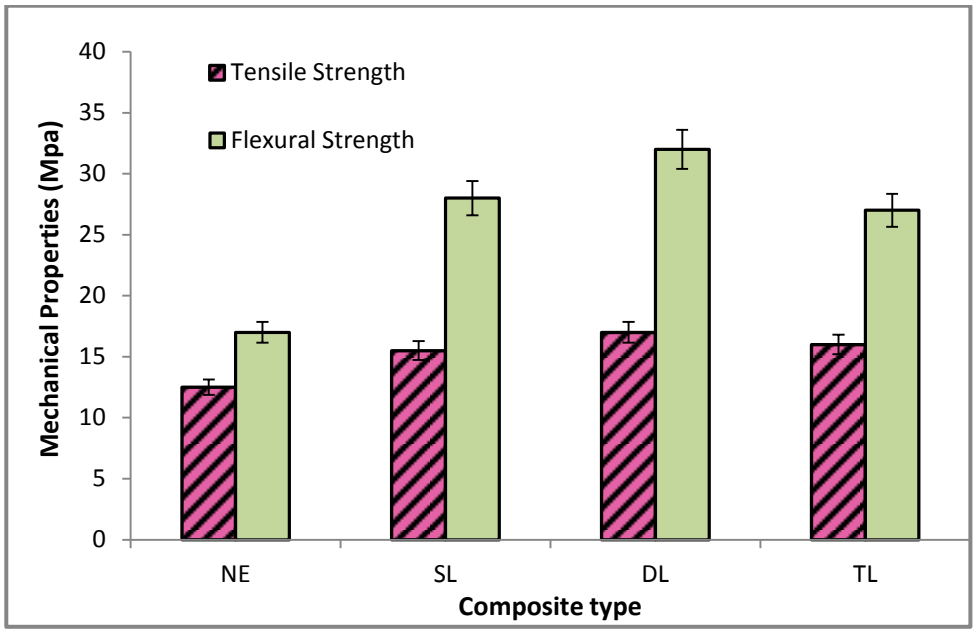

Figure-3.16 Tensile and flexural strength of Single, Double and Triple layer LC-epoxy composites.

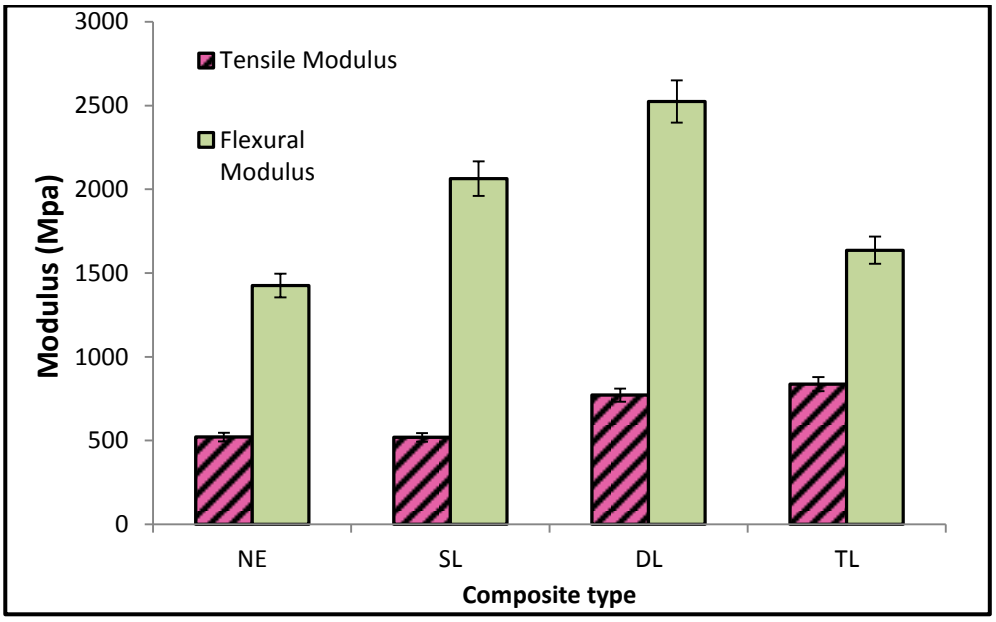

Figure-3.17 Tensile and flexural modulus of untreated Single, Double and Triple layer LC-epoxy composites.

The stresses acting on the interface of the two adjacent laminae in a layered composite are called interlaminar shear stress. These stresses cause relative deformation between the consecutive laminae and if these are sufficiently high they

may cause failure along the mid plane between two adjacent laminae. It is therefore almost important to evaluate ILSS through test in which failure of the laminates of the composite initiates in a shear (delamination mode). In the present case the ILSS value are measured and found to be appreciable increase for single, double and triple layer composites in comparisons to neat epoxy as shown in Figure-3.18.

It is observed from figure-3.18 that the impact strength of the luffa fiber epoxy composite showed an increasing trend with increase in fiber content up to double layer of fiber. However strength decreases for triple layer reinforced composite. Similar type of work [166, 167, and 168] showed an increase in impact strength with an increase in fiber content, indicating positive contribution of the fiber. Higher impact strength indicates the capability of the composite to absorb energy. It depends on the nature of the fiber, polymer and fiber-matrix interfacial bonding [169].

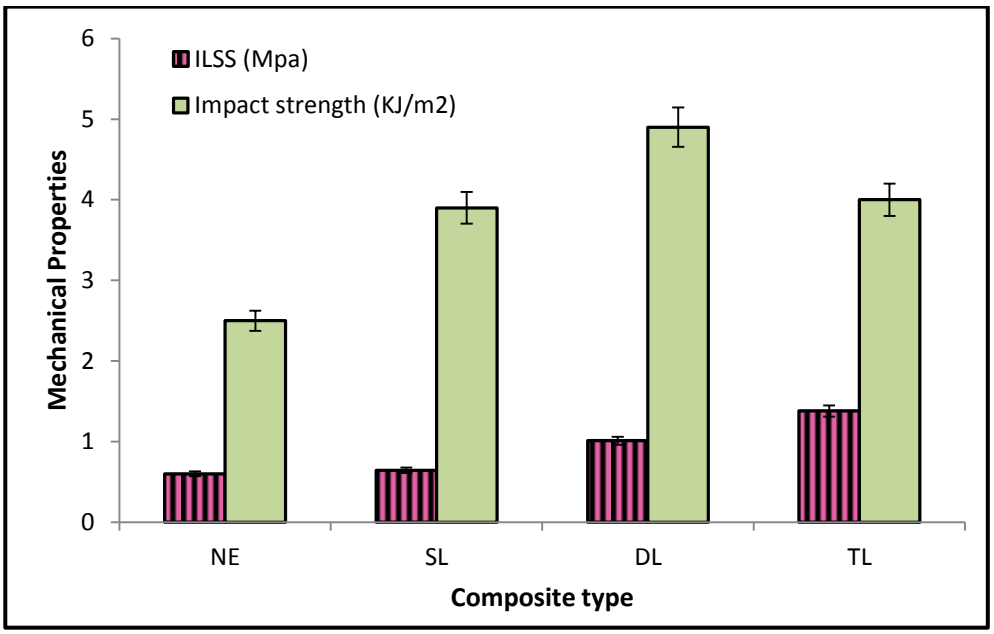

Figure-3.18 ILSS and Impact strength of untreated Single, Double and Triple layer LC-epoxy composites.

Figure-3.19 shows the micro hardness values for different layers of untreated Luffa fiber reinforced composite. It is seen that with the increase in fiber content in the composite, its hardness value improves up to double layer reinforced composite. However it decreases for triple layer composites.

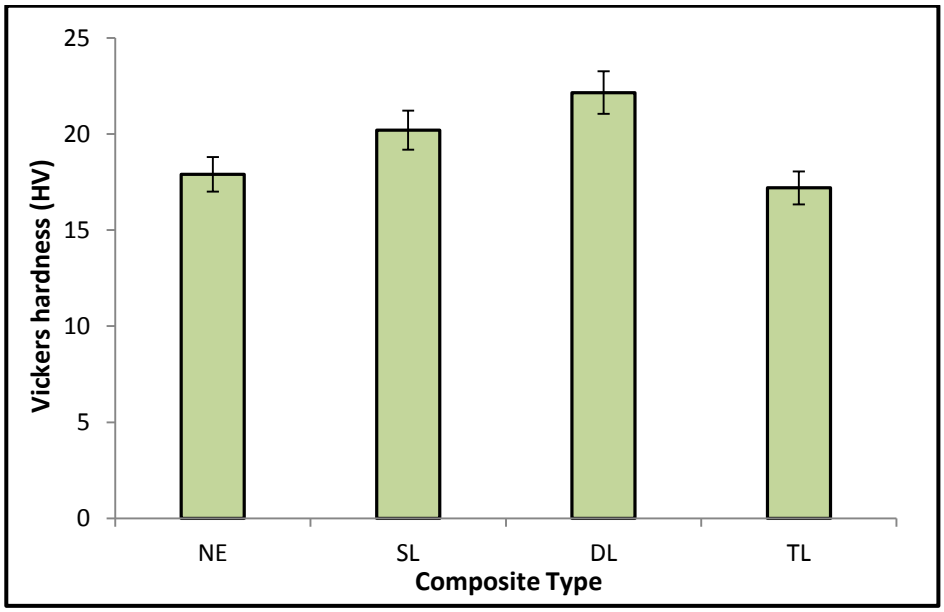

Figure-3.19 Micro hardness of untreated Single, Double and Triple layer LC-epoxy composites.

From the above investigation, it can be conclude that the composite containing double layer luffa fiber reinforced composite provided the best combination of strength and modulus. Decrease in the mechanical properties is observed at higher fiber loading i.e. triple layer luffa fiber .This may be due to poor fiber matrix adhesion which might have promoted micro-crack formation at the interface as well as non-uniform stress transfer due to fiber agglomeration within the matrix [170, 65]. Similar results have been reported by Mohanty et al. [72] and Rana et al. [171] while they worked with jute fiber.

The effect of different chemical modifications of fibers on mechanical properties of the composite have been studied by taking double layer reinforcement of luffa fiber as an optimum reinforcement as discussed earlier. It is clearly seen from Table-3.16 and Figures-3.20-3.23 that, the mechanical properties of the composite enhanced significantly due to chemical modification of fiber surface. This improvement in properties occurs due to rough fiber surface produce by removal of natural and artificial impurities, fibrillation of fiber which facilate the mechanical anchoring between fiber and matrix as explained in art-3.3.1. In addition to this the

increase of crystallinity index of fibers (art-3.3.4) due to removal of cementing materials also enhanced the properties. Higher increase in properties was observed in the case of benzoyl-chloride treated fiber followed by KMnO4 and alkali treated fiber. Nair et al. [77] Fiore et al. [172] and Kushwaha et al. [173] also reported similar observations while working with benzoylated sisal fibers, alkali treated kenaf fibers and KMnO4 treated bamboo fibers respectively.

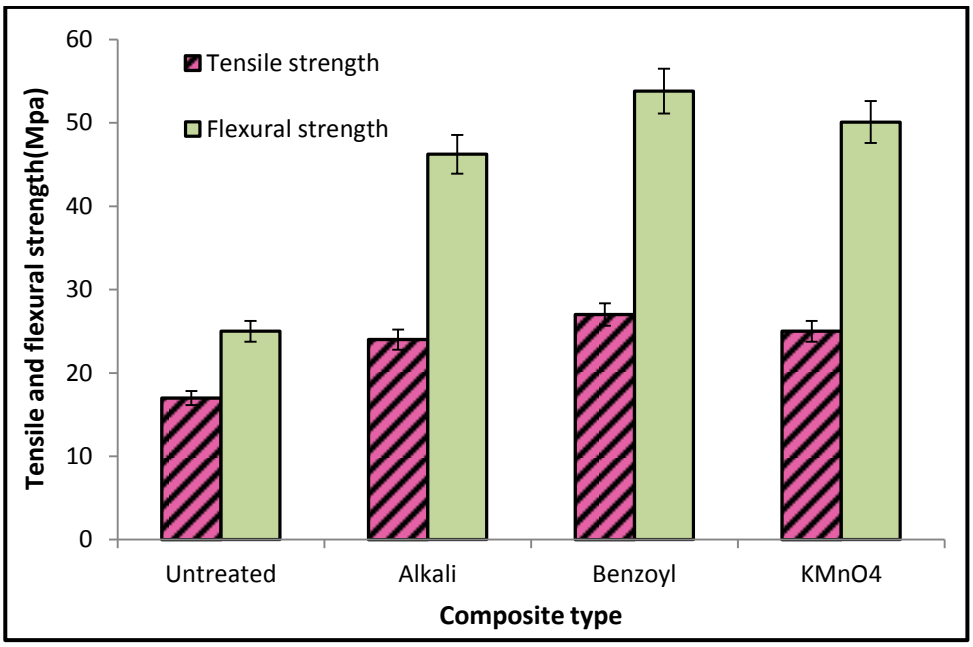

Figure-3.20. Tensile and flexural properties of treated LC-epoxy composite.

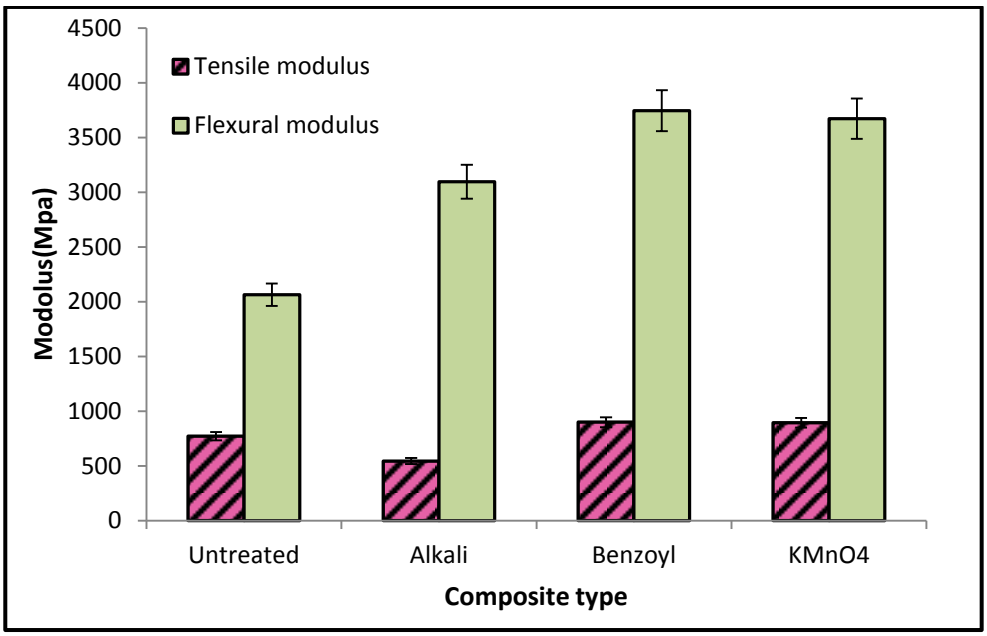

Figure-3.21. Tensile and flexural modulus of treated LC-epoxy composite

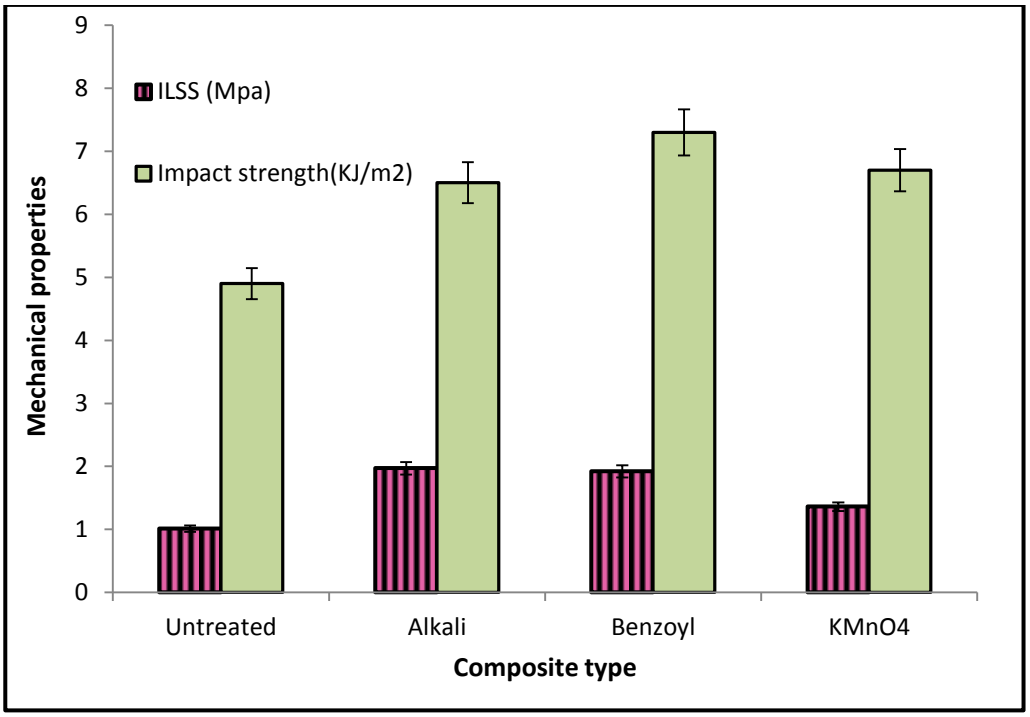

Figure-3.22. ILSS and Impact strength of treated LC-epoxy composite.

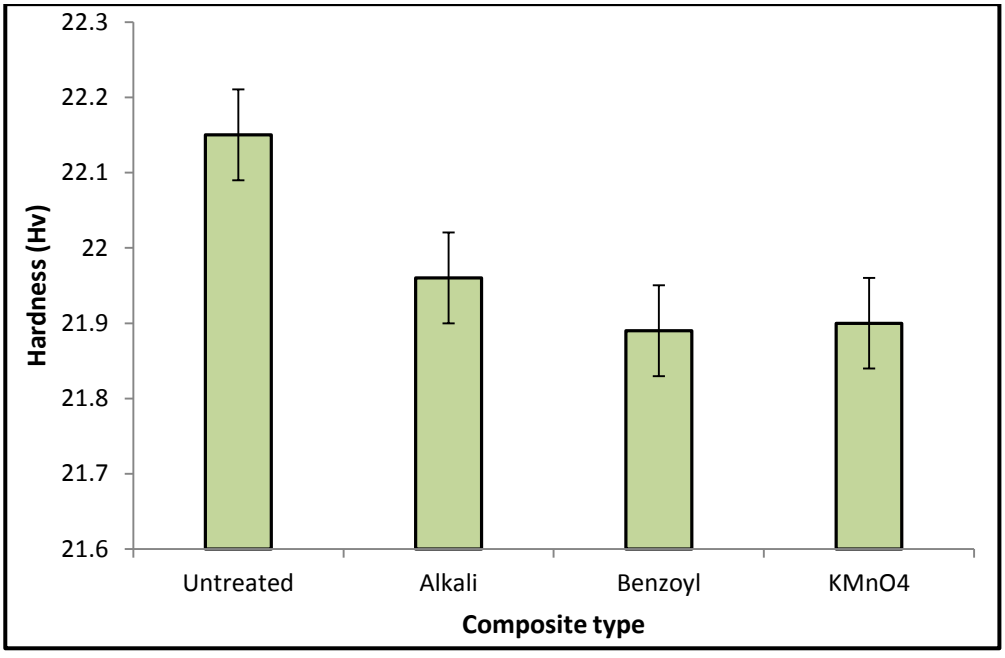

Figure-3.23 Micro hardness of treated LC-epoxy composites.

3.6.8 SEM observation of fracture surface.

Tensile failure of untreated double layer composites is shown in figure-3.24 (a). Tearing of fiber along loading direction is clearly visible. Tearing/breaking of fiber along transverse direction is not visible. The networking of structure probably restricts the breaking/tearing of fiber along the transverse direction, which mainly responsible for higher tensile strength.

Figure-3.24 (b) shows the tensile failure of untreated triple layer (19 wt. %) composite. The fiber breakage and pull out of fiber from the matrix is clearly visible. This indicates a poor fiber matrix adhesion which results in lower tensile strength as discussed earlier.

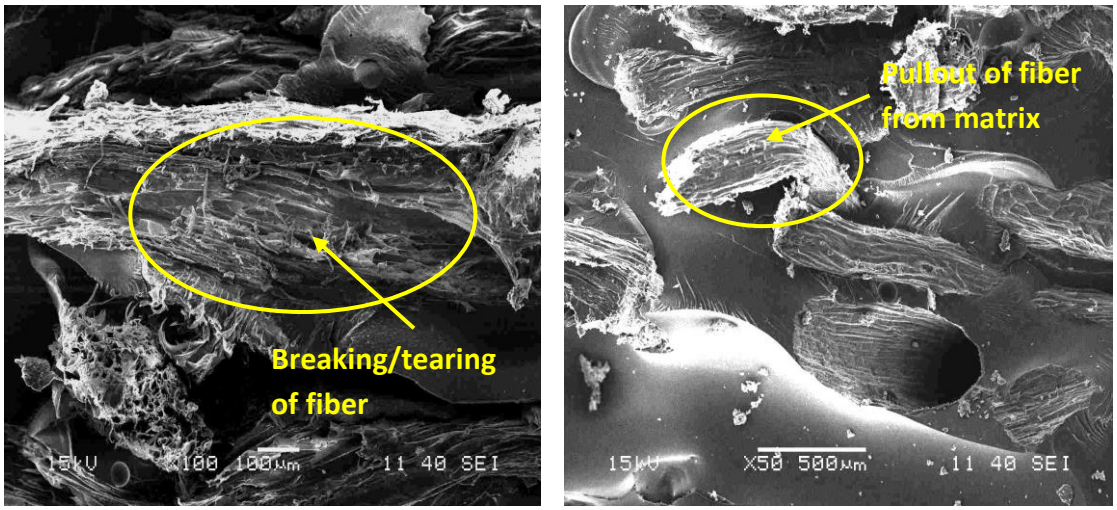

(a) (b)

Figure-3.24 SEM Micrographs of tensile fractured surface of untreated LC-Epoxy composite a) double layer and (b) triple layer under tensile load.

Figure-3.25 (a) and (b) shows the micrographs of the fracture surface of untreated double layer and triple layer of LC fiber reinforced composite during bending test. For double layer debonding of fibers at some place which creates voids are visible but most of the fibers are intact with the matrix (Figure-3.25 (a)).These voids are small in numbers and hence do not create more problem on the composite properties. For

Triple layer composite, debonding between fibers and matrix due to insufficient wetting is clearly visible. This revels that for triple layer composite, poor fiber wetting occurs due to insufficient matrix material which results in lower flexural strength of the composite.

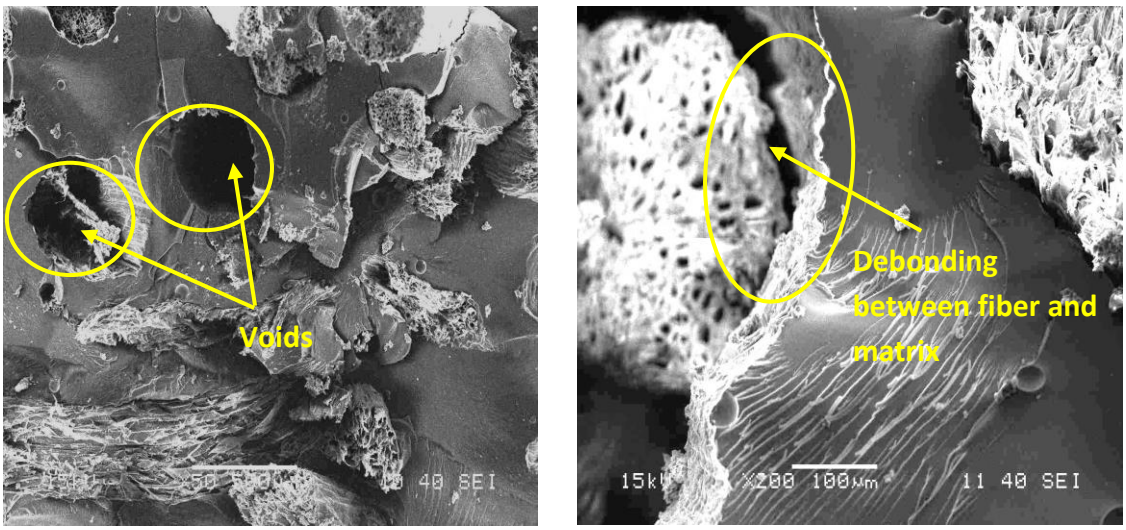

(a) **(b)**

Figure-3.25 SEM Micrographs of flexural fractured surface of untreated LC-epoxy composite (a) double layer and (b) triple layer under flexural load.

Figure-3.26 (a-c) shows the morphology of fracture surface of the treated fiber composites subjected to tensile loads. As it seen in figure-3.24 (a) for untreated Luffa fiber composite, that the phenomenon of pull-out fibers occurred in a greater extent than those of treated fiber composites. Fiber matrix debonding is clearly noticed in case untreated composite (figure-3.24(b)). Figure-3.26 (a) shows the fiber treated with NaOH. It is clearly seen that fiber breakage occurs due to tensile load, but fibers are not pulled out from the matrix. This indicates better adhesion at the interphase of fiber and the matrix. Figure-3.26 (b) shows the composite treated with KMnO4. Here also fiber breakage is visible but there is no sign of pulling out of fiber from the matrix is found. In case of benzoyl chloride fiber reinforced composite shown in figure-3.26(c). It is seen that removal or breaking of fiber from the matrix is not there rather bending of fiber is clearly visible. This bending of fiber instead breaking under the tensile load probably increases the strength of the composite. Because benzoylation of fiber improves fiber-matrix adhesion, thereby an increase in strength of the composite is

achieved [77,144]. Overall chemical modification improves the fiber-matrix adhesion that in turn enhanced the mechanical properties of composites.

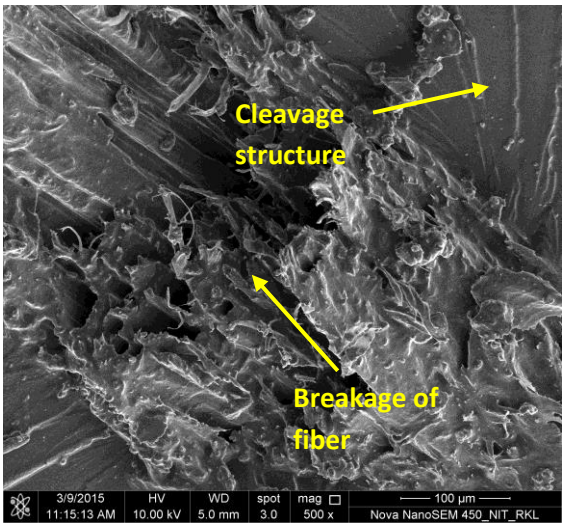

(a)

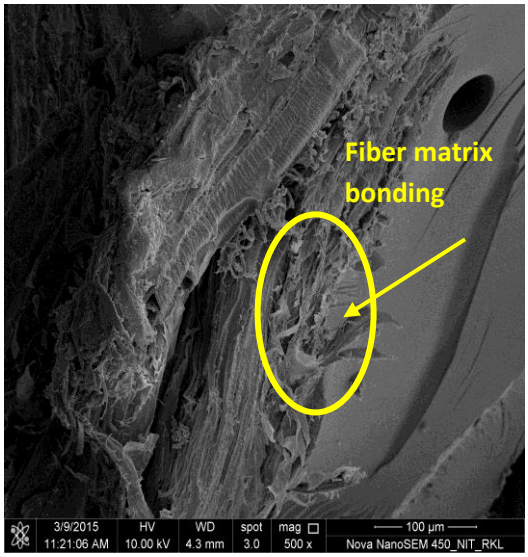

(b)

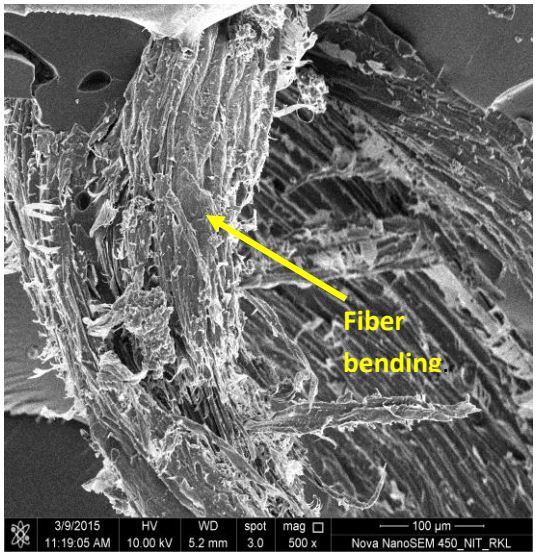

(c)

Figure-3.26 SEM micrographs of fracture surface of (a) alkali treated (b) KMnO4 treated (c) Benzolated LC-epoxy composite under tensile load.

Figure-3.27 (a-c) shows the micrographs of the fractured samples of tension side under flexural load for treated luffa fiber composite. Fracture surface of the treated fiber composite with alkali (figure-3.27 (a)) shows the breaking of fiber, but fibers seem to be intact with the matrix. This indicated a good bonding between fiber and

matrix. Some cleavages structures are also found due to flexural load. Bending of fiber instead breaking took place for the KMnO4 treated fiber composite (figure-3.27(b)). For the benzoyl chloride treated fiber composite neither bending nor breaking of fiber took place (figure- 3.27(c)). There is no sign of formation of grooves or cracks on the surface of the composite. The strength of the fiber increases with the treatment that they become capable to withstand the flexural load without any damage. Overally chemical modification improves the fiber matrix adhesion which in turn enhanced the mechanical properties of composites

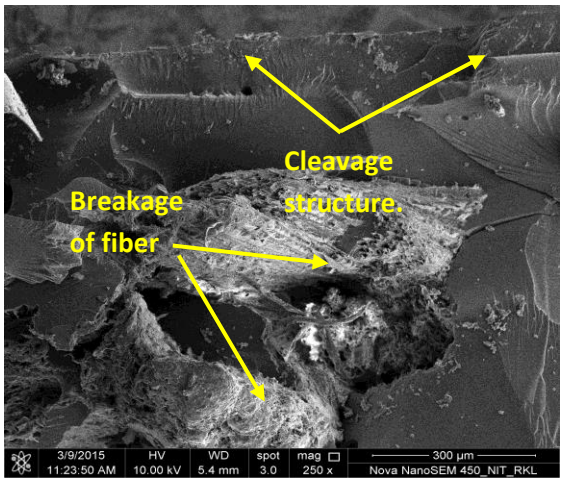

(a)

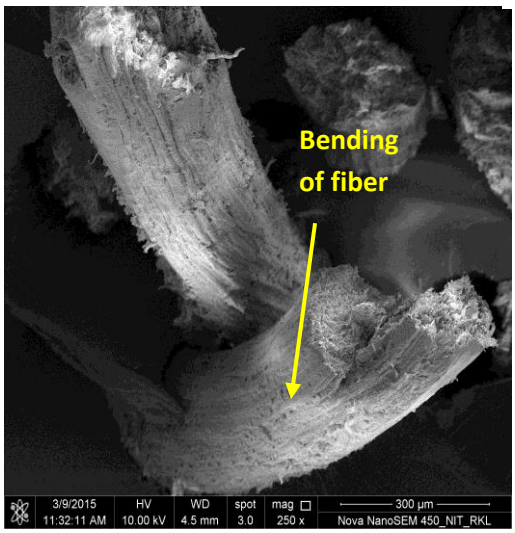

(b)

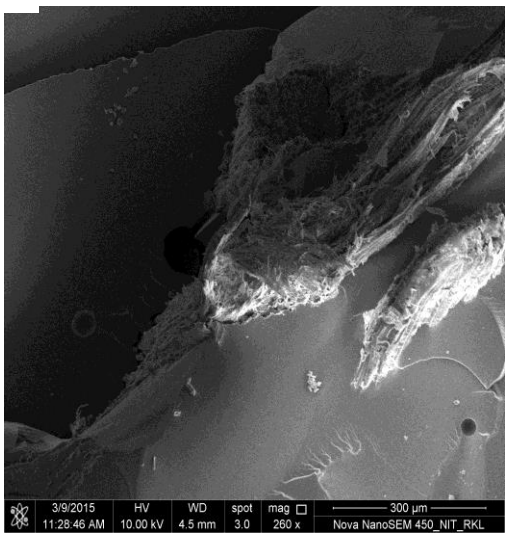

(c)

Figure-3.27 SEM micrographs of fracture surface of (a) alkali treated (b) KMnO4 treated (c) benzolated LC-epoxy composite under flexural load.

3.7 CONCLUSIONS

Based on experimental results, this study has led to the following conclusions:

- The alkali, benzoyl chloride and KMnO4 treated luffa cylindrica fiber showed a reduction in absorption spectra due to the dissolution of the non-polar covalent compound like wax, fat, etc. in the treated chemicals as compared to untreated composites. The effect is more significant in the case of benzoyl chloride treatment as this is a strong non-polar solvent that dissolves more non-polar compound.

- The crystallinity index of luffa cylindrica fiber is found to be increase upon chemical treatments. The highest crystallinity index was observed for the alkali treated fiber followed by benzoyl chloride, and KMnO4 treated fiber.

- Thermal stability of chemical treated fibers is more than the untreated fiber.KMnO4 treated fiber shows the better thermal stability.

- The luffa cylindrica fiber can successfully be used as reinforcing agent to fabricate composite by suitably bonding with epoxy resin.

- On increasing the fiber content the strength, modulus increases and the best combination is found with double layer of fiber.

- The mechanical properties of luffa cylindrica fibers were significantly improved upon surface modification of fiber by different chemical methods. Improvement in all mechanical properties occurs due to rough fiber surface produced by removal of natural and artificial impurities, fibrillation of fiber that facilitate the mechanical anchoring between fiber and matrix. Best results were achieved in the case of benzoyl chloride treated fiber composite.

- The morphology of fractured surface observed by SEM suggests that the networking of structure restricts the breaking/tearing of fibre which is responsible for higher tensile and flexural strength for double layer composite. The decrease in strength for triple layer composite due to poor fiber matrix adhesion of fibre with the matrix. However for treated fiber composite SEM photomicrographs support the strong fiber matrix adhesion.

Chapter 4

Moisture absorption behavior and its effect on mechanical properties of Luffa cylindrica fiber reinforced epoxy composite

4.1 INTRODUCTION

There are many applications of natural fibre composites in everyday life. However the main disadvantage of natural fibre is their hydrophilic nature. They also have a poor environmental and dimensional stability that prevent wider use of natural fibre composites. The possibility of using these materials in outdoor applications makes it necessary to analyse their mechanical behaviour under the influence of different weathering conditions such as humidity, saline water, sunlight or micro-organisms. The moisture absorption by composites containing natural fibres has several adverse effects on their properties and thus affects their long-term performance. For example, increased moisture absorption decreases their mechanical properties, provides the necessary condition for biodegradation, and changes their dimensions [174]. The composite absorb or release moisture depending on environmental conditions [175]. The Hydroxyl group (–OH) in amorphous cellulose, hemicellulose and lignin that are present in the natural fibre are mostly responsible for the high moisture absorption due to formation of hydrogen bond by hydroxyl groups with water molecules within the fibre cell wall. This leads to a moisture build-up in the fibre-matrix interface and causes swelling of the composite, reduction in interfacial strength, debonding of fibre and matrix, reduction in glass transition temperature and change in visco-elastic properties [176]. Therefore, it is important to study in detail the water absorption behavior in order to estimate not only the consequences that water uptake will create but also how to minimize this tendency to widened its utilization.

Moisture uptake into polymer composite happens by three different mechanisms. The primary and 1st mechanism is the diffusion of water molecules through the micro gaps between the polymer chains. The second is capillary transport into the gaps and flows at the interface between the fibres and polymers because of incomplete wettability and impregnation. The third one is the capillary transport by micro cracks in the matrix formed during the compounding process [177, 178]. All the three mechanisms can be modelled as single diffusional mechanisms. With this, there are three different diffusional behaviour such as Fickian, relaxation controlled, and non-Fickian diffusion [179]. Case 1 for Fickian diffusion, in which the rate of diffusion is much less than that of the polymer segment mobility. The equilibrium inside the polymer is rapidly reached and it is maintained with independence of time. Case 2 is

relaxation control, in which penetrant mobility is much greater than other relaxation processes. This diffusion is characterized by the development of a boundary between the swollen outer part and the inner glassy core of the polymer. The boundary advances at a constant velocity and the core diminishes in size until an equilibrium penetrant concentration is reached in the whole polymer. Case 3 is when anomalous diffusion occurs where the penetrant mobility and the polymer segment relaxation are comparable. It is an intermediate behavior between Cases 1 and 2 of diffusion. These three cases of water diffusion can be distinguished theoretically by the shape of the sorption curve represented by the following Equation [180, 181]:

$$\frac{M_t}{M_m} = kt^n \tag{4.1}$$

Where *'M_t'* is the moisture content at specific time't', *'M_m'* the equilibrium moisture content (EMC), and *'k'* and *'n'* are constants .The value of coefficient n shows different behavior between the three cases: Fickian diffusion (n=0.5), relaxation ($n \geq 1$) and anomalous diffusion ($0.5<n<1.0$) [182]. The value of n >0.5 indicates the predominant mechanism of moisture absorption is due to transport through capillary or crack. The dominant mechanism depends on several factors such as chemical structure of the polymer, dimensions and morphology of the filler, and the polymer–filler interfacial adhesion and void content in the composite. Moisture absorption in natural fiber reinforced plastics usually follows Case I Fickian behavior, so, in this present investigation is focused towards this behavior.

The moisture absorption by composite reinforced with natural fibres has several adverse effects on their performance. In view of the severity of moisture absorption and its effect on composite properties, a number of studies have already been made by several researchers on different type of fibre to address this issue. As discussed in chapter 3 art 1.1 chemical modification of fibre surface is one of the most reliable method to reduce the hydroxyl group in the natural fibres by exposing cellulose content of fibre. It also improves the roughness of fibre surface which in turn increases the fibre matrix adhesion and also improves thermal stability and mechanical strength of related composite. Different chemical treatments for surface modification of different

natural fibres like pineapple, rice husk and sisal fibre are discussed in details by different researchers [183-185,139].

George et al. [186] investigated the relationship between the moisture absorption of pineapple-leaf fibre reinforced low density polyethylene (LDPE) composites with different fibre loadings. They found that the moisture absorption increases almost linearly with the fibre loading. Similar, results also have been reported by K. Hardinnawirda et al. on rice husk –unsaturated polyester composites [187].

Joseph et al. [181] studied the environmental effects on sisal fibre reinforced PP composites. The chemically modified fibre composites showed a reduction in water uptake because of better interfacial bonding. Water uptake of the composite was found to increase with temperature since temperature activates the diffusion process. Reduction in tensile properties was observed due to the plasticization effect of water. The fibre/matrix bonding becomes weak with increasing moisture content, resulting in interfacial failure.

Stark [188] found that wood flour-polypropylene (PP) composites with 20 wt.% wood flour reached equilibrium after 1500 h in a water bath and absorbed only 1.4% moisture while composites with 40 wt.% loading reached equilibrium after 1200 hours water submersion and absorbed approximately 9.0% moisture. After the analysis, she concluded that the wood flour is inhibited from absorbing moisture due to encapsulation of the wood flour by the PP matrix and that the degree of encapsulation is greater for the 20% wood flour composite than that for the 40% wood flour composite.

Yuan et al. [189] studied the plasma treatment of sisal fibres and its effects on tensile strength and interfacial bonding. They suggested that the interfacial adhesion between the fibre and matrix could be enhanced by cleaned and chemically modified fiber surface. The strong intermolecular fiber-matrix bonding decreases the rate of moisture absorption in bio-composite.

Stamboulis et al. [190] reported that the moisture absorption and swelling of the treated flax fiber polypropylene composites is approximately 30% lower than that of composites based on untreated flax fibers.

Sreekumar et al. [191], while studying water absorption characteristics of sisal fiber polyester composites found that diffusion coefficient decreases with chemical treatment of fiber. In addition to this the chemical treatment also decreases water absorption capacity of the composite. They also showed that the composite with benzoyl-chloride treated sisal fiber composite exhibited lower water absorption capacity.

A.Athijayamani et al. [192] reported variation of mechanical properties for Roselle and sisal hybrid polyester composite at dry and wet condition. They have the opinion that the moisture absorption characteristic of the natural fiber is very important to produce the natural fiber hybrid composite material with positive hybrid effect.

Leman et al. [193] studied the moisture absorption behavior of Sugar Palm fiber reinforced epoxy composite and have reported that composite that contain higher fiber composition the moisture absorption rate is higher for them.

Deo, Acharya [194] and Acharya, Mishra, [195] studied the effect of moisture absorption and weathering behavior of chopped Lantana Camera and short bagasse fiber reinforced epoxy composites for both treated and untreated fibers. Their results indicate significant improvement on the mechanical properties of the composites due to chemical modification of fiber surface. Both the investigators modified the surface with same chemical methods. But benzoyl chloride treated fiber gives the better result for lantana- camara fiber whereas alkali treated fiber gives better result for bagasse fiber.

For potential application of natural fiber polymer composites a comprehensive study on the moisture absorption characteristic and its effect on mechanical properties are required. In this chapter, the characteristics of moisture sorption kinetics, thickness swelling and effect of moisture absorption on mechanical properties of both untreated and chemically treated luffa cylindrica epoxy composite under different environments (distilled water, saline water and sub-zero temperature) are investigated.

4.2. EXPERIMENT

4.2.1 Preparation of fiber.

The preparation of fiber and chemical modification of fiber are discussed in chapter 3, art. 3.4.1 and art 3.2 respectively.

4.2.2 Preparation of test the specimen

The preparation of the test specimens were carried out as per the procedure discussed in chapter-3, art-3.4.3. Specimens of dimension 140mm×15mm×5mm were cut from the composite slabs. Adequate care has been taken to keep the thickness constant (4mm) for all the samples.

4.2.3 STUDY OF ENVIRONMENTAL EFFECT

Since the natural fibers are hydrophilic in nature, the performances of natural luffa cylindrica reinforced epoxy composite under different environmental conditions are essential to study. Therefore effect of environment on performance of LC-epoxy composite samples for both treated and untreated fibers were subjected to various environments such as.

(a) Distilled water treatment
(b) Saline water treatment
(c) Subzero temperature treatment

4.2.3.1 Moisture absorption test

The moisture absorption and thickness swelling tests were performed in accordance with ASTM D570-98. Five samples of each composite type for tensile and flexural test were cut to a dimension of 140 mm ×15mm (length x width). They were dried in an oven at 80° C and then were allowed to cool at room temperature and kept in desiccators containing silica gel. The conditioned composites were subjected to different environmental chamber (distilled water (PH=7), saline water (5% NaCl) and sub-zero temp (-5°). The increase in weight due to moisture absorption was recorded

for each sample after exposure of every 12 hour. The specimens were taken out from the moist environments and all surface moisture was removed with a clean dry cloth or tissue paper. The specimens were weighed to the nearest 0.001 mg within 1 min. of removing them from the environment chamber. Also at the same regular time interval, the thickness of the samples was measured by a 0.001 accuracy digital caliper. The experiments were conducted continuously till the steady state is achieved. The moisture absorption was calculated by the weight difference. The percentage weight gain of the samples was calculated at different time intervals by using the following equation:

$$M_t(\%) = \frac{(W_t - W_0)}{W_o} \times 100 \quad (4.2)$$

Where 'W_o' and 'W_t' denote the dry weight and weight after time't', respectively. The Equilibrium Moisture Content (EMC) in the sample was considered when the increase in moisture content was less than 0.1% by weight.

The thickness swelling (TS) was determined by using the following equation:

$$TS(\%) = \frac{H_t - H_0}{H_0} \times 100 \quad (4.3)$$

Where 'H_t' and 'H_0' are the composite thickness after and before the water immersion respectively.

4.2.4 Test of mechanical properties

The mechanical properties such as tensile strength, flexural strength, impact strength and ILSS of environmentally treated composites are conducted according to the procedure discussed in chapter-3, art-3.5.

4.3 RESULTS AND DISCUSSION

4.3.1 Moisture absorption behaviour

The results of both untreated and treated fiber composite samples exposed to different environments are shown in table-4.1 to 4.6. Figure-4.1 to 4.3 shows the moisture absorption characteristics of composite samples with untreated fiber (SL, DL,

and TL) exposed to distilled water, saline water and sub-zero temperature environment with time. It is clearly observed from the plot that the composites absorbed water very rapidly at the initial stage and reached a saturation level where no more water can absorbed for all environments. The saturation time were different for different environments i.e., approximately 108 h for distilled water, 120 h for saline water and 84 h sub-zero temperature environment. It is also observed that as the fibre content in the composite increases the moisture uptake capacity increases and it is maximum for triple layer reinforced composite (i.e.17.23% for saline water, 19.00% for distilled water and 2.30% for sub-zero temperature). The moisture absorption behaviour of composite generally depends upon various factors such as void content in composite, fibre-matrix interfacial bonding and fibre loading [196]. But in the present case luffa cylindrica epoxy composite, the hydrophilicity nature of luffa fibre, poor fibre-matrix adhesion and void contents are responsible for this behaviour. The natural luffa fibre contains free OH group of cellulose that form hydrogen bonding with the water molecule. As the luffa fibre content increases in the composite the free OH group increases. Hence moisture uptake increases. Rashid et al. [197] while working with kenaf-polyester composites also reported same observation that as the fibre content increases in the composite the moisture absorption increases due to higher cellulose content.

Environmental conditions also play a significant role in moisture absorption process. The equilibrium moisture content (EMC) or the maximum moisture absorption of different layered composites obtained at different environmental conditions are presented in figure-4.4. It is observed that moisture absorption rate in distilled water environment is more than the saline water. This might have happened because, in case of composite immersed in saline water, NaCl ions gets deposited on the surface of fibre that increases with immersion time and slows down subsequent water diffusion [198]. Again the absorption rate of moisture in distilled water and saline water environment are much higher compared to sub-zero treatment. Less intermolecular hydrogen bonding in sub-zero treatment is responsible for this type of behaviour [194]. A similar type of results was also reported by Deo et al. [194] and Raghavendra et al. [199] while they studied with lantana camara-epoxy and jute-epoxy composite respectively.

Table - 4.1 Variation of weight gain and thickness swelling of untreated Single layer (SL), Double layer (DL) and Triple layer (TL) LC-epoxy composite exposed to saline water environment.

t (Hour)	Single layer(SL)				Double layer(DL)				Triple layer(TL)			
	Wt.(g)	%M	Ht (mm)	%TS(t)	Wt.(g)	%M	Ht (mm)	%TS(t)	Wt.(g)	%M	Ht (mm)	%TS(t)
0	11.836	0.000	5.50	0.000	12.614	0.000	5.82	0.000	19.182	0.000	8.46	0.000
12	12.045	1.765	5.51	0.181	12.914	2.378	5.85	0.515	19.808	3.263	8.53	0.827
24	12.156	2.703	5.53	0.545	13.159	4.320	5.88	1.030	20.348	6.078	8.58	1.418
36	12.298	3.903	5.55	0.909	13.471	6.794	5.90	1.374	20.885	8.878	8.62	1.891
48	12.384	4.629	5.56	1.090	13.624	8.006	5.92	1.718	21.321	11.151	8.66	2.364
60	12.514	5.728	5.57	1.272	13.821	9.568	5.94	2.061	21.567	12.433	8.70	2.836
72	12.606	6.505	5.58	1.454	13.950	10.591	5.96	2.405	21.814	13.721	8.73	3.191
84	12.712	7.401	5.59	1.636	14.100	11.780	5.98	2.749	22.000	14.690	8.76	3.546
96	12.724	7.502	5.60	1.818	14.159	12.248	5.99	2.920	22.158	15.514	8.77	3.664
108	12.783	8.001	5.61	2.000	14.210	12.652	6.00	3.092	22.347	16.499	8.78	3.782
120	12.790	8.060	5.61	2.000	14.230	12.811	6.00	3.092	22.400	16.776	8.79	3.900
132	12.790	8.060	5.61	2.000	14.250	12.969	6.00	3.092	22.487	17.229	8.79	3.900
144	12.790	8.060	5.61	2.000	14.251	12.977	6.00	3.092	22.487	17.229	8.79	3.900
156	12.790	8.060	5.61	2.000	14.251	12.977	6.00	3.092	22.487	17.229	8.79	3.900

t: Immersion time, **Wt.:** Weight of the sample at time t, **%M**: Moisture absorption percentage , Ht :Thickness at time t, **%TS(t)** : Thickness swelling percentage at time t.

Table-4.2 Variation of weight gain and thickness swelling of untreated Single layer (SL), Double layer (DL) and Triple layer (TL) LC-epoxy composite exposed to distilled water environment.

t (Hour)	Single layer(SL)				Double layer(DL)				Triple layer(TL)			
	Wt.(g)	%M	Ht (mm)	%TS(t)	Wt.(g)	%M	Ht (mm)	%TS(t)	Wt.(g)	%M	Ht (mm)	%TS(t)
0	12.761	0.000	5.9	0	12.367	0.000	4.991	0.000	19.295	0.000	6.681	0
12	12.921	1.253	5.91	0.169	12.600	1.884	5.011	0.400	19.892	3.094	6.722	0.613
24	13.100	2.656	5.93	0.508	12.845	3.865	5.031	0.801	20.400	5.726	6.761	1.197
36	13.326	4.427	5.94	0.677	13.134	6.201	5.048	1.142	21.013	8.903	6.792	1.661
48	13.468	5.540	5.95	0.847	13.435	8.635	5.071	1.602	21.518	11.521	6.821	2.095
60	13.613	6.676	5.97	1.186	13.73	11.021	5.092	2.023	21.929	13.651	6.849	2.514
72	13.721	7.522	5.98	1.355	13.949	12.792	5.111	2.404	22.258	15.356	6.881	2.993
84	13.861	8.620	5.99	1.525	14.096	13.980	5.131	2.805	22.694	17.615	6.912	3.457
96	13.900	8.925	6.01	1.864	14.165	14.538	5.162	3.426	22.900	18.683	6.942	3.906
108	13.914	9.035	6.02	2.033	14.245	15.185	5.171	3.606	22.960	18.994	6.951	4.041
120	13.915	9.043	6.03	2.203	14.246	15.193	5.171	3.606	22.961	18.999	6.951	4.041
132	13.916	9.051	6.03	2.203	14.247	15.201	5.171	3.606	22.962	19.004	6.951	4.041
144	13.917	9.058	6.03	2.203	14.247	15.201	5.171	3.606	22.962	19.004	6.951	4.041
156	13.917	9.058	6.03	2.203	14.247	15.201	5.171	3.606	22.962	19.004	6.951	4.041

t: Immersion time, **Wt.:** Weight of the sample at time t, **%M**: Moisture absorption percentage , **Ht** :Thickness at time t, **%TS(t)** : Thickness swelling percentage at time t.

Table 4.3 Variation of weight gain and thickness swelling of untreated Single layer (SL), Double layer (DL) and Triple layer (TL) LC-epoxy composite exposed to sub-zero temp environment.

t (Hour)	Single layer(SL)				Double layer(DL)				Triple layer(TL)			
	Wt.(g)	%M	Ht (mm)	%TS(t)	Wt.(g)	%M	Ht (mm)	%TS(t)	Wt.(g)	%M	Ht (mm)	%TS(t)
0	12.69	0.000	5.241	0.000	15.673	0.00	6.800	0.00	14.534	0	6.812	0
12	12.699	1.253	5.252	0.209	15.695	0.140	6.815	0.220	14.569	0.240	6.833	0.308
24	12.720	2.656	5.261	0.381	15.734	0.389	6.831	0.455	14.614	0.550	6.852	0.587
36	12.740	4.427	5.267	0.496	15.764	0.580	6.842	0.617	14.665	0.901	6.866	0.792
48	12.769	5.540	5.271	0.572	15.814	0.899	6.851	0.750	14.714	1.238	6.876	0.939
60	12.789	6.676	5.277	0.686	15.857	1.173	6.859	0.867	14.763	1.575	6.887	1.100
72	12.820	7.522	5.280	0.744	15.88	1.320	6.871	1.044	14.795	1.795	6.892	1.174
84	12.834	8.620	5.284	0.820	15.908	1.499	6.876	1.117	14.825	2.002	6.897	1.247
96	12.850	8.925	5.286	0.858	15.929	1.633	6.881	1.191	14.839	2.098	6.902	1.321
108	12.862	9.035	5.289	0.915	15.945	1.735	6.881	1.191	14.843	2.126	6.902	1.321
120	12.865	9.043	5.289	0.915	15.96	1.831	6.881	1.191	14.844	2.132	6.902	1.321
132	12.866	9.051	5.289	0.915	15.964	1.856	6.881	1.191	14.844	2.132	6.902	1.321
144	12.868	9.058	5.289	0.915	15.964	1.856	6.881	1.191	14.844	2.132	6.902	1.321
156	12.868	9.058	5.289	0.915	14.247	15.201	5.171	3.606	14.844	2.132	6.902	1.321

t: Immersion time, **Wt.:** Weight of the sample at time t, **%M**: Moisture absorption percentage , **Ht** :Thickness at time t, **%TS(t)** : Thickness swelling percentage at time t.

Table-4.4 Variation of weight gain and thickness swelling of Alkali treated, Benzoyl chloride treated and KMnO4 treated LC-epoxy composite exposed to saline water environment.

t (Hour)	Alkali treated (DL)				Benzoyl chloride (DL)				KMnO4 (DL)			
	Wt.(g)	%M	Ht (mm)	%TS(t)	Wt.(g)	%M	Ht (mm)	%TS(t)	Wt.(g)	%M	Ht (mm)	%TS(t)
0	16.183	0	4.93	0	15.227	0	6.13	0	11	0	4.23	0
12	16.32	0.846	4.94	0.202	15.261	0.223	6.132	0.032	11.04	0.363	4.233	0.071
24	16.42	1.464	4.945	0.304	15.269	0.275	6.134	0.065	11.063	0.572	4.237	0.165
36	16.513	2.039	4.955	0.507	15.283	0.367	6.138	0.130	11.081	0.736	4.241	0.260
48	16.557	2.311	4.96	0.608	15.304	0.505	6.144	0.228	11.104	0.945	4.245	0.354
60	16.679	3.064	4.965	0.709	15.306	0.518	6.147	0.277	11.104	0.945	4.248	0.425
72	16.684	3.095	4.97	0.811	15.319	0.604	6.151	0.342	11.113	1.027	4.251	0.496
84	16.695	3.163	4.976	0.933	15.33	0.676	6.154	0.391	11.128	1.163	4.254	0.567
96	16.732	3.392	4.981	1.034	15.331	0.682	6.159	0.473	11.123	1.118	4.258	0.661
108	16.736	3.417	4.986	1.135	15.344	0.768	6.162	0.522	11.149	1.354	4.261	0.732
120	16.741	3.448	4.992	1.257	15.352	0.820	6.165	0.570	11.156	1.418	4.263	0.780
132	16.745	3.472	4.997	1.359	15.377	0.985	6.169	0.636	11.188	1.709	4.266	0.851
144	16.746	3.478	5.003	1.480	15.375	0.971	6.172	0.685	11.188	1.709	4.268	0.898
156	16.747	3.485	5.008	1.582	15.378	0.991	6.175	0.734	11.189	1.718	4.272	0.992
168	16.748	3.491	5.013	1.683	15.377	0.985	6.178	0.783	11.189	1.718	4.275	1.063
180	16.749	3.497	5.017	1.764	15.344	0.768	6.182	0.848	11.19	1.727	4.278	1.134
192	16.75	3.503	5.021	1.845	15.36	0.873	6.185	0.897	11.19	1.727	4.28	1.182
204	16.751	3.5098	5.024	1.906	15.37	0.939	6.189	0.962	11.197	1.790	4.284	1.276
216	16.752	3.516	5.026	1.947	15.377	0.985	6.193	1.027	11.173	1.572	4.286	1.323
228	16.753	3.522	5.028	1.987	15.371	0.945	6.197	1.092	11.193	1.754	4.288	1.371
240	16.754	3.528	5.03	2.028	15.377	0.985	6.2	1.141	11.179	1.627	4.289	1.394
252	16.755	3.534	5.03	2.028	15.374	0.965	6.2	1.141	11.194	1.763	4.289	1.394

264	16.756	3.540	5.03	2.028	15.388	1.057	6.2	1.141	11.216	1.963	4.289	1.394
276	16.758	3.553	5.03	2.0283	15.4	1.136	6.2	1.141	11.223	2.027	4.289	1.394
298	16.758	3.553	5.03	2.0283	15.398	1.123	6.2	1.141	11.22	2.000	4.289	1.394
310	16.758	3.553	5.03	2.028	15.405	1.168	6.2	1.141	11.253	2.300	4.289	1.394
322	16.758	3.553	5.03	2.028	15.405	1.168	6.2	1.141	11.245	2.227	4.289	1.394
t: Immersion time, **Wt.:** Weight of the sample at time t, **%M**: Moisture absorption percentage , **Ht** :Thickness at time t, **%TS(t)** : Thickness swelling percentage at time t.												

Table -4.5 Variation of weight gain and thickness swelling of Alkali treated, Benzoyl-chloride treated and KMnO4 treated LC-epoxy composite exposed to distilled water environment.

t (Hour)	**Alkali treated (DL)**				**Benzoyl chloride (DL)**				**KMnO4 (DL)**			
	Wt.(g)	**%M**	**Ht (mm)**	**%TS(t)**	**Wt.(g)**	**%M**	**Ht (mm)**	**%TS(t)**	**Wt.(g)**	**%M**	**Ht (mm)**	**%TS(t)**
0	14.138	0	7.47	0	14.432	0	5.82	0	11.189	0	4.38	0
12	14.235	0.686	7.478	0.107	14.48	0.332	5.825	0.085	11.246	0.509	4.384	0.091
24	14.358	1.556	7.488	0.240	14.488	0.388	5.83	0.171	11.266	0.688	4.388	0.182
36	14.487	2.468	7.499	0.388	14.518	0.595	5.835	0.257	11.286	0.866	4.39	0.228
48	14.541	2.850	7.51	0.535	14.528	0.665	5.84	0.343	11.289	0.8937	4.393	0.296
60	14.635	3.515	7.521	0.682	14.509	0.533	5.845	0.429	11.286	0.866	4.396	0.365
72	14.741	4.265	7.529	0.789	14.518	0.595	5.85	0.515	11.297	0.965	4.398	0.410
84	14.852	5.050	7.538	0.910	14.558	0.873	5.853	0.567	11.332	1.2780	4.402	0.502
96	14.89	5.318	7.548	1.044	14.545	0.782	5.855	0.601	11.332	1.278	4.405	0.570
108	14.934	5.630	7.559	1.191	14.555	0.852	5.857	0.635	11.357	1.501	4.409	0.662
120	14.974	5.913	7.568	1.311	14.556	0.859	5.858	0.652	11.344	1.385	4.413	0.753
132	14.986	5.998	7.575	1.405	14.603	1.184	5.86	0.687	11.387	1.7695	4.416	0.821
144	14.996	6.068	7.586	1.552	14.587	1.074	5.863	0.73	11.384	1.742	4.419	0.890

156	14.999	6.089	7.597	1.700	14.588	1.080	5.866	0.790	11.384	1.742	4.423	0.981
168	15.001	6.104	7.61	1.874	14.589	1.087	5.869	0.841	11.385	1.751	4.426	1.050
180	15.015	6.203	7.615	1.941	14.591	1.101	5.874	0.927	11.379	1.698	4.43	1.141
192	15.023	6.259	7.62	2.008	14.595	1.129	5.878	0.996	11.379	1.698	4.434	1.232
204	15.028	6.295	7.625	2.074	14.598	1.150	5.881	1.048	11.402	1.903	4.439	1.347
216	15.029	6.302	7.631	2.155	14.598	1.150	5.885	1.116	11.379	1.698	4.443	1.438
228	15.03	6.309	7.636	2.222	14.607	1.212	5.888	1.168	11.407	1.948	4.446	1.506
240	15.031	6.316	7.637	2.235	14.603	1.184	5.888	1.168	11.378	1.689	4.45	1.598
252	15.032	6.323	7.638	2.248	14.609	1.226	5.888	1.168	11.411	1.984	4.45	1.598
264	15.033	6.330	7.638	2.248	14.606	1.205	5.888	1.168	11.396	1.850	4.45	1.598
276	15.033	6.330	7.638	2.248	14.624	1.330	5.888	1.168	11.438	2.225	4.45	1.598
298	15.033	6.330	7.638	2.248	14.628	1.358	5.888	1.168	11.43	2.153	4.45	1.598
310	15.033	6.330	7.638	2.248	14.636	1.413	5.888	1.168	11.457	2.395	4.45	1.598
322	15.033	6.330	7.638	2.248	14.636	1.413	5.888	1.168	11.457	2.395	4.45	1.598

t: Immersion time, **Wt.:** Weight of the sample at time t, **%M**: Moisture absorption percentage , **Ht** :Thickness at time t, **%TS(t)** : Thickness swelling percentage at time t.

Table -4.6 Variation of weight gain and thickness swelling of Alkali treated, Benzoyl chloride treated and KMnO4 treated LC-epoxy composite exposed to Sub-zero temperature environment.

t (Hour)	**Alkali treated (DL)**				**Benzoyl chloride (DL)**				**Triple layer (TL)**			
	Wt.(g)	**%M**	**Ht (mm)**	**%TS(t)**	**Wt.(g)**	**%M**	**Ht (mm)**	**%TS(t)**	**Wt.(g)**	**%M**	**Ht (mm)**	**%TS(t)**
0	11.525	0	4.93	0	12.965	0	4.82	0	10.428	0	3.95	0
12	11.541	0.138	4.936	0.1217	12.97	0.038	4.822	0.041	**10.438**	0.095	3.953	0.075
24	11.546	0.182	4.94	0.202	12.975	0.077	4.825	0.103	10.442	0.134	3.956	0.151
36	11.55	0.216	4.945	0.304	12.98	0.115	4.827	0.145	10.444	0.153	3.958	0.202

48	11.555	0.260	4.949	0.385	12.983	0.138	4.829	0.186	10.446	0.172	3.96	0.253
60	11.56	0.303	4.953	0.466	12.984	0.146	4.833	0.269	10.449	0.201	3.963	0.329
72	11.566	0.355	4.955	0.507	12.985	0.154	4.836	0.331	10.451	0.220	3.965	0.379
84	11.568	0.373	4.96	0.608	12.985	0.154	4.837	0.352	10.453	0.239	3.967	0.430
96	11.57	0.390	4.964	0.689	12.989	0.185	4.838	0.373	10.455	0.258	3.969	0.481
108	11.573	0.416	4.966	0.730	12.995	0.231	4.839	0.394	10.459	0.297	3.971	0.531
120	11.578	0.459	4.967	0.750	12.995	0.231	4.84	0.414	10.464	0.345	3.972	0.556
132	11.58	0.477	4.968	0.770	12.992	0.208	4.841	0.435	10.462	0.326	3.974	0.607
144	11.583	0.503	4.969	0.791	13	0.269	4.842	0.456	10.465	0.354	3.975	0.632
156	11.585	0.520	4.97	0.811	13.001	0.277	4.843	0.477	10.468	0.383	3.976	0.658
168	11.587	0.537	4.97	0.811	13.003	0.293	4.844	0.497	10.471	0.412	3.977	0.683
180	11.589	0.555	4.97	0.811	13.009	0.339	4.845	0.518	10.475	0.450	3.977	0.683
192	11.591	0.572	4.97	0.811	13.01	0.347	4.846	0.539	10.478	0.479	3.978	0.708
204	11.595	0.607	4.97	0.811	13.015	0.385	4.846	0.539	10.481	0.508	3.978	0.708
216	11.598	0.633	4.97	0.811	13.01	0.347	4.847	0.560	10.484	0.537	3.978	0.708
228	11.599	0.642	4.97	0.811	13.012	0.362	4.847	0.560	10.487	0.565	3.978	0.708
240	11.603	0.676	4.97	0.811	13.016	0.393	4.847	0.560	10.491	0.604	3.978	0.708
252	11.608	0.720	4.97	0.811	13.016	0.393	4.847	0.560	10.491	0.604	3.978	0.708
264	11.61	0.737	4.97	0.811	13.016	0.393	4.847	0.560	10.491	0.604	3.978	0.708
276	11.611	0.746	4.97	0.811	13.016	0.393	4.847	0.560	10.491	0.604	3.978	0.708
298	11.612	0.754	4.97	0.811	13.016	0.393	4.847	0.560	10.491	0.604	3.978	0.708
310	11.457	2.395	4.45	1.598	11.613	0.763	4.970	0.8113	13.016	0.393	4.847	0.560
322	11.457	2.395	4.45	1.598	11.614	0.772	4.970	0.8113	13.016	0.393	4.847	0.560

t: Immersion time, **Wt.:** Weight of the sample at time t, **%M**: Moisture absorption percentage , **Ht** :Thickness at time t, **%TS(t)** : Thickness swelling percentage at time t.

Figure-4.5 to 4.7 shows that the moisture absorption behavior of the chemically treated fiber (DL) reinforced epoxy composites when exposed to different environmental treatment. It is observed from plots that, for treated LC-epoxy composites, the moisture absorption rate increases slowly and continues for a longer time to achieve equilibrium moisture compared to untreated fiber composite. This increase in moisture absorption is consistent with some other studies on natural fiber reinforced composites [200-201]. Also it is observed that the treatment of fiber with alkali, benzoyl chloride, and KMnO4 reduced the affinity of fibers to moisture. Due to surface modification by chemical treatment, the fibers get masked with the epoxy resin with a stronger adhesion, resulting in greater hydrophobicity and less moisture absorption [202]. In comparison to all the chemical treatments, the Benzoyl-Chloride process showed considerable reduction in moisture absorption. In case of Benzoyl-Chloride treated fiber composite, the maximum moisture absorption was reduced by 91.01% in saline water, while it is 90% in distilled water and 60% in subzero environment (Figure-4.8). Similar type of observation is also reported by other chemical treated NF reinforced composites subjected to water absorption [203].

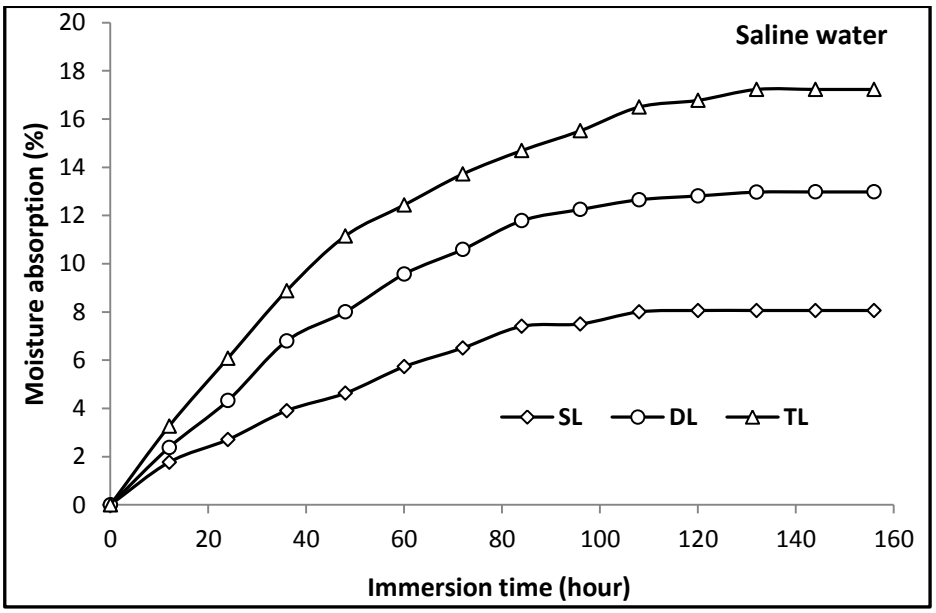

Figure-4.1 Variation of moisture absorption of the untreated LC-epoxy composites with immersion time exposed at saline water.

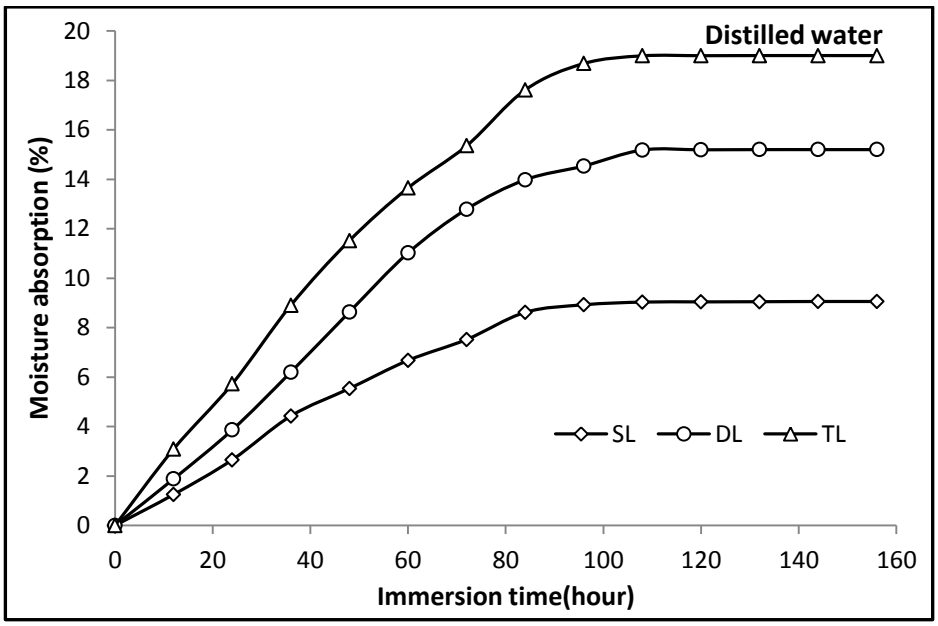

Figure-4.2 Variation of moisture absorption of the untreated LC-epoxy composites with immersion time exposed at distilled water.

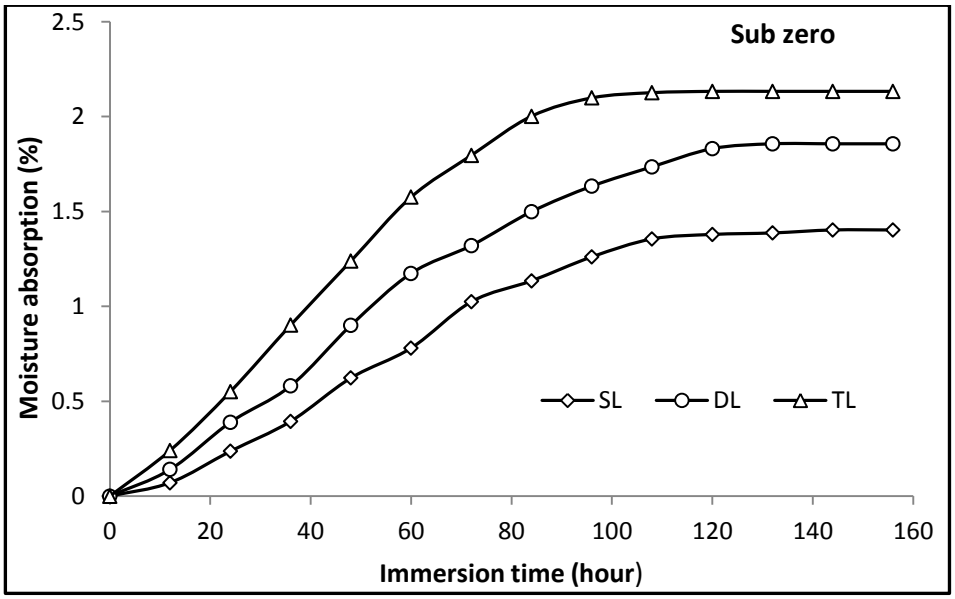

Figure-4.3 Variation of moisture absorption of the untreated LC- epoxy composites with immersion time exposed at sub-zero temperature.

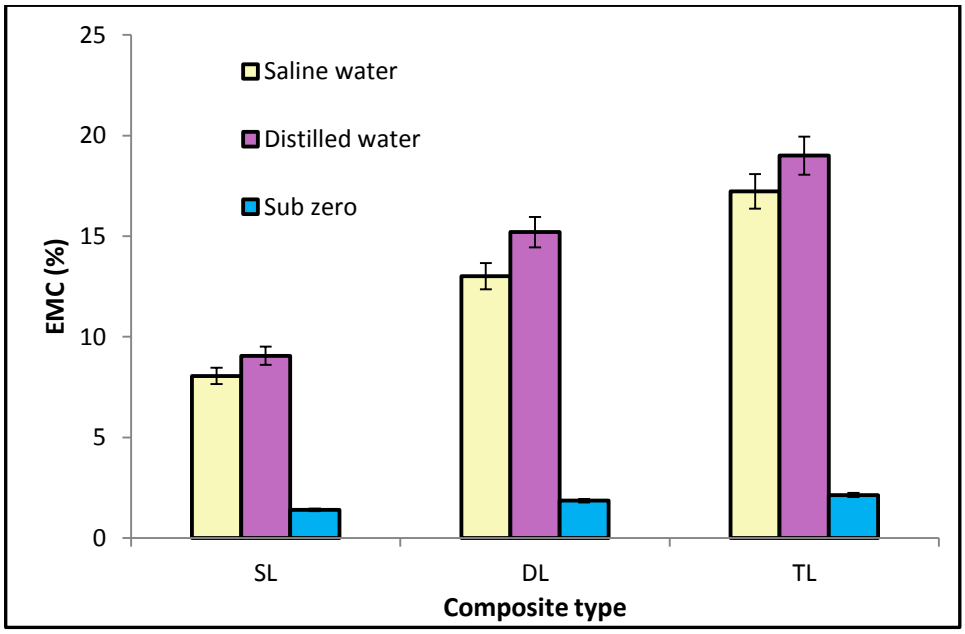

Figure-4.4 Maximum moisture absorption of untreated LC-epoxy composite versus fiber loading exposed in different environments.

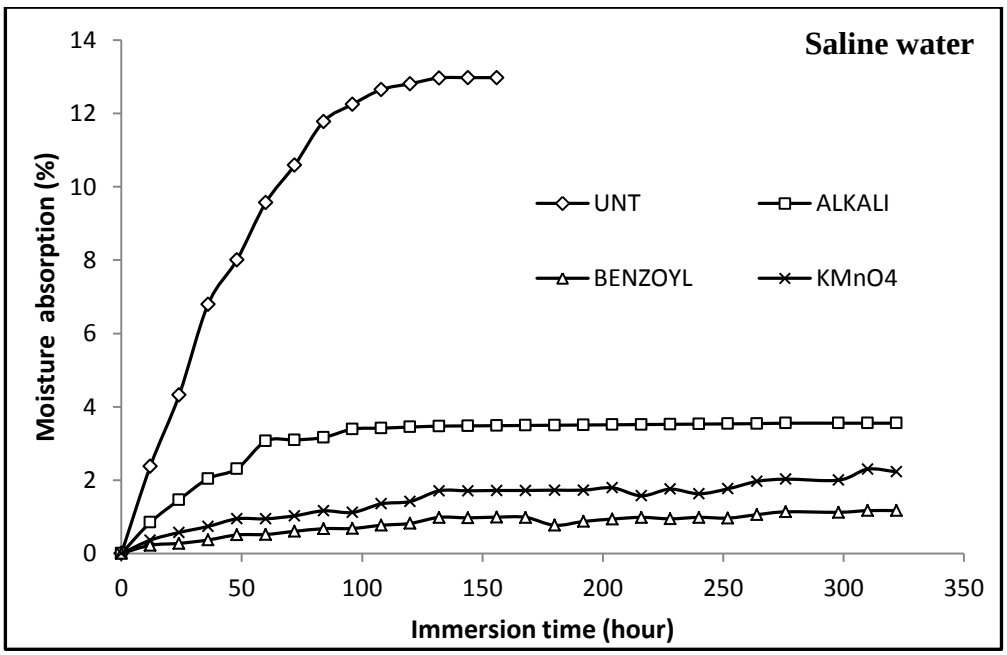

Figure-4.5 Variation of moisture absorption of the treated LC- epoxy composites with immersion time exposed at saline water.

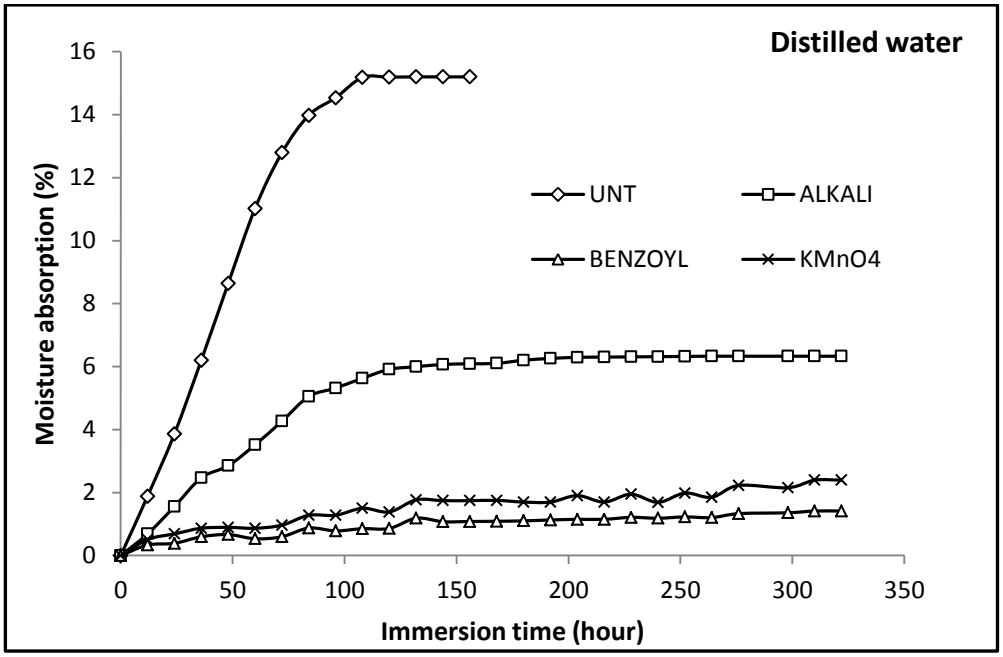

Figure-4.6 Variation of moisture absorption of the treated LC- epoxy composites with immersion time exposed at distilled water.

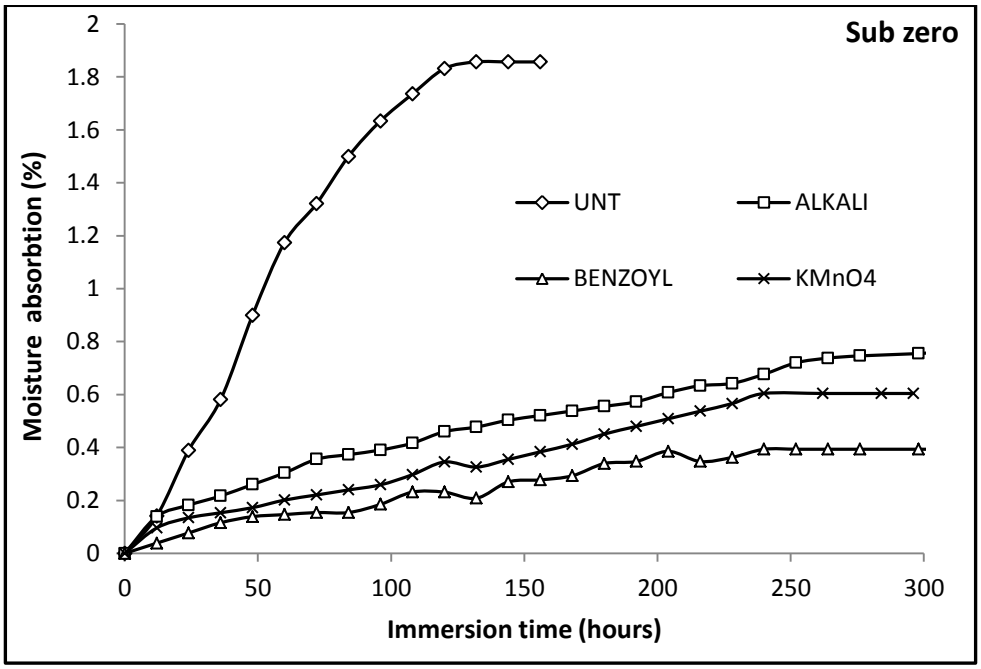

Figure-4.7 Variation of moisture absorption of the treated LC- epoxy composites with immersion time exposed at sub-zero temp.

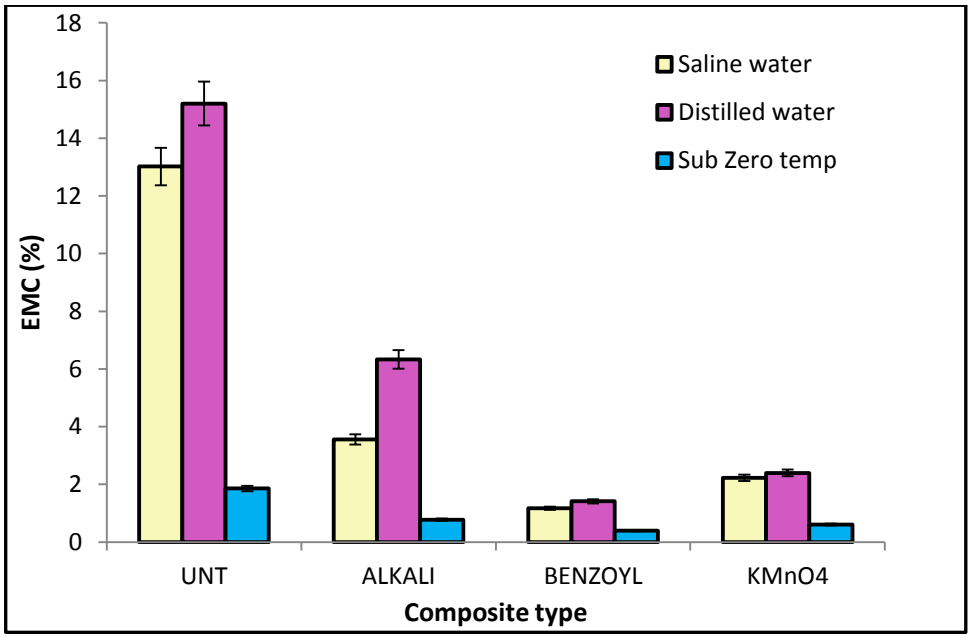

Figure-4.8 Maximum moisture absorption of treated LC-epoxy composite versus fiber loading exposed in different environment.

4.3.1.1 Mechanism of Water Transport

The water sorption kinetics in LC-epoxy composite has been studied based on the Fick's theory and adjusting the experimental values to the following equation which is derived from Eq. (4.1).

$$\log (M_t / M_m) = \log (k) + n \log (t) \qquad (4.4)$$

The value of k and n were determined from the slope and the intercept of M_t / M_m versus 't' in the log plot which was drawn from experimental data of moisture absorption with time. Figure-4.9 to 4.11 and Figure-4.12 to 4.14 showed the typical curve of log (M_t/M_m) as a function of log (t) for untreated and treated Luffa cylindrica reinforced epoxy composite respectively. The values of k and n resulting from the fitting of all formulations are shown in Table-4.7. It was observed that the value of n is close to 0.5 for both untreated and treated composites. This confirms that the Fickian diffusion in lignocellulosic composites, can be adequately describe the moisture absorption in the composite, which is consistent with previous studies [204, 174]. Deo et al [194] and Espert et al [177] also observed that the value of n is closed to 0.5 while

they studied with lantana camara and pine oreucalyptus wood, one-year crops such as coir, sisal reinforced polymer composite respectively. A higher value of n and k indicates that the composite needs shorter time to attain equilibrium water absorption. The value of k was found to increases with increasing fiber content for LC-epoxy composite in all environments resulting higher moisture absorption initially. However the K values are lower for treated fiber composite as compared to untreated fiber composites.

Next step was the performance of an analysis of the parameters of this theoretical model.The diffusion coefficient (D) is one of the important parameters of Fick's model, and that shows the ability of water molecules to diffusion into the composite structures. The values of D can be calculated by weight gain measurements of samples by considering the initial slope of moisture absorption (Mt) vs. square root of time by using the following equation [205].

$$D = \pi \left[\frac{h}{4M_m}\right]^2 \left[\frac{M_2 - M_1}{\sqrt{t_2} - \sqrt{t_1}}\right]^2 \quad (4.5)$$

Where 'M_m' is the moisture content at saturation point, 'h' is the sample thickness, 't_1' and 't_2' are the selected points for time in the initial linear portion of M_t vs. $\sqrt{t}$ curve. 'M_1' and 'M_2' are moisture content at time t_1 and t_2. Figure-4.15 to 4.20 shows the diffusion coefficient curve-fitting plot for M_t verses square root of time (t) composites immersed in different environments. The calculated values of D are listed in Table-4.8. From the table it is observed that the diffusion coefficient (D) values increases with an increase in fiber content in all three environments. The increase is more pronounced for the specimens subjected to distilled water than those subjected to saline water and sub-zero environments. Higher fiber-loaded samples triple layer reinforced epoxy composites shows highest diffusivity due to higher cellulose content for all the environmental conditions. Also it can be seen that the (D) for treated composites are lower compared to the untreated fiber composite for all environments. This type of behavior occurs because the rate of diffusion is less with treated fiber with better fiber-matrix adhesion which decreases the velocity of diffusion in interfacial gap and blocking of Hydroxyl group [177]. The value of diffusion coefficient was found in the range of 9.89×10^{-7} to 1.41×10^{-10} mm^2/sec which is in conformity with the work of H Amari et al. with recycled cellulose fiber reinforced epoxy composites [206].

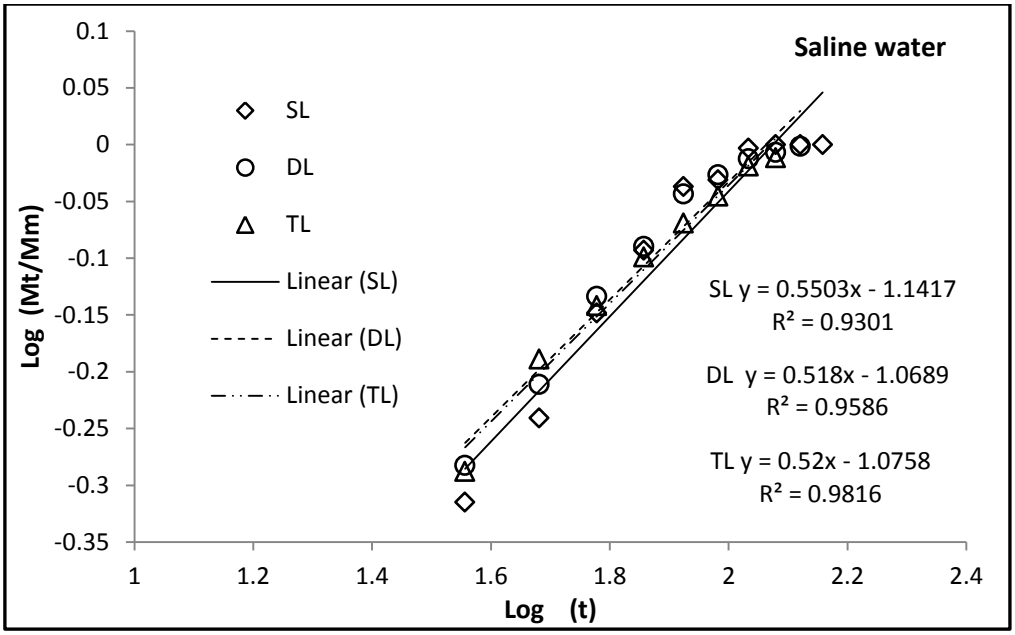

Figure-4.9 Diffusion curve fitting for untreated LC-epoxy composites under saline water environment.

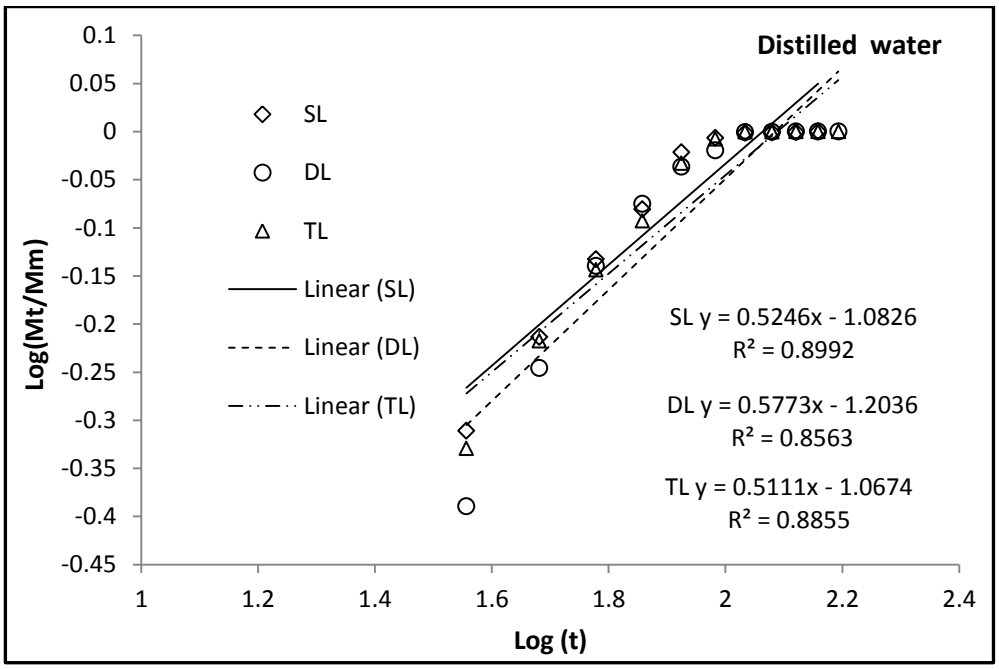

Figure-4.10 Diffusion curve fitting for untreated LC-epoxy composites under distilled water environment.

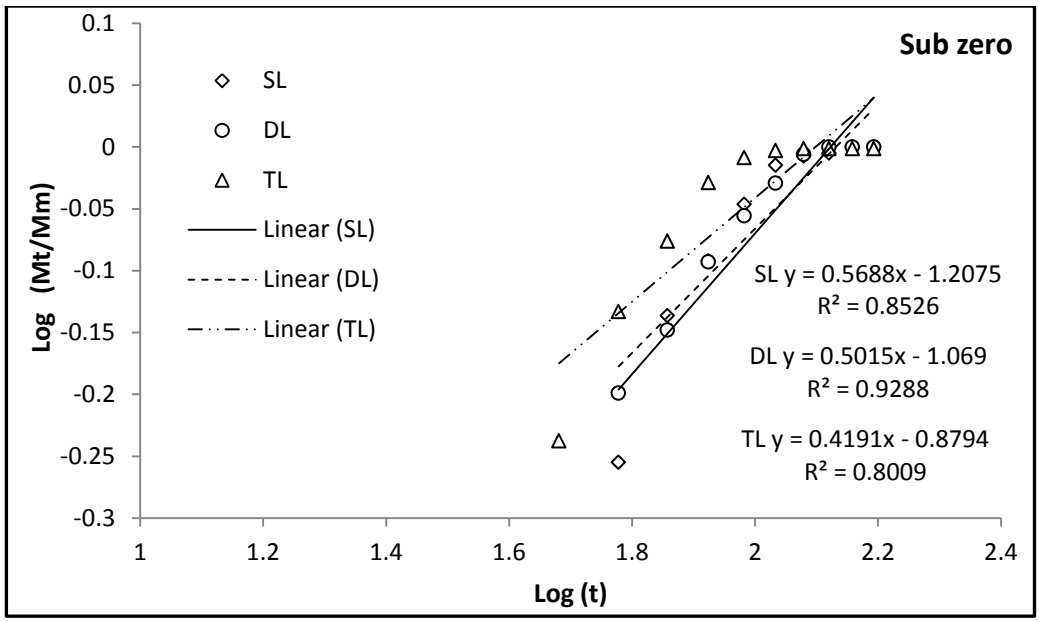

Figure-4.11 Diffusion curve fitting for untreated LC-epoxy composites under sub-zero temperature environment.

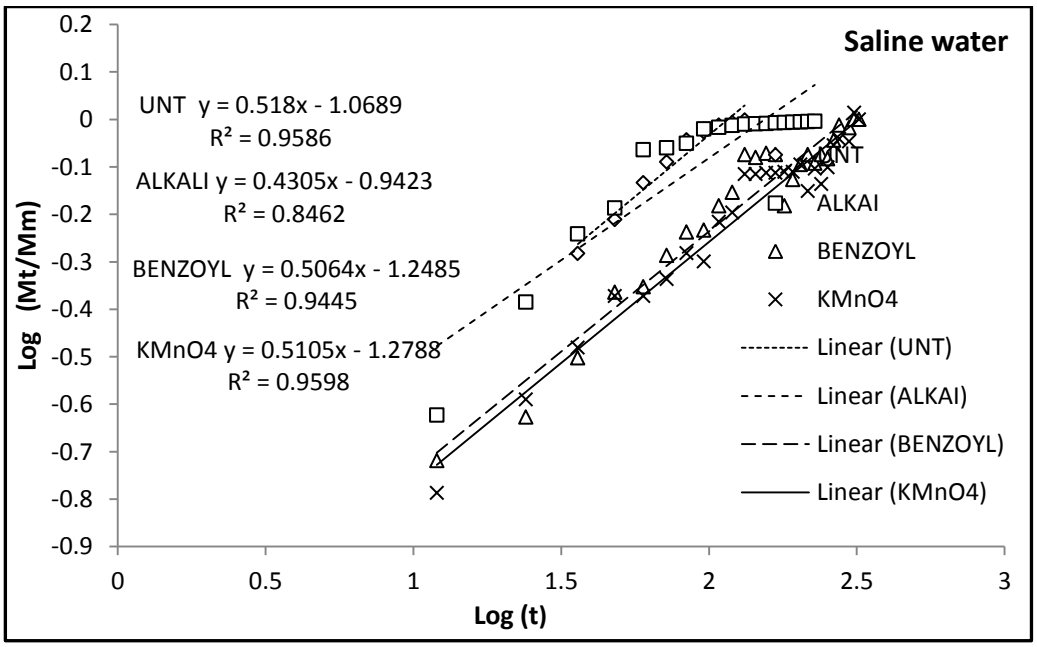

Figure-4.12 Diffusion curve fitting for Treated LC- epoxy composites under saline water environment.

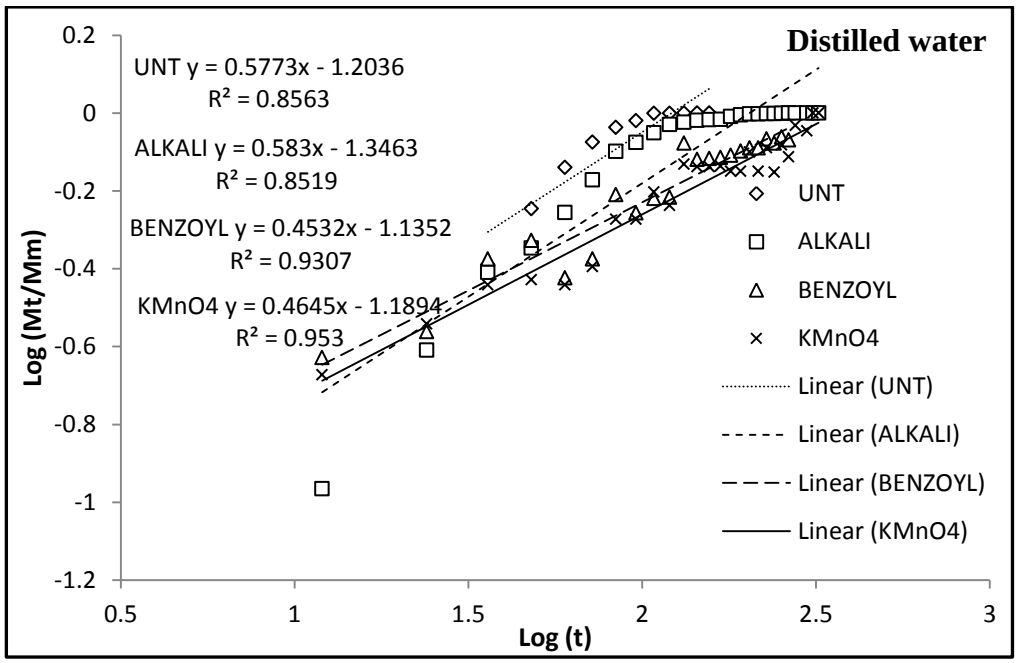

Figure-4.13 Diffusion curve fitting for Treated LC- epoxy composites under distilled water environment.

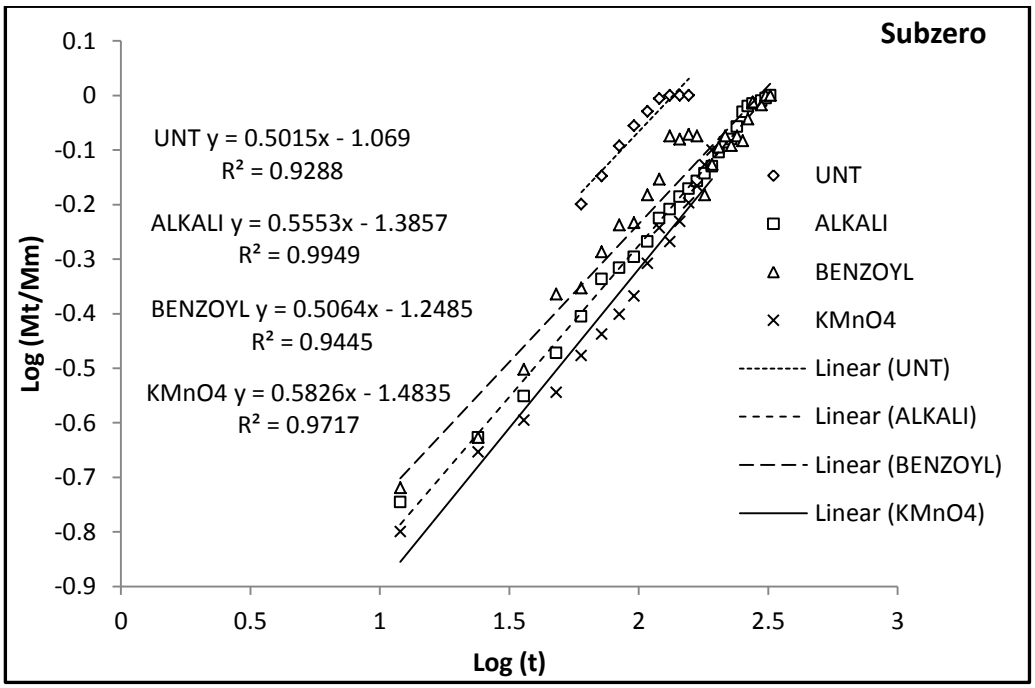

Figure-4.14 Diffusion curve fitting for treated LC-epoxy composites under sub-zero temperature environment.

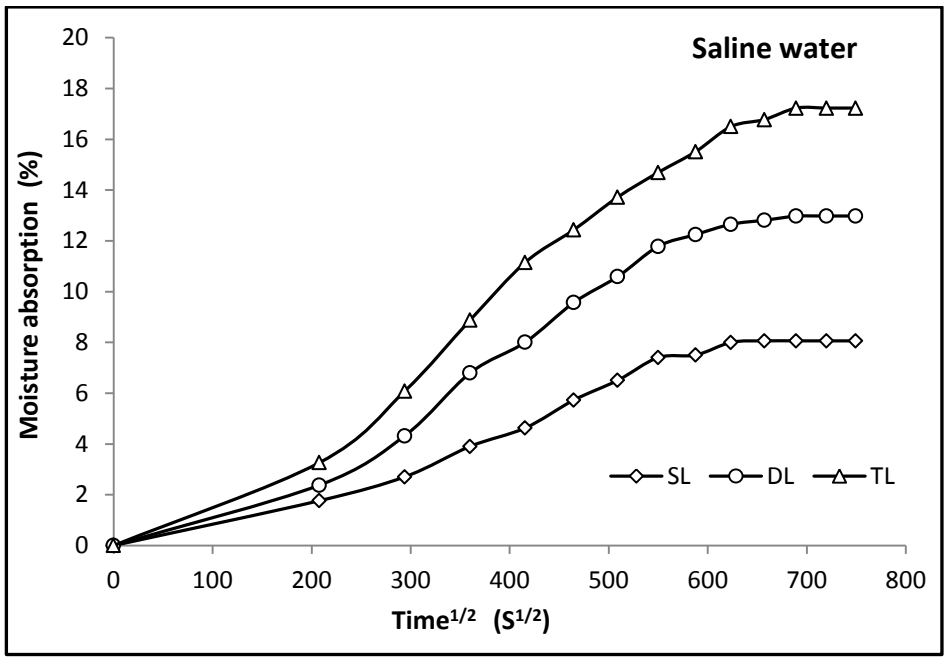

Figure-4.15 Variation of moisture absorption of untreated LC- epoxy composites with square root of immersion time at saline water environment.

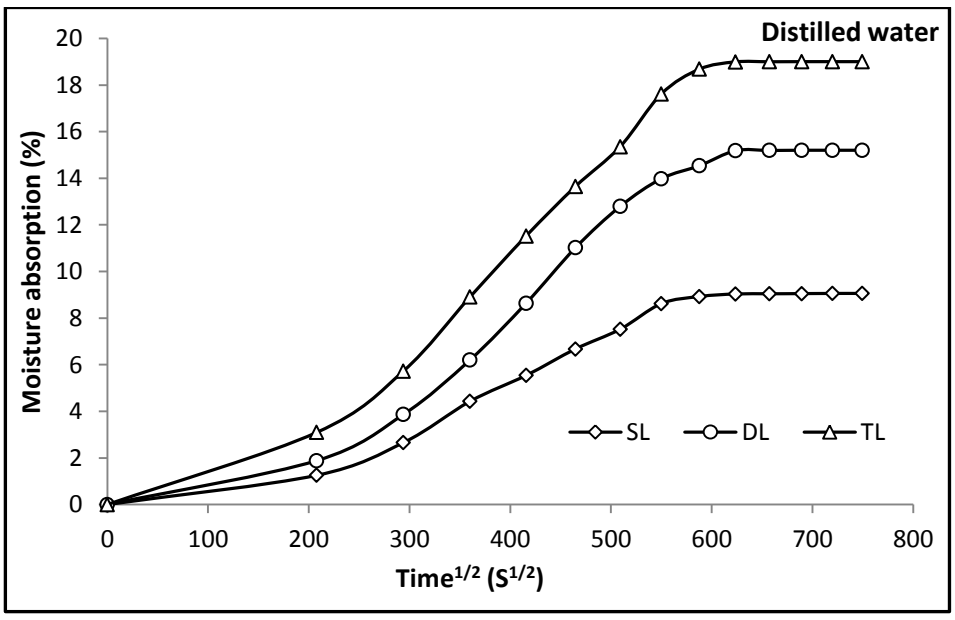

Figure-4.16 Variation of moisture absorption of untreated LC-epoxy composites with square root of immersion time at distilled water environment.

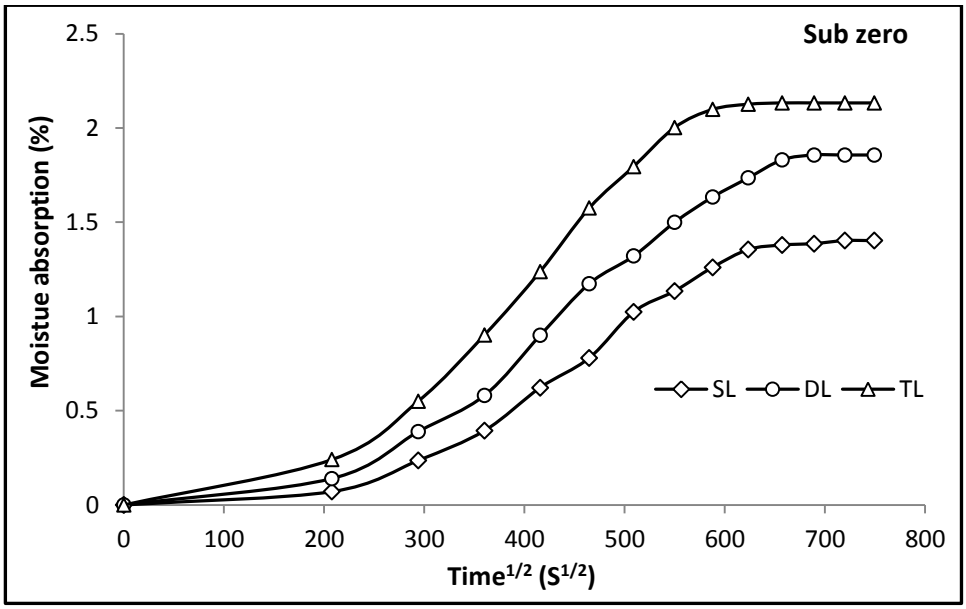

Figure-4.17 Variation of moisture absorption of untreated LC- epoxy composites with square root of immersion time at sub-zero temperature environment.

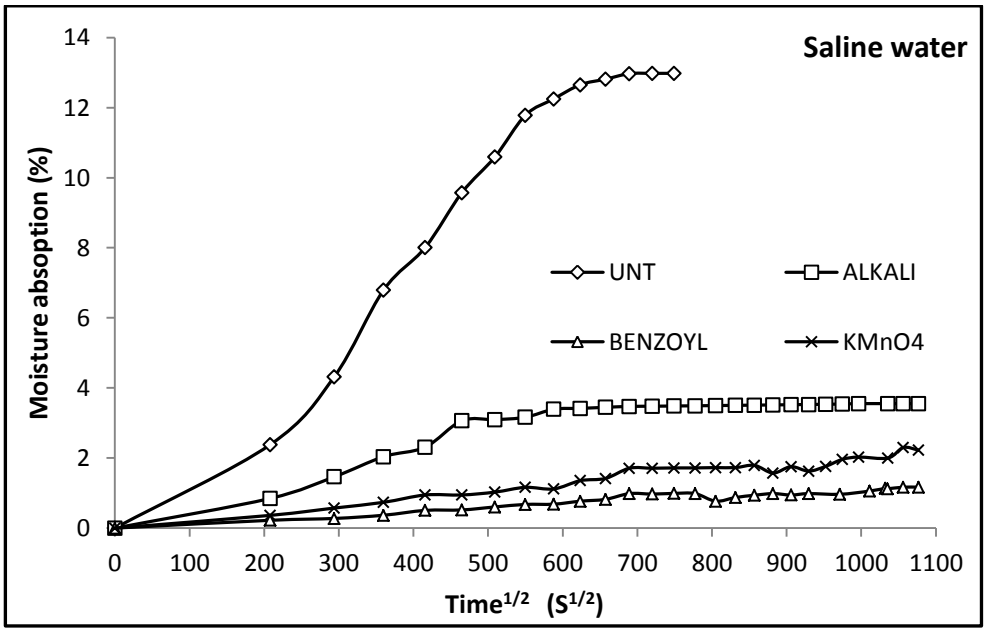

Figure-4.18 Variation of moisture absorption of treated LC-epoxy composites with square root of immersion time at saline water environment.

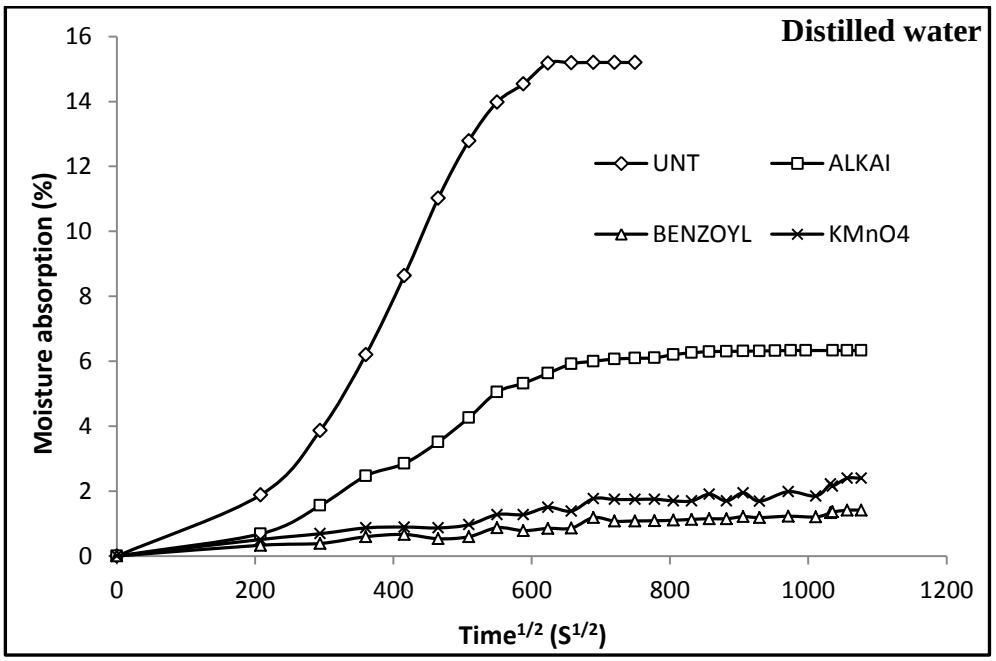

Figure-4.19 Variation of moisture absorption of treated LC- epoxy composites with square root of immersion time at distilled water environment.

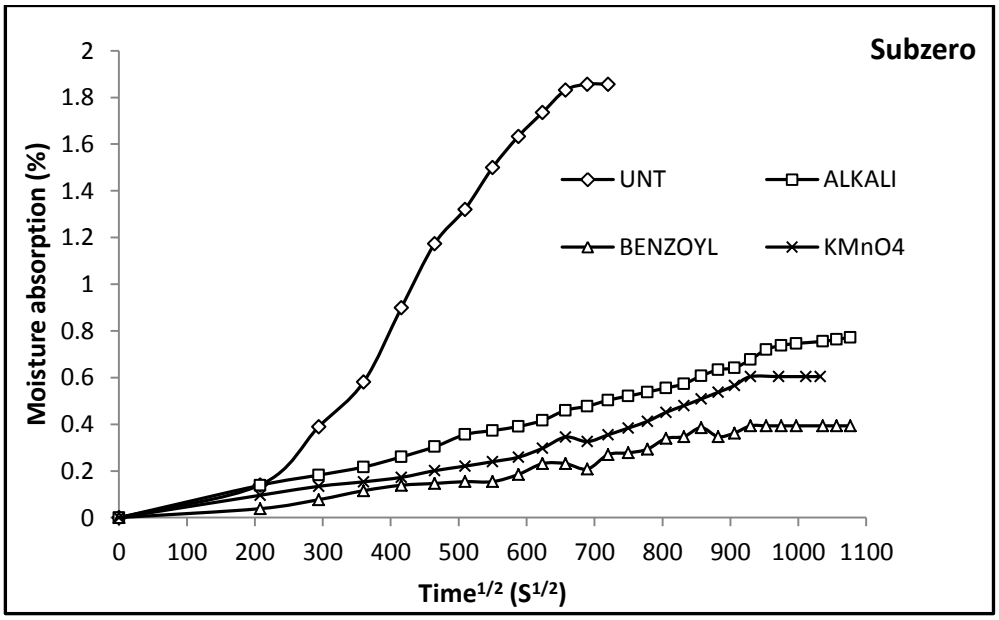

Figure-4.20 Variation of moisture absorption of treated LC - epoxy composites with square root of immersion time at sub-zero temperature environment.

Table-4.7 Diffusion case selection parameters of untreated and treated LC-epoxy composites at different environments.

Environment	Fiber content	Type of Fiber	n	K	R^2
Saline water	SL	Untreated	0.5503	0.072	0.9301
	DL	Untreated	0.518	0.085	0.9586
	TL	Untreated	0.52	0.083	0.9816
	DL	Alkali	0.4305	0.1142	0.8462
	DL	Benzoyl	0.506	0.0564	0.9445
	DL	KMnO4	0.5105	0.0526	0.9598
Distilled water	SL	Untreated	0.5246	0.082	0.8992
	DL	Untreated	0.5773	0.063	0.8563
	TL	Untreated	0.5111	0.084	0.8855
	DL	Alkali	0.583	0.045	0.8519
	DL	Benzoyl	0.4532	0.0732	0.9307
	DL	KMnO4	0.4645	0.0646	0.953
Sub-Zero Temperature	SL	Untreated	0.5688	0.062	0.8526
	DL	Untreated	0.5015	0.085	0.9288
	TL	Untreated	0.4191	0.132	0.8009
	DL	Alkali	0.5553	0.0411	0.9949
	DL	Benzoyl	0.5064	0.0564	0.9445
	DL	KMnO4	0.5826	0.0328	0.9717

Table-4.8 Diffusibility of untreated and treated LC-epoxy composites at different environments.

Environment	Fiber content	Type of Fiber	EMC (%)	Diffusibility D (mm2/s)
Saline water	SL	Untreated	8.05	3.02×10^{-7}
	DL	Untreated	13.01	5.50×10^{-7}
	TL	Untreated	17.23	5.82×10^{-7}
	DL	Alkali Treated	3.55	4.06×10^{-7}
	DL	Benzoyl	1.168	1.78×10^{-8}
	DL	KMnO4	2.227	4.29×10^{-8}
Distilled water	SL	Untreated	9.05	5.99×10^{-7}
	DL	Untreated	15.20	3.83×10^{-7}
	TL	Untreated	19.01	9.89×10^{-7}
	DL	Alkali Treated	6.33	4.04×10^{-7}
	DL	Benzoyl	1.41	1.41×10^{-10}
	DL	KMnO4	2.39	2.4×10^{-8}
Sub-Zero Temperature	SL	Untreated	1.40	4.65×10^{-8}
	DL	Untreated	1.85	6.73×10^{-8}
	TL	Untreated	2.13	1.71×10^{-7}
	DL	Alkali Treated	0.77	4.43×10^{-8}
	DL	Benzoyl	0.39	1.00×10^{-7}
	DL	KMnO4	0.60	7.41×10^{-9}

4.3.2 Thickness swelling behavior

The thickness swelling processes for LC-epoxy composites at different environments has been studied by considering the thickness swelling (TS) and swelling rate parameter (K_{SR}). The value of K_{SR} was evaluated through a non-linear regression curve fitting method to fit the experimental data (table-4.9) in equation-4.6 [207], using computer software with curve fitting routines.

$$TS(t) = \left[\frac{H_\infty}{H_0+(H_\infty-H_0)e^{-K_{SR}\,t}} - 1\right] \times 100 \qquad (4.6)$$

Where *'TS (t)'* is the thickness swelling at a specific time (t), *'H_0'* is the initial thickness and *'H_∞'* is the equilibrium thickness of the composite.

Figure-4.21 to 4.23 shows the thickness swelling behavior of untreated LC-epoxy composites at various environments. Since the natural Luffa fibers are highly cellulosic in nature, contains free OH group can readily absorb moisture when immersed in water and hence thickness swelling of the composite occurs. The absorption of moisture occurs during immersion is mainly due to fibers hydrophilic nature and micro pores which give passage for capillary action [177, 208]. From the figures, it can be seen that the thickness swelling rate increases with an increase in fiber loading and aging time for all the environmental conditions. The triple-layer composite shows the highest thickness swelling rate, i.e. 3.90%, 4.04% and 1.32% for saline water, distilled water and sub-zero environments respectively (Figure-4.24). The swelling tendency is always more in distilled water environment followed by saline water and then subzero environment for both treated and untreated LC-epoxy composite.

However, the chemical treatments reduce the swelling character of LC-epoxy composite which is evident from Figure-4.25 to 4.27. The thickness swelling character of LC-epoxy composite was reduced by 30-37.77% for alkali, 52-67% for benzoyl chloride and 39-55% for KMnO4 treatment of Luffa fiber subjected to different environmental conditions. From the obtained result it is observed that benzoyl-chloride treated fiber composite shows the highest reduction of thickness swelling compare to alkali and KMnO4 treatment (Figure-4.28).

The value of K_{SR} was evaluated through a non-linear regression curve fitting method to fit the experimental data using computer software with curve fitting routines using equation 4.6. Table-4.9 presents the value of K_{SR} for both untreated and treated LC epoxy composites obtained through non-linear curve fitting. The swelling parameter quantifies the rate of the composites approaching the equilibrium value for thickness swelling after sufficient time of water immersion. From the Table-4.9, it is clearly observed that the swelling rate parameter of the composites increases with increase in fiber content. This result might have happened because of the increased micro voids caused by the larger amount of poorly bonded area between the hydrophilic luffa and the hydrophobic epoxy resin [182]. From table it is also observed that the value of K_{SR} reduces significantly with chemical treatment of fiber surface. The higher value of K_{SR} indicates, the higher rate of swelling along with reaching of equilibrium thickness swelling in a shorter period [209]. For example, the composite of untreated fiber approached the equilibrium thickness swelling about 36.59, 41, and 54% faster than the alkali, KMnO4 and benzoyl chloride treated fiber reinforced composite respectively immersed in the saline water environment. This swelling rate of chemically modified fiber reinforced composites were found to slower compared to untreated one may be due to the improved compatibility between the polymer and chemically modified fiber [210].

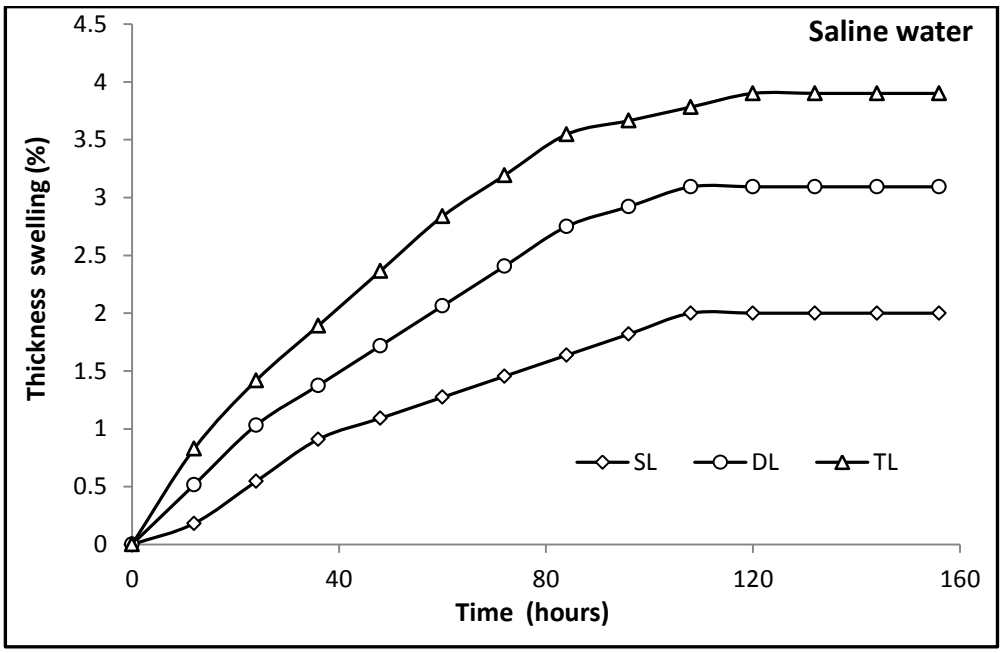

Figure-4.21 Variation of thickness swelling of untreated LC-epoxy composites with immersion time at Saline water environment.

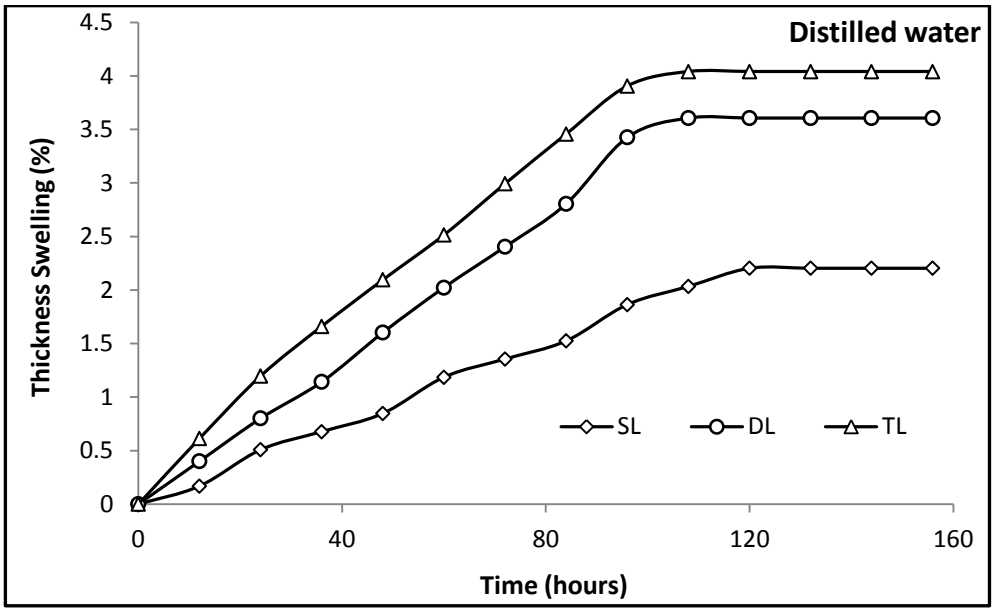

Figure-4.22 Variation of thickness swelling of untreated LC-epoxy composites with immersion time at saline water environment.

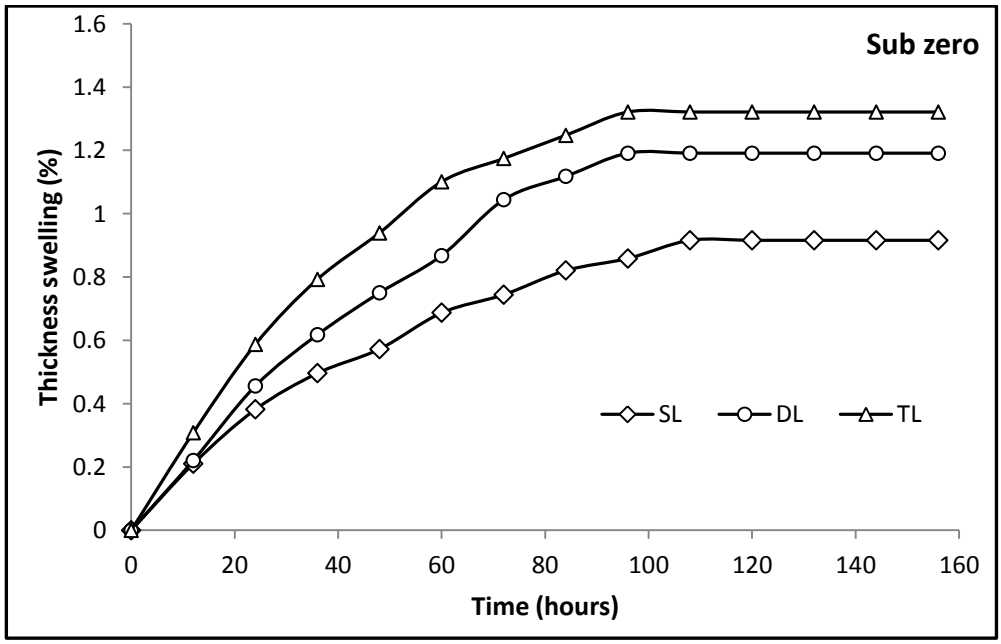

Figure-4.23 Variation of thickness swelling of untreated LC-epoxy composites with immersion time at subzero temperature environment.

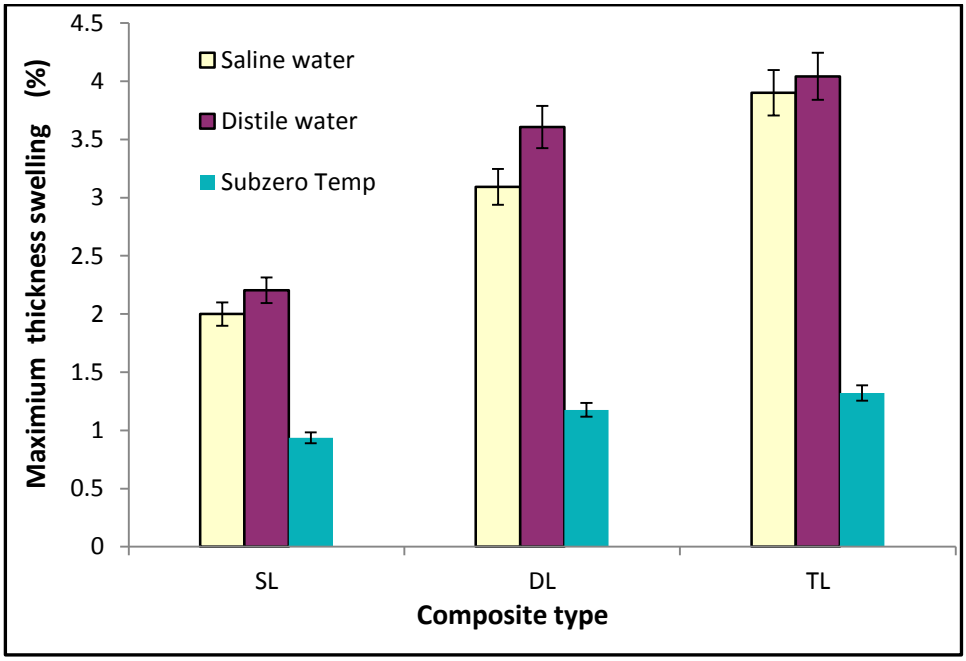

Figure-4.24 Maximum thickness swelling of untreated LC-epoxy composite versus fiber loading exposed in different environment.

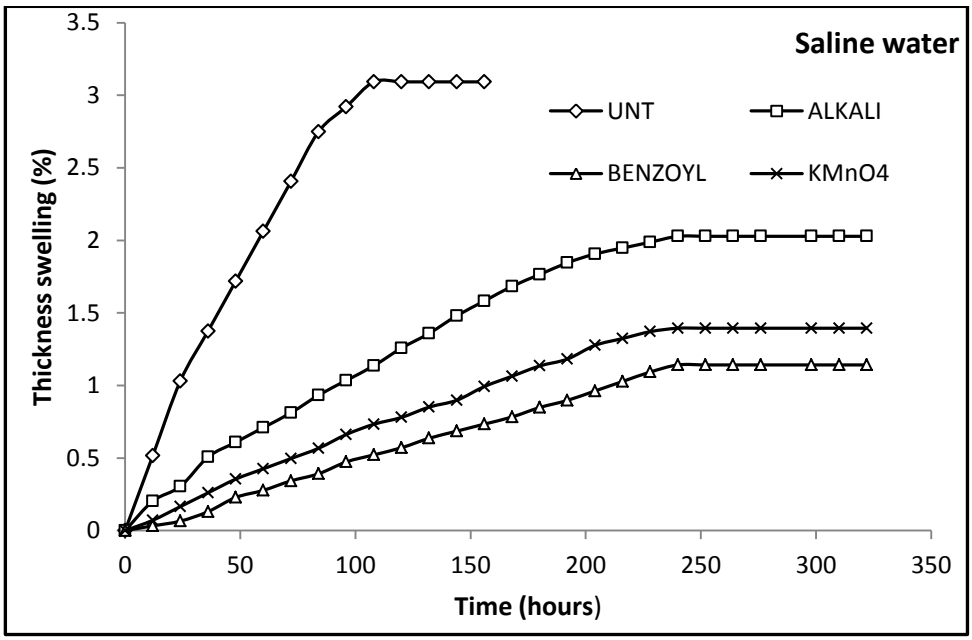

Figure-4.25 Variation of thickness swelling of treated fiber epoxy composites with immersion time at saline water environment.

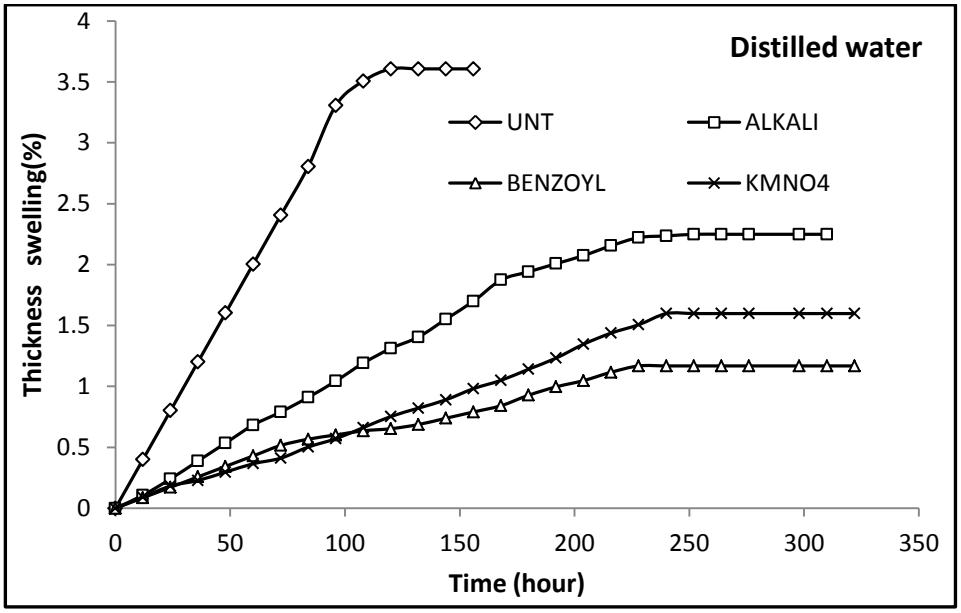

Figure-4.26 Variation of thickness swelling of treated LC- epoxy composite with immersion time at distilled water environment.

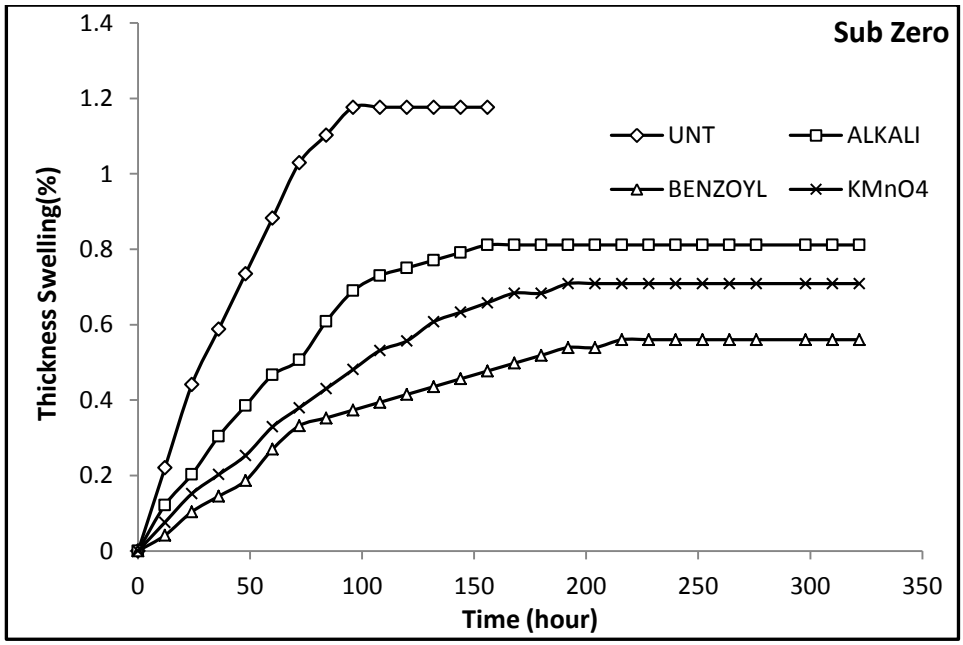

Figure-4.27 Variation of thickness swelling of treated LC- epoxy composites with immersion time at subzero temperature environment.

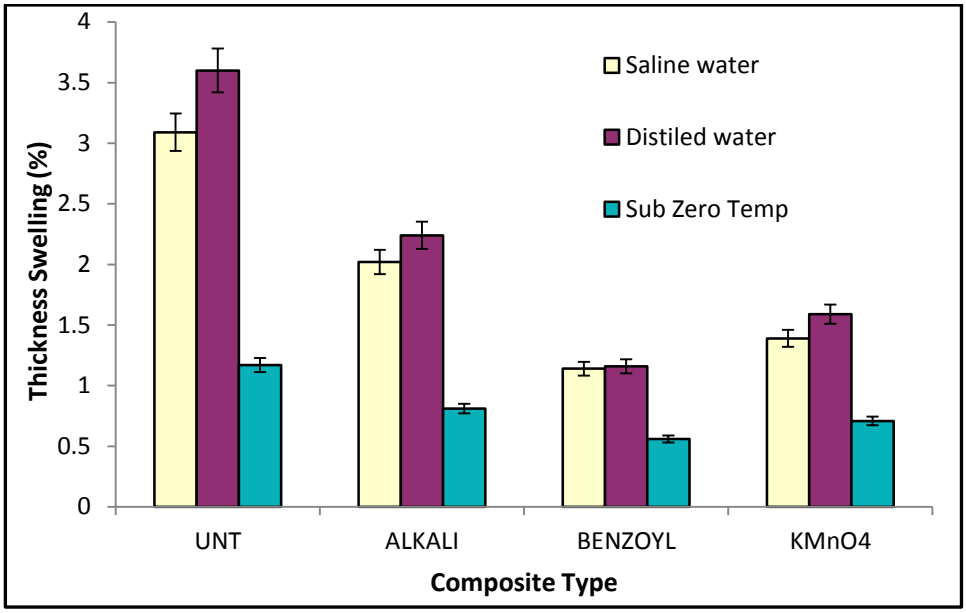

Figure-4.28 Maximum thickness swelling of treated LC- epoxy composite versus fiber loading exposed in different environments.

Table-4.9 Swelling rate parameter of treated and untreated LC-epoxy composite in different environments.

Environment	**% of Fiber**	**Type of Fiber**	**T_0 (mm)**	**T_∞ (mm)**	**TS (%)**	**Swelling Rate Parameter (K_{SR}) $\times 10^{-3}$ (h^{-1})**
Saline Water	SL	Untreated	5.5	5.61	2	28.5
	DL	Untreated	5.82	6	3.09	23.5
	TL	Untreated	8.46	8.79	3.90	32
	DL	Alkali treated	4.93	5.03	2.03	14.9
	DL	Benzoyl chloride treated	6.13	6.2	1.14	10.8
	DL	KMnO4 treated	4.23	4.289	1.399	13.7
	SL	Untreated	5.9	6.03	2.21	21

Distilled water	DL	Untreated	4.991	5.171	3.61	25.7
	TL	Untreated	6.681	6.951	4.04	30.1
	DL	Alkali treated	7.47	7.638	2.25	17.5
	DL	Benzoyl chloride treated	5.82	5.888	1.17	11
	DL	KMnO4 treated	4.38	4.45	1.59	10.02
Sub-Zero Temperature	SL	Untreated	5.241	5.289	0.92	27.8
	DL	Untreated	6.8	6.881	1.19	31.5
	TL	Untreated	6.812	6.902	1.33	30.1
	DL	Alkali treated	4.93	4.97	0.81	24.8
	DL	Benzoyl chloride treated	4.82	4.847	0.56	15.6
	DL	KMnO4 treated	3.95	3.978	0.70	18.7

4.3.2 Effect of moisture absorption on mechanical properties

The moisture absorption has a significant influence on the mechanical properties of the natural fiber polymer composite. Table-4.10 shows the result of mechanical properties of the composite for both treated and untreated fiber reinforced composite after expose to different moist environment. It has been observed that, the mechanical properties of all composite decreases after moisture absorption. This reduction in the strength properties is attributed due to the changes occurring in the fiber, and the interface between fiber and matrix. When fiber/matrix interface is accessible to moisture from the environment, the cellulosic fibers tend to swell, thereby developing shear stresses at the interface, which favors ultimate debonding of the fibers, which in turn causes a reduction in strength [181]. It is also observed that the reduction in properties was greatly influenced by the fiber loading and nature of environment. The maximum reduction in strength properties is observed in case of distilled water environment. However Minimum reduction in strength properties is in subzero environment that might be due to less moisture absorption as discussed in the previous section. Comparing to dry composites, the reduction in tensile strength of SL,

DL and TL composites are 17%, 26% and 31 % respectively for distilled water environmental conditions. However the flexural strength decreases by 14.28% for SL, 19% for DL and 22.2 % for TL composites compared to respective dry composites subjected to distilled water environments. Similar trend was obtained for other mechanical properties as presented in table-4.10. From the obtained result it is clear that with an increase in the fiber content, the strength properties of environmentally treated composites decreases progressively due to the increase in moisture content [192]. This reduction in mechanical properties may be attributable to the reduction of bonding strength of fiber and matrix those results in ineffective stress transfer between fiber and matrix. Dhakal et al. [211] and Alamri et al. [206] also reported the similar type of result while they worked with hemp-polyester composite and recycled cellulose-epoxy composite respectively. Further it is also noticed that the extent of decrease in mechanical properties is reduced with chemical modification of fiber. The benzoyl-chloride treated fiber composite exhibits the best result in all environments in comparison to other two treated fiber composite. Because the benzoyl-chloride treatments reduces the hydrophilic nature of the fiber to great extent which leads to less moisture absorption as reported in art-4.3.1.

Table-4.10 Mechanical properties of both untreated and treated LC- epoxy composite after exposed to different environments.

Type of Environment	**Fiber content (%)**	**Type of fiber**	**Tensile strength (MPa)**	**Young's Modulus (MPa)**	**Flexural strength (MPa)**	**Flexural Modulus (MPa)**	**ILSS (Mpa)**	**Impact strength (KJ/m^2)**
Dry	SL	Untreated	16.5	650	28	2525	0.64	3.9
	DL	Untreated	18	699	32	2064	1.01	4.9
	TL	Untreated	16	725	27	1636	1.38	4
	DL	Alkali	24	788	46.23	3097	1.97	6.5
	DL	Benzoyl	27	890	53.8	3745	1.92	7.3
	DL	KMnO4	25	900	50.1	3672	1.36	6.7
Saline water	SL	Untreated	14	578	25	3001	0.7	3.6
	DL	Untreated	15	635	27	3211	0.98	4
	TL	Untreated	12.75	627	25	2942	1	3.5

	DL	Alkali	20.5	705	44	3700	1.8	5
	DL	Benzoyl	24.5	935	48.11	3942	1.74	6.7
	DL	KMnO4	21	856	42.97	3398	1.28	5.5
Distilled water	SL	Untreated	13	645	24	2930	0.599	2.9
	DL	Untreated	12.5	588	26	3200	0.89	3.5
	TL	Untreated	11	598	21	2852	1.01	3.3
	DL	Alkali	19.5	1130	40.47	2940	1.7	5.2
	DL	Benzoyl	23	900	46.34	2840	1.65	6.1
	DL	KMnO4	20.58	896	42.81	3186	1.34	5
Sub-zero temperature	SL	Untreated	15.34	599	28	2699	0.601	3.5
	DL	Untreated	17	687	31	2671	0.982	4.2
	TL	Untreated	12.75	600	28	2602	1.21	3.7
	DL	Alkali	25	938	42.19	3053	1.07	5.9
	DL	Benzoyl	26	799	50	3090	1.36	6.2
	DL	KMnO4	24.5	900	41.98	2597	1.36	5.8

4.3.3 Morphology of fractured surface.

Figure-4.29 (a-b) shows the micrographs of the fracture surface of untreated and benzoyl-chloride treated composite subjected to distilled water treatment under flexural load. For untreated fiber reinforced composite (figure-4.29(a)), fiber-matrix debonding is clearly visible that might be due to poor compatibility between fiber and matrix. Fractured surface of treated fiber composite with benzoyl-chloride (figure-4.29(b)) indicates breakage of fiber, but there is no trace of debonding of fiber with the matrix as it happens for untreated fibers. This bonding between fiber and matrix is the result of fiber modification by chemical treatment. During chemical treatments, dissolution of cellulose took place due to which voids are being created in the fiber structure. This void gives rise to water absorption due to which swelling of composites occurs that finally leads to deterioration of fiber strength. Due to decrease in fiber

strength original structure of luffa fiber gets destroyed and the splitting of fibers to filaments can be seen in figure-4.29 (b).

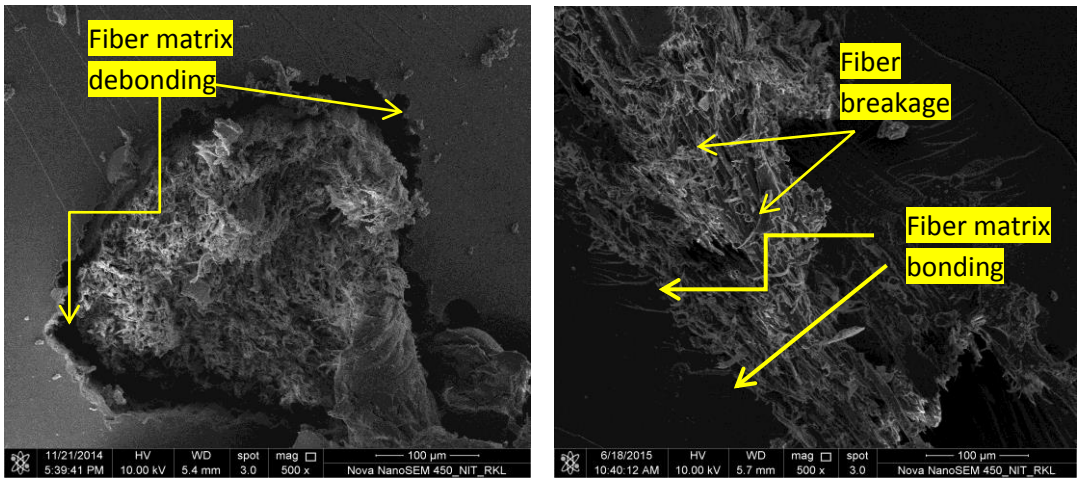

(a) (b)

Figure-4.29. SEM micrographs of facture surface under flexural load of (a) untreated and (b) benzoyl chloride treated LC-epoxy composite undergone treatment in distilled water.

Figure-4.30 (a-b) shows the fracture surface of the untreated and benzoyl-chloride treated fiber composite subject to saline water treatment under flexural load. For untreated composite (figure-4.30(a)), fiber-matrix debonding is clearly visible. This might have happened due to swelling of fiber and also because of poor compatibility between fiber and the matrix. For benzoyl chloride treated fiber reinforced composites (figure- 4.30(b)), though breaking of fibers took place but there is no sign of pulling out fiber from the matrix is visible. The pulling out of fiber is restricted probably due to improvement of fiber-matrix interface bonding. This might happened due to less propagation of moisture through the fibrillation surface that occurs due to ion exchange (Na+ Cl-) in between fiber and matrix [51]. This might be the reason for higher strength with regards to distilled water treatment.

Figure-4.31 (a)-(b) shows the fracture surface of the both untreated and benzoyl- chloride treated fiber composites subjected to subzero temperature under flexural load. For untreated fiber composite subjected to subzero environment (figure-4.31(a)) also indicates same type of behavior occurred as in distilled water and saline water treatment. For treated fiber composite bending of fibers instead of breaking took

place under flexural load (figure-4.31(b)) .Cleavages are formed on the matrix surface when subject subzero condition. This might have happened due to higher strength attainment of the matrix at this temperature (-25°), which does not allow the fibers to come out from the matrix. The absorption of water is also less due to less intermolecular hydrogen bonding and hence higher strength of the composite when subjected to subzero temperature [209].

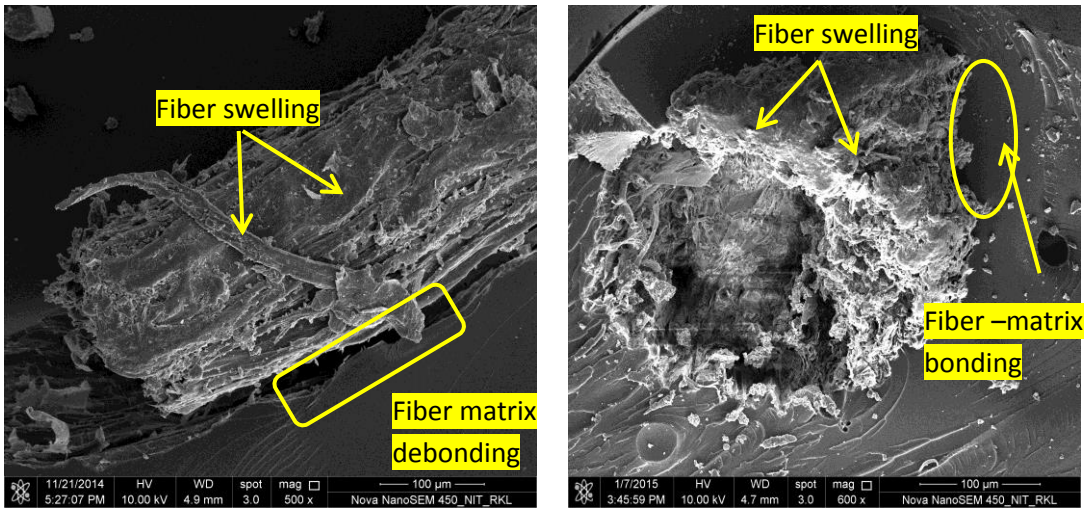

(a) (b)

Figure-4.30 SEM micrographs of facture surface under flexural load (a) untreated and (b) benzoyl chloride treated LC-epoxy composite undergone treatment in saline water.

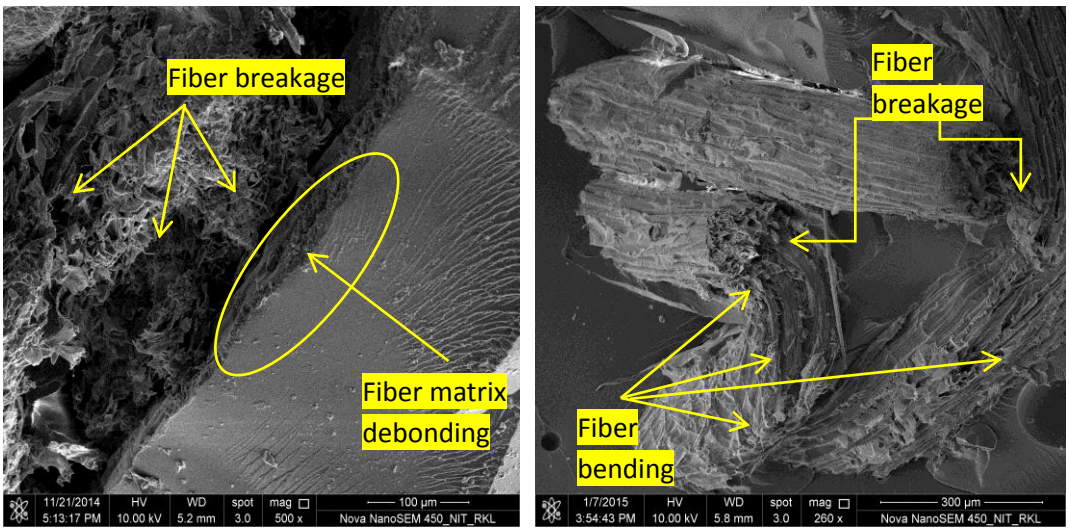

(a) (b)

Figure-4.31. SEM micrographs of facture surface under flexural load of (a) untreated and (b) benzoyl chloride treated LC-epoxy composite undergone treatment in sub-zero temperature.

Figure-4.32 (a)-(d) shows the micrographs of the fracture surface of untreated and benzoyl chloride treated fiber composite subjected to different environments under tensile load. Figure-4.32(a) shows the fracture surface of untreated fiber reinforced composite subjected to distilled water environment. Fiber pullout under tensile load and fiber matrix debonding due to swelling of fiber is clearly visible. Fractured surface of benzoyl chloride treated fiber composite subjected to distilled water environment shows the breakage of fiber under tensile load but fibers seems to be intact with the matrix (figure-4.32 (b)). Matrix cracking due to swelling of fiber is also visible. Figure-4.32 (c) shows the benzoyl chloride treated fibre composite subjected to saline water. Breakage of fibres and cavity due to fibre pull-out under tensile load is observed. But there is no sign of debonding of fiber with matrix as it happens for untreated fibers composite. Figure-4.32(d) shows the benzoyl chloride treated fibre composite subjected to sub-zero temperature environment. There is no sign fibre-matrix debonding due to swelling of fibre is observed. This indicates good bonding between fiber and matrix due to surface modification of fiber. Overall chemical modification improves the fiber-matrix adhesion that in turn prevents the reduction of tensile strength up to certain extent due to environmental effect discussed in Art 4.3.2.

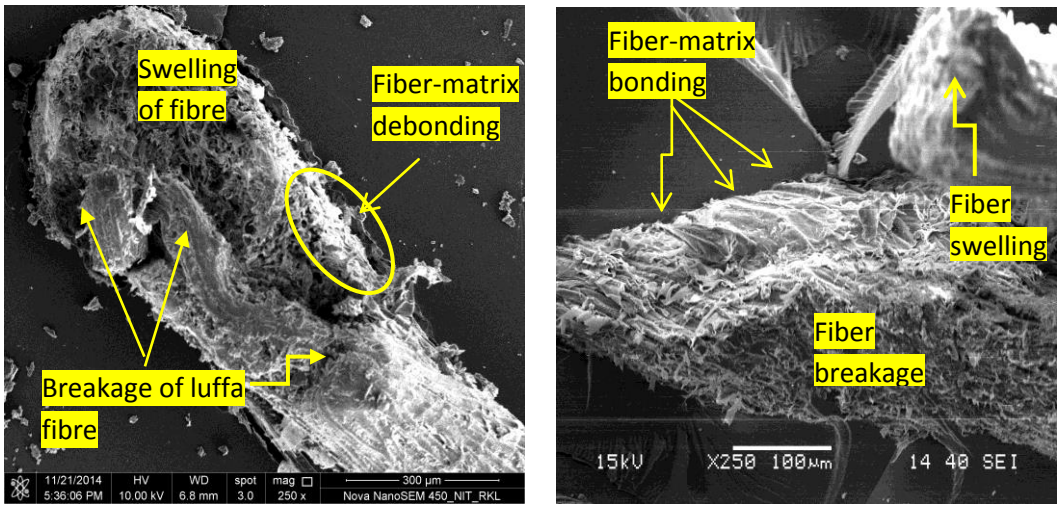

(a) (b)

Figure-4.32. SEM micrographs of fracture surface under tensile load (a) untreated LC-epoxy composite subjected to distilled water (b) Benzoyl chloride treated LC-epoxy composite subjected to distilled water.

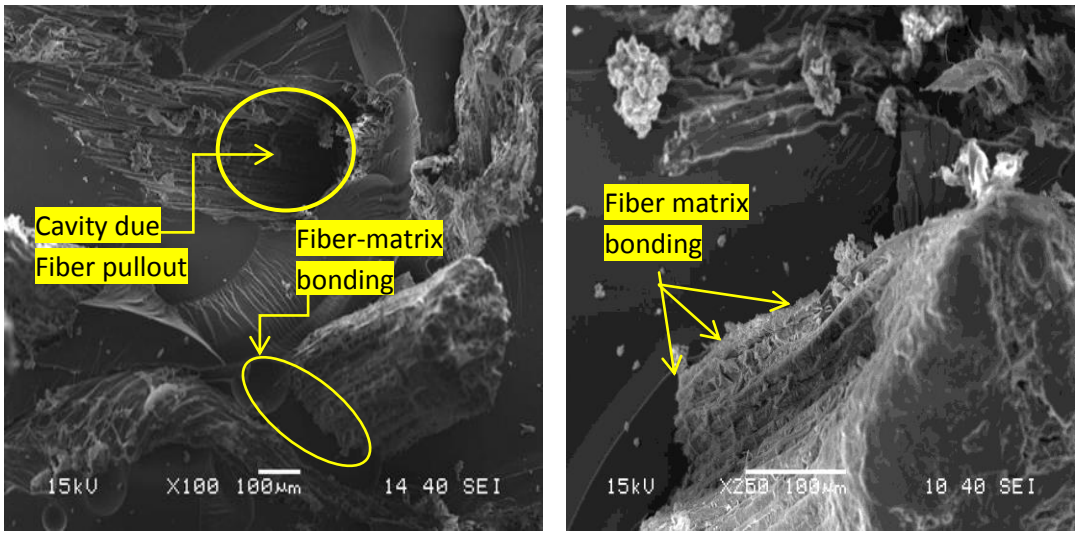

(c) (d)

Figure-4.32. SEM micrographs of fracture surface under tensile load (c) benzoyl chloride treated LC-epoxy composite subjected to saline water (d) benzoyl chloride treated LC-epoxy composite subjected to sub-zero temperature.

4.4 CONCLUSION

Based on experimental results, this study has led to the following conclusions:

- As the luffa fiber loading increases in the composite, the moisture absorption and thickness swelling increases due to a rise of cellulose content for all the environments. However chemical treatments such as alkali, KMnO4 and benzoyl chloride reduce moisture absorption and thickness swelling up to certain extent. But the benzoyl chloride treatment is very effective of all.

- Environmental conditions also play a significant role in moisture absorption process. The composites subjected to sub-zero environment absorbed less moisture than the saline water and distilled water environment.

- The moisture absorption pattern of untreated as well as treated LC-epoxy composites is found to follows Fickian diffusion behavior under all

environment conditions. The values of diffusion coefficient are more pronounced for distilled water environment, followed by saline water and sub-zero temperature environment. The values of diffusion coefficient are decreased upon chemical treatment of fiber surface. They are found in the range of 4.65×10^{-08} - $9.89x10^{-07}$ (mm^2/s) and 1.41×10^{-10} - 4.06×10^{-7} (mm^2/s) for untreated and treated LC-epoxy composite respectively.

- The swelling rate parameter (K_{SR}) of the composites increases with increase in fiber layer. However The K_{SR} value decreases with different chemical modification of fiber surface. It is least in benzoyl chloride treated fiber composites. It is found in the range of 30.5×10^{-3} h^{-1} - 10.02×10^{-3} h^{-1}.

- Under all environmental condition the mechanical properties are decreases as compare to the dry composite samples. The maximum degradation of properties occurs in case of distilled water environment followed by saline water and sub-zero environment. However chemical treatment of fiber helps to prevent the reduction of mechanical properties due to environmental effect up to certain extent.

- SEM images of the composites confirm that fiber-matrix debonding are predominate mode of failure due to swelling of fiber for untreated LC-epoxy composite. However chemical modification of fiber surface improves fiber-matrix interfacial bonding.

Chapter 5

Solid particle erosion studies of Luffa cylindrica fiber reinforced epoxy composite

5.1 INTRODUCTION

Tribology deals with relative motion of surfaces which comprises friction, wear of materials, scratching and rubbing. Further a sophistic definition portrays tribology as a science and technology of surfaces, in contact and relative motion, as well as support of activities that should diminishes the costs resulting from friction and wear [212-213]. Economic consequences of materials' wear are clearly described in the Rabinowicz book 4 – quoting a report to the British Government of 1966 when the word 'tribology' was used for the first time [214]. Increasing applications of polymeric materials require knowledge of their tribological properties – different from much better understood tribological properties of metals and ceramics [215]. A significant part of tribology deals with the selection of materials and surface processing in as much as they affect wear [216].

Wear is a kind of loss of materials to a solid surface which occur due to relative motion of substance with respect to another substance. Formerly wear was defined as damaged to a surface. The most common form of that damage is loss or displacement of material and volume can be used as a measure of wear volume of material removed or volume of material displaced. For scientific purposes this is frequently the measure used to quantify wear. In many studies, particularly material investigations, mass loss is frequently the measure used instead of volume. This is carried out because of the relative ease of performing a weight loss measurement.

Wear causes a huge annual expenditure by industry and consumers. Most of this is replacing or repairing equipment that has worn to the extent that it no longer performs a useful function. In most of the agricultural industries 40% of the machine components replaced on equipment failed through wear. Estimates of direct cost of wear to industrialized nations vary from 1% to 4% of GNP and it is estimated that 10% of all energy generated by man is dissipated in various friction processes. This direct cost includes replacements of wear part, an increase in the work load and time, loss of productivity, as well as loss of energy and the increased environmental liability.

In 1960s a systematic exertions in wear research had investigated in the industrial nations. Thus the magnitude of losses caused to mankind (which can be expressed in percentage points of GDP) makes it absolutely necessary to study ways to

minimize it. Thus minimizing wear, affects the economics of production in a major way. Even though in the twenty-first century there are still wear problems present in industrial applications. This actually reveals the complexity of the wear phenomenon [216].

There are different types of wear such as abrasive, adhesive, fatigue and erosive wear, for polymer composite erosive wear is particularly interesting. In addition, composites acquire a significant place when it comes to operating in a dusty environment where resistance to erosion becomes an important aspect.

Solid particle erosion occurs whenever hard particles along with gas or liquid medium impinged on a surface at any significant velocity which results in progressive loss of material from a solid surface due to mechanical interaction between that surface and the erodent particles. The erosive wear is one of the most encountered types of wear and has recently been a subject of a number of researches [217-219]. The effect of particle erosion on structural and engineering components has been recognized for a long time [220]. Damage caused by erosion has been reported in several industries for a wide range of situations.

Most recently polymers are combining with the various natural fibers and fillers and finding increased application such as aerospace, pipe line carrying sand slurries, water turbines, helicopter rotor blades, pump impeller blades, high speed vehicles and aircrafts, water turbines, aircraft engine blades, missile components, canopies, radomes, wind screens and outer space applications etc. In such applications, one important characteristic is the erosion behavior as these parts operate very often in dusty environments [221–224] because of their outstanding specific mechanical and tribological properties by Guadagnoa et al. [225] and McIntyre et al. [226]. Also, there have been various reports of applications of polymers and their composites in erosive wear situations in the literature [223, 227-228]. Hence, study on the erosive wear behavior of such composites is important. Some studies have been emphasized that the erosive wear behavior of polymer based natural fiber composite is not intrinsic behavior and it strongly depend on many processing parameters such as operating parameters, characteristics of polymer martial, physical and interfacial adhesion properties of fiber, additives and contact condition.

5.2 MECHANISM OF EROSIVE WEAR

Barkoula and Karger-Kocsis [229] presented in 2002 a review article on the solid particle erosion of polymers and polymeric composites focusing on the dominating mechanisms, the most discussed influencing parameters and the different trends observed in the literature. A detailed analysis was given on the effect of experimental conditions (erodent velocity, erodent characteristics, erodent flux rate) and target material characteristics (morphological-, thermal-, thermo mechanical-, and mechanical properties) on the erosive response of polymers and polymer matrix composites.

Erosive wear involves several wear mechanisms which are largely controlled by the various parameters such as particle material, the angle of impingement, the impact velocity, and the particle size. Figure-5.1 summarizes the most important ones. All have important effects on erosive wear; this effect tends to show variations depending upon whether the material tested are ductile, semi ductile or brittle.

According to Bitter [230], erosion is a material damage caused by the attack of particles entrained in a fluid system impacting the surface at high speed. Hutchings [231] defines it as an abrasive wear process in which the repeated impact of small particles entrained in a moving fluid against a surface result in the removal of material from the surface. Erosion due to the impact of solid particles can either be constructive (material removal desirable) or destructive (material removal undesirable), and therefore, it can be desirable to either minimize or maximize erosion, depending on the application. The constructive applications include sand blasting, high-speed water-jet cutting, blast stripping of paint from aircraft and automobiles, blasting to remove the adhesive flash from bonded parts, erosive drilling of hard materials. Whereas the solid particle erosion is destructive in industrial applications such as erosion of machine parts, surface degradation of steam turbine blades, erosion of pipelines carrying slurries and particle erosion in fluidized bed combustion systems. In most erosion processes, target material removal typically occurs as the result of a large number of impacts of irregular angular particles, usually carried in pressurized fluid streams.

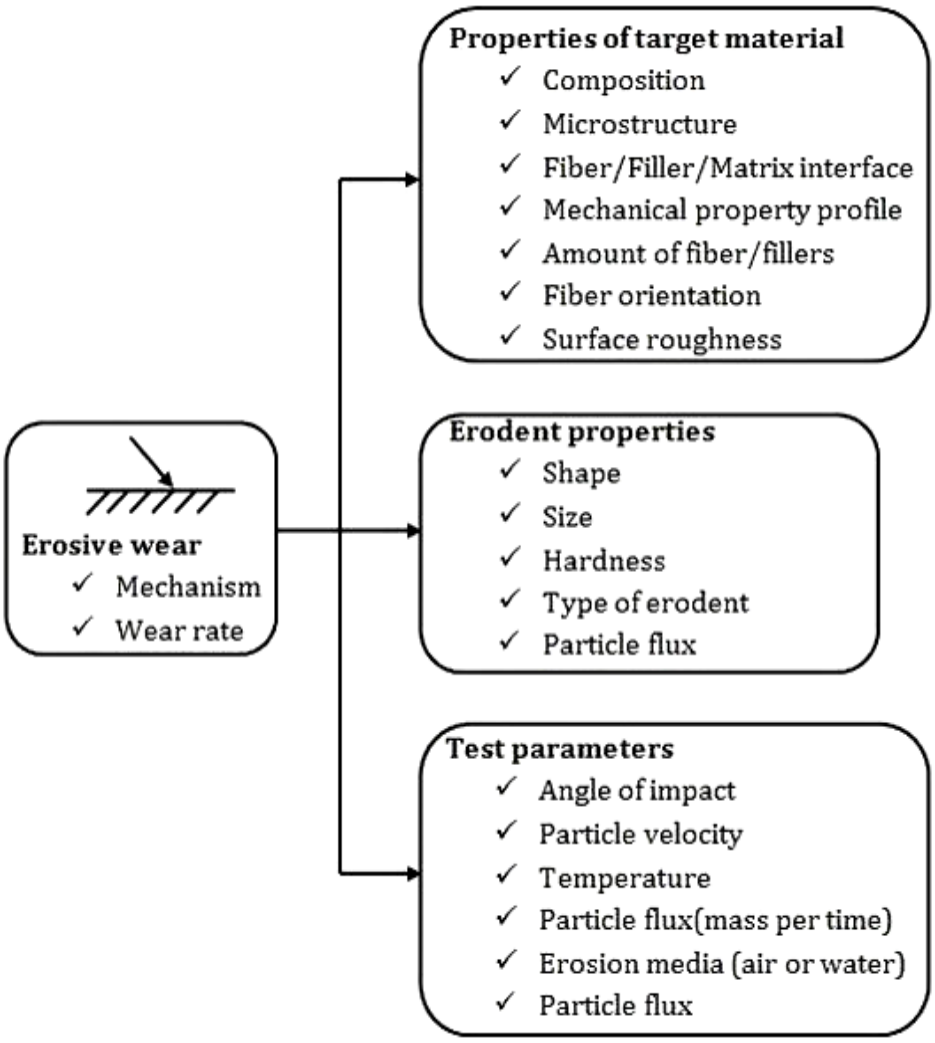

Figure-5.1 Influence of material, erodent and test parameters on erosive wear performance of polymers and their composites.

It is generally recognized that erosive wear is a characteristic of a system and is influenced by many parameters. Laboratory scale investigation if designed properly allows careful control of the tribo system whereby the effects of different variables on wear behavior of PMC scan be isolated and determined. The data generated through such investigation under controlled conditions may help in correct interpretation of the results. General factors influencing erosion test are given in table-5.1. E is the mass removed divided by the mass of particles [223].

Table-5.1 General factors influencing erosion [223]

Eroded surface properties Hardness	Ductile: ***E*** is inversely proportional to the Vickers hardness Brittle: very little correlation
Stress level	Ductile: little effect on ***E*** Brittle: more effect on ***E***
Surface finish	Rougher surfaces raise ***E*** (this is a transient initial effect)
Eroding particle properties Size	Ductile: no effect for particle diameters ≥ 100 pm; lower ***E*** for particle diameters ≤ 100 /Jrn Brittle: ductile behavior for particle diameters ≥10 /μm
Shape	Angular particles produce more wear
Hardness	Harder particles produce more wear (they also tend to be more angular)
Flow and environmental conditions Angle of impingement	Ductile: maximum erosion at about 20° Brittle: maximum erosion at about 90°
Particle velocity	Ductile: $E \alpha U_0^{2-3}$ Brittle: $E \alpha U_0^{3-5}$
Particle flux (mass per time)	Generally small effect on ***E***
Temperature	Less effect than predicted from corresponding change in hardness (for temperatures less than half the melting point in Kelvins)

5.2.1 Influence of impact angle (α) on erosive wear rate

Among the various parameters, Impact angle is one of the most important parameters for the erosion behavior of composite materials. Dependence of erosion rate on the impact angle is largely determined by the nature of the target material and other operating conditions. The impact angle is usually defined as the angle between the

trajectory of the eroding particles and the sample surface. Impact can range from 0° to 90°.

At zero impact angle there is negligible wear because the eroding particles do not impact the surface, although even at relatively small impact angles of about 20°, severe wear may occur if the particles are hard and the surface is soft. If erosion rate goes through a maximum at intermediate impact angles, typically in the range 15°<α<30°, it is concluded that the '**ductile mode of erosive wear**' prevails. Ductile material erosion wear involves the removal of material by plastic deformation. Conversely if the maximum erosion rate occurs at high impact angles i.e. α=90°, then the behavior of the material is purely '**brittle mode**' is assumed. Brittle erosion involving the removal of material by fracture processes. It is generally seen that reinforced composites have been found to exhibit **semi-ductile behaviour** with the maximum erosion rate at intermediate angles, i.e. 45°< α< 60°. The relationship between the wear rate and impact angle for ductile and brittle materials is shown in Figure-5.2.

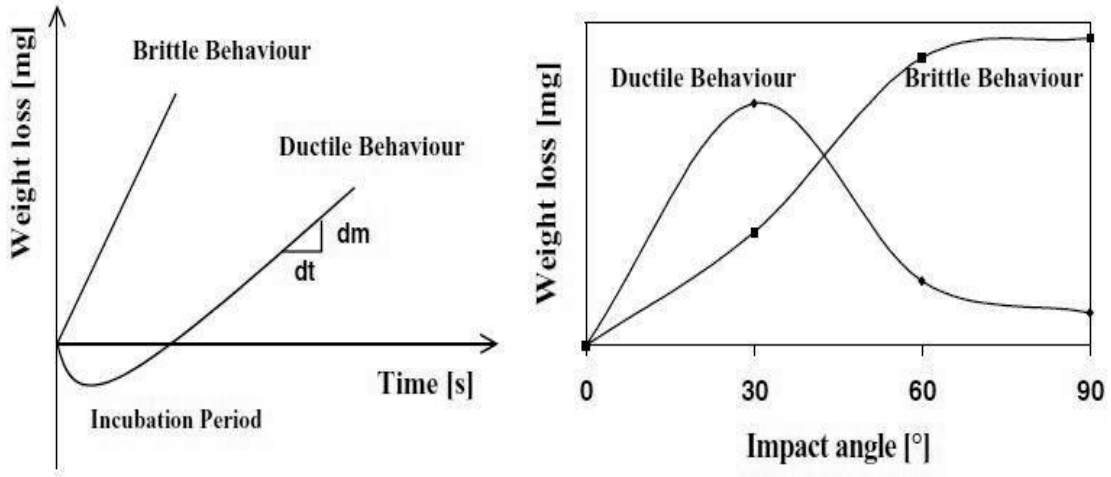

Figure-5.2 Schematic representation of the effect of impact angle on wear rates of ductile and brittle materials [229].

5.2.2 Influence of impact velocity (υ) on erosive wear rate

The velocity (υ) of the erosive particle has very strong effect on the wear process. If the velocity is very low then stresses at impact are insufficient for plastic deformation to occur and wear proceeds by surface fatigue [232]. When the velocity is increased it is possible for the eroded material to deform plastically. In this case, wear is caused by

repetitive plastic deformation. At brittle wear response, wear proceeds by sub surface cracking. At very high particle velocities melting of the impacted surface may even occur.

From medium to high velocity, once steady state conditions have reached erosion rate (E_r) can be expressed as a simple power function of impact velocity (v) [232] equation:

$$E_r = kv^n \tag{5.1}$$

Where 'k' is an empirical constant of proportionality includes the effect of all the other variables. The value of 'n' and 'k' can be found by least-square fitting of the data points in plots which represent the erosion rate dependence on impact velocity by using the power law. The characteristics of the erodent and that of the target material determine the value of the exponent 'n'. It has been stated that 'n' varies in the range of 2–3 for polymeric materials behaving in a ductile manner, while for polymer composites behaving in brittle fashion the value of 'n' is in the range of 3–5 [223].

5.3 SOLID PARTICLE EROSION WEAR OF POLYMER COMPOSITE

The most important factors influencing the erosion rate of the polymer composite materials can be summarized under four categories; (i) The properties of the target materials (matrix material properties and morphology, reinforcement type, amount and orientation, interface properties between the matrices and reinforcements, etc.), (ii) Environment and testing conditions (temperature, chemical interaction of erodent with the target), (iii) Operating parameters (angle of impingement, impinging velocity, particle flux–mass per unit time, etc.) and (iv) The properties of the erodent (size, shape, type, hardness, etc.) [233,212]. Thus it seems that the erosion resistance of the material can be evaluated after investigating the combination of above parameters.

Numerous research works have been carried out to evaluate the resistance of various polymers such as nylon, epoxy, polypropylene, bismileimide etc. and their composite using various natural filler for the tribological application. In recent years some work has been done on natural fiber like oil palm [234], jute [235], betelnut [236] and bamboo [237]. Chin and Yousif [238] attempted to use kenaf fibers reinforced

epoxy composite for bearing application. In all these work it is stated that, the wear resistance of polymeric composites can be improved when natural fiber is used as a reinforcing material.

Patnaik et al. [239] presented a review articles on solid particle erosion behaviour of fiber and particulate filled polymer composites. Various predictions models have been proposed to describe the erosion rate with their suitable applications on real life conditions.

Arjula et al. [240] evaluated erosion efficiency (η) of polymers and polymeric composites by collecting the available data from the literature pertaining to solid particle erosion under normal impact conditions. The result indicates the influence of hardness of various polymers and polymer composites on their erosion resistance.

Mohanty et al. [241] studied solid particle erosion behavior of short date palm leaf (DPL) fiber reinforced polyvinyl alcohol (PVA) composite using silica sand particles (200 ± 50 μm) as an erodent at different impingement angles (15°–90°) and impact velocities (48–109m/s).The neat PVA shows maximum erosion rate at 30° impingement angle whereas PVA/DPL composites exhibit maximum erosion rate at 45° impingement angle irrespective of fiber loading showing semi ductile behavior.

Mishra and Acharya [242], Deo and Acharya [243] reported the tribo potential of sugarcane, lantana camara and bamboo fiber reinforcement in thermoset polymers for enhancing erosive wear resistance. In their studies it is concluded that fiber volume fraction has a significant influence on the erosion rate.

New developments are still under way to explore innovative fields for tribo-application of natural fiber base material. Hence in this present investigation an attempt has been made to study the erosive wear behaviors of luffa cylindrica reinforced epoxy composite. For this the influence of impinging velocity, impingement angle, fiber loading and effect of fiber surface modification on erosive wear has been carried out and results of these investigations are presented in the subsequent sections.

5.4 EXPERIMENT

5.4.1 Preparation of fiber

The details of preparation fiber and surface modification of luffa cylindrica fibers are discussed in chapter-3, art 3.4.1 and 3.2.

5.4.2 Preparation for the test specimens

The preparation of the test specimens were carried out as per the procedure discussed in chapter-3, art-3.4.3. Specimens of dimension 30 mm × 30 mm ×5.0 mm were cut from the composite slabs. Adequate care has been taken to keep the thickness constant (5 mm) for all the samples.

5.4.3. Measurement of impact velocity of erodent particles: Double disc method

The most commonly used method for measuring impact velocity of the erodent particle is the double disc method. It consists of a pair of metal disc mounted on a common shaft and the stream of erodent particles is arranged to strike the upper disc, which has a thin radial slit cut in it. The exit particles from nozzle impinge on the upper disc with some of the particles passing through the slit, which eventually erode a mark on lower disc. Two erosion exposures are made, one with stationary disc and other with rotating disc at known rpm. These exposures give rise to erosion marks A and B on the lower disc (figure-5.3). Measurement of the angular displacement between these marks gives a measure of the flight time of the particles as they cross the space between the discs. The particle velocity can be found by using the following equation [244].

$$v = \frac{L}{t} = \frac{Lv360^0}{\theta} \tag{5.2}$$

Where L is separation of two discs, t is time in second, v is rotation speed of disc per second and θ is angular displacement between the marks. The above equation can also be expressed as

$$v = \frac{2\pi rvL}{S} \tag{5.3}$$

Where r is radius from the disc center, and S is linear separation of two marks. The details of impact velocity calibration at various pressures are given in table-5.2.

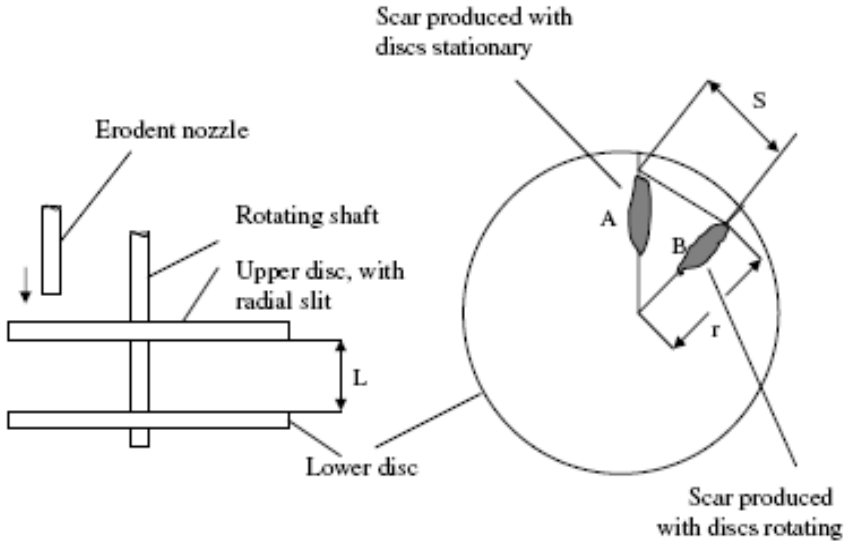

Figure- 5.3 Schematic diagram of methodology used for velocity calibration

Table-5.2 Impact velocity calibration at various pressures.

Pressure (bar)	**Speed of rotating disc(rpm)**	**Angle θ (°)**	**Velocity (m/s)**	**Avg. impact velocity(m/s)**
1 bar	2000	7.0	42.85	47.25
		6.5	46.15	
		6.0	50.00	
		6.0	50.00	
2 bar	2000	4.0	75.00	69.16
		4.5	66.67	
		4.0	75.00	
		5.0	60.00	
3 bar	2000	4.5	66.67	81.845
		4.0	75.00	
		3.5	85.71	
		3.0	100.00	

5.4.4 Test apparatus & Experiment

The schematic figure of the erosion test apparatus used for the present investigation designed as per ASTM-G76 standard is shown in Figure-5.4. The rig consists of an air compressor, a particle feeder, and an air particle mixing and accelerating chamber. The compressed dry air is mixed with the erodent particles, which are fed at a constant rate from a conveyor belt-type feeder in to the mixing chamber and then accelerated by passing the mixture through a tungsten carbide converging nozzle of 4 mm diameter. These accelerated particles impact the specimen, and the specimen could be held at various angles with respect to the impacting particles using an adjustable sample holder. The test apparatus has also been fitted with a rotating double disc to measure the velocity of the erodent particle. The impact velocities of the erodent particles has been evaluated experimentally using this rotating double disc method as mentioned in art 5.4.3.

The conditions under which the erosion test has been carried out are given in Table-5.3. A standard test procedure is employed for each erosion test. The samples are cleaned in acetone, dried and weighed to an accuracy of 1×10^{-3} g using an electronic balance, prior and after each test. The test samples after loading in the test rig were eroded for 3 min. at a given impingement angle and then weighed again to determine weight loss **(Δw)**. The erosion rate (E_r) is then calculated by using the following equation:

$$E_r = \frac{\Delta w}{w_e} \tag{5.4}$$

Where Δw is the mass loss of test sample in gm and w_e is the mass of eroding particles (i.e., testing time × particle feed rate). This procedure has been repeated until the erosion rate attains a constant steady-state value. In the present study the same procedure is repeated for 7 times (i.e. expose time was 21min).

Erosive experiments were conducted with specimen reinforced with untreated Luffa cylindrical fiber with different with single, double and triple layers. As it is discussed in earlier section double layer luffa cylindrica fiber reinforced composite shows optimum strength. The fiber surfaces were modified with alkali, benzoyl chloride and KMnO4 treatment to increase the performance of the fiber in composite.

Experiments were also carried out on the treated fiber composite with double layer of luffa fiber. Experimental results for untreated and treated Luffa fiber epoxy composite for different layer of fiber with different impingement angle and velocities are tabulated and presented in Table-5.4 to 5.9. Based on these tabulated results various graphs were plotted and presented in the subsequent sections for discussions

1 Sand hopper

2 Conveyor belt system for sand flow

3 Pressure transducer

4 Particle-air mixing chamber

5 Nozzle

6 X–Y and Θ axes assembly.

7 Sample holder

Figure- 5.4 Solid particle erosion test set up.

Table-5.3 Experimental condition for the erosion test

Test parameters	
Erodent:	Silica sand
Erodent size (μm):	200±50
Erodent shape:	Angular
Hardness of silica particles (H_V):	1420±50
Impingement angle (α^0):	30, 45, 60 and 90
Impact velocity (m/s):	48, 70, 82 and 109.
Erodent feed rate (gm/min):	3±0.02
Test temperature:	(27 ^{0}C)
Nozzle to sample distance (mm):	10

Table-5.4 Weight loss and Erosion rate of Single layer (SL) untreated LC-epoxy composite with respect to impingement angle due to erosion for a period of 21 min.

Velocity (m/s)	**Impact Angle (α)**	**SL**	
		Weight loss 'Δw' g	**Erosion rate × 10^{-4} (g/g)**
48	30^0	0.012	1.667
	45^0	0.016	2.222
	60^0	0.015	2.083
	90^0	0.008	1.111
70	30^0	0.027	3.750
	45^0	0.031	4.306
	60^0	0.026	3.611
	90^0	0.021	2.917
82	30^0	0.048	6.667
	45^0	0.056	7.778
	60^0	0.051	7.530
	90^0	0.045	6.250
109	30^0	0.049	8.056
	45^0	0.09	12.500
	60^0	0.09	13.100
	90^0	0.06	8.750

Table-5.5 Weight loss and Erosion rate of Double layer (DL) untreated LC- epoxy composite with respect to impingement angle due to erosion for a period of 21 min.

Velocity (m/s)	**Impact Angle (α)**	**DL**	
		Weight loss 'Δw' g	**Erosion rate × 10^{-4} (g/g)**
48	30^0	0.01	1.389
	45^0	0.018	2.500
	60^0	0.016	2.222
	90^0	0.008	1.111
70	30^0	0.03	4.167
	45^0	0.039	5.417
	60^0	0.034	4.722
	90^0	0.031	4.306
82	30^0	0.045	6.250
	45^0	0.054	7.500
	60^0	0.051	7.083
	90^0	0.039	5.417
109	30^0	0.058	6.806
	45^0	0.087	10.560
	60^0	0.076	12.080
	90^0	0.063	8.333

Table-5.6 Weight loss and Erosion rate of Triple layer (TL) untreated LC-epoxy composite with respect to impingement angle due to erosion for a period of 21 min.

Velocity (m/s)	**Impact Angle (α)**	**TL**	
		Weight loss 'Δw' g	**Erosion rate × 10^{-4} (g/g)**
48	30^0	0.01	1.389
	45^0	0.02	2.778
	60^0	0.025	3.472
	90^0	0.021	2.917
70	30^0	0.038	5.278
	45^0	0.042	5.833
	60^0	0.044	6.111
	90^0	0.033	4.583
82	30^0	0.047	6.528
	45^0	0.059	8.194
	60^0	0.06	8.333
	90^0	0.046	6.389
109	30^0	0.064	8.889
	45^0	0.098	13.61
	60^0	0.104	14.44
	90^0	0.07	9.722

Table-5.7 Weight loss and Erosion rate of Double Layer (DL) alkali treated LC-epoxy composite with respect to impingement angle due to erosion for a period of 21 min**.**

Velocity (m/s)	**Impact Angle (α)**	**Alkali (DL)**	
		Weight loss 'Δw' g	**Erosion rate × 10^{-4} (g/g)**
48	30°	0.011	1.528
	45°	0.016	2.222
	60°	0.016	2.000
	90°	0.008	1.111
70	30°	0.023	3.194
	45°	0.03	4.167
	60°	0.027	3.750
	90°	0.03	4.167
82	30°	0.041	5.694
	45°	0.057	7.917
	60°	0.044	6.890
	90°	0.036	5.000
109	30°	0.047	6.528
	45°	0.071	9.444
	60°	0.068	10.20
	90°	0.062	8.600

Table-5.8 Weight loss and Erosion rate of Double Layer (DL) benzoyl chloride treated LC-epoxy composite with respect to impingement angle due to erosion for a period of 21 min.

Velocity (m/s)	**Impact Angle (α)**	**Benzoyl Chloride (DL)**	
		Weight loss 'Δw' g	**Erosion rate × 10^{-4} (g/g)**
48	30°	0.008	1.000
	45°	0.013	1.800
	60°	0.011	1.530
	90°	0.007	9.722
70	30°	0.015	2.210
	45°	0.03	4.167
	60°	0.026	3.611
	90°	0.023	3.194
82	30°	0.033	4.583
	45°	0.046	6.389
	60°	0.034	5.620
	90°	0.034	4.722
109	30°	0.041	5.694
	45°	0.059	8.194
	60°	0.059	8.720
	90°	0.051	7.083

Table-5.9 Weight loss and Erosion rate of Double Layer (DL) KMn04 treated LC-epoxy composite with respect to impingement angle due to erosion for a period of 21 min.

Velocity (m/s)	**Impact Angle (α)**	**KMnO4 (DL)**	
		Weight loss 'Δw'(g)	**Erosion rate × 10^{-4} (g/g)**
48	30°	0.01	1.389
	45°	0.014	1.944
	60°	0.012	1.667
	90°	0.007	9.722
70	30°	0.022	3.056
	45°	0.034	4.722
	60°	0.031	4.306
	90°	0.026	3.611
82	30°	0.036	5.000
	45°	0.054	7.500
	60°	0.037	6.140
	90°	0.029	4.028
109	30°	0.046	6.389
	45°	0.069	8.472
	60°	0.061	9.583
	90°	0.058	8.056

5.4.5 Erosion efficiency

The surface hardness of material cannot give sufficient correlation with erosion rate because it determines the volume displaced by each impact and not really the volume of material eroded. Thus a parameter which will reflect the efficiency with which the volume that is displaced is removed should be combined with hardness to obtain a better correlation. The erosion efficiency is one such parameter which is proposed by Sundararajan et al. [245] for erosion at normal impact angle as

$$\boldsymbol{n = \frac{2ErH}{\rho V^2}} \tag{5.5}$$

But considering impact of erodent at any angle α to the surface, the actual erosion efficiency can be obtained by modifying Eq. (5.5) [246-247]

$$\boldsymbol{n = \frac{2ErH}{\rho V^2 sin^2\alpha}} \tag{5.6}$$

Where E_r is erosion rate (g/g), H is hardness of eroded material (MPa) and *v* is the impact velocity (m/s). 'ρ' is the density of the eroding material (g/cm^3).

The magnitude of 'η' can be used to characterize the nature and mechanism of erosion. For example, ideal micro-ploughing involving just the displacement of the material from the crater without any fracture (and hence no erosion) has zero efficiency (η=0). In contrast, if the material removal is by ideal micro-cutting, 'η' is unity (η=1.0 or 100%). If erosion occurs by lip or platelet formation and their fracture by repeated impact, as is usually the case in ductile materials, the magnitude of η will be very low, i.e. η ≤ 100%. In the case of brittle materials, erosion occurs usually by spall and removal of large chunks of materials resulting from the interlinking of lateral or radial cracks and thus η can be expected to be even greater than 100% [239].

The values of erosion efficiencies of composites under this study are calculated using equation 5.6 and are listed in table-5.10 for both treated and untreated LC-epoxy composite along with their hardness values and operating parameters.

Table-5.10 Erosion efficiency of both treated and untreated LC- epoxy composites.

Impact Velocity 'v' (m/s)	**Impact angle 'α'**	**Erosion efficiency (η)**					
		SL	**DL**	**TL**	**Alkali (DL)**	**Benzolated (DL)**	**KMnO4 (DL)**
		H=190.3 Mpa	H=161.8 Mpa	H=191.2 Mpa	H=202.9 Mpa	H=201.5 Mpa	H=192.7 Mpa
		ρ=1.02 g/cm3	ρ=.975 g/cm3	ρ=.969 g/cm3	ρ=1.17 g/cm3	ρ=1.83 g/cm3	ρ=1.178 g/cm3
30^0	48	10.70	8.00	9.52	9.52	5.91	7.78
	70	11.32	11.29	17.00	9.09	6.15	8.16
	82	14.66	12.34	15.32	11.75	9.29	9.73
	109	8.47	9.00	11.81	7.63	6.53	7.04
45	48	7.13	7.78	9.52	6.78	5.32	5.54
	70	6.50	7.20	9.40	5.90	5.79	6.31
	82	8.55	7.34	9.62	8.17	6.47	7.30
	109	7.78	7.40	9.04	5.76	4.70	5.28
60	48	4.46	4.27	7.93	4.02	3.02	3.05
	70	3.63	4.26	6.56	3.54	3.35	3.83
	82	5.52	4.66	6.52	4.20	3.19	3.33
	109	5.19	3.93	6.40	3.68	3.13	3.11
90	48	1.78	1.60	5.00	1.52	1.36	1.39
	70	2.20	2.92	3.69	2.95	2.22	2.41
	82	3.44	2.67	3.75	2.58	2.39	1.96
	109	2.59	2.44	3.23	2.51	2.03	2.22

5.5 RESULTS AND DISCUSSION

5.5.1 Effect of impact angle (α) on erosion rate of LC-epoxy composite

Figure-5.5-5.8 shows the influence of impingement angle (α) on the erosion rate of untreated single, double and triple layered LC-epoxy composites for different impact velocities (48,70,82 and 109 m/s). It is clear from the plot that the erosion rate increases with the increase of impingement angle and attains a maximum value at 45° impingement angle for single and double layered composite. However, the peak erosion shifts from 45° to 60° for higher fiber loaded triple layer composite for all the velocities. Figure-5.9- 5.12 shows the influence of impingement angle (α) on the erosion rate of untreated, alkali, benzoyl chloride and KMnO4 treated fiber reinforced composite. From figures it is observed that treated Luffa fiber shows peak erosion rate ($E_{r\ max}$) at 45^o impact angle at low impact velocity (48, 70, 82 m/sec). However the peak erosion shift towards 60^o as the velocity of impingement increases (i.e. 109 m/s). As mentioned earlier (art 5.2.1) impact angle is one of the most important parameter for classifying the erosion behavior of any material. From this present investigation it is seen that maximum erosion occurs for different layer composite in the range 45°-60°. Hence it can be concluded that the present LC-epoxy composite behaves neither in a purely ductile nor in a purely brittle nature. This behavior can be termed as semi ductile in nature. Deo and Acharya [243] while studying with lantana camara fiber also found that maximum erosion at 45° impact angle showing semi ductile behavior. The same type of behavior was also reported by Mohanty et al. [241] and Ojha et al. [248] while they studying the erosive behavior of date palm leave and wood apple shell reinforced polymer composite respectively. N.Sari et al. [249] while studying the erosive wear behavior of carbon fibre/polyetherimide composites under low particle speed have reported increase in particle speed results in more brittle response of the material, the angle which causes highest wear rate shift to higher angle. However the interesting point here is that at higher velocity 109 m/s the maximum erosion from 45^o shifted towards 60^o impact angle for the untreated as well as treated Luffa fiber composite. This gives an indication that at higher impact velocity the ductile behavior of the composite shifted towards the brittle behavior. For comparison of the erosion

rate of other natural fiber with luffa cylindrica fiber is presented in table 5.11. It can be seen that this fiber has better erosion resistance compared to many other natural fiber.

Table-5.11 Comparison table of erosion rate of some natural fiber polymer composite with luffa cylindrica epoxy composite.

Natural fiber polymer composite	**Erosion rate (g/g)**	**Nature of erosion response**	**Reference**
Raw wood apple shell particle/epoxy	0.940×10^{-4} to 1.110×10^{-4}	Semi ductile	[248]
Luffa cylindrica/epoxy	**6.250×10^{-4} to 7.000×10^{-4}**	**Semi ductile**	Present study
Date palm leaf/PVA	5.000×10^{-4} to 10.000×10^{-4}	Semi ductile	[241]
Rice husk/epoxy	8.727×10^{-4} to11.945×10^{-4}	Semi ductile	[250 a]
Lantana camara/epoxy	8.182×10^{-4} to 21.818×10^{-4}	Semi ductile	[243]
Bagasse/epoxy	01.747×10^{-3} to 5.418×10^{-3}	Brittle	[242]

It is further noticed that irrespective of impact velocity and impact angle, the erosion rate increases with increase in fiber layer for lower impact velocity (48 and 70 m/s). The erosion rate is lowest for single layer reinforced composite for lower impact velocities. However erosion rate is lowest for double layered reinforced composite for higher impact velocities (82 and 109 m/s). Further it is observed that treated fiber composite shows lower erosion rate with respect to untreated Luffa cylindrica composite. This happened because the compatibility between Luffa cylindrica fiber and epoxy resin increases due to fiber surface treatment. This is possible because the treatment completely wet the surface of luffa cylindrica and more and more OH groups are used for chemical bonding [250]. Benzoyl chloride treated fiber composite shows the best erosion resistance capacity followed by KMnO4 and alkali treated fiber reinforced composite.

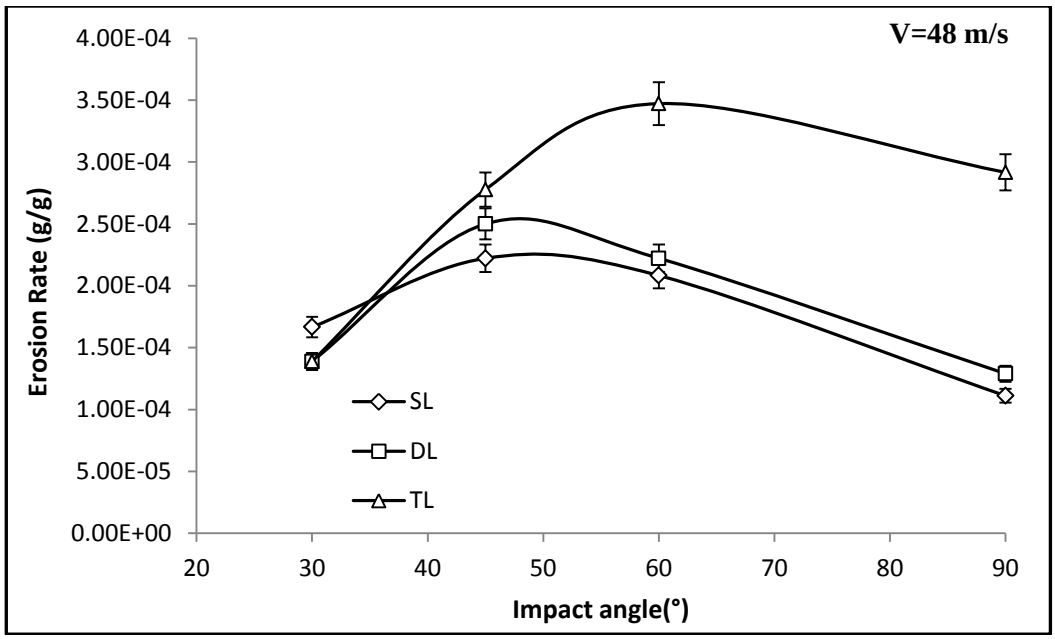

Figure-5.5 Variation of erosion rate with different impact angle of untreated LC-epoxy composite at impact velocity 48 m/s.

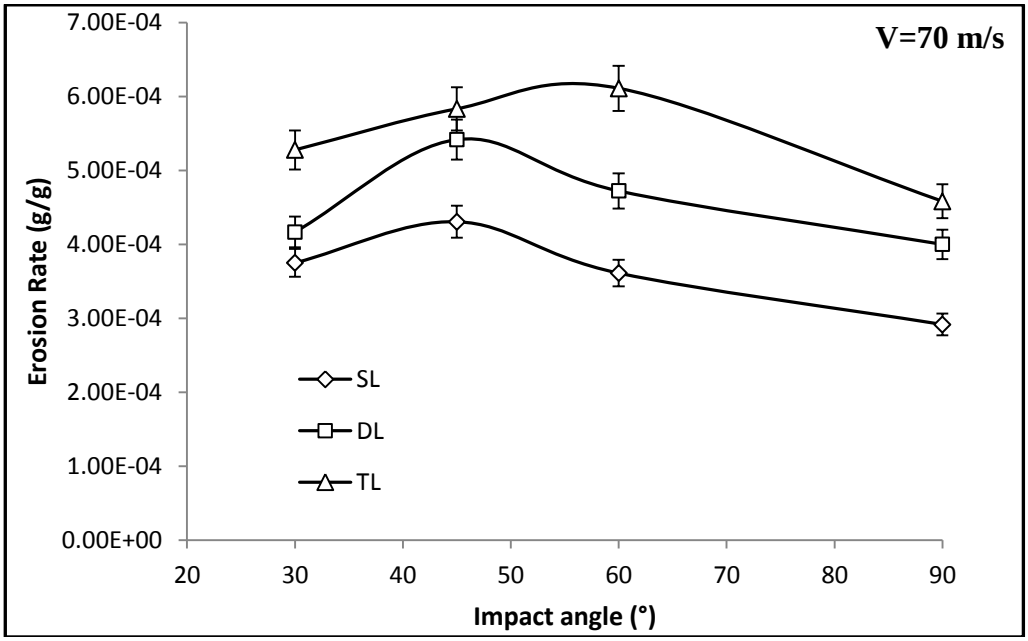

Figure-5.6 Variation of erosion rate with different impact angle of untreated LC-epoxy composite at impact velocity 70 m/s.

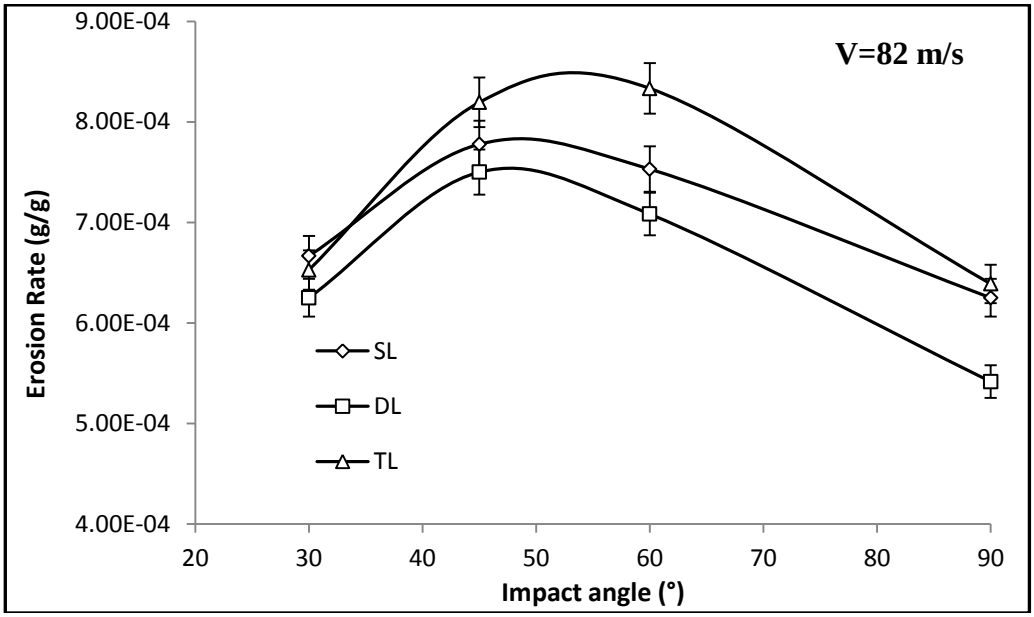

Figure-5.7 Variation of erosion rate with different impact angle of untreated LC-epoxy composite at impact velocity 82 m/s.

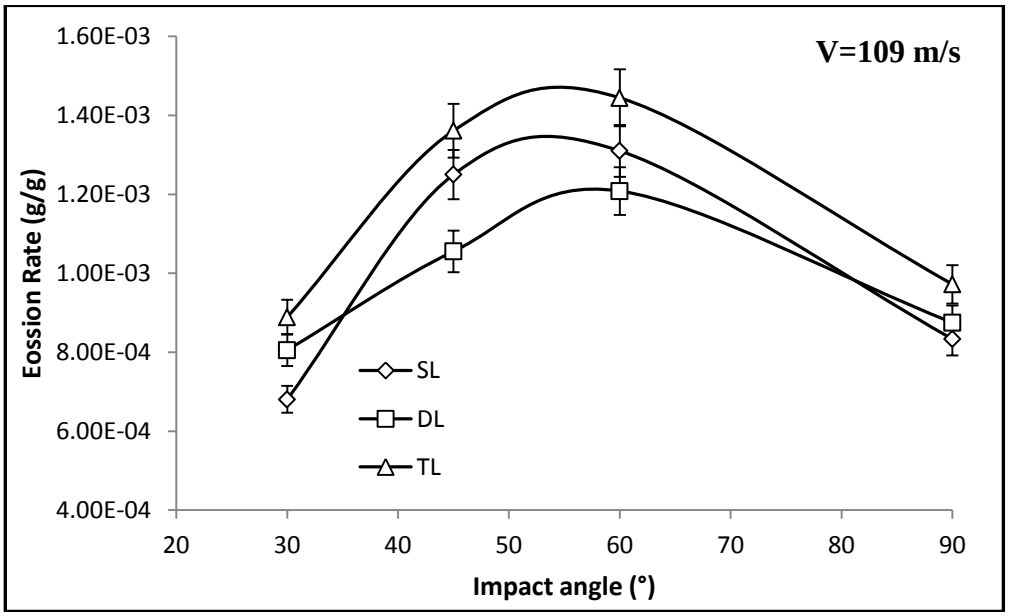

Figure-5.8 Variation of erosion rate with different impact angle of untreated LC-epoxy composite at impact velocity 109 m/s.

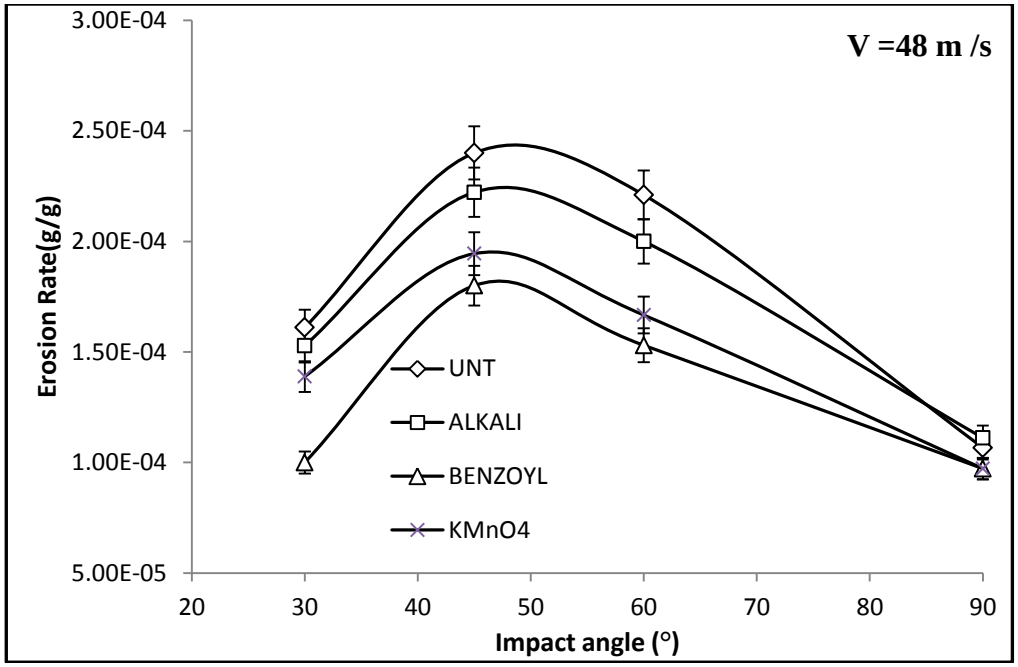

Figure-5.9 Variation of erosion rate with different impact angle of treated double layer LC- epoxy composite at impact velocity 48 m/s.

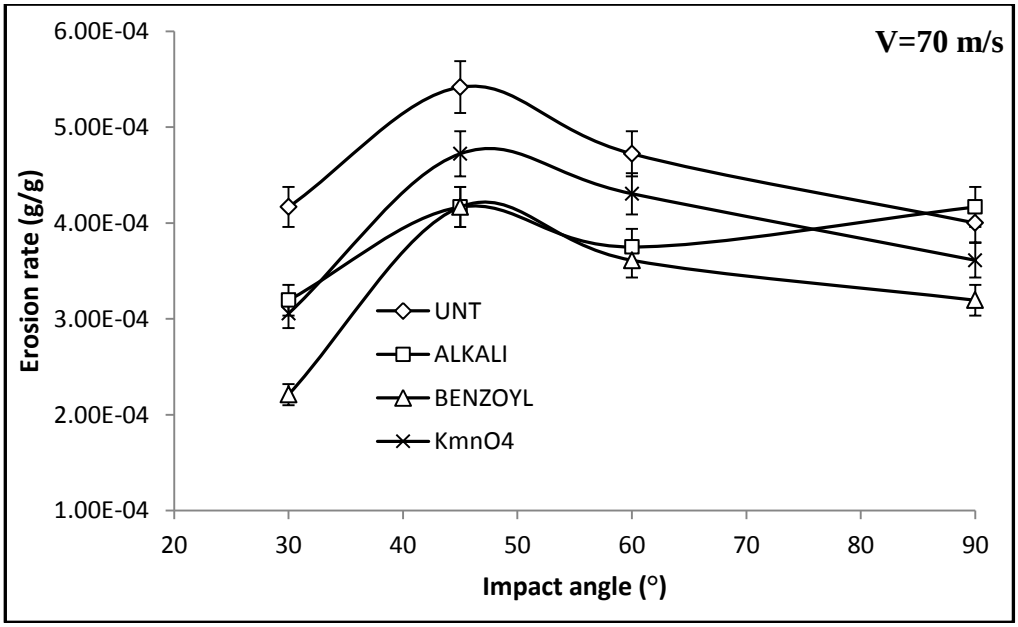

Figure-5.10 Variation of erosion rate with different impact angle of treated double layer LC- epoxy composite at impact velocity 70 m/s.

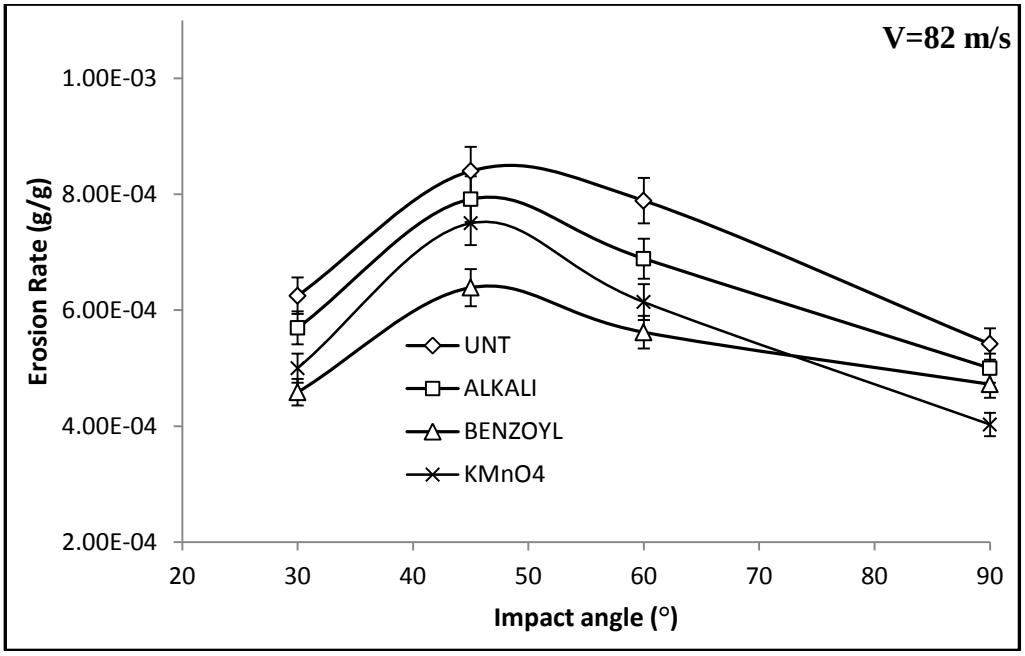

Figure-5.11 Variation of erosion rate with different impact angle of treated double layer LC- epoxy composite at impact velocity 82 m/s.

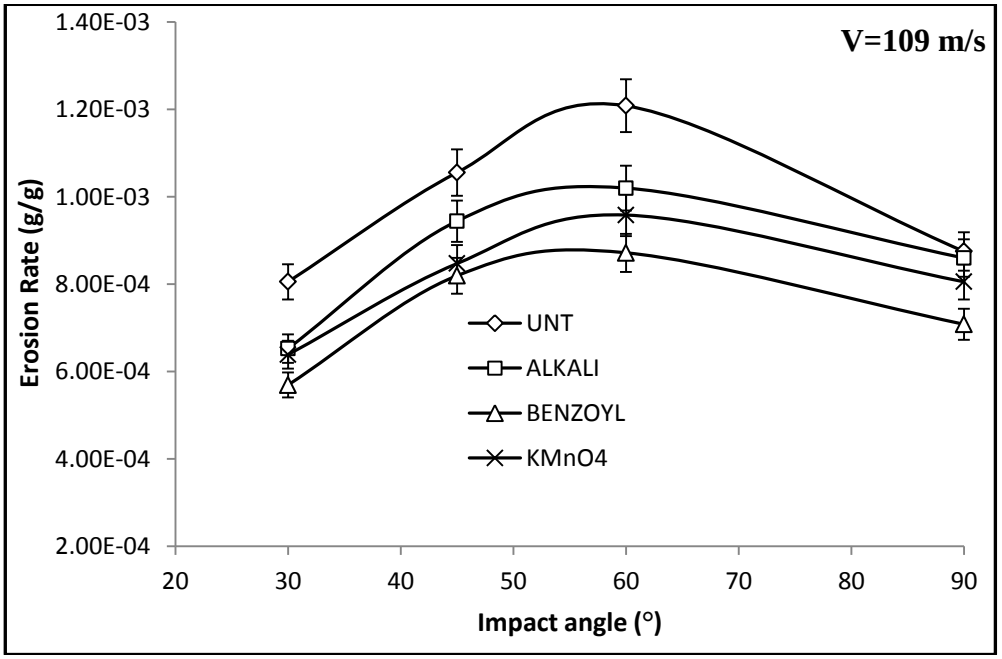

Figure-5.12 Variation of erosion rate with different impact angle of treated double layer LC- epoxy composite at impact velocity 109 m/s.

5.5.2 Effect of impact velocity (v) on erosion rate of LC-epoxy composite

The variation of steady-state erosion rate of untreated SL, DL, TL LC-epoxy composite samples with impact velocity at different impact angles are shown in the form of a histogram in Figure-5.13 to 5.16. It can be observed from these histograms that erosion rate of all composite samples increases with increase in the impact velocity. It is observed from the plots that there is no significant variation in the wear rate at low impact velocities (48 m/s). However for the increase in the velocity to 70, 82 and 109 m/s it is found that erosion rate increase to higher values. This might have happened due to creation of severe plastic deformation on the composite surface at higher velocities. Same type of behavior was also reported by Rout et al. [251], while working with Rice husk filled composite.

The similar observations were also found in treated LC-epoxy composites which are shown in Figure-5.17 to 5.20. Minimum erosion rate was also observed for benzoyl chloride treated fiber composite with all impact velocities followed by KMnO4 and alkali treated composite.

As mentioned earlier (art 5.2.2) influence of impact velocity (υ) on erosive wear rate is one of the most important parameter for classifying the erosion behavior of any material. Figure-5.21-5.24 illustrates the erosion rate with impact velocity at impingement angle (30-90°) for untreated (SL, DL and TL) fiber composite and Figure- 5.25 to 5.28 shows for double layer treated (Alkali, benzoyl chloride and KMnO4 treated) fiber composite. From these figures it is clear that steady state erosion rate of all treated and untreated reinforced epoxy composites increases with increase in impact velocity. The least-square fits to data point were obtained by using power law (equation 5.1) and the values of '*n*' and '*k*' are summarized in Table- 5.12. The velocity exponents found for untreated SL, DL, TL are in the range of 1.82-2.57, 1.85-2.52 and 1.48-2.03 respectively for different impact angles and impact velocities studied. However for alkali, KMnO4, benzoyl chloride treated LC composites are in the range of 1.86-2.48, 1.90-2.46 and 1.92-2.54 respectively. This velocity exponent at various impingement angles are in conformity with Harsha et al. [252]. Observing the values of velocity exponent 'n' it can be concluded the present LC-epoxy exhibited semi-ductile behaviour. This conclusion was drawn by following the classifications

made by KV pool [223] as mentioned in art 5.2.2. Similar results are also observed by Mohanty et al. [241] in their study of date palm reinforced epoxy composite.

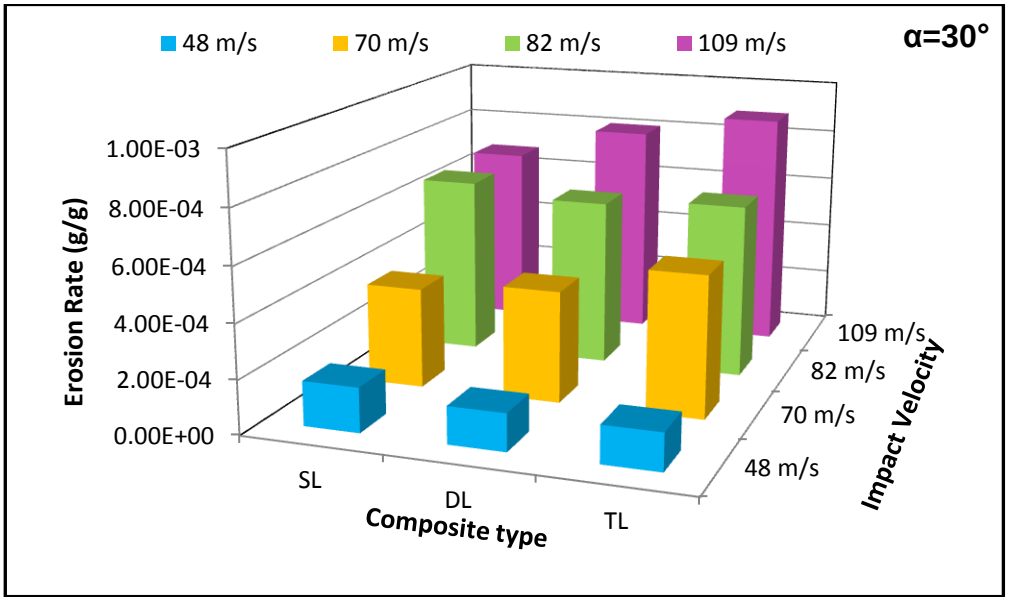

Figure-5.13 Histogram showing the erosive wear rates untreated LC-epoxy composite at four impact velocities (i.e. at 48, 70, 82 and 109 m/s) for 30° impact angle.

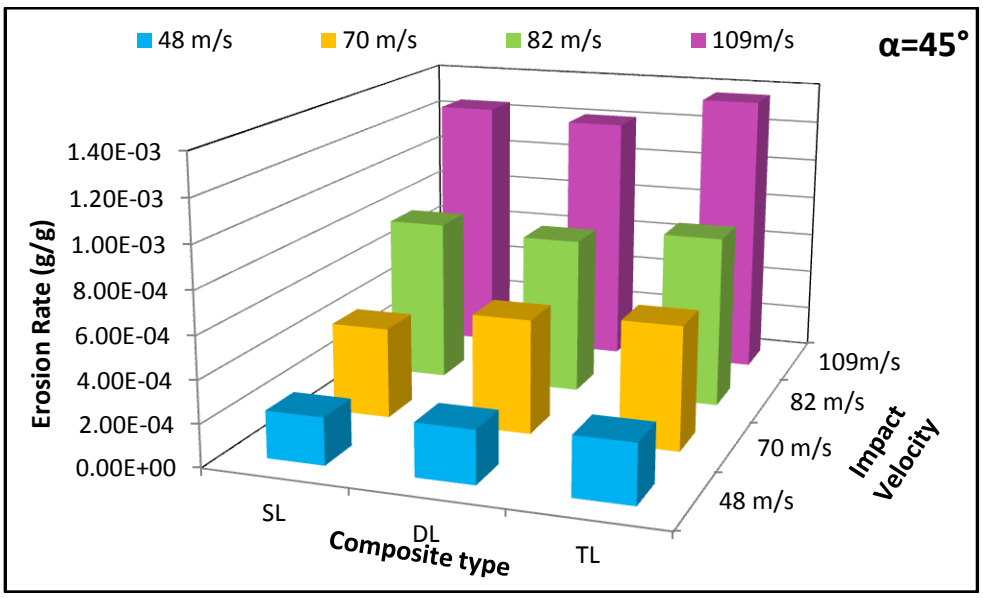

Figure-5.14 Histogram showing the erosive wear rates untreated LC-epoxy composite at four impact velocities (i.e. at 48, 70, 82 and 109 m/s) for 45° impact angle.

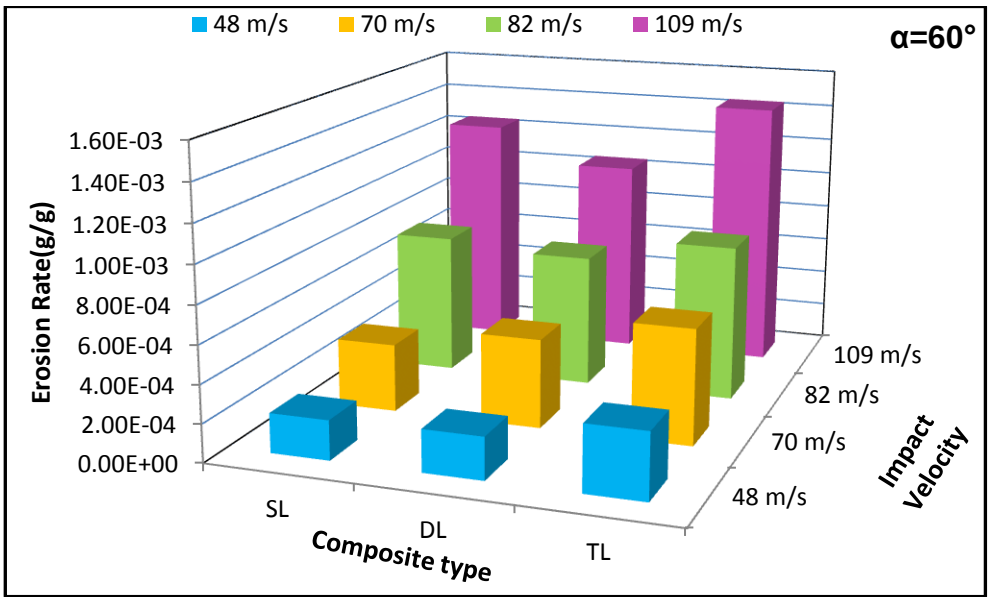

Figure-5.15 Histogram showing the erosive wear rates untreated LC-epoxy composite at four impact velocities (i.e. at 48, 70, 82 and 109 m/s) for 60° impact angle.

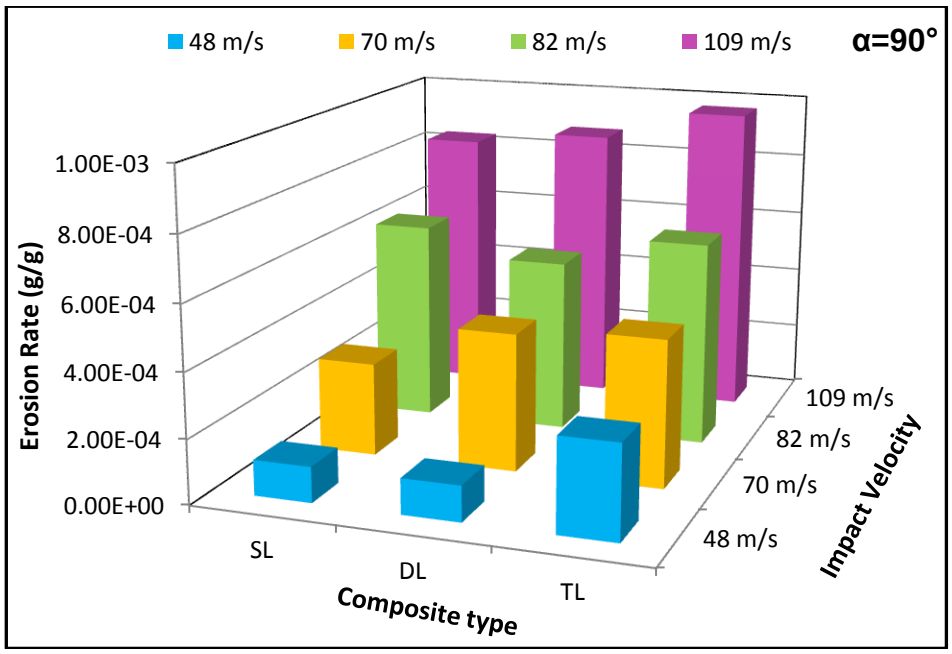

Figure-5.16 Histogram showing the erosive wear rates untreated LC-epoxy composite at four impact velocities (i.e. at 48, 70, 82 and 109 m/s) for 90 ° impact angle.

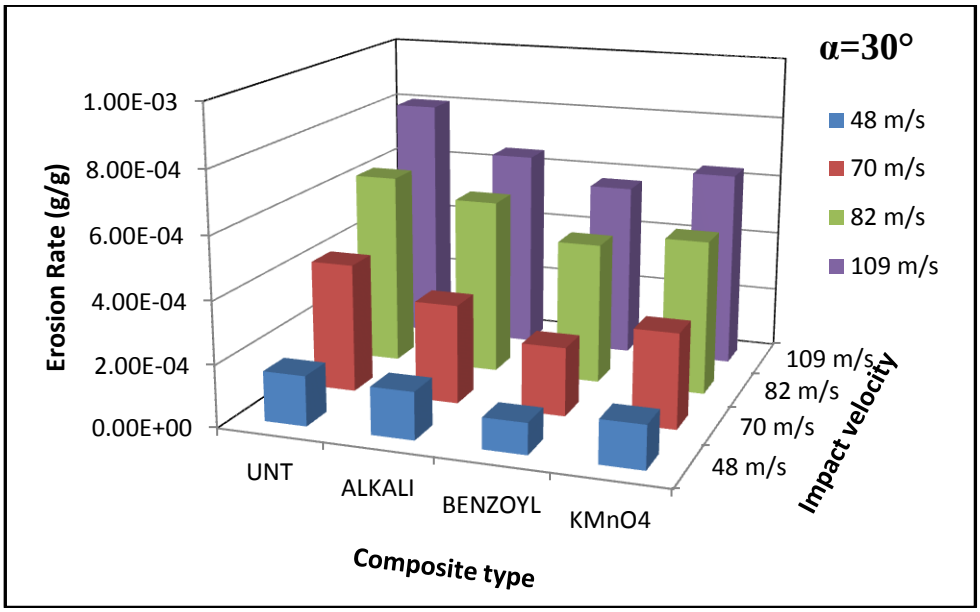

Figure-5.17 Histogram showing the erosive wear rates of treated double layer LC-epoxy composite at four impact velocities (i.e. at 48, 70, 82 and 109 m/s) for 30° impact angle.

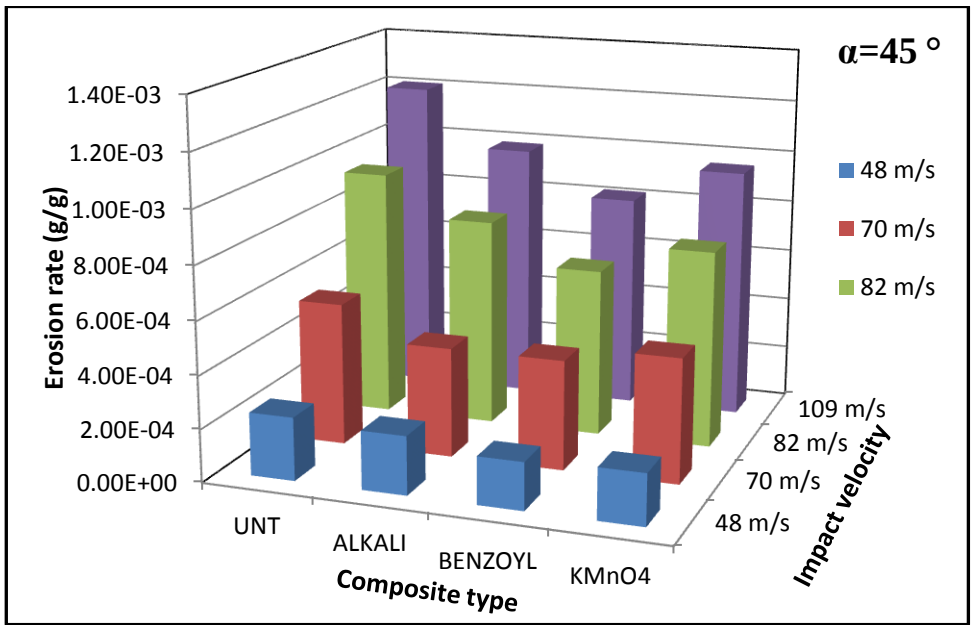

Figure-5.18 Histogram showing the erosive wear rates treated double layer LC-epoxy composite at four impact velocities (i.e. at 48, 70, 82 and 109 m/s) for 45° impact angle.

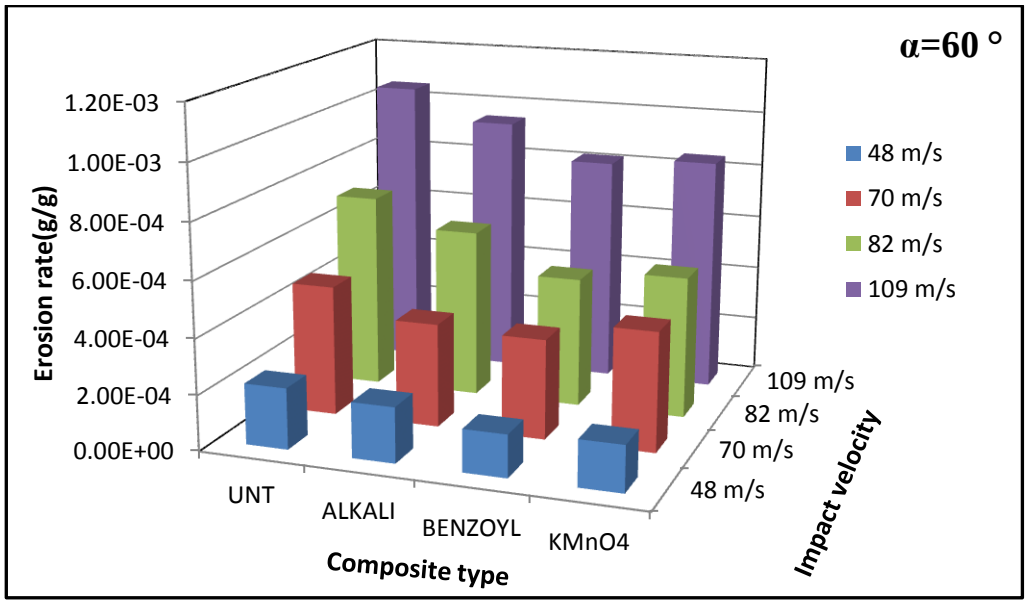

Figure-5.19 Histogram showing the erosive wear rates treated double layer LC-epoxy composite at four impact velocities (i.e. at 48, 70, 82 and 109 m/s) for 60 ° impact angle.

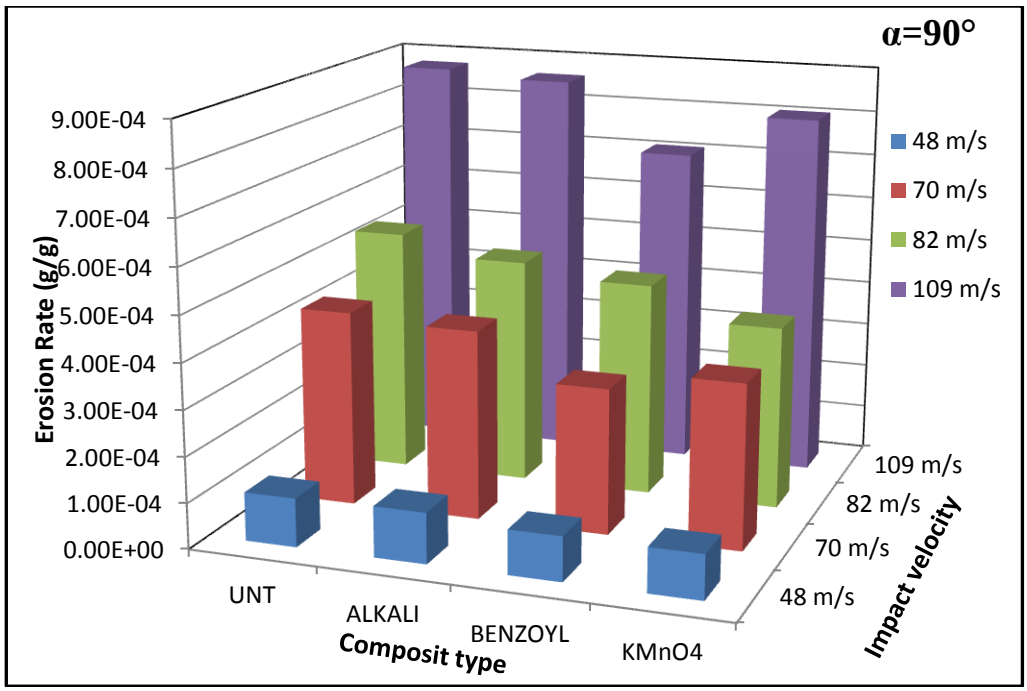

Figure-5.20 Histogram showing the erosive wear rates treated double layer LC-epoxy composite at four impact velocities (i.e. at 48, 70, 82 and 109 m/s) for 90° impact angle.

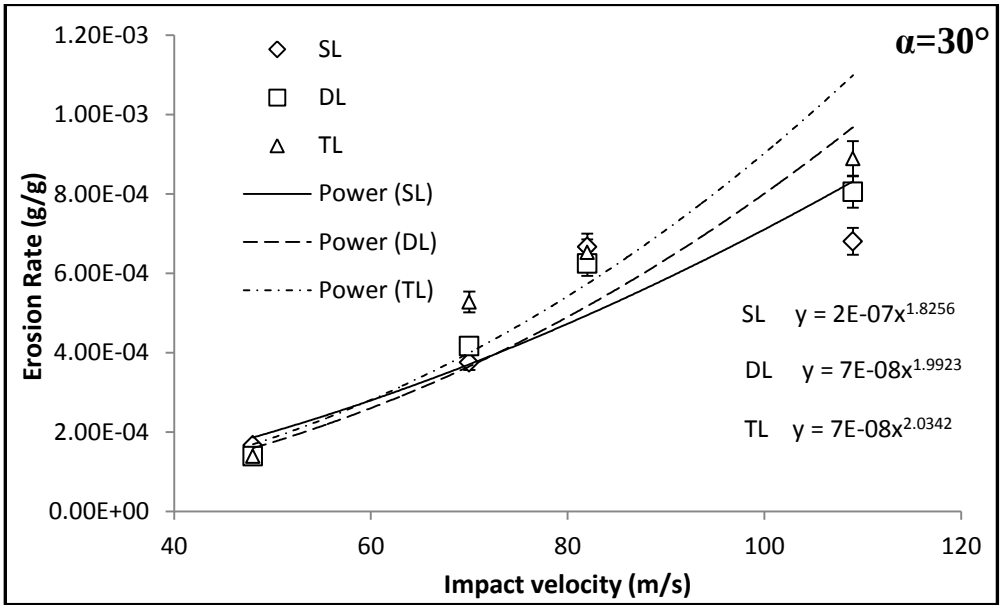

Figure-5.21 Erosion parameter for untreated LC-epoxy composite at impingement angle 30^0.

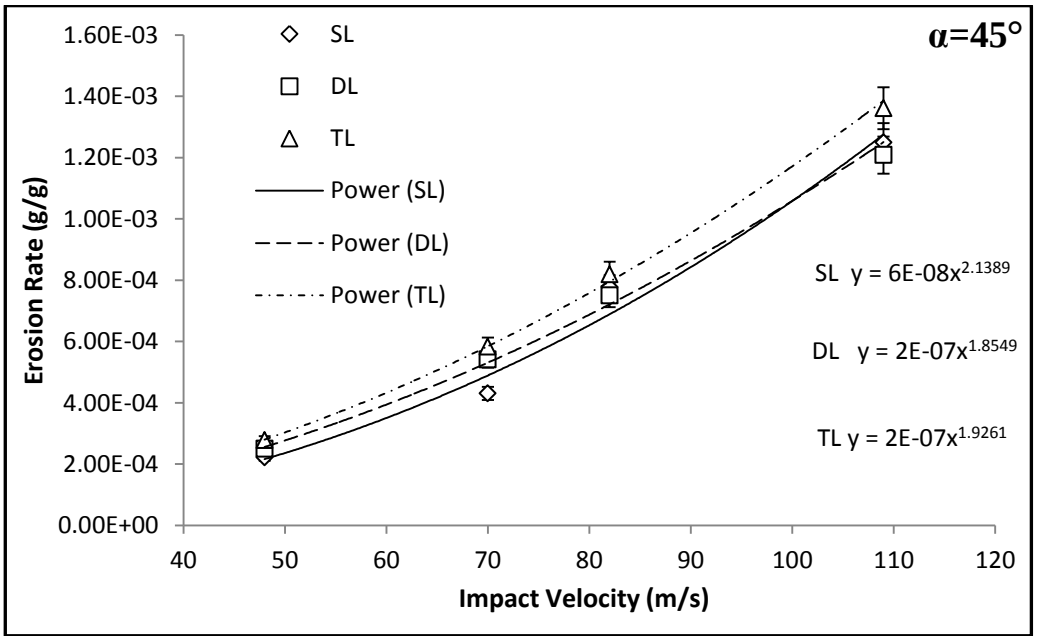

Figure-5.22 Erosion parameter for untreated LC-epoxy composite at impingement angle 45^0.

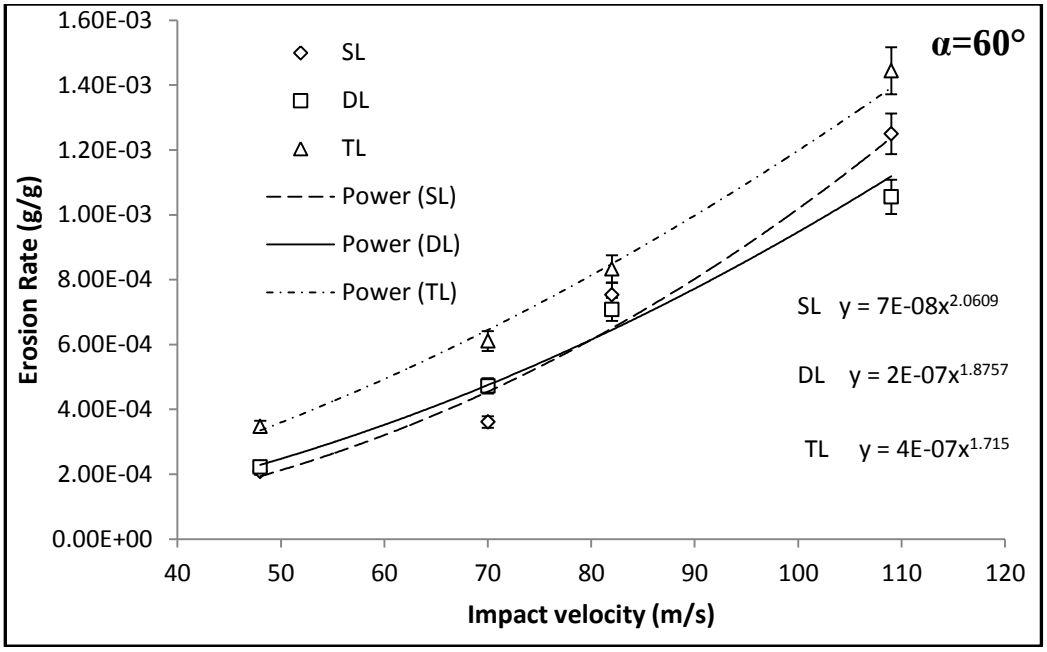

Figure-5.23 Erosion parameter for untreated LC-epoxy composite at impingement angle 60^0.

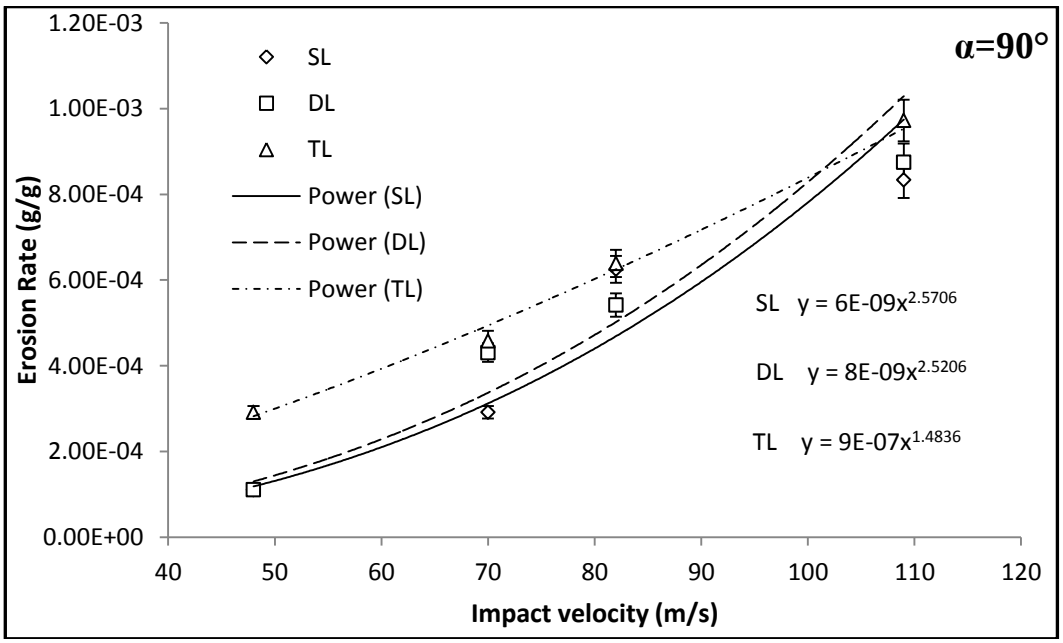

Figure-5.24 Erosion parameter for untreated LC-epoxy composite at impingement angle 90^0.

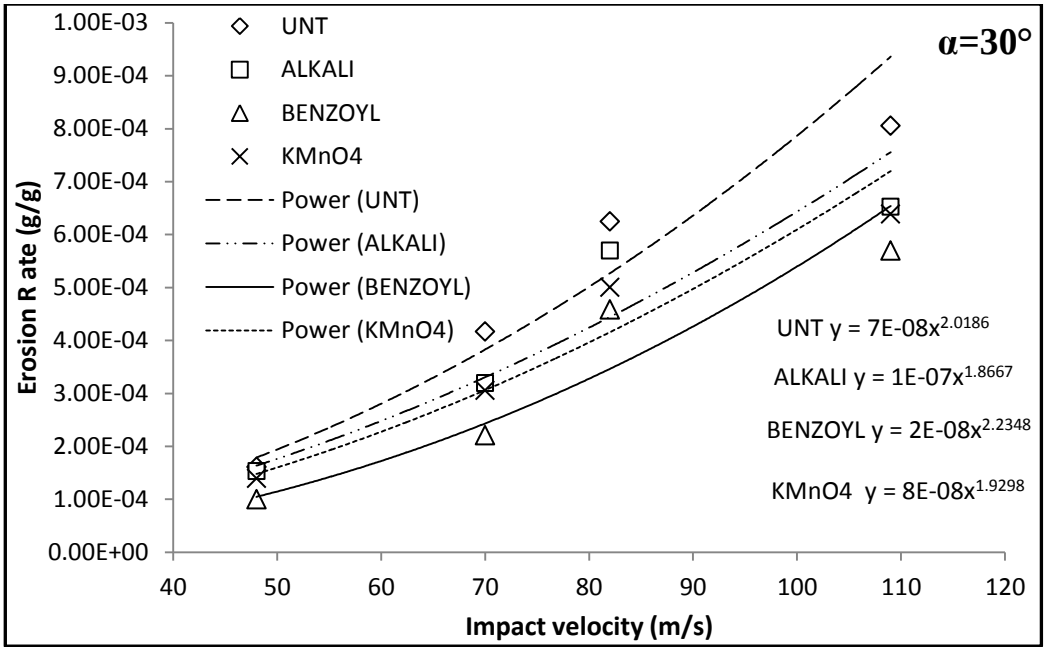

Figure-5.25 Erosion parameter for treated LC-epoxy composite at impingement angle 30^0.

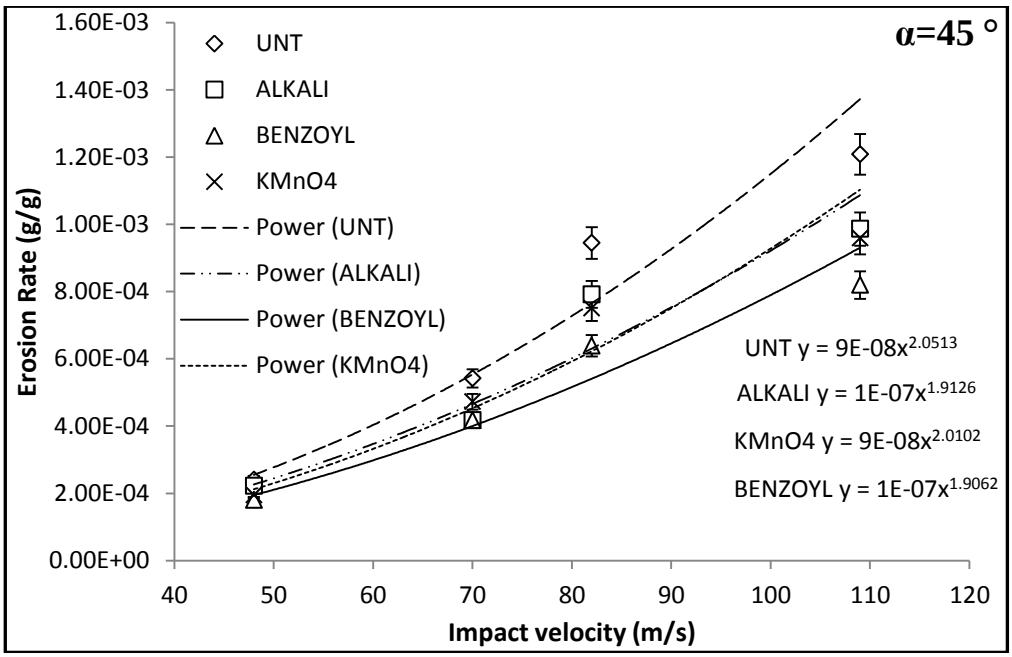

Figure-5.26 Erosion parameter for treated LC-epoxy composite at impingement angle 45^0.

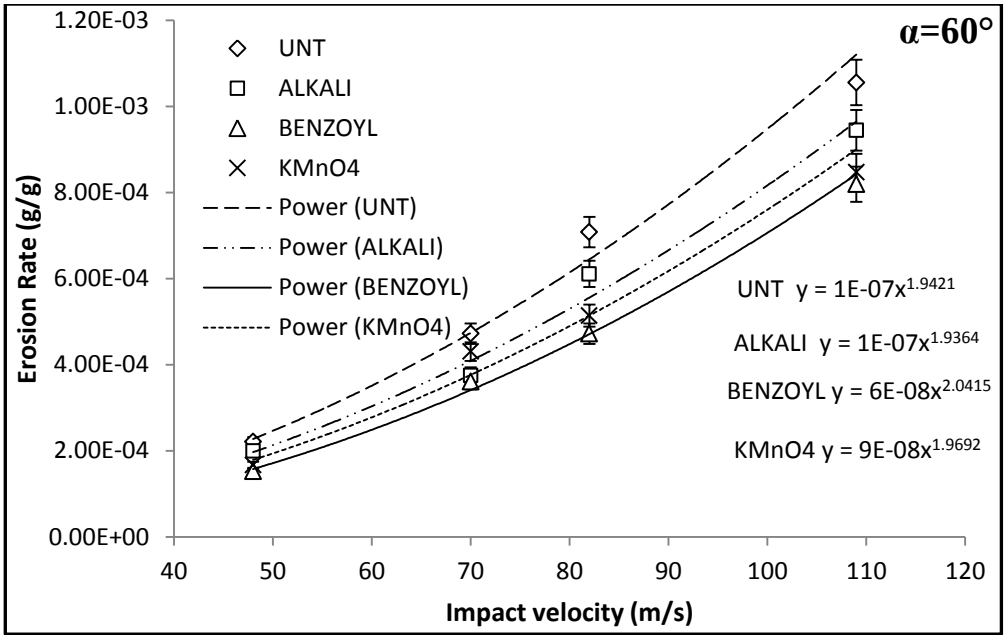

Figure-5.27 Erosion parameter for treated LC-epoxy composite at impingement angle 60^0.

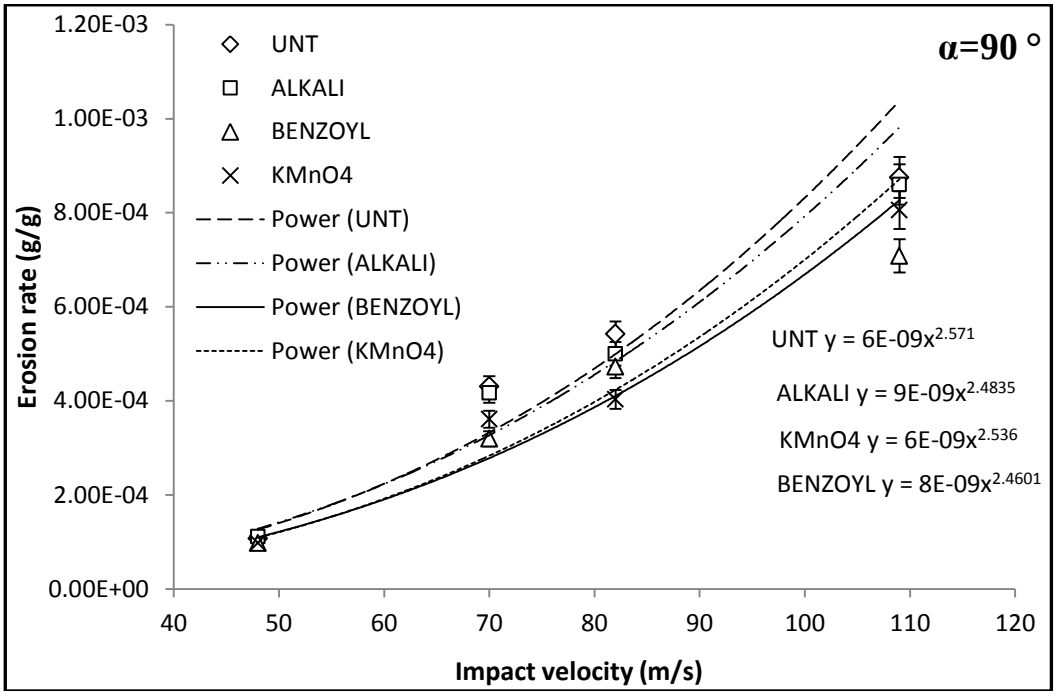

Figure-5.28 Erosion parameter for treated LC-epoxy composite at impingement angle 45^0.

Table-5.12 Parameters characterizing the velocity dependence of erosion rate of untreated and treated LC-epoxy composite.

Fiber content (%)	**Impact Angle(α)**	**k× 10^{-7}**	**n**	**R^2**
SL Untreated	30°	2.00	1.8256	0.892
	45°	0.60	2.1389	0.9797
	60°	0.70	2.0609	0.9448
	90°	0.06	2.5706	0.9525
DL Untreated	30°	0.70	1.9923	0.8819
	45°	2.00	1.8549	0.9916
	60°	2.00	1.8757	0.9838
	90°	0.08	2.5206	0.9501
TL Untreated	30°	0.70	2.0342	0.8335
	45°	2.00	1.9261	0.9984
	60°	4.00	1.715	0.9956
	90°	9.00	1.4836	0.9903
Alkali Treated	30°	1.00	1.8667	0.932
	45°	1.00	1.9126	0.9455
	60°	1.00	1.9364	0.9871
	90°	0.09	2.4835	0.9568
Benzoyl chloride Treated	30°	0.20	2.2348	0.9415
	45°	1.00	1.9062	0.9609
	60°	0.60	2.0415	0.9966
	90°	0.08	2.4601	0.9647
KMnO4 Treated	30°	0.80	1.9298	0.9615
	45°	0.90	2.0102	0.9569
	60°	0.90	1.9692	0.9806
	90°	0.06	2.536	0.9657

5.5.3 Erosion efficiency of LC-epoxy composite

As discussed earlier (art 5.4.4) erosion efficiency is also one of the important parameter for classifying the erosion behavior of any material. The erosion efficiency of both untreated and treated luffa fibre reinforced composite were calculated by using equation (5.6). The calculated results are presented in Table-5.11 along with their hardness values and operating conditions. The erosion efficiencies is found to be in the range of 1.78-14.63%, 1.60-12.34%, 3.23-17% for untreated SL,DL and TL LC-epoxy composite respectively and 1.52-11.75%,1.36-9.29% and 3.05-9.73% for alkali, benzoyl chloride and KMnO4 treated LC-epoxy composite for different impact velocities and impact angles studied. Thus, by observing the erosion efficiency and the velocity exponent (*n*), the erosion response of the LC-epoxy composites can be broadly categorized as semi-ductile. This conclusion was drawn by following the classifications made by Sundararajan and Roy [245]. Similar observations of the erosion efficiency for different polymeric composites have also been reported in the literature [253,241]. Further the data shown in table-5.11 also indicates that the erosion efficiency of luffa cylindrica epoxy composite varies with increase in fiber content and sometime with impact velocity. Similar observations are also reported by Srivastava et al. [254] for glass fiber epoxy composite. The treated reinforced composites show the lower erosion efficiency indicates a better erosion resistance. Also among all treated fiber reinforced composite benzoyl chloride treated composite shows lowest erosion efficiency is an indication of higher erosion resistance. The highest values of erosion efficiencies of untreated LC-epoxy composite indicate poor erosion resistance.

5.5.4 Surface morphology

Figure-5.29 (a) shows the SL composites eroded at a 45° impingement angle with a particle velocity of 82 m/s. It is observed from the SEM imaging that both micro ploughing and micro cutting together were responsible for material removal. Figure-5.29 (b,c) shows the micrographs of the eroded surface of DL and TL composites at a 45° impingement angle with a particle velocity of 82 m/s. It was observed by Sari et al. [249] that fibres in composites, when subjected to solid particle erosion, encountered intensive debonding and breakage. This was because the fibres in this particular situation were not effectively supported by the matrix material. The same type of

behaviour was observed in this experiment; the maximum erosion rate that occurred for the TL composite may have been because of insufficient matrix material.

Figure-5.30 (a-c) shows the micrographs of eroded surfaces of double layer of Luffa cylindrica reinforced epoxy composite for alkali, benzoyl chloride and KMno4 treated fiber composite at a 45° impingement angle with a particle velocity of 82 m/s. It is observed from the SEM figure that in all the treated fiber composite due to good compatibility of fiber with the matrix there is less removal of material. Matrix cracking and cavity due to impingement of silica sand is visible in alkali treated fiber composite (Figure-5.30 (a)). For KMnO4 treated fiber composite (Figure-5.30(b)) and benzoyl chloride treated fiber composite (Figure-5.30(c)) surface damage is found very less as compared to the untreated fiber composite (Figure-5.29). This means there is good bonding between fiber and matrix that helps in reducing wear of the composite. This also confirms the experimental results that benzoyl chloride treated fiber composite gives the minimum erosion rate.

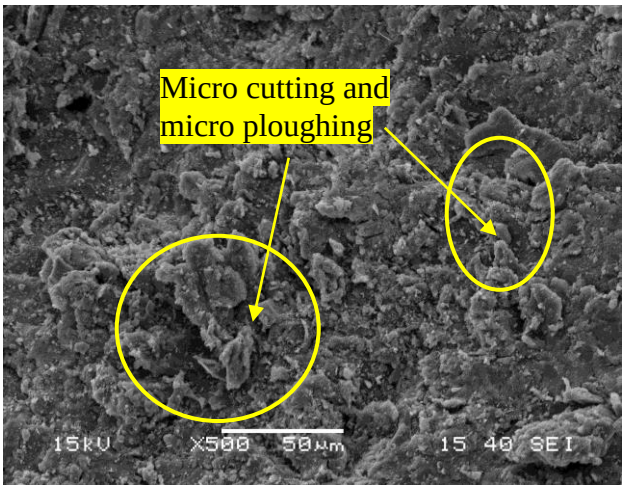

(a)

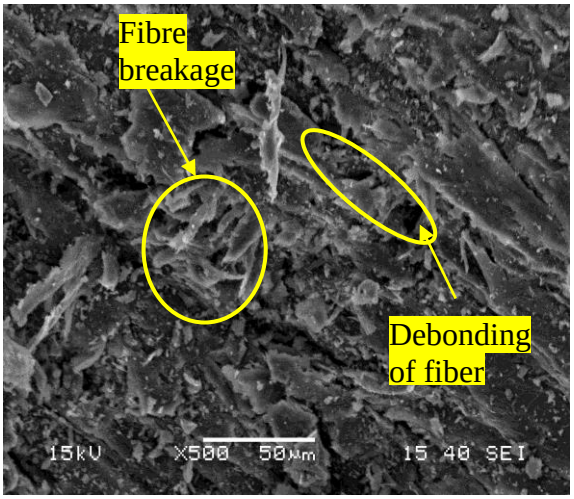

(b)

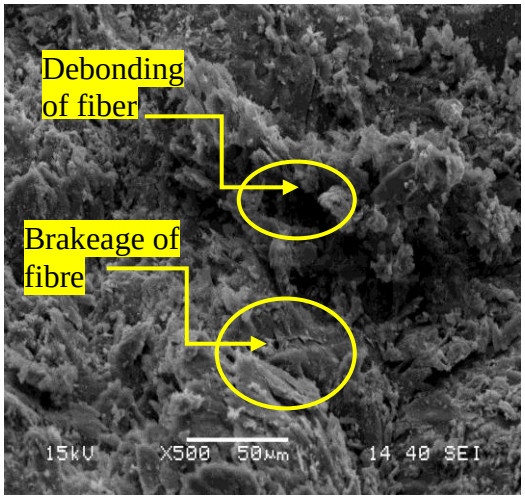

(c)

Figure-5.29 SEM micrographs of eroded surface of (a) single layer (b) double layer c) triple layer LC-epoxy composite at 45° impingement angle at impact velocity 82 m/s.

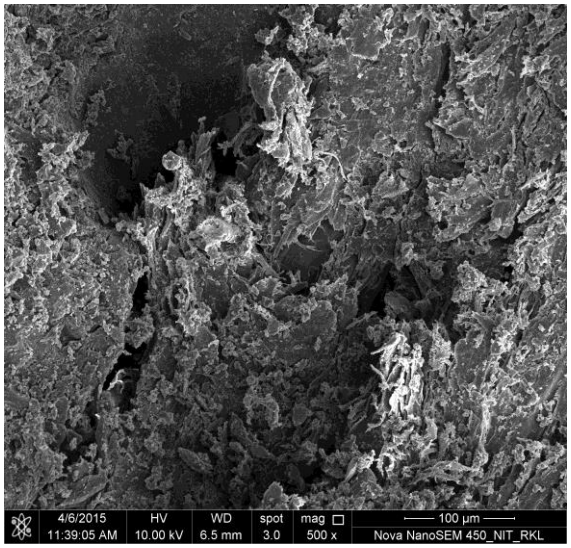

(a)

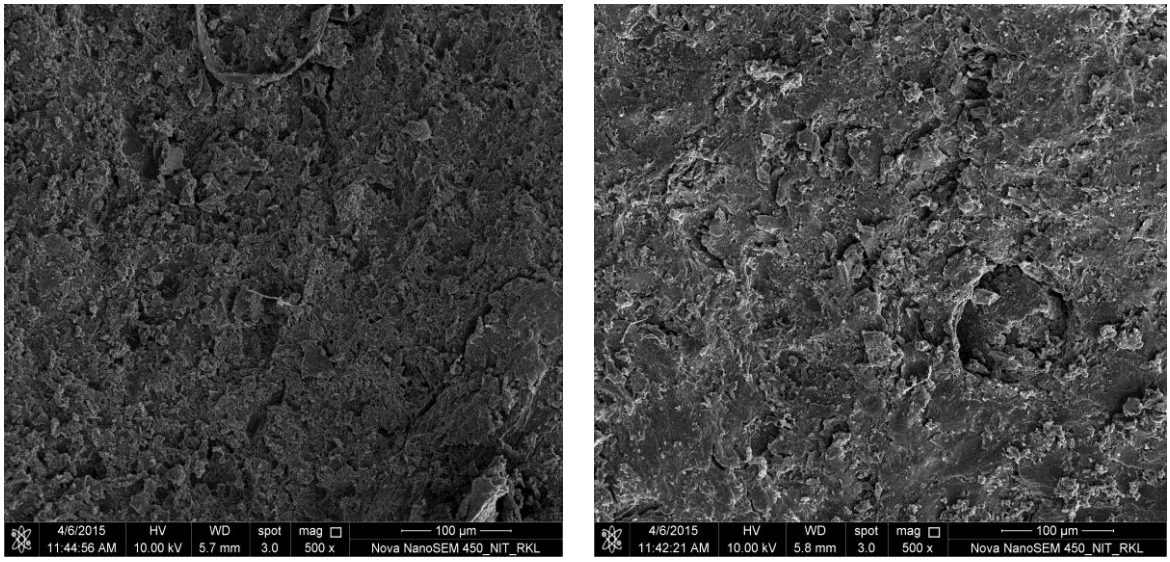

(b) (c)

Figure-5.30 SEM micrographs of eroded surface of (a) alkali and (b) KMnO4 (c) benzoyl chloride treated composite at 45° impingement angle at impact velocity 82 m/s.

5.6 CONCLUSIONS

Experiments were conducted to study the solid particle erosion of both untreated and treated luffa cylindrica reinforced epoxy composites with silica sand as erodent. Polymer composites are experimented at various impingement angles and impact velocities. Based on the studies, the following conclusions are drawn.

- Study of influence of impingement angle on erosion rate of the composites with both untreated and treated luffa fiber reveals their semi ductile nature with respect to erosive wear. The peak erosion rate is found to be occurring at 45° impingement angle at lower to medium impact velocities and at 60° at higher velocities for both untreated and treated composites.

- The erosion rate for all of the composites increases with increase of impact velocity. It is observed that the erosion rate followed the power law behavior

with respect to impact velocity, $Er = kV^n$, and the value of the velocity exponent n is obtained in the range of 1.2 to 3.3, conforming that the LC-epoxy composite exhibits a semi-ductile behavior.

- The erosion efficiency of the LC- epoxy composites is found to be1.52-17% for different impact angle and different impact velocities studied conforming that the LC-epoxy composite exhibits semi-ductile behavior.

- The chemical treatment of luffa cylindrica fiber reduces the erosion rate. The chemical treatment of luffa cylindrica with benzoyl chloride offers maximum erosion resistance.

- The morphology of the eroded surface observed by SEM suggested that the overall erosion damage of the composite is mainly due to breaking of fiber and subsequent removal from the matrix. This removal of fiber might be due to softening of matrix material due to impacting particles velocities. This removal of fiber from the matrix is the result of both micro ploughing and micro cutting due to impacting velocities.

- From the experiment it is believed that possible use of these particulate composites can be made in the areas such as pipe lines carrying coal dust, slurries, desert structure, low cost housing, boats/sporting equipment, partition boards, doors and window panels.

Chapter 6

Mechanical and tribological behavior of Luffa cylindrica fiber reinforced Hybrid epoxy composite

6.1 INTRODUCTION

Multicomponent composite materials comprising of two or more families of fibers have recently attracted the attention of researchers. This is because the use of one type of fiber alone has proved to be inadequate in satisfactorily tackling all the technical and economic problems that comes in the path of fiber reinforced composites. There are basically two types of fibers: natural and synthetic fibers. Lot of work has been carried out by several researchers on the composites based on these fibers [114,255-256]. Both the fibers as reinforcing material have proved to be advantage and disadvantage in different situations. For instance, a natural fiber such as cotton, jute, and sisal as far as cost is concerned much cheaper than synthetic fibers such as glass, nylon, and carbon etc. But the mechanical properties of these natural fiber composites are much lower than those of the synthetic fiber composites. Though synthetic fibers have very good mechanical properties, from environmental point of view they are not suitable because of their recycling problem. In contrast, natural fibers are renewable raw materials and they are recyclable [103]. Another advantage of synthetic fibers is their moisture repellency, whereas poor resistance to moisture absorption made the use of natural fiber-reinforced composites less attractive [257]. Therefore researchers are focusing their attention towards combining both these fibers to produce hybrid composite by taking best properties from these fiber by which an optimal, superior but economical composite can be obtained. Accordingly several attempts are being made to combined different natural fibers with synthetic fiber for various applications.

Kalaprasad et al. [258] have studied the low-density polyethylene-based short sisal–glass hybrid composites and found a considerable enhancement in the mechanical properties. Nayak et al. [116] studied the dynamic mechanical and thermal properties of sisal–glass-fiber-reinforced PP hybrid composites and found a positive hybrid effect for the mechanical strength.

Pavithran et al.[259] determined the work of fracture by impact testing on sisal–glass hybrid composites with two arrangements, one with sisal shell and glass core and the other with glass shell and sisal core. They showed that the sisal shell laminate had the higher work of fracture compared with glass shell hybrid laminates of equivalent volume fraction of sisal and glass fibers. Mishra et al. [147] studied the effect of glass

fiber addition on tensile and flexural strength and izode impact strength of pine apple leaf fiber (PALF) and sisal fiber reinforced polyester composites. K. John et al. [260-262] have studied the unsaturated polyester based sisal glass composites with 5% and 8% volume fraction and found a considerable enhancement in impact, compression, flexural and tensile properties.

Abdul Khalil et al. [114] reported the enhancement in the mechanical properties (tensile, flexural, impact, and hardness) of oil palm- polyester composites by incorporating chopped strand mat (CSM) glass fibers with oil palm empty fruit fiber (EFB). Almeida et al. [263] evaluated the enhancement in the mechanical properties of curaua polyester composites by incorporating chopped glass fibres with chopped curaua fibre.

Pavithran et al. [264] evaluated the enhancement in the properties of coir-polyester composites by incorporating glass as intimate mix with coir. Mohan et al. [265] reported that jute provided a reasonable core material in jute-glass hybrid laminates. They evaluated flexural properties and compressive properties of the jute-glass reinforced epoxy laminates fabricated by filament winding technique using flat mandrel. Four different hybrid combinations were studied with different glass fiber volume fractions and the results were compared with jute reinforced plastic. They found substantial increase in flexural and compressive properties with hybridization.

Patel et al. [266] reported that the erosive wear resistance of jute/epoxy composite can be improved significantly by hybridizing with synthetic fibre glass.

In this chapter, effect of hybridization of glass and layering sequence effect on mechanical properties properties and tribological properties of luffa-glass fiber hybrid composites is studied. As an initial investigation in the present work the influence of impinging velocity, impingement angle and laminate stacking sequence on erosive wear has been carried out and results of these investigations are presented in the subsequent sections.

6.2 COMPOSITE FABRICATION

6.2.1 Raw materials used

Raw materials used in this experimental work are listed below:

1. Luffa cylindrica fiber
2. E-glass fiber
3. Epoxy resin
4. Hardener

6.2.1.1 Luffa cylindrica fiber

The details of the luffa cylindrica fiber preparation used for the present investigation are same as explained in chapter 3, art 3.4.1.The natural luffa cylindrica mat cut to size 150 mm ×100 mm from the outer core of the sponge guard is shown in Figure-6.1.

Figure-6.1 Natural luffa fiber mat.

6.2.1.2 E-glass fiber

Glass fiber is a generic name like carbon fiber or steel. A variety of different chemical compositions is commercially available. Common glass fibers are silica based (50-60% SiO_2) and contains a host of other oxides of calcium boron, sodium, aluminum, and iron. Table -6.1 gives the composition of some common used glass

fibers for different applications. The designation E stands for electrical. E-glass is a good electrical insulator in addition to have a good strength and a reasonable Young's Modulus. C stands for corrosion and this glass has a better resistance to chemical corrosion; S stands for high silica content that makes S glass to withstand higher temperature than other glasses. It should be pointed out that most of the continuous glass fiber produced is of the E glass type but, notwithstanding the designation E. Electrical use of E glass fiber are only small fraction of the total market.

Table-6.1 Approximate chemical composition of some glass fibers (wt. %).

composition	E glass	C glass	S glass
SiO_2	55.2	65.0	65.0
Al_2O_3	8.0	4	25.0
CaO	18.7	14.0	_
MgO	4.6	3.0	10
Na_2O	0.3	8.5	0.3
K_2O	0.2	-	_
B_2O_3	7.3	5.0	_

Limitation of glass fiber

Glass fiber reinforced composites suffer from three important limitations:

1. Comparatively low modulus of elasticity (the specific modulus of unidirectional fiber glass composites being of same order as aluminium,titanium, magnesium and steel)
2. Low Interlaminar shear strength in relation to tensile strength.
3. Low compressive properties in relation to tensile properties (the comparison allowable for unidirectional layup being less than one half of tensile strength)

The low modulus of glass-reinforced composites has limited their usefulness in applications where buckling stability or high natural frequency is an important criteria. Both shear and compressive deficiencies of this fiber have restricted its performance in bending.

Glass fiber used in the present investigation along with luffa fiber is shown in figure-6.2. E-glass fiber 360 roving supplied by Saint Gobian ltd was used for making hybrid polymer matrix composite. The fibers were cut to sizes 150 mm ×100 mm from the long sheet.

Figure-6.2 E-Glass fiber mats.

6.2.1.3 Epoxy resin and Hardener

The details of the epoxy resin and hardener used for the preparation of test specimen are same as explained in chapter 3 art 3.4.2.

6.2.1.4 Preparation of composites

Hybrid laminates of luffa and glass fiber were prepared by hand lay-up technique. A wooden mold of 150 mm ×100 mm ×5 mm was used for manufacturing the composite. The procedure of preparation of test specimens were carried out as per the procedure discussed in chapter 3, art 3.4.3. Five groups of laminate composite samples with total 4 plies were manufactured by varying stacking sequence of luffa and glass fabrics. Table-6.2 shows the various stacking sequence with their designations along with the volume fraction of fibre and thickness of composite. Care was taken to keep the thickness of the samples to 5mm as far as possible. After curing the laminate was cut into required size for mechanical and erosive wear tests by diamond cutter. The total volume fraction of fibre is calculated using equation 6.1.

$$V_f = \frac{(W_l/\rho_l)+(W_g/\rho_g)}{(W_l/\rho_l)+(W_g/\rho_g)+(W_m/\rho_m)} \quad (6.1)$$

Where W_l, Wg and Wm are the known weights of the luffa cylindrica fibre, glass fibre and epoxy resin, respectively, and ρ_l, ρ_g *and* ρ_m are the densities of luffa cylindrica, glass fibre and epoxy resin. The density of epoxy resin, luffa cylindrica and glass fibre is found to be 1.1 g/cm^3, 0.56 g/cm^3 and 2.55 g/cm^3 respectively.

Table-6.2 Laminate stacking sequence

Symbol	Laminate stacking sequence	Total Fibre		Thickness (mm)
		Weight fraction (%)	Volume fraction (%)	
S1	LLLL	18.52	30.86	5.6
S2	LGLG	24.42	28.99	5.12
S3	LGGL	17.72	19.12	5.12
S4	GLLG	18.50	19.87	5.13
S5	GGGG	14.27	6.7	5.00
L-Luffa cylindrica layer , G-Glass fibre layer				

6.3 EXPERIMENTS

6.3.1 Mechanical testing of the luffa-glass hybrid composite

6.3.1.1 Density and Void Fraction

The test procedure for density and void fraction are well explained in chapter 3, art 3.5.1. The obtained result of density and void fractions are listed in Table-6.3.

6.3.1.2 Tensile Strength,Flexural and Interlaminar shear strength

The test procedure for tensile, flexural and interlaminar shear strength (ILSS) is explained in chapter 3, art 3.5.2 and 3.5.3. The results obtained from these tests are presented in Table-6.4.

6.3.1.2 Micro hardness.

The test procedure for micro hardness is explained in chapter 3, art 3.5.5. The results obtained from the tests are also presented in same table-6.4.

Table-6.3. Measured and theoretical densities of the luffa-glass hybrid epoxy composites.

Stacking sequence	Theoretical density (g/cm^3)	Measured density (g/cm^3)	Volume fraction of voids (%)
Neat epoxy	1.2	1.18	1.66
S1	1.01	1.009	1.2
S2	1.18	1.178	0.89
S3	1.187	1.177	0.878
S4	1.188	1.179	0.78
S5	1.3054	1.297	0.65

Table-6.4 Mechanical properties of luffa-glass hybrid epoxy composites.

Composite type	Tensile strength (Mpa)	Young's Modulus (Mpa)	Flexural strength (MPa)	Flexural Modulus (MPa)	ILSS (Mpa)	Vickers Hardness (Hv)
NE	12.50	521.00	17	1150	0.60	17.90
S1	17.63	768	39.10	1210	2.148	19.94
S2	25.87	906.88	107.93	3864	5.628	20.74
S3	32.17	831.89	63.116	2869	3.656	19.95
S4	35.34	1085	108.36	4075	5.161	20.65
S5	79.02	1248	154.41	6035	7.841	20.39

6.3.2 Erosive wear test

6.3.2.1 Test apparatus & Experiment

The erosion test apparatus for the present case is one which is used earlier. The details of the test apparatus, procedure and the conditions under which the test has been carried out is same for this investigation also and has been discussed in details in chapter 5, art-5.4.4.

The experimental results of the weight loss and erosion rate for luffa-glass hybrid composites with different impact angle and impact velocities are tabulated and presented in table-6.5 to 6.9.

Table-6.5 Weight loss and Erosion rate of laminate stacking sequence S1 (LLLL) with respect to impingement angle due to erosion for a period of 21 min.

Velocity (m/s)	**Impact Angle (°)**	**S1 (LLLL)**	
		Weight loss 'Δw' g	**Erosion rate × 10^{-4} (g/g)**
48	30^0	0.006	1.333
	45^0	0.008	1.778
	60^0	0.011	2.444
	90^0	0.004	0.888
70	30^0	0.012	2.667
	45^0	0.017	3.778
	60^0	0.018	4.000
	90^0	0.015	3.330
82	30^0	0.023	5.111
	45^0	0.028	6.222
	60^0	0.037	8.222
	90^0	0.029	6.444
109	30^0	0.03	6.667

	45^0	0.04	8.900
	60^0	0.04	8.990
	90^0	0.038	8.444

Table-6.6 Weight loss and Erosion rate of laminate stacking sequence S2 (LGLG) with respect to impingement angle due to erosion for a period of 21 min.

Velocity (m/s)	**Impact Angle (°)**	**S2 (LGLG)**	
		Weight loss 'Δw' g	**Erosion rate × 10^{-4} (g/g)**
48	30^0	0.006	1.333
	45^0	0.007	1.556
	60^0	0.008	1.778
	90^0	0.004	0.888
70	30^0	0.012	2.667
	45^0	0.0156	3.467
	60^0	0.016	3.556
	90^0	0.01	2.222
82	30^0	0.016	3.556
	45^0	0.022	4.890
	60^0	0.024	5.333
	90^0	0.02	4.444
109	30^0	0.022	4.889
	45^0	0.035	7.778
	60^0	0.034	7.500
	90^0	0.031	6.889

Table-6.7 Weight loss and Erosion rate of laminate stacking sequence S3 (LGGL) with respect to impingement angle due to erosion for a period of 21 min.

Velocity (m/s)	**Impact Angle (°)**	**S3 (LGGL)**	
		Weight loss 'Δw' g	**Erosion rate × 10^{-4} (g/g)**
48	30^0	0.004	0.888
	45^0	0.005	1.111
	60^0	0.01	2.222
	90^0	0.005	1.111
70	30^0	0.014	3.111
	45^0	0.018	4.000
	60^0	0.019	4.222
	90^0	0.016	3.556
82	30^0	0.018	4.000
	45^0	0.025	5.556
	60^0	0.027	6.000
	90^0	0.022	4.889
109	30^0	0.022	4.889
	45^0	0.038	8.444
	60^0	0.032	7.111
	90^0	0.027	6.000

Table-6.8 Weight loss and Erosion rate of laminate stacking sequence S4 (GLLG) with respect to impingement angle due to erosion for a period of 21 min.

Velocity (m/s)	**Impact Angle (°)**	**S4 (GLLG)**	
		Weight loss 'Δw' g	**Erosion rate × 10^{-4} (g/g)**
48	30^0	0.004	0.888
	45^0	0.006	1.333
	60^0	0.0065	1.444
	90^0	0.005	1.111
70	30^0	0.006	1.333
	45^0	0.011	2.444
	60^0	0.011	2.444
	90^0	0.008	1.778
82	30^0	0.014	3.111
	45^0	0.021	4.667
	60^0	0.019	4.220
	90^0	0.017	3.778
109	30^0	0.02	4.444
	45^0	0.029	6.444
	60^0	0.027	6.100
	90^0	0.024	5.333

Table-6.9 Weight loss and Erosion rate of laminate stacking sequence S4 (GLLG) with respect to impingement angle due to erosion for a period of 21 min.

Velocity (m/s)	**Impact Angle (°)**	**S5(GGGG)**	
		Weight loss 'Δw' g	**Erosion rate × 10^{-4} (g/g)**
48	30^0	0.004	0.888
	45^0	0.006	1.333
	60^0	0.004	0.888
	90^0	0.003	0.667
70	30^0	0.004	0.889
	45^0	0.008	1.778
	60^0	0.007	1.556
	90^0	0.005	1.111
82	30^0	0.011	2.444
	45^0	0.018	4.000
	60^0	0.016	3.556
	90^0	0.0132	2.933
109	30^0	0.014	3.111
	45^0	0.026	5.778
	60^0	0.021	4.667
	90^0	0.02	4.444

6.3.3 Scanning electron microscopy

The fracture surfaces of the specimens after mechanical test and worn surface of the sample after erosion wear are examined directly by field emission scanning electron microscope Nova Nano SEM 450. This test procedure is explained in chapter 3, art 3.5.6.

6.3 RESULTS AND DISCUSSIONS

6.4.1 Mechanical characterization luffa-glass hybrid composite

6.4.1.1 Density and Void fraction

Density is one of the primary factors that determine the properties of the composite. Often it is found that the theoretical values of the density will not match with the experimentally measured values. This is primarily due to presence of voids or air bubbles in the composite. This has a greater contribution which affects the mechanical properties and the performance of the composite in the actual work place. Higher void contents usually mean lower fatigue resistance, greater susceptibility to water penetration, and weathering [164]. Thus the knowledge of void content is desirable for estimation of the quality of the composites. It is understandable that a good composite should have fewer voids. However, the presence of void is unavoidable in composite making particularly through hand-lay-up technique.

The theoretical and measured densities of the developed composites along with the corresponding volume fraction of voids for the present case are presented in table-6.3. As shown in table in all laminate stacking sequences, the volume fractions of voids are found to be reasonably small i.e. <1.5%.

Figure-6.3 shows the density of the composites for different stacking sequences. It is seen that density for sequences S1 is the lowest since it contains only the luffa layers. From S2 sequence onwards up to S5 density increases and it is maximum for sequences S5. This increase in density is due to the incorporation of glass layer for which density is higher than luffa fiber.

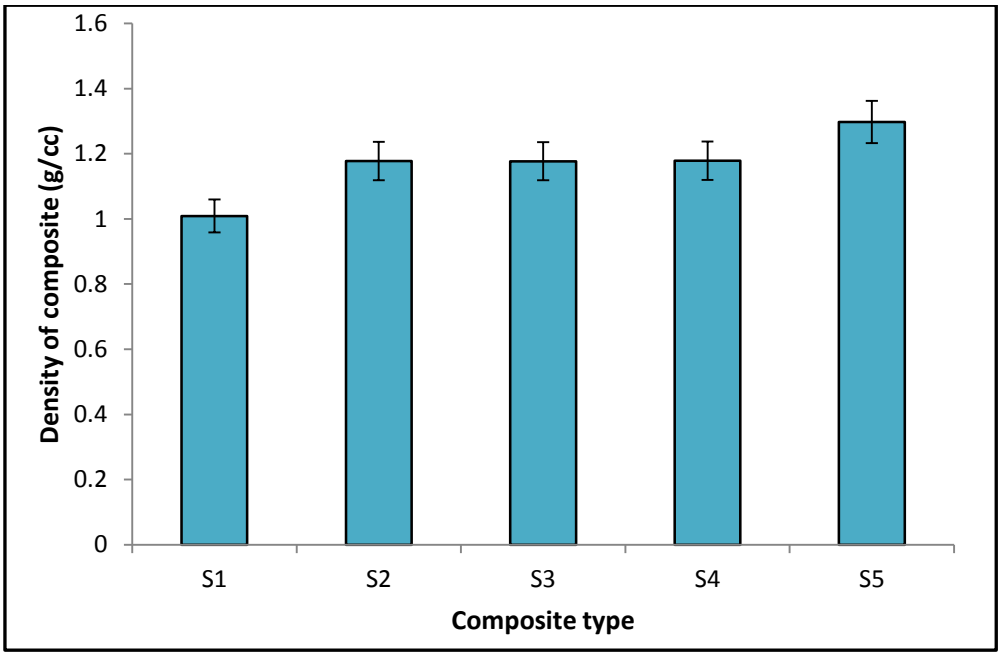

Figure-6.3 Density of the composite laminates.

6.4.1.2 Tensile strength

It is well known that fibre strength is mainly responsible for strength properties of the composite. Therefore variation in tensile strength of the composite with various fibres loading is obvious. The variation of tensile strength for different laminate stacking sequences is presented in table-6.4 and shown in figure-6.4. It is found that with only luffa cylindrica fibre laminates; the tensile strength of the composite is 17.628Mpa.With different sequence of luffa with glass fibre the tensile strength varies between 25.87 and 35.34 Mpa. It is found to be maximum for the sequence S4 (i.e.) two glass fibre at the extreme layer with two luffa cylindrica fibre at the middle among all hybrid laminate sequences. It is interesting to note that by incorporating glass fibre with luffa cylindrica fibre the tensile strength increases to about 46.6, 82 and 100.4% for the sequences S2,S3 and S4 in comparisons to sequence S1 (i.e.) only luffa cylindrica fibre. Similar types of results are also reported by raghavendra et al. [267] while they worked with jute-glass hybrid composite.

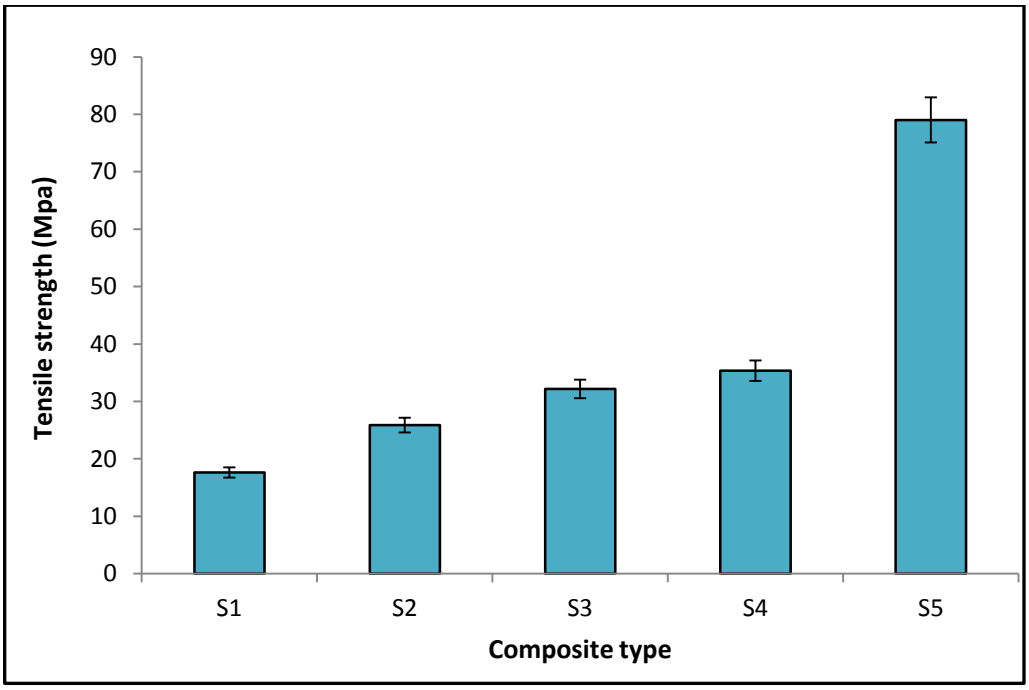

Figure-6.4 Tensile strength of the composite laminates.

6.4.1.3 Flexural strength

The variation of flexural strength for various laminate stacking sequences is presented in Table-6.4 and shown in figure-6.5. The flexural strength of the only luffa cylindrica reinforced epoxy resin is found to be 39.1 MPa. An increase in the flexural strength of 130, 176 and 177 % is observed for Luffa-glass fibre-reinforced hybrid laminate for sequences S2, S3 and S4 composites when compared to that of only luffa cylindrica laminate (i.e.) S1. It is also found that Flexural strength for the sequences S3 and S4 are maximum (i.e.) when the glass fibre layers are placed at the extreme layer compared to other hybrid laminate stacking sequences. This can be said from this type of observation that the flexural strength is controlled by the extreme layer of reinforcement. Same type of observation is also reported by Gouda et al. [268] while they worked with untreated jute fabric-reinforced polyester composites.

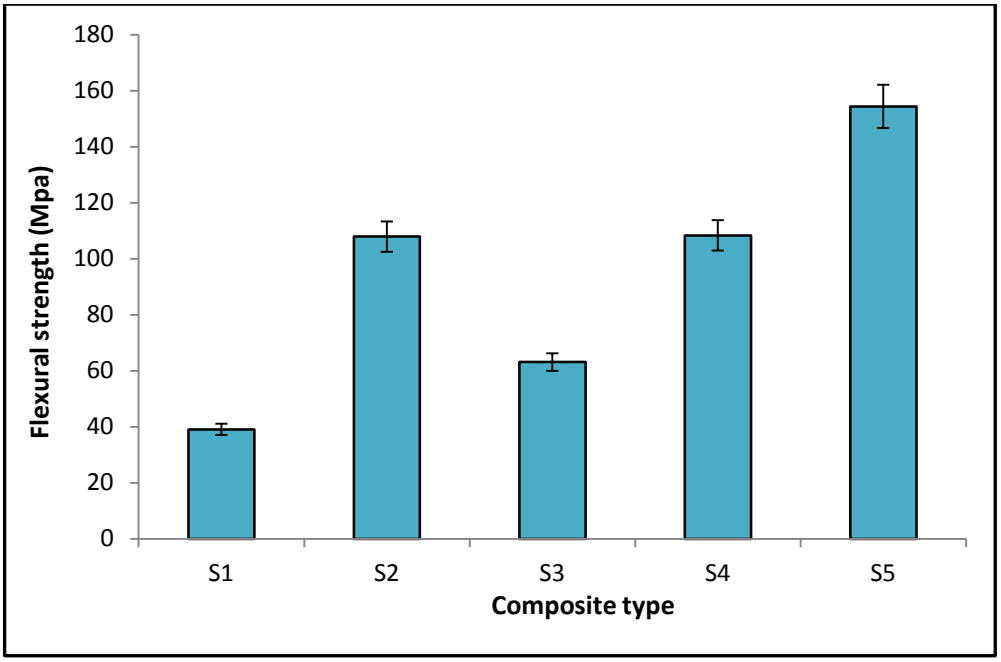

Figure-6.5 Flexural strength of the composite laminates.

6.4.1.4 Tensile and Flexural modulus

The variation tensile modulus for various laminate stacking sequences of luffa-glass fiber epoxy hybrid composites is shown in Figure-6.6 and 6.7. The higher modulus was recorded for the conventional glass fiber composites in both cases. The tensile and flexural moduli of the only luffa cylindrica fiber are 768Mpa and 1210 Mpa respectively. Addition of glass fiber with luffa fiber with various stacking sequences increases the tensile and flexural modulus and it is found to be maximum for laminate stacking sequence S4. Similar observations were reported by Raghavendra et al. [267] while they worked with jute-glass hybrid composite.

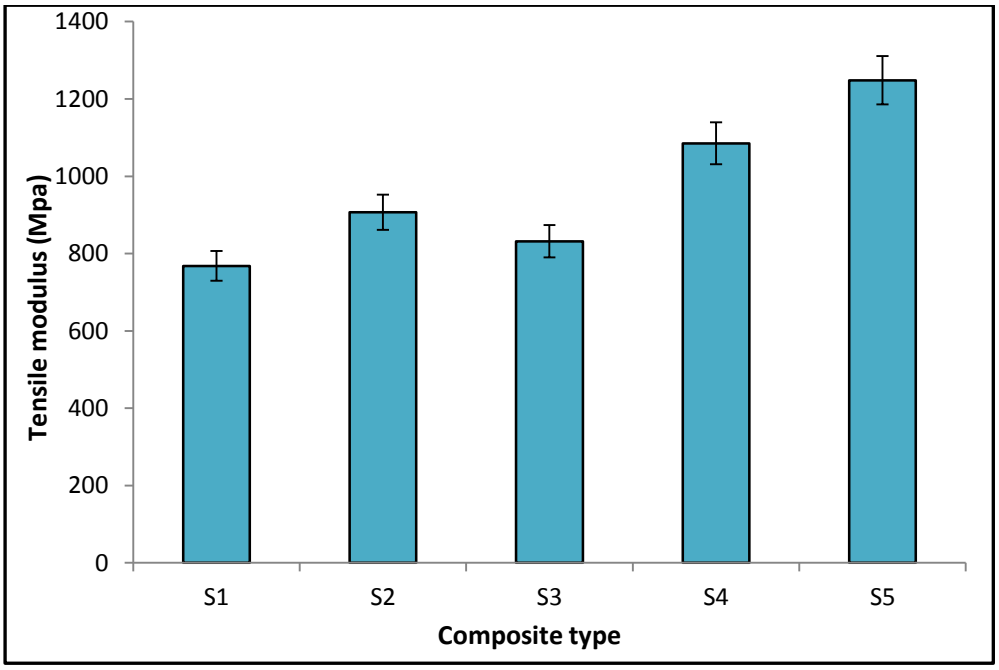

Figure-6.6 Tensile modulus of the composite laminates.

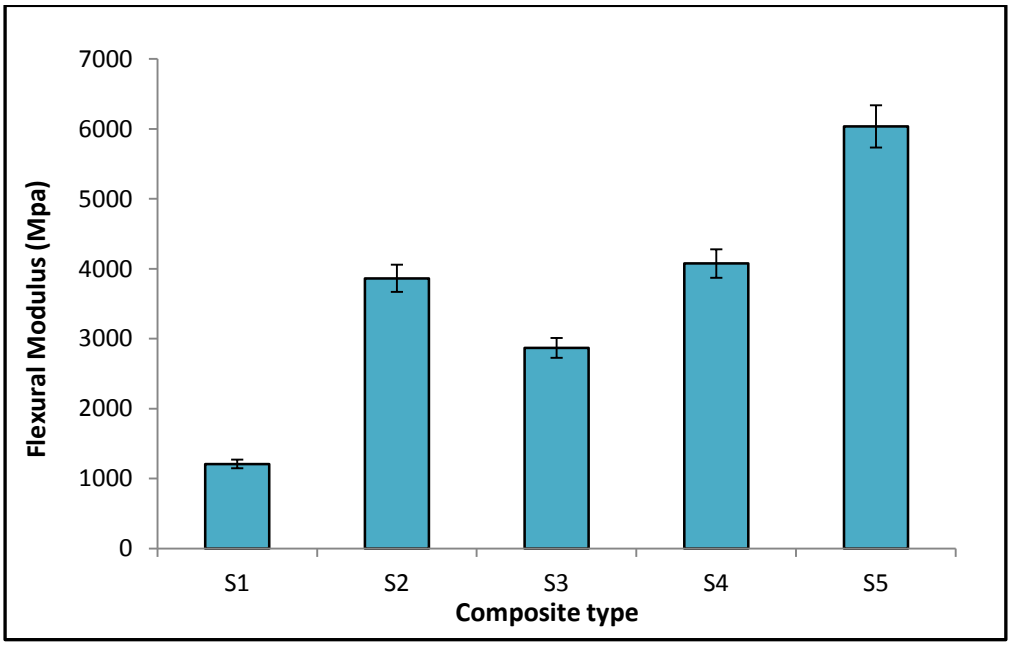

Figure-6.7 Flexural modulus of the composite laminates.

6.4.1.5 Interlaminar shear strength

The ILSS of the laminates for different stacking sequences shows similar trend in line with flexural strength as shown in figure-6.8. The laminate stacking sequence S1 i.e. only luffa cylindrica laminate exhibit an average Interlaminar shear stress value of 2.148 MPa. Addition of glass fiber plies increases the ILSS value of composite and the highest ILSS value of 5.628 Mpa is observed for laminate S3 among all hybrid laminate sequences. Similar types of observations are also reported by Dalbehera et al. [269] while they worked with jute-glass hybrid composite.

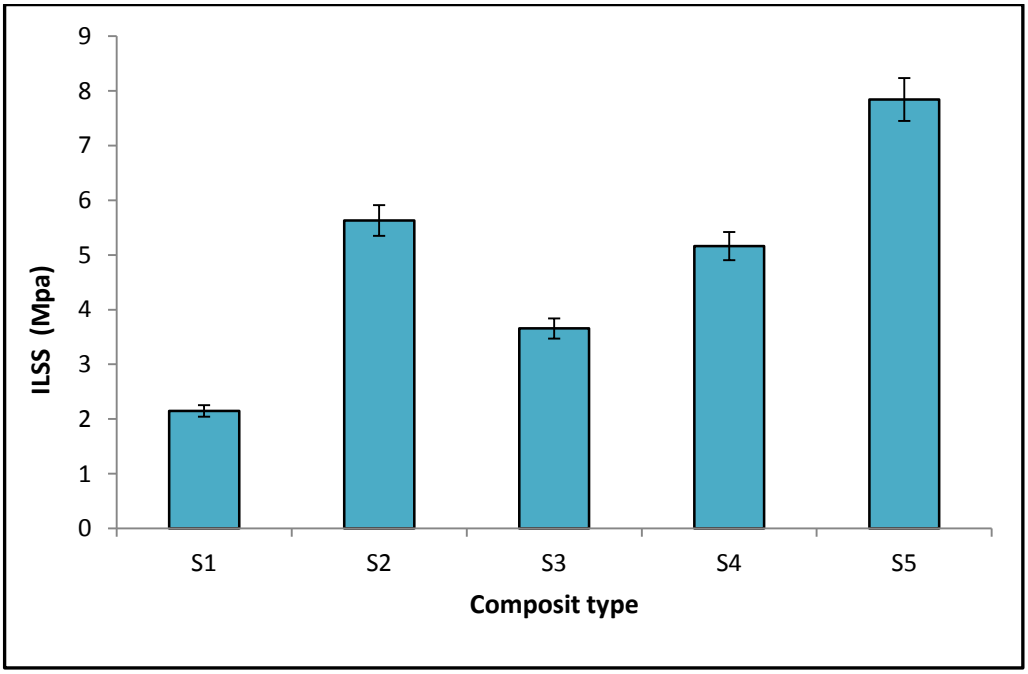

Figure-6.8 Interlaminar shear strength of the composite laminates.

6.4.1.6 Micro hardness

Figure-6.9 shows the micro-hardness of the composite for different stacking sequences. The micro hardness value is different for different stacking sequences. The maximum value is found for sequence S4.

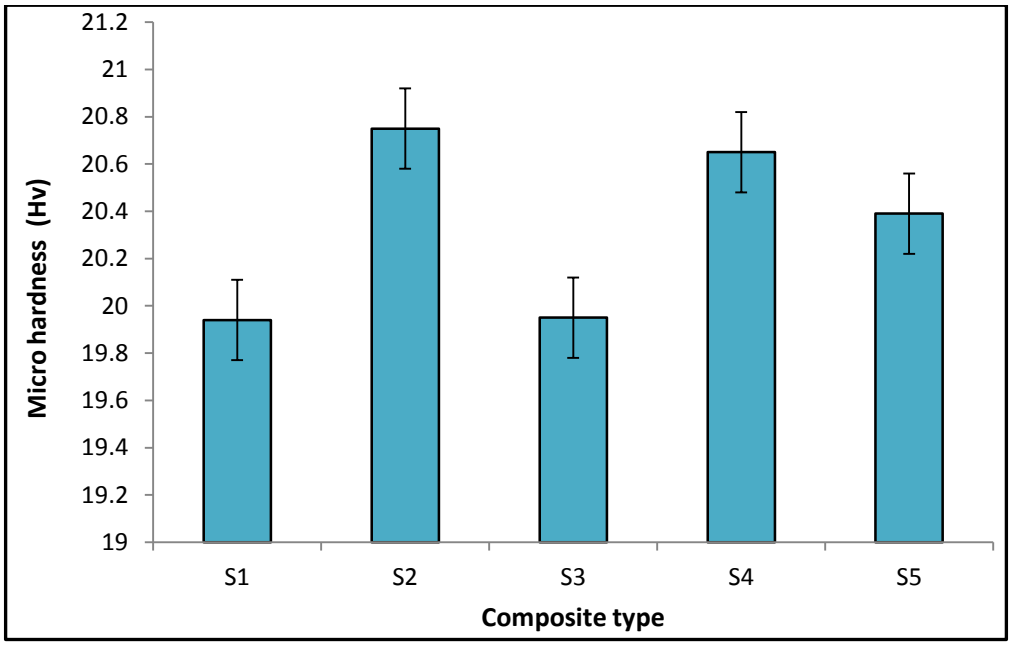

Figure-6.9 Micro hardness of the composite laminates.

6.4.1.6. Fracture surface morphology of laminates

Figure-6.10 shows the SEM image of fractured surface of only luffa cylindrica reinforced epoxy composite i.e. for sequence S1 under tensile load .The fiber breakage and pull out of fiber along loading direction from the matrix is clearly visible. The formation of voids due to fibre pull out is also noticed because of poor resin compatibility with natural fibres. Figure-6.11 shows the tensile failure of luffa cylindrica-glass fiber hybrid laminate (S4).The stretching and bending of glass fibre are visible due to the applied tensile load. Also breakage of luffa fibre without any stretching is clearly visible. The stretching of glass fibre indicates that the strength of the composite increased due to the incorporation of glass fibre, and this supplement to the results shown in figure-6.4.

Figure-6.12 shows the SEM micrograph of flexural specimen for tensile side of the laminate S1 under flexural load. Debonding of fiber with the matrix is clearly visible. Enlargement of fiber tissue due to flexural load probably reduced the strength of laminate S1. Figure-6.13 shows the SEM micrograph of hybrid laminate S4 representing the failure on the tension side of the specimen under flexural load. Greater extensibility of the glass fibres leading to fibre pull out and matrix failure is clearly visible. No delamination between the luffa cylindrica and glass plies is noticed for

flexural specimens. This probably is the main reason for increased flexural strength for hybrid laminates S4. Similar observations are reported by Sabeel Ahmeda et al. [270] while they worked for jute-glass hybrid laminates.

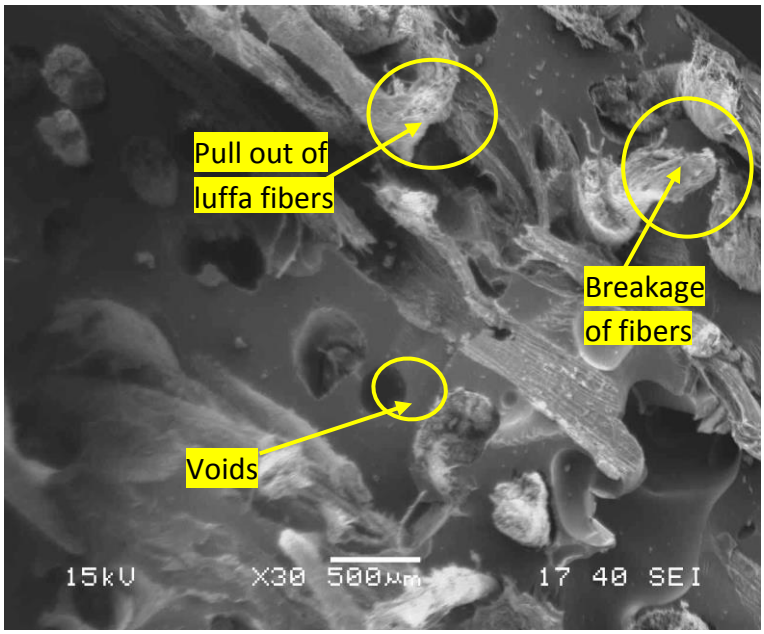

Figure-6.10 SEM image of fractured surface of laminate S1 under tensile load.

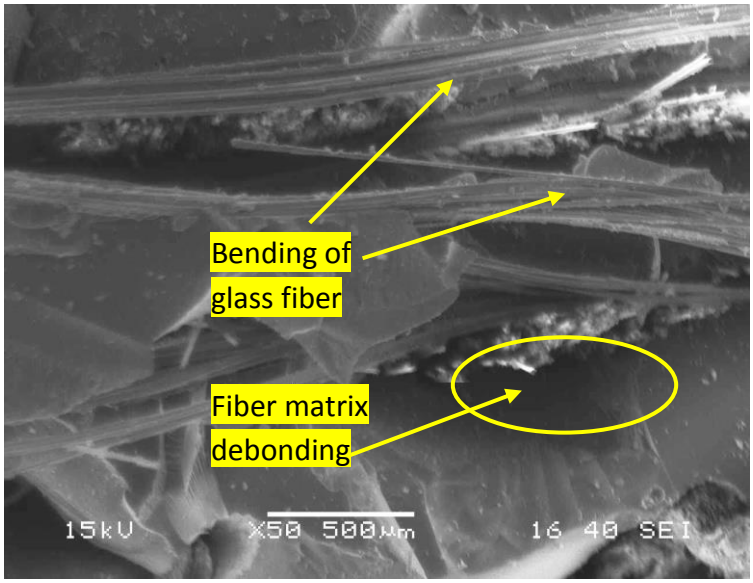

Figure-6.11 SEM image of fractured surface of laminate S4 under tensile load.

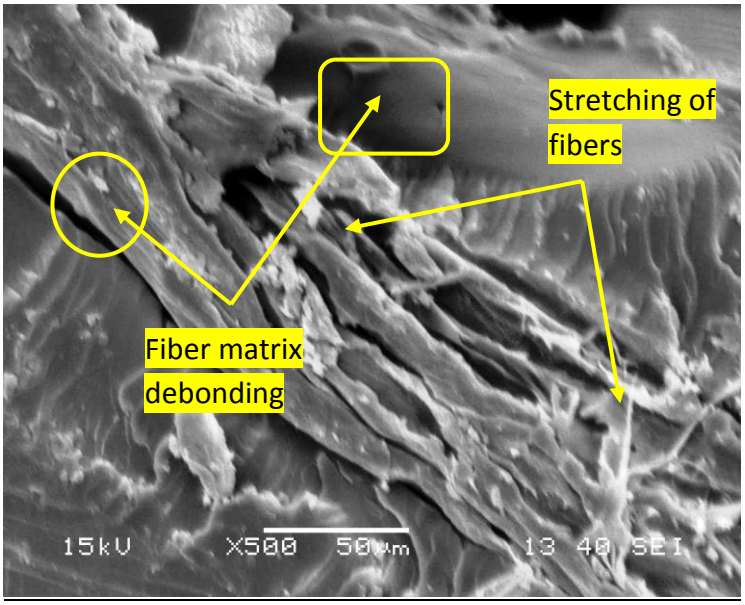

Figure-6.12 SEM image of tensile fractured surface of laminate S1 under flexural load.

.

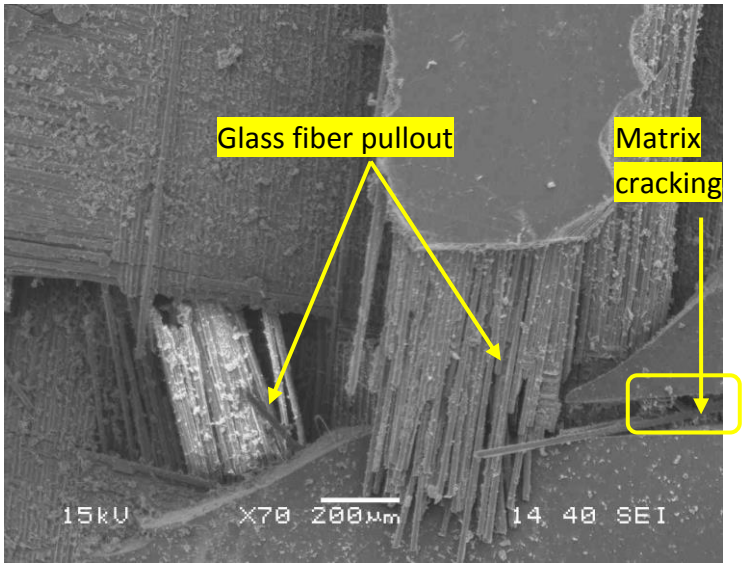

Figure-6.13 SEM image of tensile fractured surface of laminates S4 under flexural load.

6.4.2 EROSION WEAR

Based on the tabulated results various graphs were plotted and presented in Figure-6.14 to 6.25 for different stacking sequence of luffa-glass hybrid composite under different test conditions.

6.4.2.1 Effect of impact angle (α) on erosion wear of luffa-glass hybrid composite

Figure-6.14 to 6.17 illustrate the erosion wear rates of luffa cylindrica reinforced epoxy hybrid composite as a function of impingement angle under different impact velocities (48,70,82 and 109m/s). It is observed that laminate stacking sequence S4 and S5 shows peak erosion rate ($E_{r\ max}$) at 45° impact angle at different velocities and the peak erosion shift towards 60^o for the laminate stacking sequences S1,S2 and S3. Minimum erosion rate ($E_{r\ min}$) is observed at an impact angle of 30° for all laminate stacking sequence under all velocity of impact. As mentioned earlier in chapter 5, art 5.2.1 impact angle is one of the most important parameter for classifying the ductile or brittle erosion response of any material.The ductile behaviour is characterized by maximum erosion rate at low impingement angle typically $15< \alpha <30^0$. On the other hand, if the maximum erosion rate occurs at normal impact ($\alpha=90^0$) the behaviour of the material is brittle. However the maximum erosion occurring in the angular range 45^0-60^0 indicates the semi ductile behaviour of the material. From the present experimental results it is clear that the developed hybrid composites respond to solid particle impact neither behaves in a purely ductile nor in a brittle manners. Since maximum erosion of all hybrid composite occurs in the range of 45°-60° impact angles for all impact velocities. Therefore it can be concluded that the erosion response of luffa cylindrica-glass fibre reinforced epoxy hybrid composites behaves in a semi- ductile nature. Same type of behavior was also reported by Biswas et al. [271] for the erosive behavior of red mud filled Bamboo-epoxy composite. It is interesting to note that when luffa fiber as the outer layer as for laminate stacking sequence S1, S2 and S3 the maximum erosion shifts towards 60° impact angle. However when the glass fiber layer is the outer layer such as for laminate stacking sequence S4 and S5 maximum erosion shifts toward 45° impact angle for all impact

velocities. This gives an indication that the brittle behavior shifted towards the ductile erosion response of the composite.

It is further noticed that irrespective of impact velocity and impact angle, the erosion rate of laminate stacking sequence S4 is lowest as compared to other hybrid laminate stacking sequences. Laminate stacking sequences S1 shows the highest erosion wear. Here it can be conclude that erosion resistance of the luffa cylindrica fiber composite can be improved by the placing the glass fiber at the outer layer.

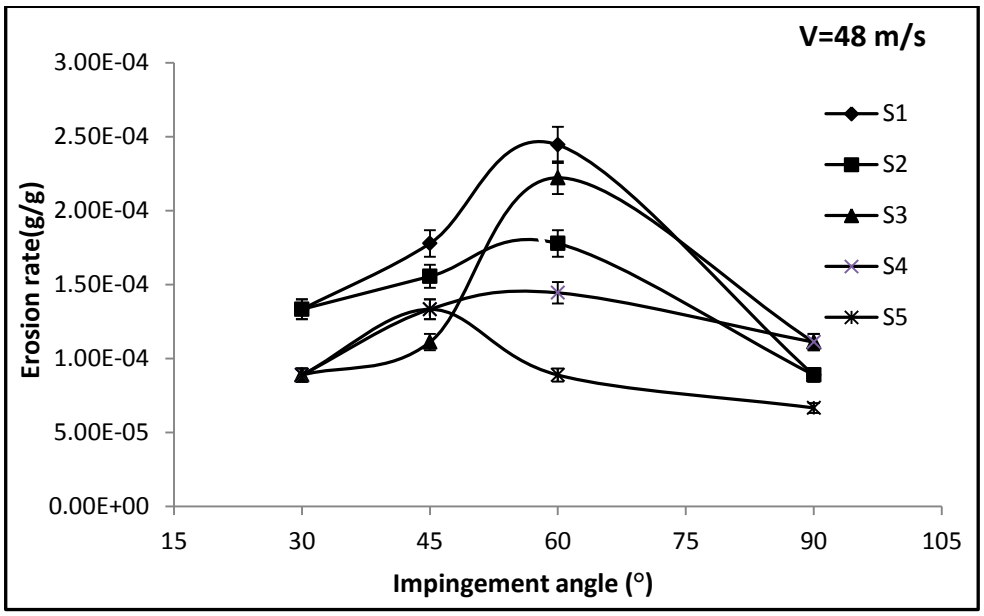

Figure-6.14 Erosion rate as a function of impingement angle for different composite laminates at 48 m/s impact velocity.

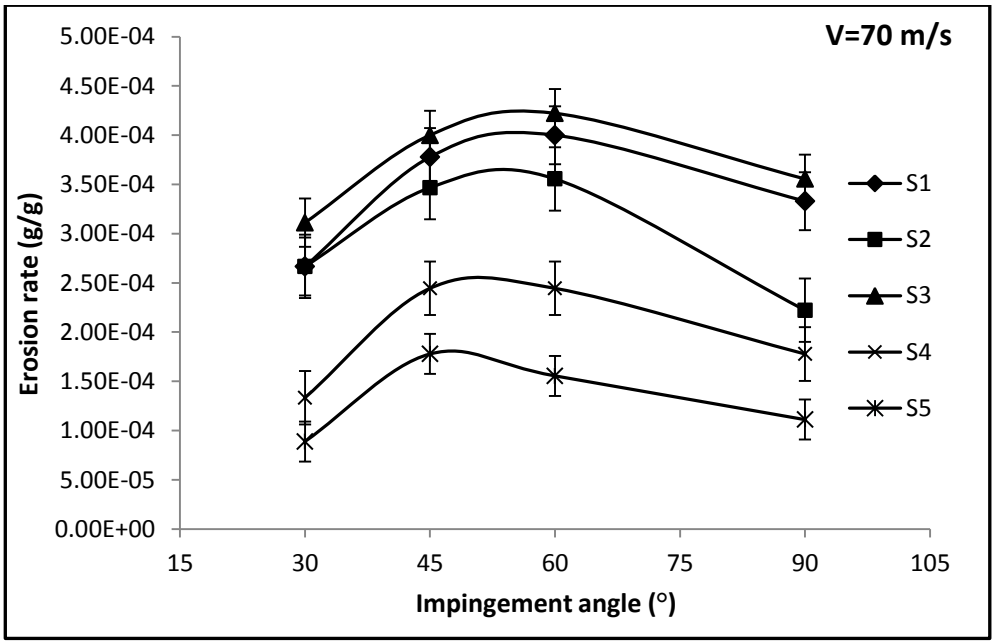

Figure-6.15 Erosion rate as a function of impingement angle for different composite laminates at 70 m/s impact velocity.

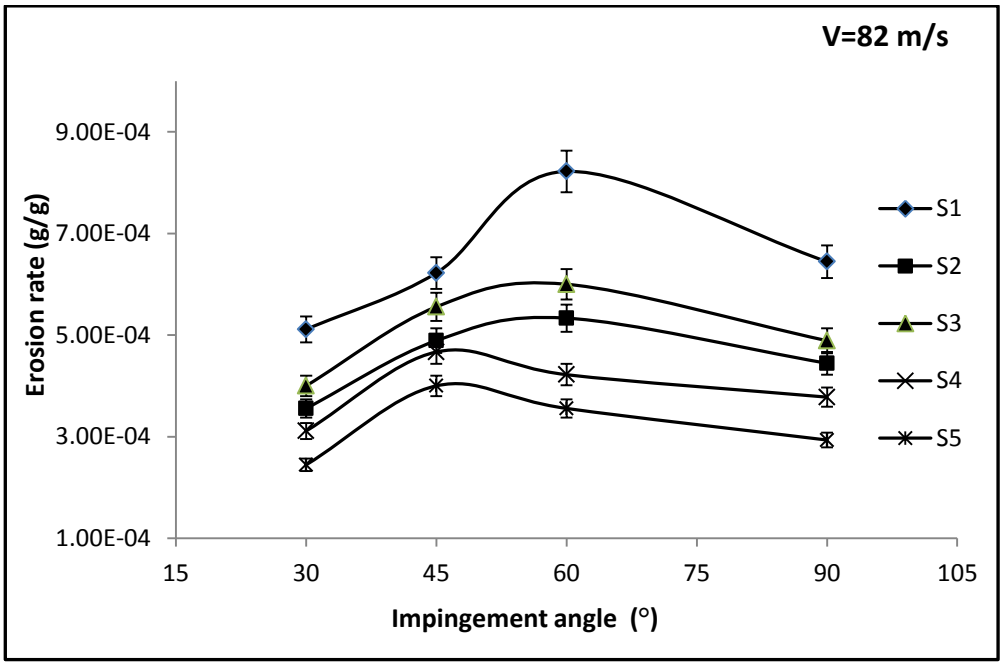

Figure-6.16 Erosion rate as a function of impingement angle for different composite laminates at 82 m/s impact velocity.

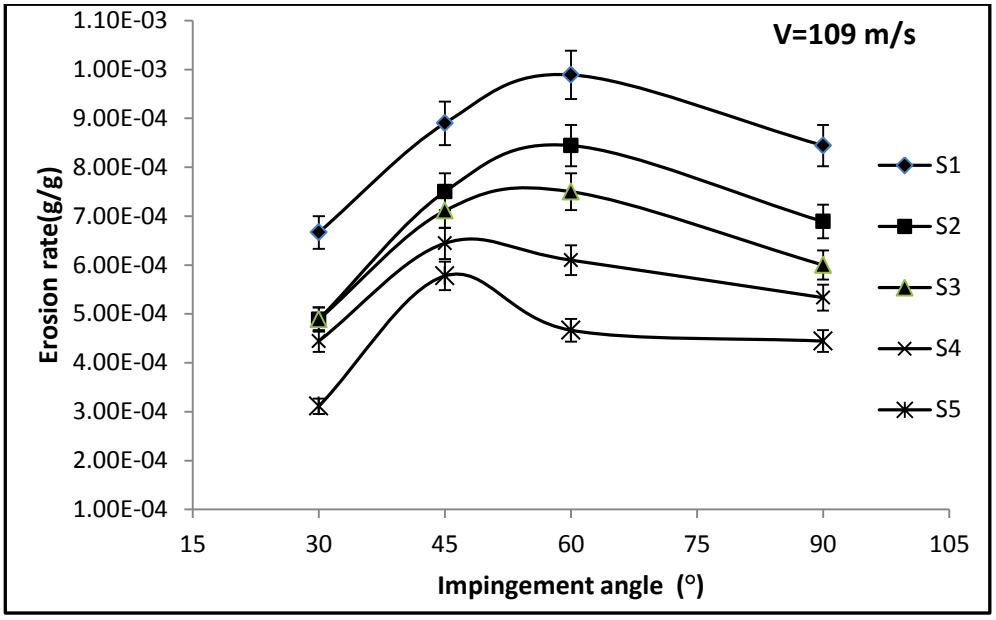

Figure-6.17 Erosion rate as a function of impingement angle for different composite laminates at 109 m/s impact velocity.

6.4.2.2 Effect of impact velocity (v) on erosion wear of luffa-glass hybrid composite

The variation of steady-state erosion rate of all laminate stacking sequences with impact velocity at different impact angles are shown in the form of a histogram in Figure-6.18 to 6.21. It can be observed from these histograms that erosion rate of all composite samples increases with increase in the impact velocity. It is also observed that irrespective of impingement angle and impact velocity, erosion rate of laminate stacking sequences S4 is low as compared to other laminate stacking sequences.

As mentioned earlier (art 5.2.2) influence of impact velocity (υ) on Erosive wear rate is one of the most important parameter for classifying the erosion behavior of any material. Figure-6.22-6.25 shows the variation of erosion rate with impact velocity at various impingement angles (45^0–90^0) for different laminate stacking sequences. From these figures it is clear that steady-state erosion rate of all laminate stacking sequences for different impingement angles increases with increase in impact velocity. The velocity of erosive particle has a very strong effect on erosion rate. It was found that the erosion rate follows power low behaviour with particle velocity as discussed in

chapter art 5.3.2. The least-square fits to data point were obtained by using power law (equation 5.1) and the values of '*n*' and '*k*' are summarized in table-6.10. The velocity exponents found for laminate stacking sequence S1 i.e. only Luffa layer, are in the range of 1.75-2.84 and for laminate stacking sequence S5 i.e. only glass layers is in the range of 1.65-2.44 for different impact angles and impact velocities studied. However it is in the range of 1.60-2.58, 1.46-2.50, 1.81-2.07, for luffa-glass hybrid composite with laminate stacking sequences S2, S3, S4, respectively. These values indicated that the erosion response of luffa cylindrica-glass reinforced epoxy hybrid composite behaves in semi-ductile nature. The velocity exponents (1.46–2.84) in the present study at various impingement angles are in conformity with Harsha et al. [252].

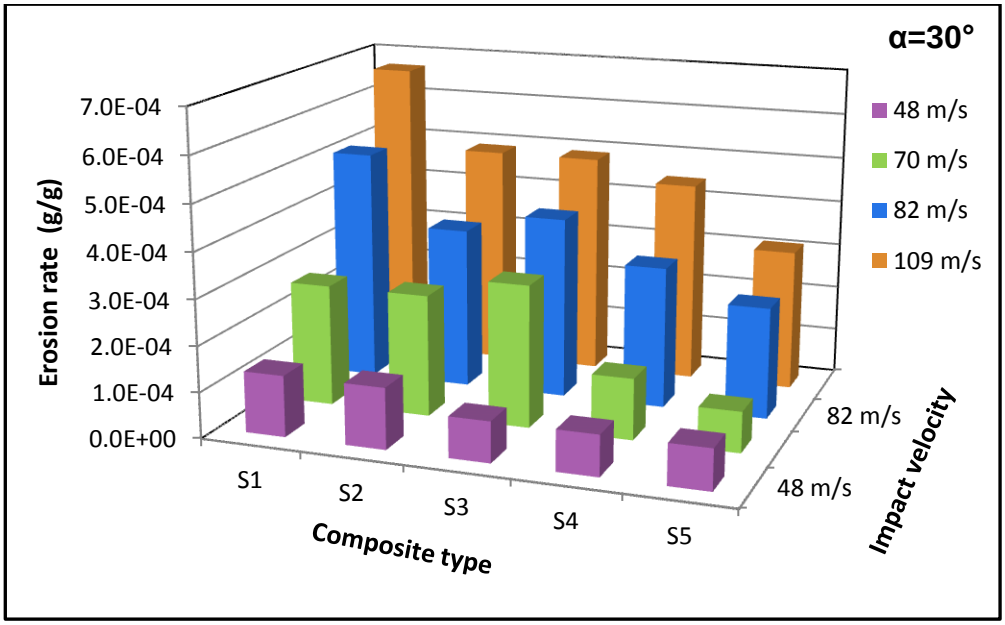

Figure-6.18 Histogram showing the erosive wear rates of different composite laminates at four impact velocities (i.e. at 48, 70, 82 and 109m/s) for 30° impact angle.

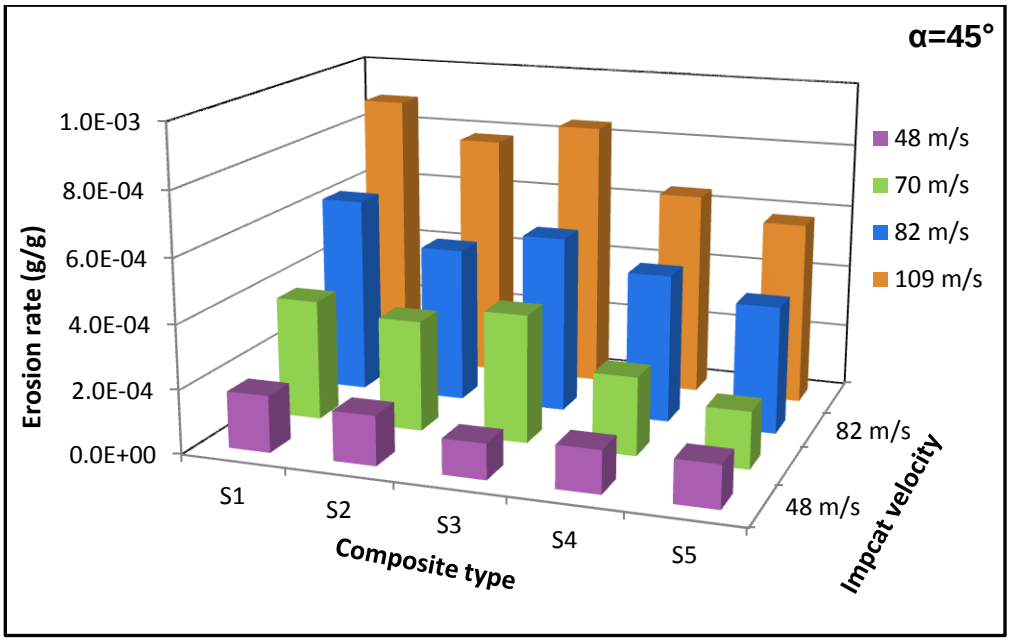

Figure-6.19 Histogram showing the erosive wear rates of different composite laminates at four impact velocities (i.e. at 48, 70, 82 and 109 m/s) for 45° impact angle.

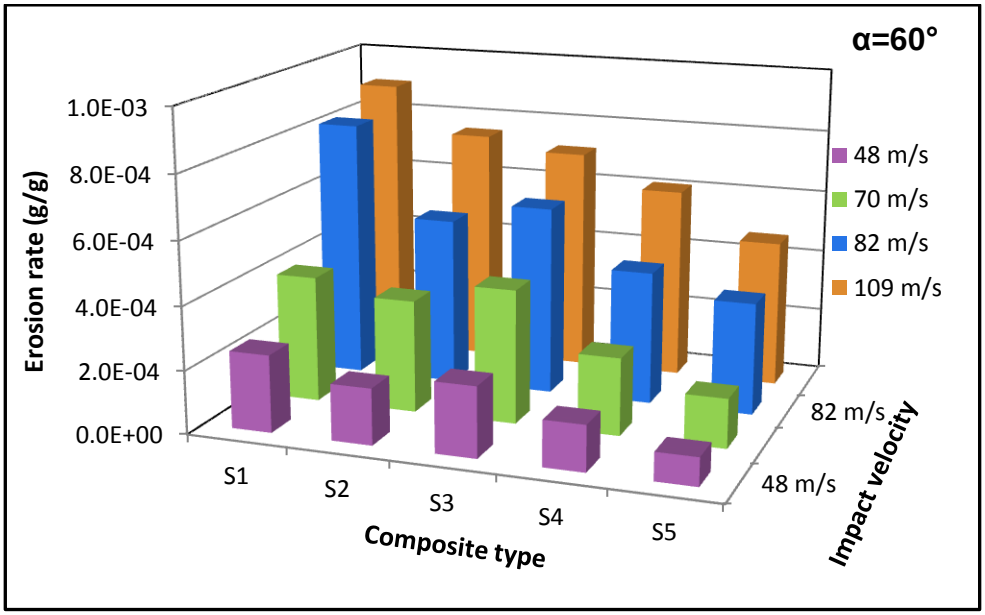

Figure-6.20 Histogram showing the erosive wear rates of different composite laminates at four impact velocities (i.e. at 48, 70, 82 and 109 m/s) for 60° impact angle.

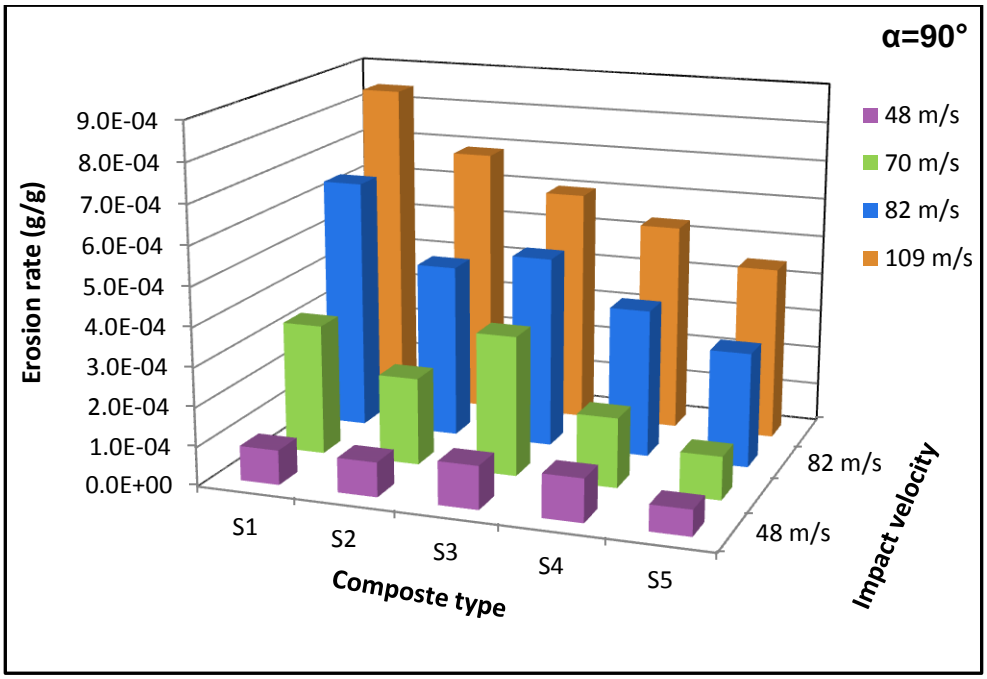

Figure-6.21 Histogram showing the erosive wear rates of different composite laminates at four impact velocities (i.e. at 48, 70, 82 and 109 m/s) for 60° impact angle.

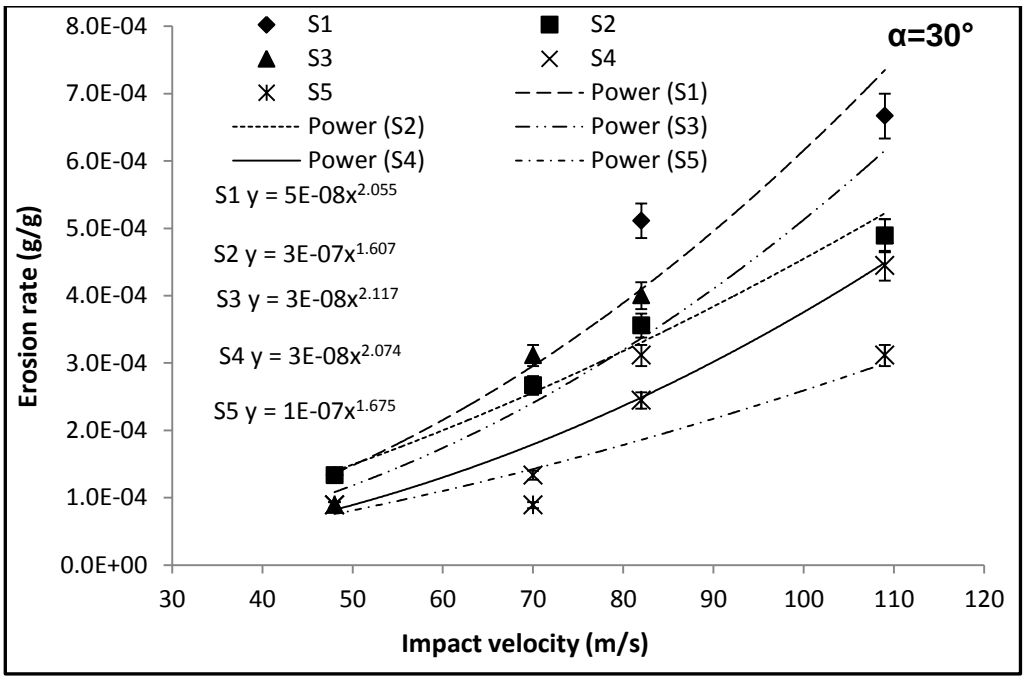

Figure-6.22 Erosion parameter for different composite laminates at impingement angle 30^0.

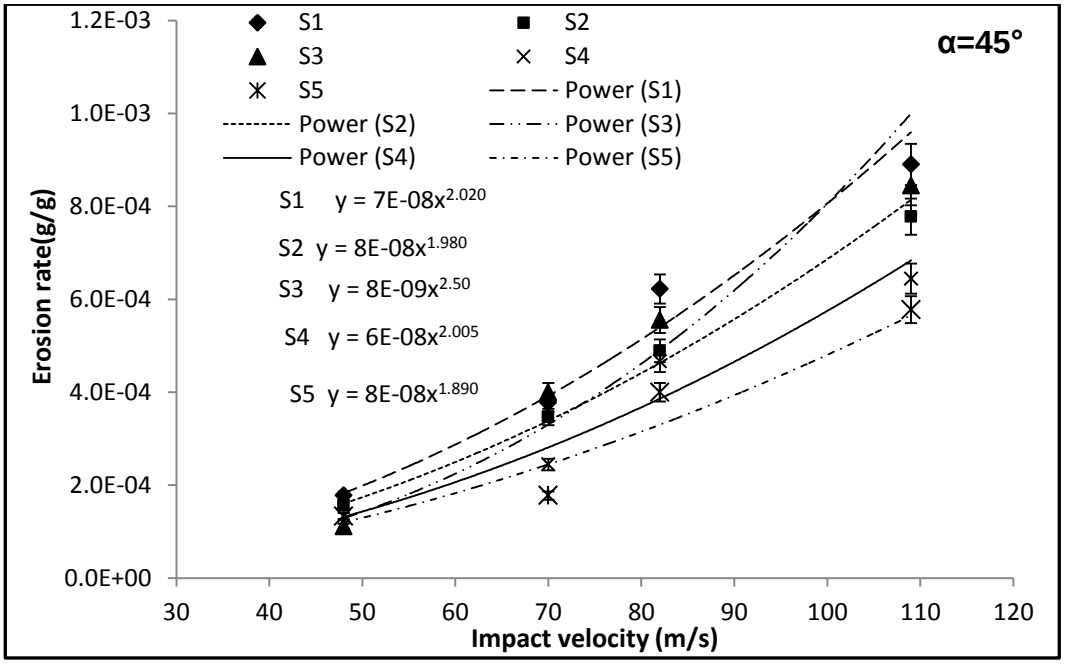

Figure-6.23 Erosion parameter for different composite laminates at impingement angle 45^0.

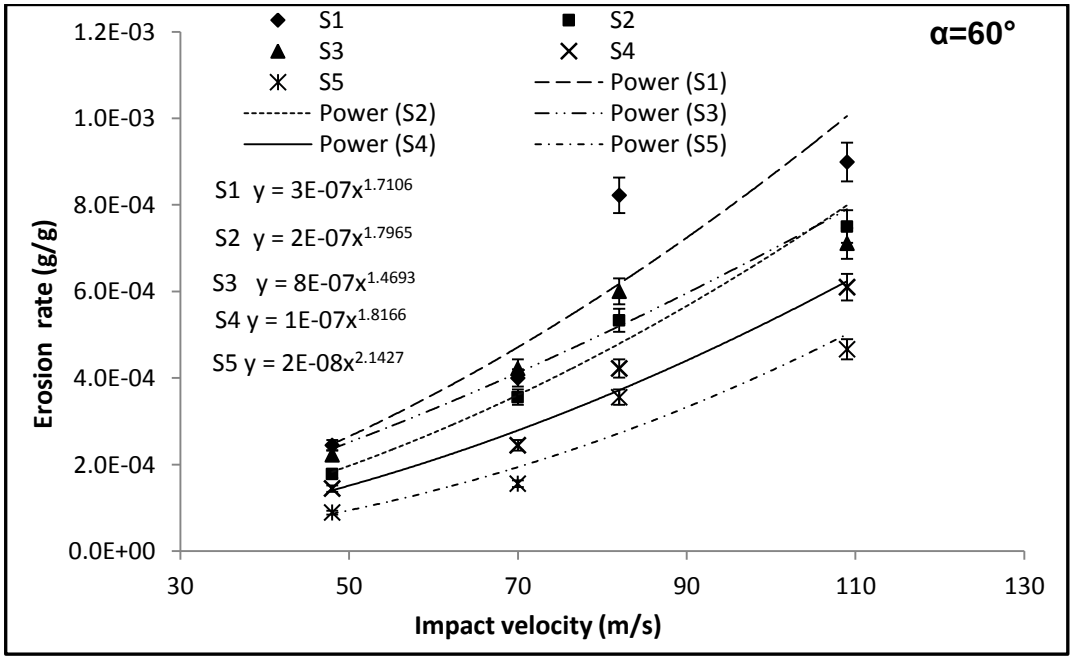

Figure-6.24 Erosion parameter for different composite laminates at impingement angle 60^0.

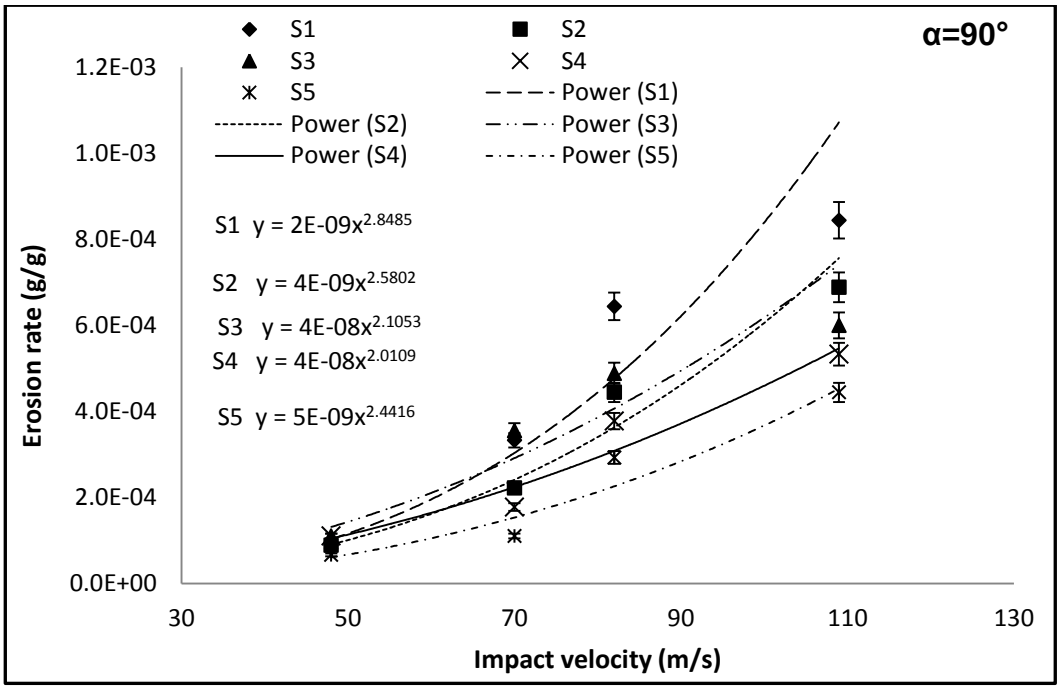

Figure-6.25 Erosion parameter for different composite laminates at impingement angle 90^0.

Table-6.10 Parameters characterizing the velocity dependence of erosion rate of luffa-glass hybrid epoxy composites.

Fiber content (%)	**Impact Angle**	**k× 10^{-8}**	**n**	**R^2**
S1 (LLLL)	30°	5.00	2.0552	0.955
	45°	7.00	2.0204	0.9808
	60°	30.00	1.7106	0.8944
	90°	0.20	2.8485	0.9405
S2 (LGLG)	30°	30.00	1.6076	0.9854
	45°	8.00	1.9802	0.9953
	60°	20.00	1.7965	0.9856
	90°	0.40	2.5802	0.9761

S3 (LGGL)	30°	3.00	2.1178	0.8938
	45°	0.80	2.5005	0.9556
	60°	80.00	1.4693	0.9545
	90°	4.00	2.1053	0.9139
S4 (GLLG)	30°	3.00	2.0746	0.9129
	45°	6.00	2.0052	0.9599
	60°	10.00	1.8166	0.9709
	90°	4.00	2.0109	0.9348
S5 (GGGG)	30°	10.0	1.6758	0.7519
	45°	8.00	1.8907	0.8927
	60°	2.00	2.1437	0.9276
	90°	0.50	2.4416	0.9205

6.4.2.3. Erosion efficiency of luffa-glass hybrid composite

As mentioned earlier (art 5.4.4) erosion efficiency is also one of the important parameter for classifying the erosion behavior of any material. The erosion efficiency of the luffa-glass hybrid composites were calculated by using equation 5.6 and listed in table-6.11. The erosion efficiency of laminate stacking sequences S1, S2, S3, S4 and S5 are in the range of 2.29-11.79%, 1.33-8.00%, 1.60-8.44%, 1.25-6.36% and 0.67-4.55% respectively studied at different impact angles and impact velocities. Thus, by observing erosion efficiency and velocity exponent (n) of luffa cylindrica-glass epoxy hybrid composite erosive wear behaviour can be categorize as semi-ductile. Similar observations on erosion efficiency for different polymer composites have also been reported by different investigators [252,241]. The laminate stacking sequence S4 shows lower erosion efficiency (1.25-6.36%) among all hybrid laminate at different impact velocities pointed towards a better erosion resistance. The higher values of erosion efficiencies (2.50-11.79%) of laminate stacking sequence S1 (i.e. all luffa layers) indicate its poor erosion resistance. Hence it can be concluded that erosion

resistance of luffa cylindrica epoxy composite can be improved by hybridising it with glass fibre.

Table-6.11 Erosion efficiency (η) of luffa-glass hybrid epoxy composites.

Impact Velocity 'v' (m/s)	**Impact angle 'α'**	**Erosion efficiency (η)**				
		S1	**S2**	**S3**	**S4**	**S5**
		H=195.6 ρ=1.009	**H=203.5 P=1.178**	**H=195.6 P=1.177**	**H=202.5 P=1.179**	**H=191.2 P=1.297**
30^0	48	8.97	8.00	5.13	5.30	4.55
	70	8.44	7.52	8.44	3.74	2.14
	82	11.79	7.31	7.91	6.36	4.29
	109	8.70	5.69	5.47	5.14	3.09
45	48	5.98	4.67	3.21	3.98	3.41
	70	5.98	4.89	5.43	3.43	2.14
	82	7.18	5.03	5.49	4.77	3.51
	109	5.81	4.52	4.72	3.73	2.87
60	48	5.48	3.52	4.27	2.87	1.52
	70	4.22	3.34	3.82	2.28	1.25
	82	6.32	3.65	3.95	2.87	2.08
	109	3.91	3.19	2.65	2.35	1.54
90	48	2.29	1.33	1.60	1.66	0.85
	70	2.50	1.57	2.41	1.25	0.67
	82	3.72	2.28	2.42	1.93	1.29
	109	2.76	2.00	1.68	1.54	1.10

6.4.2.4 Surface morphology of eroded surface

The surface microstructures of the eroded composite samples are examined by Scanning electron microscope (JEOL JSM-6480LV). Figure-6.26 and 6.27 shows the SEM micrographs of the composite laminate for stacking sequence S1 and S2 at 60º impingements angle for impact velocity 82 m/s. Pulling out of fibres from the matrix is not visible. At some places craters are being formed due to penetration of silica sand which causes damage to the matrix material.

Figure-6.28 shows the damage caused to the fibres for the sequence S3.The meshing of the original structure is totally damaged and smooth surfaces are being formed. Figure-6.29 shows the surface damage caused to sequence S4. Breakings of glass fibres in the micrograph are found but there is no chipping up fibres from the matrix is visible. Damage to the luffa fibre is totally eliminated because of position of glass fibre at the outer layer.

Figure-6.30 and 6.31 shows the micrographs of the eroded surface for laminate stacking sequence S3 and S4 at higher velocity (109 m/s). For sequences S3 after eroding the luffa fibre surface the erodent particles enters to the glass fibre surface. Breaking of glass fibres is seen but chipping out of fibres from the matrix is prevented. This might be due to a good bonding between the fibres and the matrix and the time it gets to erode the glass fibre is less.

Figure-6.31 shows the damage caused to sequence S4 due to higher velocity (109 m/s). Formation of cavity is clearly visible which is formed by micro ploughing and cutting. Also extensive damage caused at this velocity to the luffa fibre surface is seen. It can be concluded that natural fibre alone is not capable of resisting wear caused by particle impact but resistance can significantly be improved by placing the synthetic fibre (i.e.) glass fibre at the extreme layer.

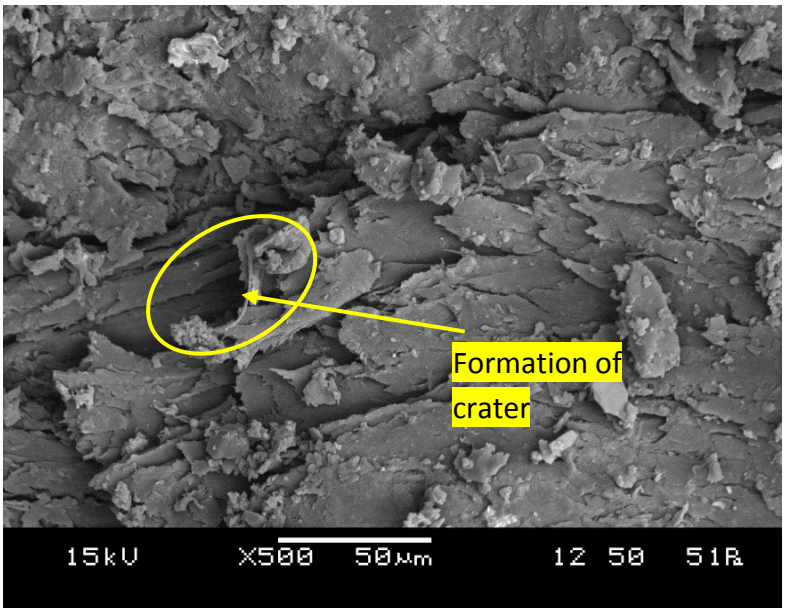

Figure-6.26 SEM micrograph of eroded surface for laminate stacking sequence S1 at impingement angle 60°, impact velocity 82 m/s.

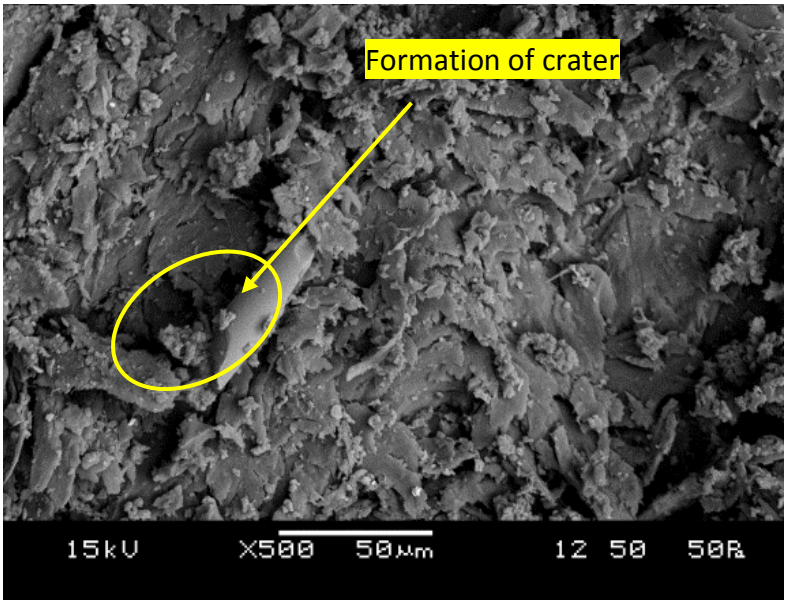

Figure-6.27. SEM micrograph of eroded surface for laminate stacking sequence S2 at impingement angle 60°, impact velocity 82 m/s.

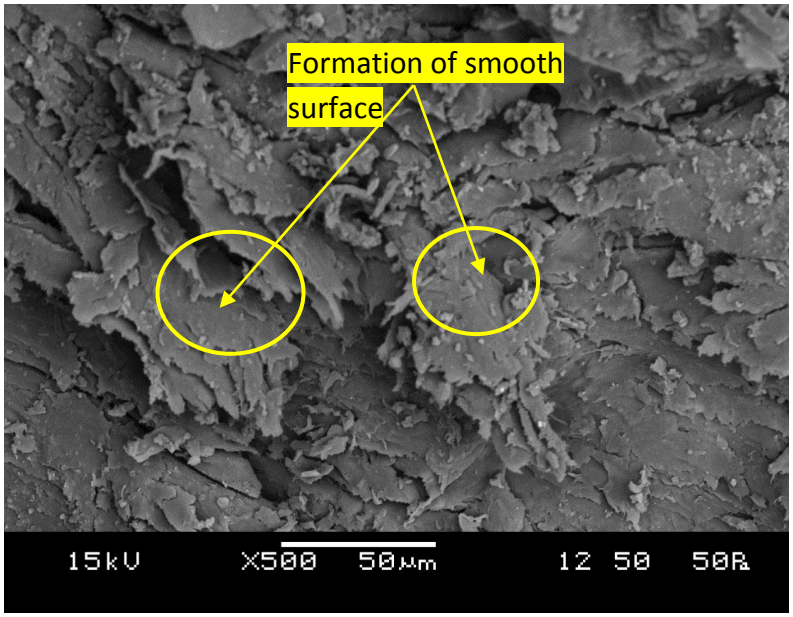

Figure-6.28 SEM micrograph of eroded surface for laminate stacking sequence S3 at impingement angle 60°, impact velocity 82 m/s.

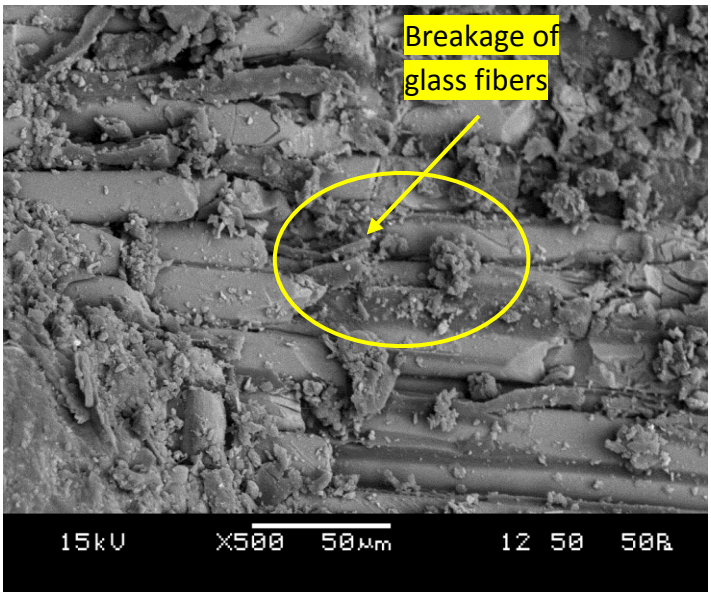

Figure-6.29 SEM micrograph of eroded surface for laminate stacking sequence S4 at impingement angle 60°, impact velocity 82 m/s.

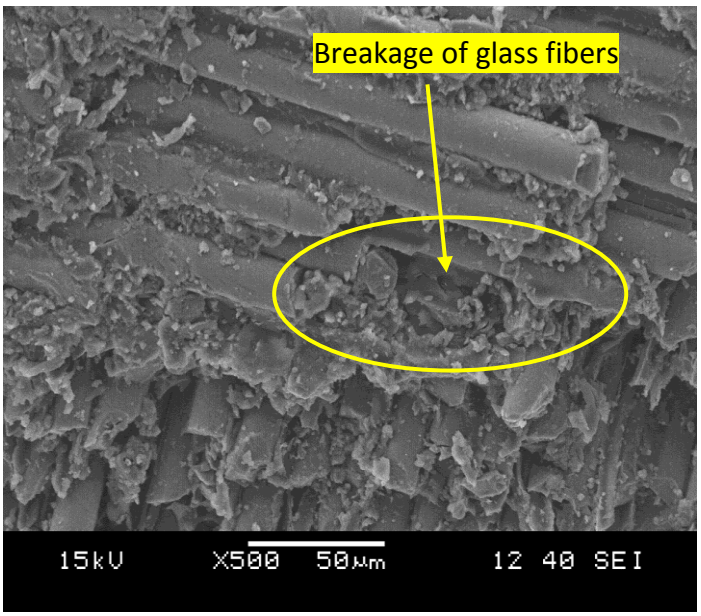

Figure-6.30 SEM micrograph of eroded surface for laminate stacking sequence S3 at impingement angle 60°, impact velocity 109 m/s.

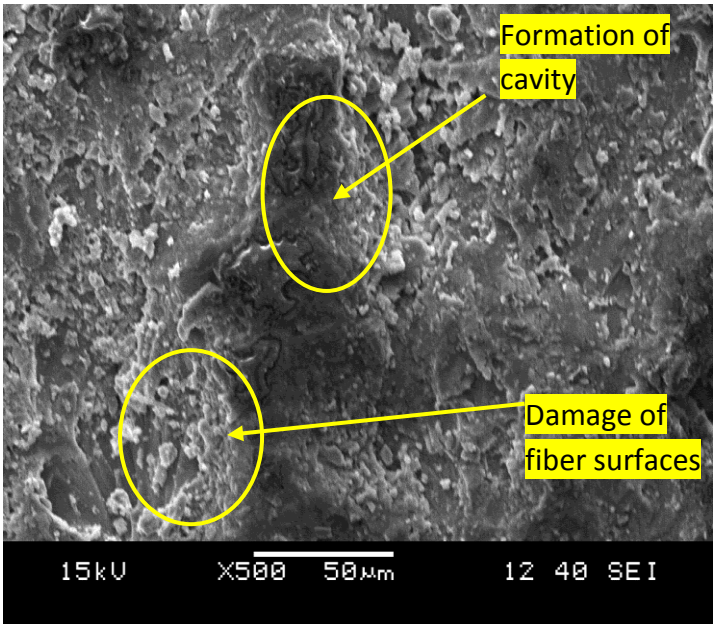

Figure-6.31 SEM micrograph of eroded surface for laminate stacking sequence S4 at impingement angle 60°, impact velocity 109 m/s.

6.5 CONCLUSION

Experiments were carried out to study the effect of luffa and glass fiber stacking sequence on the mechanical properties and erosion wear rate of Luffa glass hybrid composite at various impingement angles, impact velocities for different stacking sequence with silica sand as erodent. Based on the results the following conclusions are drawn.

1. A new type of hybrid laminate composite with luffa and glass fibre has been fabricated successfully in the laboratory.

2. The Tensile strength and Flexural strength of luffa- glass fibre-reinforced hybrid composite is found to be maximum for the stacking sequence (S4) among all hybrid laminates.

3. The maximum ILSS of 5.628 Mpa is observed for laminate S3 among all hybrid laminates.

4. Comparing the properties of the designed hybrid laminates, it is found that the optimum mechanical properties are achieved from hybrid laminate S4 with two glass piles on both side and two luffa fibre layers are at the middle.

5. The influence of impingement angle on erosive wear of all laminate stacking sequence under consideration exhibit semi ductile behaviour with maximum wear rate at 45-60^0 impingement angles.

6. Erosion rate (Er) of different laminate stacking sequences displays power law behaviour with particle velocity (v) as $E \alpha V^n$. The velocity exponents are in the range of 1.46–2.84 for various materials studied for different impingement angles (30°–90°) and impact velocities (48–109 m/s).

7. The erosion efficiency is found to be in the range of 1.26-11.79% for different laminate stacking sequence at different impact velocity and impact angles

conforming that the luffa-glass hybrid composite exhibited semi-ductile behaviour.

8. The laminate stacking sequence S4 (two glass piles on both side and two luffa fibre layers are at the middle) shows best erosion resistance when compared with the all other laminate stacking sequence.

9. The morphologies of the eroded surfaces observed by SEM suggest that overall erosion damage of the composite is mainly due to breaking of fibre. Fibre pull out is prevented due to good bonding between the fibre and the matrix.

10. It is clear from this study that erosive strength of natural luffa cylindrica fibre can be increased by hybridization with synthetic fibre.

Chapter 7

Conclusion and Scope for Future Work

7.1 CONCLUSIONS

The conclusions drawn from the present investigations are as follows:

1. The luffa cylindrica can successfully be used as reinforcing agent to fabricate composite by suitably bonding with resin for the development of value added products.
2. On increasing the fiber content the strength, modulus increases. Double layer (13 wt. %) of luffa cylindrica reinforcement gives the best combination among the tested composites.
3. The surface modification of luffa cylindrica significantly improves the fiber matrix adhesion which in turn enhances the mechanical properties of the composite. The benzoyl-chloride treatment provides the highest improvement in strength and modulus in-comparison to alkali and potassium permanganate treatment.
4. Fickian's diffusion can be used to describe the moisture absorption behavior of both treated and untreated luffa cylindrica reinforced epoxy composite.
5. Study of influence of impingement angle on erosion rate of the composites with both untreated and treated luffa fiber reveals their semi ductile nature with respect to erosive wear.
6. The erosion efficiency (η) values (1.52% to 17%) obtained experimentally also confirm that the luffa cylindrica reinforced epoxy composites exhibit semi-ductile erosion response.
7. The chemical treatment of luffa cylindrica fiber reduces the erosion rate. The chemical treatment of luffa cylindrica with benzoyl chloride offers maximum erosion resistance.

8. Comparing the properties of the designed hybrid laminates, it is found that the optimum mechanical properties are achieved from hybrid laminate S4 with two glass piles on outer side and two luffa fibre layers at the middle.

9. The influence of impingement angle on erosive wear of all laminate stacking sequence under consideration exhibit semi ductile behavior with maximum wear rate at 45-60° impingement angles.

10. The laminate stacking sequence S4 (two glass fiber layers at extreme end and two luffa layer at middle) shows best erosion resistance when compared with the all other laminate stacking sequence. It is clear from this study that erosive strength of natural fiber luffa cylindrica can be increased by hybridization with synthetic fiber.

7.2 RECOMMENDATION FOR FURTHER RESEARCH

1. In the present investigation hand-lay-up technique is used to fabricate the composite. However there exists other manufacturing process for polymer matrix composite. They could be tried and analyzed, so that a final conclusion can be drawn there from. However the results provided in this thesis can act as a base for the utilization of this fiber.

2. From this work it is found that chemical modification of the fiber with alkali, benzoyl-chloride and potassium permanganate significantly improves the mechanical performance of the composite. Other chemical modification methods such as silane treatment, acetylation treatment, acrylation treatment, isocynates treatment, acetone treatment and maleated coupling agents could be tried and a final conclusion can be drawn thereafter.

3. In the erosion test sand particle of 200±50 microns only have been used. This work can be further extended to other particle size and types of particle like glass bead etc., to study the effect of particle size and type of particles on wear behavior of the composite.

Bibliography

1. Khanam, P. N., Reddy, M. M., Raghu, K., John, K., & Naidu, S. V. (2007). Tensile, flexural and compressive properties of sisal/silk hybrid composites. *Journal of Reinforced Plastics and Composites*, *26*(10), 1065-1070.
2. Agarwal B. D & Broutman L. J, (1990). *Analysis and performance of fiber composites*, Second edition, John wiley & Sons, Inc, 2-16.
3. Wetter, R., (1970).*Kunststoffe in der Luft-und Raumfahrt*, Kunststoffe, 60, Heft-10.
4. Schmidt, K. A. F., (1967). *Verstarkungsfasern in Glasfaserverstärkte Kunstoffe*, Ed. P. H. Selden, Springer-Verlag, Berlin, 159-221
5. Berghezan, A., (1966).*Non-ferrous Materials*, Nucleus, 8, 5–11.
6. Van Suchtelen, J. (1972). Product properties: a new application of composite materials. *Philips Res. Rep*, *27*(1), 28-37.
7. Outwater Jr, J. O. (1956). The mechanics of plastics reinforcement in tension. *Modern Plastics*, *33*(7), 156.
8. Rout, J., Misra, M., Tripathy, S. S., Nayak, S. K., & Mohanty, A. K. (2001). The influence of fiber treatment on the performance of coir-polyester composites. *Composites Science and Technology*, *61*(9), 1303-1310.
9. Li, Q., & Matuana, L. M. (2003). Surface of cellulosic materials modified with functionalized polyethylene coupling agents. *Journal of Applied Polymer Science*, *88*(2), 278-286.
10. Mohanty, A. K., Misra, M., & Drzal, L. T. (2002). Sustainable bio-composites from renewable resources: opportunities and challenges in the green materials world. *Journal of Polymers and the Environment*, *10*(1-2), 19-26.
11. Wambua, P., Ivens, J., & Verpoest, I. (2003). Natural fibers: can they replace glass in fiber reinforced plastics. *Composites science and technology*, *63*(9), 1259-1264.
12. Gamstedt, E., & Almgren, K. (2007). Natural fiber composites–with special emphasis on effects of the interface between cellulosic fibers and polymers. *In Proceedings of the 28th International Symposium on Materials Science*.
13. Mohanty, A. K., Khan, M. A., & Hinrichsen, G. (2000). Influence of chemical surface modification on the properties of biodegradable jute fabrics—polyester

amide composites. *Composites Part A: Applied Science and Manufacturing*, *31*(2), 143-150.

14. Joseph, P. V., Joseph, K., & Thomas, S. (1999). Effect of processing variables on the mechanical properties of sisal-fiber-reinforced polypropylene composites. *Composites Science and Technology*, *59*(11), 1625-1640.
15. Mukherjee, P. S., & Satyanarayana, K. G. (1986). Structure and properties of some vegetable fibers. *Journal of materials science*, *21*(1), 51-56.
16. Jain, S., Kumar, R., & Jindal, U. C. (1992). Mechanical behavior of bamboo and bamboo composite. *Journal of Materials Science*, *27*(17), 4598-4604.
17. Nishino, T., Hirao, K., Kotera, M., Nakamae, K., & Inagaki, H. (2003). Kenaf reinforced biodegradable composite. *Composites Science and Technology*, *63*(9), 1281-1286.
18. Vazquez, A., Dominguez, V. A., & Kenny, J. M. (1999). Bagasse fiber-polypropylene based composites. *Journal of Thermoplastic Composite Materials*, *12*(6), 477-497.
19. Holbery, J., & Houston, D. (2006). Natural-fiber-reinforced polymer composites in automotive applications. *Jom*, *58*(11), 80-86.
20. Clemons, C. (2002). Wood-plastic composites in the United States: The interfacing of two industries. *Forest Products Journal*, *52*(6), 10.
21. Plackett, D. (2002). The Natural Fiber-Polymer Composite Industry in Europe-Technology and Markets. *Progress in Woodfibre-Plastic Composites*. Toronto, Canada
22. Nickel, J., & Riedel, U. (2003). Activities in bio composites. *Materials Today*, *6*(4), 44-48.
23. Mazali, I. O., & Alves, O. L. (2005). Morphosynthesis: high fidelity inorganic replica of the fibrous network of loofa sponge (Luffa cylindrica). *Anais da Academia Brasileira de Ciências*, *77*(1), 25-31.
24. Boynard, C. A., & d'Almeida, J. R. M. (2000). Morphological characterization and mechanical behavior of sponge gourd (Luffa cylindrica)–polyester composite materials. *Polymer-Plastics Technology and Engineering*, *39*(3), 489-499.
25. Oboh, I. O., & Aluyor, E. O. (2009). Luffa cylindrica-an emerging cash crop. *African Journal of Agricultural Research*, *4*(8), 684-688.

26. BAL, K. E., Bal, Y., & Lallam, A. (2004). Gross morphology and absorption capacity of cell-fibers from the fibrous vascular system of Loofah (Luffa cylindrica). *Textile research journal*, *74*(3), 241-247.
27. Partap, S., Kumar, A., Sharma, N. K., & Jha, K. K. (2012). Luffa Cylindrica: An important medicinal plant. *Journal of Natural Product & Plant Resources*, *2*(1).
28. Shen, J., Xie, Y. M., Huang, X., Zhou, S., & Ruan, D. (2012). Mechanical properties of luffa sponge. *Journal of the mechanical behavior of biomedical materials*, *15*, 141-152.
29. Siqueira, G., Bras, J., & Dufresne, A. (2010). Luffa cylindrica as a lignocellulose source of fiber, micro fibrillated cellulose and cellulose nanocrystals. *Bio Resources*, *5*(2), 727-740.
30. Seki, Y., Sever, K., Erden, S., Sarikanat, M., Neser, G., & Ozes, C. (2012). Characterization of Luffa cylindrica fibers and the effect of water aging on the mechanical properties of its composite with polyester. *Journal of Applied Polymer Science*, *123*(4), 2330-2337.
31. Demir, H., Atikler, U., Balköse, D., & Tıhmınlıoğlu, F. (2006). The effect of fiber surface treatments on the tensile and water sorption properties of polypropylene–luffa fiber composites. *Composites Part A: Applied Science and Manufacturing*, *37*(3), 447-456.
32. Laidani, Y., Hanini, S., & Henini, G. (2011). Use of fiber luffa cylindrica for waters treatment charged in copper. Study of the possibility of its regeneration by desorption chemical. *Energy Procedia*, *6*, 381-388.
33. Oboh, I. O., Aluyor, E. O., & Audu, T. O. (2011). Application of Luffa cylindrica in natural form as biosorbent to removal of divalent metals from aqueous solutions-kinetic and equilibrium study. *InTech*, 195–212.
34. Ghali, L., Msahli, S., Zidi, M., & Sakli, F. (2009). Effect of pre-treatment of Luffa fibers on the structural properties. *Materials letters*, *63*(1), 61-63.
35. Paglicawan, M. A., Cabillon, M. S., Cerbito, R. P., & Santos, E. O. (2005). Loofah fiber as reinforcement material for composite. *Philippine Journal of Science*, *134*(2), 113.
36. Tanobe, V. O., Sydenstricker, T. H., Munaro, M., & Amico, S. C. (2005). A comprehensive characterization of chemically treated Brazilian sponge-gourds (Luffa cylindrica). *Polymer Testing*, *24*(4), 474-482.

37. Chen, J. P., & Lin, T. C. (2005). Loofa sponge as a scaffold for culture of rat hepatocytes. *Biotechnology progress*, *21*(1), 315-319.

38. Zampieri, A., Mabande, G. T., Selvam, T., Schwieger, W., Rudolph, A., Hermann, R. & Greil, P. (2006). Biotemplating of Luffa cylindrica sponges to self-supporting hierarchical zeolite macrostructures for bio-inspired structured catalytic reactors. *Materials Science and Engineering: C*, *26*(1), 130-135.

39. De Sousa, J. T., Henrique, I. N., Oliveira, R., Lopes, W. S., & Leite, V. D. (2008). Nitrification in a submerged attached growth bioreactor using Luffa cylindrica as solid substrate. *African Journal of Biotechnology*, *7*(15).

40. Franck, R.R. (2005), *Bast and Other Plant Fibers*, Cambridge: Woodhead Publishing Limited.

41. Rong, M. Z., Zhang, M. Q., Liu, Y., Yang, G. C., & Zeng, H. M. (2001). The effect of fiber treatment on the mechanical properties of unidirectional sisal-reinforced epoxy composites. *Composites Science and Technology*, *61*(10), 1437-1447.

42. Abdul Khalil, H. P. S., Bhat, A. H., & Ireana Yusra, A. F. (2012). Green composites from sustainable cellulose nanofibrils: a review. *Carbohydrate Polymers*, *87*(2), 963-979.

43. Carvalho, W., Canilha, L., Ferraz, A., & Milagres, A. M. F. (2009). Uma visão sobre a estrutura, composição e biodegradação da madeira. *Química Nova*, *32*(8), 2191-2195.

44. Silva, R., Haraguchi, S. K., Muniz, E. C., & Rubira, A. F. (2009). Aplicações de fibras lignocelulósicas na química de polímeros e em compósitos. *Química Nova*, *32*(3), 661-671.

45. Pietak, A., Korte, S., Tan, E., Downard, A., & Staiger, M. P. (2007). Atomic force microscopy characterization of the surface wettability of natural fibers. *Applied Surface Science*, *253*(7), 3627-3635.

46. Pereira, P. H. F., Rosa, M. D. F., Cioffi, M. O. H., Benini, K. C. C. D. C., Milanese, A. C., Voorwald, H. J. C., & Mulinari, D. R. (2015). Vegetal fibers in polymeric composites: a review. *Polímeros*, *25*(1), 9-22.

47. Thygesen, A., Thomsen, A. B., Daniel, G., & Lilholt, H. (2007). Comparison of composites made from fungal defibrated hemp with composites of traditional hemp yarn. *Industrial Crops and Products*, *25*(2), 147-159.

48. Rowell, R.M., Young, R.A., and Rowell, J.K. (1997). *Chemical Composition of fibers: Paper and Composites from Agro-based Resources*, *Lewis Publishers,* CRC 194Press, 85-91.

49. Bjerre, A. B., & Schmidt, A. S. (1997). Development of chemical and biological processes for production of bioethanol: Optimization of the wet oxidation process and characterization of products. *Riso-R-967(EN), Riso National Laboratory*. pp. 5-9

50. Morvan, C., Jauneau, A., Flaman, A., Millet, J., & Demarty, M. (1990). Degradation of flax polysaccharides with purified endo-polygalacturonase. *Carbohydrate polymers*, *13*(2), 149-163.

51. Madsen, B., (2004), *Properties of plant fiber yarn polymer composites – An experimental study,* PhD Thesis, Department of civil Engineering, Technical University of Denmark.

52. Mohanty, A. K., Misra, M., & Drzal, L. T. (Eds.). (2005). *Natural fibers, biopolymers, and biocomposites*. CRC Press.

53. Sakakibara, A. and Shiraishi, N.(1991) *Wood and Cellulose Chemistry*, New York: Marcel Dekker.

54. Rowell, R. M. (1995). A new generation of composite materials from agro-based fiber. In *Polymers and Other Advanced Materials* (pp. 659-665). Springer US.

54 a. Boerjan W, Ralph J, Baucher M (2003) .Lignin biosynthesis. *Annu Rev Plant Biol* 54,519-546.

54 b. Ralph, J., Lundquist, K., Brunow, G., Lu, F., Kim, H., Schatz, P. F., & Boerjan, W. (2004). Lignins: natural polymers from oxidative coupling of 4-ydroxyphenyl-propanoids. *Phytochemistry Reviews*, *3*(1-2), 29-60.

55. Lilholt, H., & Lawther, J. M. (2000). Natural organic fibers. *Comprehensive composite materials*, *1*, 303-325.

56. Maldas, D., & Kokta, B. V. (1994). Role of coupling agents on the performance of wood flour-filled polypropylene composites. *International Journal of Polymeric Materials*, *27*(1-2), 77-88.

57. Yildiz, S., Gezer, E. D., & Yildiz, U. C. (2006). Mechanical and chemical behavior of spruce wood modified by heat. *Building and Environment*, *41*(12), 1762-1766.

58. Ray, D., Sarkar, B. K., Basak, R. K., & Rana, A. K. (2002). Study of the thermal behavior of alkali-treated jute fibers. *Journal of applied polymer science*, *85*(12), 2594-2599.

59. Islam, M. S., Pickering, K. L., Beckermann, G. W., & Foreman, N. J. (2005). The effect of fiber treatment using alkali on industrial hemp fiber/epoxy resin composites. *ICME*.

60. Vichnevsky, S., Fuhr, B., & Melnichuk, J. (2003). Characterization of wood and non-wood mechanical pulps by differential thermal analysis. *Journal of pulp and paper science*, *29*(1), 17-20.

61. Sanadi, A. R., Caulfield, D. F., & Jacobson, R. E. (1997). Agro-fiber thermoplastic composites. *Paper and composites from agro-based resources*, 377-401.

62. Rowell, R. M. (1997). *Chemical modification of agro-resources for property enhancement* (Vol. 54, pp. 351-375). Lewish Publisher, London.

63. Joseph, P. V., Rabello, M. S., Mattoso, L. H. C., Joseph, K., & Thomas, S. (2002). Environmental effects on the degradation behavior of sisal fiber reinforced polypropylene composites. *Composites Science and Technology*, *62*(10), 1357-1372.

64. Kahraman, R., Abbasi, S., & Abu-Sharkh, B. (2005). Influence of epolene G-3003 as a coupling agent on the mechanical behavior of palm fiber-polypropylene composites. *International Journal of Polymeric Materials*, *54*(6), 483-503.

65. El-Shekeil, Y. A., Sapuan, S. M., Abdan, K., & Zainudin, E. S. (2012). Influence of fiber content on the mechanical and thermal properties of Kenaf fiber reinforced thermoplastic polyurethane composites. *Materials & Design*, *40*, 299-303.

66. Al-Oqla, F. M., & Sapuan, S. M. (2014). Natural fiber reinforced polymer composites in industrial applications: feasibility of date palm fibers for sustainable automotive industry. *Journal of cleaner production*, *66*, 347-354.

67. Öztürk, S. (2010). Effect of Fibre Loading on the Mechanical Properties of Kenaf and Fiberfrax Fibre-reinforced Phenol-Formaldehyde Composites. *Journal of Composite Materials 44*, 2265.

68. Bowen, C. R., Dent, A. C., Stevens, R., Cain, M., & Steward, M. (2005). Determination of critical and minimum volume fraction for composite sensors and actuators. *Proceedings 4M*, 483-487.

69. Alger, M. S. (1997). *Polymer science dictionary*. Springer Science & Business Media.

70. El-Shekeil, Y. A., Sapuan, S. M., & Algrafi, M. W. (2014). Effect of fiber loading on mechanical and morphological properties of cocoa pod husk fibers reinforced thermoplastic polyurethane composites. *Materials & Design*, *64*, 330-333.

71. Lu, J. Z., Qinglin, W., & McNabb Jr, H. S. (2000). Chemical coupling in wood fiber and polymer composites: a review of coupling agents and treatments. *Wood and Fiber Science*, *32*(1), 88-104.

72. Mohanty, A. K., Misra, M., & Drzal, L. T. (2001). Surface modifications of natural fibers and performance of the resulting bio composites: an overview. *Composite Interfaces*, *8*(5), 313-343.

73. Agrawal, R., Saxena, N. S., Sharma, K. B., Thomas, S., & Sreekala, M. S. (2000). Activation energy and crystallization kinetics of untreated and treated oil palm fiber reinforced phenol formaldehyde composites. *Materials Science and Engineering: A*, *277*(1), 77-82.

74. Jahn, A., Schroder, M.W., Futing, M. and Schezel, K, Diepenbrock, (2002), Wear, Spectrochim,Acta A: Mol Biomol Spectrosc 58: p.2271.

75. Valadez-Gonzalez, A., Cervantes-Uc, J. M., Olayo, R., & Herrera-Franco, P. J. (1999). Effect of fiber surface treatment on the fiber–matrix bond strength of natural fiber reinforced composites. *Composites Part B: Engineering*, *30*(3), 309-320.

76. Paul, S., Nanda, P., & Gupta, R. (2003). PhCOCl-Py/basic alumina as a versatile reagent for benzoylation in solvent-free conditions. *Molecules*, *8*(4), 374-380.

77. Nair, K. C., Diwan, S. M., & Thomas, S. (1996). Tensile properties of short sisal fiber reinforced polystyrene composites. *Journal of Applied Polymer Science*, *60*(9), 1483-1497.

78. Joseph, K., Mattoso, L. H. C., Toledo, R. D., Thomas, S., De Carvalho, L. H., Pothen, L., & James, B. (2000). Natural fiber reinforced thermoplastic composites. *Natural Polymers and Agro fibers Composites*, *159*.

79. Wang, B. (2004), MSc. Thesis. University of Saskatchewan.

80. Rahman, M. M., Mallik, A. K., & Khan, M. A. (2007). Influences of various surface pretreatments on the mechanical and degradable properties of photografted oil palm fibers. *Journal of applied polymer science*, *105*(5), 3077-3086.

81. Paul, S. A., Joseph, K., Mathew, G. G., Pothen, L. A., & Thomas, S. (2010). Influence of polarity parameters on the mechanical properties of composites from polypropylene fiber and short banana fiber. *Composites Part A: Applied Science and Manufacturing*, *41*(10), 1380-1387.

82. Li, X., Panigrahi, S. A., Tabil, L. G., & Crerar, W. J. (2004, September). Flax fiber-reinforced composites and the effect of chemical treatments on their properties. In *North central ASAE/CSAE Conference*.

83. Ray, D., Sarkar, B. K., Rana, A. K., & Bose, N. R. (2001). Effect of alkali treated jute fibers on composite properties. *Bulletin of materials science*, *24*(2), 129-135.

84. Vallo, C., Kenny, J. M., Vazquez, A., & Cyras, V. P. (2004). Effect of chemical treatment on the mechanical properties of starch-based blends reinforced with sisal fiber. *Journal of Composite Materials*, *38*(16), 1387-1399.

85. Ouajai, S., & Shanks, R. A. (2005). Composition, structure and thermal degradation of hemp cellulose after chemical treatments. *Polymer Degradation and Stability*, *89*(2), 327-335.

86. Cao, Y., Shibata, S., & Fukumoto, I. (2006). Mechanical properties of biodegradable composites reinforced with bagasse fiber before and after alkali treatments. *Composites part A: Applied science and Manufacturing*, *37*(3), 423-429.

87. Mwaikambo, L. Y., Tucker, N., & Clark, A. J. (2007). Mechanical Properties of Hemp-Fiber-Reinforced Euphorbia Composites. *Macromolecular Materials and Engineering*, *292*(9), 993-1000.

88. Li, X., Tabil, L. G., & Panigrahi, S. (2007). Chemical treatments of natural fiber for use in natural fiber-reinforced composites: a review. *Journal of Polymers and the Environment*, *15*(1), 25-33.

89. Gu, H. (2009). Tensile behaviours of the coir fibre and related composites after NaOH treatment. *Materials & Design*, *30*(9), 3931-3934.

90. Boopalan, M., Umapathy, M. J., & Jenyfer, P. (2012). A Comparative Study on the Mechanical Properties of Jute and Sisal Fiber Reinforced Polymer Composites. *Silicon*, *4*(3), 145-149.

91. Karsli, N. G., & Aytac, A. (2014). Properties of alkali treated short flax fiber reinforced poly (lactic acid)/polycarbonate composites. *Fibers and Polymers*, *15*(12), 2607-2612.

92. Manshor, M. R., Anuar, H., Aimi, M. N., Fitrie, M. A., Nazri, W. W., Sapuan, S. M., & Wahit, M. U. (2014). Mechanical, thermal and morphological properties of durian skin fibre reinforced PLA biocomposites. *Materials & Design*, *59*, 279-286.

93. Khan, J. A., Khan, M. A., & Islam, R. (2012). Effect of potassium permanganate on mechanical, thermal and degradation characteristics of jute fabric-reinforced polypropylene composite. *Journal of Reinforced Plastics and Composites*, 0731684412458716.

94. Sathishkumar, T. P., Navaneethakrishnan, P., Shankar, S., & Rajasekar, R. (2013). Investigation of chemically treated randomly oriented sansevieria ehrenbergii fiber reinforced isophthallic polyester composites. *Journal of Composite Materials*, 0021998313503589.

95. Thiruchitrambalam, M., & Shanmugam, D. (2012). Influence of pre-treatments on the mechanical properties of palmyra palm leaf stalk fiber–polyester composites. *Journal of Reinforced Plastics and Composites*, *31*(20), 1400-1414.

96. Dhanalakshmi, S., Ramadevi, P., & Basavaraju, B. (2015). Effect of Chemical Treatments on Tensile Strength of Areca Fiber Reinforced Natural Rubber Composites. *IOSR Journal of Applied Chemistry (IOSR-JAC)*, *8*(5), 43-52.

97. Zaman, H. U., Khan, M. A., Khan, R. A., Rahman, M. A., Das, L. R., & Al-Mamun, M. (2010). Role of potassium permanganate and urea on the improvement of the mechanical properties of jute polypropylene composites. *Fibers and Polymers*, *11*(3), 455-463.

98. Yang, Y., Ota, T., Morii, T., & Hamada, H. (2011). Mechanical property and hydrothermal aging of injection molded jute/polypropylene composites.*Journal of Materials Science*, *46*(8), 2678-2684.

99. Shubhra, Q. T., Alam, A. K. M. M., Beg, M. D. H., Khan, M. A., & Gafur, M. A. (2010). Mechanical and degradation characteristics of natural silk and

synthetic phosphate glass fiber reinforced polypropylene composites. *Journal of Composite Materials*, *45*(12),1305- 1313

100. Prasad, A. R., Rao, K. M., Gupta, A. V. S. S. K. S., & Reddy, B. V. (2011). A Study on flexural properties of wild cane grass fiber-reinforced polyester composites. *Journal of Materials Science*, *46*(8), 2627-2634.
101. Suardana, N. P. G., Piao, Y., & Lim, J. K. (2011). Mechanical properties of hemp fibers and hemp/pp composites: effects of chemical surface treatment. *Materials Physics and Mechanics*, *11*(1), 1-8.
102. Athijayamani, A., Thiruchitrambalam, M., Manikandan, V., & Pazhanivel, B. (2010). Mechanical properties of natural fibers reinforced polyester hybrid composite. *International Journal of Plastics Technology*, *14*(1), 104-116.
103. Ku, H., Wang, H., Pattarachaiyakoop, N., & Trada, M. (2011). A review on the tensile properties of natural fiber reinforced polymer composites.*Composites Part B: Engineering*, *42*(4), 856-873.
104. Malkapuram, R., Kumar, V., & Negi, Y. S. (2008). Recent development in natural fiber reinforced polypropylene composites. *Journal of Reinforced Plastics and Composites*. *28*(10), 1169–1189.
105. Shubhra, Q. T., Alam, A. K. M. M., Gafur, M. A., Shamsuddin, S. M., Khan, M. A., Saha, M., & Ashaduzzaman, M. D. (2010). Characterization of plant and animal based natural fibers reinforced polypropylene composites and their comparative study. *Fibers and Polymers*, *11*(5), 725-731.
106. Nam, T. H., Ogihara, S., Tung, N. H., & Kobayashi, S. (2011). Effect of alkali treatment on interfacial and mechanical properties of coir fiber reinforced poly (butylene succinate) biodegradable composites. *Composites Part B: Engineering*, *42*(6), 1648-1656.
107. Santulli, C. (2007). Impact properties of glass/plant fibre hybrid laminates. *Journal of materials science*, *42*(11), 3699-3707.
108. Alawar, A., Hamed, A. M., & Al-Kaabi, K. (2009). Characterization of treated date palm tree fiber as composite reinforcement. *Composites Part B: Engineering*, *40*(7), 601-606.
109. Gururaja, M. N., & Rao, A. H. (2012). A review on recent applications and future prospectus of hybrid composites. *Int J Soft Comput Eng*, *1*(6), 352-355.

110. Velmurugan, R., & Manikandan, V. (2005). Mechanical properties of glass/palmyra fiber wastesandwich composites. *Indian Journal of Engineering and Materials Sciences*, *12*(6), 563.

111. Ho, M. P., & Lau, K. T. (2012). Design of an impact resistant glass fibre/epoxy composites using short silk fibres. *Materials & Design*, *35*, 664-669.

112. Ahmed, K. S., & Vijayarangan, S. (2008). Tensile, flexural and interlaminar shear properties of woven jute and jute-glass fabric reinforced polyester composites. *Journal of materials processing technology*, *207*(1), 330-335.

113. Mirbagheri, J., Tajvidi, M., Hermanson, J. C., & Ghasemi, I. (2007). Tensile properties of wood flour/kenaf fiber polypropylene hybrid composites. *Journal of Applied Polymer Science*, *105*(5), 3054-3059.

114. Khalil, H. A., Hanida, S., Kang, C. W., & Fuaad, N. N. (2007). Agro-hybrid composite: the effects on mechanical and physical properties of oil palm fiber (EFB)/glass hybrid reinforced polyester composites. *Journal of Reinforced Plastics and Composites*, *26*(2), 203-218.

115. Reddy, G. V., Naidu, S. V., & Rani, T. S. (2008). Kapok/glass polyester hybrid composites: Tensile and hardness properties. *Journal of Reinforced Plastics and Composites*.

116. Nayak, S. K., & Mohanty, S. (2010). Sisal glass fiber reinforced PP hybrid composites: Effect of MAPP on the dynamic mechanical and thermal properties. *Journal of Reinforced Plastics and Composites*, *29*(10), 1551-1568.

117. Idicula, M., Malhotra, S. K., Joseph, K., & Thomas, S. (2005). Dynamic mechanical analysis of randomly oriented intimately mixed short banana/sisal hybrid fibre reinforced polyester composites. *Composites Science and Technology*, *65*(7), 1077-1087.

118. Prabhakaran, R. D., Toftegaard, H., Markussen, C. M., & Madsen, B. (2014). Experimental and theoretical assessment of flexural properties of hybrid natural fibre composites. *Acta Mechanica*, *225*(10), 2775-2782.

119. Bhushan, B., & Gupta, B. K. (1995). Micromechanical characterization of Ni-P coated aluminium-magnesium, glass, and glass-ceramic substrates and finished magnetic thin-film rigid disks. *Advances in Information Storage Systems*, *6*, 193-208.

120. Archard, J. (1953). Contact and rubbing of flat surfaces. *Journal of applied physics*, *24*(8), 981-988.

121. Bhansali, K. J. (1980). Wear coefficients of hard-surfacing materials. *Wear control handbook (eds) MB Peterson and WO Winer (New York: ASME) pp*, 373-383.
122. Archard, J. F., & Hirst, W. (1957, January). An examination of a mild wear process. In Proceedings of the Royal Society of London A: Mathematical, Physical and Engineering Sciences (Vol. 238, No. 1215, pp. 515-528). The Royal Society.
123. Hokkirigawa, K. (1997). Wear maps of ceramics. *Ceramics Japan, 32*, 19-25.
124. Holm, R. (1946), Electric Contact, Almquist and Wiksells, Stockholm, Section 40.
125. Lancaster, J. K. (1978). Wear mechanisms of metals and polymers. Transactions of the Institute of Metal Finishing, 56(4), 145-153.
126. Rabinowicz, E. (1980). Wear coefficients-metals. *Wear Control Handbook*, 475-506.
127. Lim, S. C., & Ashby, M. F. (1987). Overview no. 55 wear-mechanism maps.*Acta metallurgica*, *35*(1), 1-24.
128. Hokkirigawa, K., & Kato, K. (1988). An experimental and theoretical investigation of ploughing, cutting and wedge formation during abrasive wear. *Tribology International*, *21*(1), 51-57.
129. Burwell, J. T. (1957). Survey of possible wear mechanisms. *Wear*, *1*(2), 119-141.
130. Stokes, J. (2008). Theory and application of the high velocity oxy-fuel (HVOF), Thermal spray process. Dublin City University. ISBN 1-87232-753-2, ISSN 1649-8232.
131. Benedict, G. H. (1968). Correlation of Disk Machines and Gear Tests. *Lubrication Engineering*, *24*(12), 591.
132. Yahagi, Y., & Mizutani, Y. (1984). Corrosive wear of steel in gasoline-ethanol-water mixtures. *Wear*, *97*(1), 17-25.
133. Yahagi, Y., Nagasawa, Y., Hotta, S., & Mizutani, Y. (1986). Corrosive wear of cast iron under reciprocating lubrication *(No. 861599). SAE Technical Paper*.
134. Rengstorff, G. W., Miyoshi, K., & Buckley, D. H. (1986). Interaction of sulphuric acid corrosion and mechanical wear of iron. *ASLE transactions*, *29*(1), 43-51.

135. Acharya, S. K., Mishra, P., & Mehar, S. K. (2011). Effect of surface treatment on the mechanical properties of bagasse fiber reinforced polymer composite. *BioResources*, *6*(3), 3155-3165.

136. Khan, F., & Ahmad, S. R. (1996). Chemical modification and spectroscopic analysis of jute fibre. *Polymer degradation and stability*, *52*(3), 335-340.

137. Espert, A., Vilaplana, F., & Karlsson, S. (2004). Comparison of water absorption in natural cellulosic fibres from wood and one-year crops in polypropylene composites and its influence on their mechanical properties. *Composites Part A: Applied science and manufacturing*, *35*(11), 1267-1276.

138. John, M. J., & Anandjiwala, R. D. (2008). Recent developments in chemical modification and characterization of natural fiber-reinforced composites. *Polymer composites*, *29*(2), 187-207.

139. Joseph, K., Thomas, S., & Pavithran, C. (1996). Effect of chemical treatment on the tensile properties of short sisal fibre-reinforced polyethylene composites. *Polymer*, *37*(23), 5139-5149.

140. Yan, L., Chouw, N., & Yuan, X. (2012). Improving the mechanical properties of natural fibre fabric reinforced epoxy composites by alkali treatment. *Journal of Reinforced Plastics and Composites*, *31*,425–437.

141. Yan, L. (2012). Effect of alkali treatment on vibration characteristics and mechanical properties of natural fabric reinforced composites. *Journal of Reinforced Plastics and Composites*, *31*(13), 887-896.

142. Ray, D., & Sarkar, B. K. (2001). Characterization of alkali-treated jute fibers for physical and mechanical properties. *Journal of Applied Polymer Science*, *80*(7), 1013-1020.

143. Kushwaha, P., & Kumar, R. (2009). Enhanced mechanical strength of BFRP composite using modified bamboos. *Journal of reinforced plastics and composites*, *28*(23), 2851-2859.

144. Wang, B., (2004), MSc. Thesis. University of Saskatchewan

145. Nair, K. M., Thomas, S., & Groeninckx, G. (2001). Thermal and dynamic mechanical analysis of polystyrene composites reinforced with short sisal fibres. *Composites Science and Technology*, *61*(16), 2519-2529.

146. Sreekala, M. S., Kumaran, M. G., & Thomas, S. (1997). Oil palm fibers: Morphology, chemical composition, surface modification, and mechanical properties. *Journal of Applied Polymer Science*, *66*(5), 821-835.

147. Mishra, S., Mohanty, A. K., Drzal, L. T., Misra, M., Parija, S., Nayak, S. K., & Tripathy, S. S. (2003). Studies on mechanical performance of biofibre/glass reinforced polyester hybrid composites. *Composites Science and Technology*, *63*(10), 1377-1385.

148. Bledzki, A. K., & Gassan, J. (1999). Composites reinforced with cellulose based fibers. *Progress in polymer science*, *24*(2), 221-274.

149. Sreekala, M. S., & Thomas, S. (2003). Effect of fibre surface modification on water-sorption characteristics of oil palm fibres. *Composites Science and Technology*, *63*(6), 861-869.

150. Kreže, T., Iskrač, S., Smole, M. S., Stana-Kleinschek, K., Strnad, S., & Fakin, D. (2005). Flax fibers sorption properties influenced by different pretreatment processes. *Journal of natural fibers*, *2*(3), 25-37.

151. Dairo, F. A. S., Aye, P. A., & Oluwasola, T. A. (2007). Some functional properties of loofah gourd (Luffa cylindrica L., MJ Roem) seed. *Journal of food agriculture and environment*, *5*(1), 97.

152. Khan, M. A., Hassan, M. M., & Drzal, L. T. (2005). Effect of 2-hydroxyethyl methacrylate (HEMA) on the mechanical and thermal properties of jute-polycarbonate composite. *Composites Part A: Applied Science and Manufacturing*, *36*(1), 71-81.

153. Tsuboi, M. (1957). Infrared spectrum and crystal structure of cellulose.*Journal of Polymer Science*, *25*(109), 159-171.

154. Sinha, E., & Rout, S. K. (2009). Influence of fibre-surface treatment on structural, thermal and mechanical properties of jute fibre and its composite. *Bulletin of Materials Science*, *32*(1), 65-76.

155. Jahan, M. S., & Mun, S. P. (2005). Effect of tree age on the cellulose structure of Nalita wood (Trema orientalis). *Wood science and technology*,*39*(5), 367-373.

156. Mwaikambo, L. Y., & Ansell, M. P. (2002). Chemical modification of hemp, sisal, jute, and kapok fibers by alkalization. *Journal of Applied Polymer Science*, *84*(12), 2222-2234.

156. a Segal, L., Creely, J.J., Martin, A.E., & Conrad, C.M. (1959). An empirical method for estimating the degree of crystallinity of native cellulose using the X-ray diffractometer. *Textile Res. J.* 29, 786–794.

157. Kaith, B. S., Singha, A. S., & Sharma, S. K. (2003). Graft copolymerization of flax fibers with binary vinyl monomer mixtures and evaluation of swelling,

moisture absorbance and thermal behavior of the grafted fibers. *Journal of Polymer Materials, 20*(2), 195-200.

158. Roncero, M. B., Torres, A. L., Colom, J. F., & Vidal, T. (2005). The effect of xylanase on lignocellulosic components during the bleaching of wood pulps.*Bioresource Technology*, *96*(1), 21-30.
159. Tserki, V., Matzinos, P., Kokkou, S., & Panayiotou, C. (2005). Novel biodegradable composites based on treated lignocellulosic waste flour as filler. Part I. Surface chemical modification and characterization of waste flour. *Composites Part A: Applied Science and Manufacturing*, *36*(7), 965-974.
160. Nordin, N. I. A. A., Ariffin, H., Andou, Y., Hassan, M. A., Shirai, Y., Nishida, H., & Ibrahim, N. A. (2013). Modification of oil palm mesocarp fiber characteristics using superheated steam treatment. *Molecules*, *18*(8), 9132-9146.
161. Nguyen, T., Zavarin, E., & Barrall, E. M. (1981). Thermal Analysis of lignocellulosic materials: Part I. Unmodified materials. *Journal of Macromolecular Science—Reviews in Macromolecular Chemistry*, *20*(1), 1-65.
162. Wong, S., Shanks, R., & Hodzic, A. (2004). Interfacial improvements in poly (3-hydroxybutyrate)-flax fibre composites with hydrogen bonding additives.*Composites science and technology*, *64*(9), 1321-1330
163. Kaushik, V. K., Kumar, A., & Kalia, S. (2012). Effect of mercerization and benzoyl peroxide treatment on morphology, thermal stability and crystallinity of sisal fibers. *International Journal of Textile Science*, *1*(6), 101-105.
164. Agarwal, B. D., Broutman, L. J., & Chandrashekhara, K. (2006). Analysis and performance of fiber composites. *John Wiley & Sons. Chicago.*
165. Acharya, S. K., Mishra, P., & Mishra, S. C. (2008). Effect of environment on the mechanical properties of fly ash-jute-polymer composite. *Indian journal of engineering &material science*.*15*, 483-488.
166. Joseph, S., Sreekala, M. S., Oommen, Z., Koshy, P., & Thomas, S. (2002). A comparison of the mechanical properties of phenol formaldehyde composites reinforced with banana fibres and glass fibres. *Composites Science and Technology*, *62*(14), 1857-1868.
167. Lin, J. C., Chang, L. C., Nien, M. H., & Ho, H. L. (2006). Mechanical behavior of various nanoparticle filled composites at low-velocity impact. *Composite Structures*, *74*(1), 30-36.

168. Jayaraman, K. (2003). Manufacturing sisal–polypropylene composites with minimum fibre degradation. *Composites Science and technology, 63*(3), 367-374.

169. Joseph, P. V., Mathew, G., Joseph, K., Groeninckx, G., & Thomas, S. (2003). Dynamic mechanical properties of short sisal fibre reinforced polypropylene composites. *Composites Part A: applied science and manufacturing, 34*(3), 275-290.

170. Karmarkar, A., Chauhan, S. S., Modak, J. M., & Chanda, M. (2007). Mechanical properties of wood–fiber reinforced polypropylene composites: Effect of a novel compatibilizer with isocyanate functional group. *Composites Part A: Applied Science and Manufacturing, 38*(2), 227-233.

171. Rana, A. K., Mandal, A., & Bandyopadhyay, S. (2003). Short jute fiber reinforced polypropylene composites: effect of compatibiliser, impact modifier and fiber loading. *Composites Science and Technology, 63*(6), 801-806.

172. Fiore, V., Di Bella, G., & Valenza, A. (2015). The effect of alkaline treatment on mechanical properties of kenaf fibers and their epoxy composites. *Composites Part B: Engineering, 68*, 14-21.

173. Kushwaha, P. K., & Kumar, R. (2010). Influence of chemical treatments on the mechanical and water absorption properties of bamboo fiber composites. *Journal of Reinforced Plastics and Composites.*

174. Wang, W., Sain, M., & Cooper, P. A. (2006). Study of moisture absorption in natural fiber plastic composites. *Composites Science and Technology, 66*(3), 379-386.

175. Shen, C. H., & Springer, G. S. (1976). Moisture absorption and desorption of composite materials. *Journal of Composite Materials, 10*(1), 2-20..

176. Abot, J. L., Yasmin, A., & Daniel, I. M. (2005). Hygroscopic behavior of woven fabric carbon-epoxy composites. *Journal of reinforced plastics and Composites, 24*(2), 195-207.

177. Espert, A., Vilaplana, F., &Karlsson, S. (2004). Comparison of water absorption in natural cellulosic fibres from wood and one-year crops in polypropylene composites and its influence on their mechanical properties. *Composites Part A: Applied science and manufacturing, 35*(11), 1267-1276.

178. Lin, Q., Zhou, X., & Dai, G. (2002). Effect of hydrothermal environment on moisture absorption and mechanical properties of wood flour–filled

polypropylene composites. *Journal of Applied Polymer Science*, *85*(14), 2824-2832.

179. Bond, D. A., & Smith, P. A. (2006). Modeling the transport of low-molecular-weight penetrants within polymer matrix composites. *Applied Mechanics Reviews*, *59*(5), 249-268.
180. Davies, P., Mazeas, F., &Casari, P. (2001). Sea water aging of glass reinforced composites: shear behaviour and damage modelling. *Journal of composite materials*, *35*(15), 1343-1372.
181. Joseph, P. V., Rabello, M. S., Mattoso, L. H. C., Joseph, K., & Thomas, S. (2002). Environmental effects on the degradation behaviour of sisal fibre reinforced polypropylene composites. *Composites Science and Technology*, *62*(10), 1357-1372.
182. Shakeri, A., &Ghasemian, A. (2010). Water absorption and thickness swelling behavior of polypropylene reinforced with hybrid recycled newspaper and glass fiber. *Applied Composite Materials*, *17*(2), 183-193.
183. Li, X., Tabil, L. G., &Panigrahi, S. (2007). Chemical treatments of natural fiber for use in natural fiber-reinforced composites: a review. *Journal of Polymers and the Environment*, *15*(1), 25-33.
184. Kabir, M. M., Wang, H., Aravinthan, T., Cardona, F., & Lau, K. T. (2011, April). Effects of natural fibre surface on composite properties: A review. In*Proceedings of the 1st International Postgraduate Conference on Engineering, Designing and Developing the Built Environment for Sustainable Wellbeing (eddBE2011)* (pp. 94-99). Queensland University of Technology.
185. John, M. J., &Anandjiwala, R. D. (2008). Recent developments in chemical modification and characterization of natural fiber-reinforced composites. *Polymer composites*, *29*(2), 187.
186. George, J., Bhagawan, S. S., & Thomas, S. (1998). Effects of environment on the properties of low-density polyethylene composites reinforced with pineapple-leaf fibre. *Composites Science and Technology*, *58*(9), 1471-1485.
187. K. Hardinnawirda and I. SitiRabiatull Aisha, (2012), "Effect of rice husks as filler in polymer matrix composites", *Journal of Mechanical Engineering and Sciences (JMES*) e-ISSN: 2231-8380; Volume 2: pp. 181-186.

188. Stark, N. (2001). Influence of moisture absorption on mechanical properties of wood flour-polypropylene composites. *Journal of thermoplastic composite materials, 14*(5), 421-432.

189. Yuan, X., Jayaraman, K., & Bhattacharyya, D. (2002). Plasma treatment of sisal fibres and its effects on tensile strength and interfacial bonding. *Journal of adhesion science and technology, 16*(6), 703-727.

190. Stamboulis, A., Baillie, C. A., Garkhail, S. K., Van Melick, H. G. H., &Peijs, T. (2000). Environmental durability of flax fibres and their composites based on polypropylene matrix. *Applied composite materials, 7*(5-6), 273-294.

191. Sreekumar, P. A., Thomas, S. P., marc Saiter, J., Joseph, K., Unnikrishnan, G., & Thomas, S. (2009). Effect of fiber surface modification on the mechanical and water absorption characteristics of sisal/polyester composites fabricated by resin transfer molding. *Composites Part A: Applied Science and Manufacturing, 40*(11), 1777-1784.

192. Athijayamani, A., Thiruchitrambalam, M., Natarajan, U., &Pazhanivel, B. (2009). Effect of moisture absorption on the mechanical properties of randomly oriented natural fibers/polyester hybrid composite. *Materials Science and Engineering: A, 517*(1), 344-353.

193. Leman, Z., Sapuan, S. M., Saifol, A. M., Maleque, M. A., & Ahmad, M. M. H. M. (2008). Moisture absorption behavior of sugar palm fiber reinforced epoxy composites. *Materials & Design, 29*(8), 1666-1670.

194. Deo, C., & Acharya, S. K. (2010). Effect of moisture absorption on mechanical properties of chopped natural fiber reinforced epoxy composite. *Journal of Reinforced Plastics and Composites, 29*(16), 2513-2521.

195. Acharya, S. K., Mishra, P. P., &Mehar, S. K. (2009). The influence of fiber treatment on the performance of bagasse fiber-reinforced polymer composite. *Journal of Reinforced Plastics and Composites, 28*(24), 3027-3036.

196. Mariatti, M., Jannah, M., Bakar, A. A., & Khalil, H. A. (2008). Properties of banana and pandanus woven fabric reinforced unsaturated polyester composites. *Journal of Composite Materials, 42*(9), 931-941.

197. Rashdi, A. A. A., Sapuan, S. M., Ahmad, M. M. H. M., & Khalina, A. (2009). Water absorption and tensile properties of soil buried kenaf fibre reinforced unsaturated polyester composites (KFRUPC). *Journal of Food, Agriculture & Environment, 7*(9), 908–11.

198. Zamri, M. H., Akil, H. M., Bakar, A. A., Ishak, Z. A. M., & Cheng, L. W. (2011). Effect of water absorption on pultruded jute/glass fibre-reinforced unsaturated polyester hybrid composites. *Journal of Composite Materials, 46*: 51–61.

199. Raghavendra, G., Kumar, K. A., Kumar, M. H., Raghu Kumar, B., &Ojha, S. (2015). Moisture absorption behavior and its effect on the mechanical properties of jute-reinforced epoxy composite. *Polymer Composites*.

200. Baghaei, B., Skrifvars, M., Salehi, M., Bashir, T., Rissanen, M., &Nousiainen, P. (2014). Novel aligned hemp fibre reinforcement for structural biocomposites: Porosity, water absorption, mechanical performances and viscoelastic behaviour. *Composites Part A: Applied Science and Manufacturing, 61*, 1-12.

201. Fang, H., Zhang, Y., Deng, J., &Rodrigue, D. (2013). Effect of fiber treatment on the water absorption and mechanical properties of hemp fiber/polyethylene composites. *Journal of applied polymer science, 127*(2), 942-949.

202. Jannah, M., Mariatti, M., Bakar, A. A., & Khalil, H. A. (2008). Effect of chemical surface modifications on the properties of woven banana-reinforced unsaturated polyester composites. *Journal of Reinforced Plastics and Composites*.

203. Rodríguez, L. J., Cardona, C. A., &Orrego, C. E. (2015). Water uptake, chemical characterization, and tensile behavior of modified banana–plantain fiber and their polyester composites. *Polymer Composites.*

204. Marcovich, N. E., Reboredo, M. M., &Aranguren, M. I. (1999). Moisture diffusion in polyester–woodflour composites. *Polymer, 40*(26), 7313-7320.

205. Merdas, I., Thominette, F., Tcharkhtchi, A., &Verdu, J. (2002). Factors governing water absorption by composite matrices. *Composites Science and Technology, 62*(4), 487-492..

206. Alamri, H., & Low, I. M. (2012). Mechanical properties and water absorption behaviour of recycled cellulose fibre reinforced epoxy composites. *Polymer testing, 31*(5), 620-628.

207. Shi, S. Q., & Gardner, D. J. (2006). Effect of density and polymer content on the hygroscopic thickness swelling rate of compression molded wood fiber/polymer composites. *Wood and fiber science, 38*(3), 520-526.

208. Jawaid, M., Khalil, H. A., Khanam, P. N., & Bakar, A. A. (2011). Hybrid composites made from oil palm empty fruit bunches/jute fibers: Water

absorption, thickness swelling and density behaviors. *Journal of Polymers and the Environment*, *19*(1), 106-109.

209. Adhikary, K. B., Pang, S., & Staiger, M. P. (2008). Long-term moisture absorption and thickness swelling behavior of recycled thermoplastics reinforced with Pinusradiata sawdust. *Chemical Engineering Journal*, *142*(2), 190-198.
210. Islam, M. S., Pickering, K. L., & Foreman, N. J. (2010). Influence of hygrothermal ageing on the physico-mechanical properties of alkali treated industrial hemp fibre reinforced polylactic acid composites. *Journal of Polymers and the Environment*, *18*(4), 696-704.
211. **D**hakal, H. N., Zhang, Z. Y., & Richardson, M. O. W. (2007). Effect of water absorption on the mechanical properties of hemp fibre reinforced unsaturated polyester composites. *Composites Science and Technology*, *67*(7), 1674-1683
212. Bhushan, B. (2013). *Principles and applications of tribology*. John Wiley & Sons.
213. Ivusic, V. (1998). *Hrvatsko drustvo za materijale i tribologiju*.
214. Rabinowicz, E. (1965). *Friction and wear of materials.*
215. Brostow, W., Deborde, J. L., Jaclewicz, M., & Olszynski, P. (2003). Tribology with emphasis on polymers: friction, scratch resistance and wear. *Journal of Materials Education*, 25(4/6), 119-132.
216. Kivikyto-Reponen, P. (2006). Correlation of material characteristics and wear of powder metallurgical metal matrix composites. Helsinki University of Technology.
217. Biswas, S., Satapathy, A., & Patnaik, A. (2009). Erosion wear behaviour of polymer composites: a review. *Journal of Reinforced Plastics and Composites*.
218. Drensky, G., Hamed, A., Tabakoff, W., & Abot, J. (2011). Experimental investigation of polymer matrix reinforced composite erosion characteristics. *Wear*, 270(3), 146-151.
219. Mahapatra, S. S., & Patnaik, A. (2009). Study on mechanical and erosion wear behavior of hybrid composites using Taguchi experimental design. *Materials & Design*, 30(8), 2791-2801.
220. Wahl H, Hartenstein F. (1946). Strahlverschleiss, rankhscheVerlagshandlung, Stuttgart
221. T.H. Tsiang. (1986). *Journal of Composite Technology and Research* 8(4) 154.

222. Tilly, G. P., & Sage, W. (1970). The interaction of particle and material behaviour in erosion processes. *Wear, 16*(6), 447-465.

223. Pool, K. V., Dharan, C. K. H., & Finnie, I. (1986). Erosive wear of composite materials. *Wear, 107*(1), 1-12.

224. Smeltzer, C. E., Gulden, M. E., & Compton, W. A. (1970). Mechanisms of metal removal by impacting dust particles. *Journal of Fluids Engineering, 92*(3), 639-652.

225. Guadagnoa, L., Vertuccioa, L., Sorrentinoa, A., Raimondoa, M., Naddeoa, C., Vittoriaa,V., (2009). Mechanical and barrier properties of epoxy resin filled with multi-walled carbon nanotubes. *Carbon, 47*(10), 2419-2430.

226. McIntyre, S., Kaltzakorta, I., Liggat, J. J., Pethrick, R. A., & Rhoney, I. (2005). Influence of the epoxy structure on the physical properties of epoxy resin nanocomposites. *Industrial & engineering chemistry research*, 44(23), 8573-8579

227. Kulkarni, S. M. (2001). Influence of matrix modification on the solid particle erosion of glass/epoxy composites. *Polymers & polymer composites*, 9(1), 25-30.

228. Aglan, H. A., & Chenock, T. A. (1993). Erosion damage features of polyimide thermoset composites. *SAMPE quarterly*, *24*(2), 41-47.

229. Barkoula, N. M., & Karger-Kocsis, J. (2002). Review processes and influencing parameters of the solid particle erosion of polymers and their composites. *Journal of materials science*, 37(18), 3807-3820.

230. Bitter, J. G. A. (1963). A study of erosion phenomena: Part II. *Wear, 6*(3), 169-190.

231. Hutchings, I. M., Winter, R. E., & Field, J. E. (1976, March). Solid particle erosion of metals: the removal of surface material by spherical projectiles. *In Proceedings of the Royal Society of London A: Mathematical, Physical and Engineering Sciences* (Vol. 348, No. 1654, pp. 379-392). The Royal Society.

232. Stachowiak, G. W., Batchelor, A. W., & Stolarski, T. A. (1994). Engineering tribology: Elsevier, 1993, ISBN 0-444-89235-4, pp 960.

233. Barkoula, N. M., & Karger-Kocsis, J. (2002). Solid particle erosion of unidirectional GF reinforced EP composites with different fibre/matrix adhesion. *Journal of reinforced plastics and composites*, 21(15), 1377-1388.

234. Yousif, B. F., & El-Tayeb, N. S. M. (2008). Adhesive wear performance of T-OPRP and UT-OPRP composites. *Tribology letters*, 32(3), 199-208.

235. Chand, N., & Dwivedi, U. K. (2006). Effect of coupling agent on abrasive wear behaviour of chopped jute fibre-reinforced polypropylene composites. *Wear, 261*(10), 1057-1063.

236. Yousif, B. F., Lau, S. T., & McWilliam, S. (2010). Polyester composite based on betelnut fibre for tribological applications. *Tribology international*, *43*(1), 503-511.

237. Nirmal, U., Hashim, J., & Low, K. O. (2012). Adhesive wear and frictional performance of bamboo fibres reinforced epoxy composite. *Tribology International*, *47*, 122-133.

238. Chin, C. W., & Yousif, B. F. (2009). Potential of kenaf fibres as reinforcement for tribological applications. *Wear, 267*(9), 1550-1557.

239. Patnaik, A., Satapathy, A., Chand, N., Barkoula, N. M., & Biswas, S. (2010). Solid particle erosion wear characteristics of fibre and particulate filled polymer composites: A review. *Wear, 268*(1), 249-263.

240. Arjula, S., & Harsha, A. P. (2006). Study of erosion efficiency of polymers and polymer composites. *Polymer testing*, *25*(2), 188-196.

241. Mohanty, J. R., Das, S. N., Das, H. C., Mahanta, T. K., & Ghadei, S. B. (2014). Solid particle erosion of date palm leaf fiber reinforced polyvinyl alcohol composites. *Advances in Tribology*, 2014.

242. Mishra, P., & Acharya, S. K. (2010). Anisotropy abrasive wear behaviour of bagasse fibre reinforced polymer composite. *International Journal of Engineering, Science and Technology*, *2*(11).

243. Deo, C., & Acharya, S. K. (2009). Solid particle erosion of lantana camaran fibre-reinforced polymer matrix composite. *Polymer-Plastics Technology and Engineering*, *48*(10), 1084-1087.

244. Ruff, A. W., & Ives, L. K. (1975). Measurement of solid particle velocity in erosive wear. *Wear, 35*(1), 195-199.

245. Sundararajan, G., Roy, M., & Venkataraman, B. (1990). Erosion efficiency-a new parameter to characterize the dominant erosion micromechanism. *Wear, 140*(2), 369-381.

246. Patnaik, A., Satapathy, A., Mahapatra, S. S., & Dash, R. R. (2008). A modeling approach for prediction of erosion behavior of glass fiber–polyester composites. *Journal of Polymer Research*, *15*(2), 147-160.

247. Patnaik, A., Satapathy, A., Mahapatra, S. S., & Dash, R. R. (2009). Tribo-performance of polyester hybrid composites: damage assessment and parameter optimization using Taguchi design. *Materials & Design*, *30*(1), 57-67.

248. Ojha, S., Raghavendra, G., & Acharya, S. K. (2014). A comparative investigation of bio waste filler (wood apple-coconut) reinforced polymer composites. *Polymer Composites*, *35*(1), 180-185.

249. Sarı, N., & Sınmazçelik, T. (2007). Erosive wear behaviour of carbon fiber/polyetherimide composites under low particle speed. *Materials & design*, *28*(1), 351-355.

250. Majhi, S., Samantarai, S. P., & Acharya, S. K. (2012). Tribological behavior of modified rice husk filled epoxy composite. Internaton Journal of Scientific and Engineering Research, 3, 1-5.

250 a. Samantarai, S. P (2014). Tribological behaviour of rice husk reinforced polymer matrix composite. PhD thesis, NIT Rourkela.

251. Rout, A. K., & Satapathy, A. (2012). Study on mechanical and tribo-performance of rice-husk filled glass–epoxy hybrid composites. *Materials & Design*, *41*, 131-141.

252. Harsha, A. P., & Thakre, A. A. (2007). Investigation on solid particle erosion behaviour of polyetherimide and its composites. *Wear*, *262*(7), 807-818

253. Satapathy, A., Patnaik, A., & Pradhan, M. K. (2009). A study on processing, characterization and erosion behavior of fish (Labeo-rohita) scale filled epoxy matrix composites. *Materials & Design*, *30*(7), 2359-2371.

254. Srivastava, V. K., & Pawar, A. G. (2006). Solid particle erosion of glass fibre reinforced fly ash filled epoxy resin composites. *Composites Science and Technology*, *66*(15), 3021-3028.

255. Bisanda, E. T. N., & Ansell, M. P. (1991). The effect of silane treatment on the mechanical and physical properties of sisal-epoxy composites. *Composites Science and Technology*, *41*(2), 165-178.

256. DiBenedetto, A. T. (2001). Tailoring of interfaces in glass fiber reinforced polymer composites: a review. Materials Science and Engineering: A,302(1), 74-82.

257. Acharya, S. K., Mishra, P., Dikshit, V., & Mehar, S. K. (2007). Weathering behavior of bagasse fiber reinforced polymer composite. *Journal of Reinforced Plastics and Composites, 27,* 1839.

258. Kalaprasad, G., Thomas, S., Pavithran, C., Neelakantan, N. R., & Balakrishnan, S. (1996). Hybrid effect in the mechanical properties of short sisal/glass hybrid fiber reinforced low density polyethylene composites.*Journal of reinforced plastics and composites, 15*(1), 48-73.

259. Pavithran, C., Mukherjee, P. S., Brahmakumar, M., & Damodaran, A.D. (1991). Impact properties of sisal-glass hybrid laminates. *Journal of materials science, 26*(2), 455-459.

260. John, K., & Venkata Naidu, S. (2004). Sisal fibre/glass fibre hybrid composites: impact and compressive properties. *Journal of Reinforced Plastic Composite. 23* (12), 1253–1258.

261. John, K., & Venkata Naidu, S. (2004). Effect of fibre content and fibre treatment of flexural properties of sisal fibre/glass fibre hybrid composites. *Journal of Reinforced Plastic Composite. 23* (15), 1601–1605.

262. John, K., & Venkata Naidu, S. (2004). Tensile properties of unsaturated polyester based sisal fibre-glass fibre hybrid composites. *Journal of Reinforced Plastic Composite. 23* (17), 1815–1819.

263. Almeida, J. H. S., Amico, S. C., Botelho, E. C., & Amado, F. D. R. (2013). Hybridization effect on the mechanical properties of curaua/glass fiber composites. *Composites Part B: Engineering*, *55*, 492-497

264. Pavithran, C., Mukherjee, P. S., & Brahmakumar, M. (1991). Coir-glass intermingled fibre hybrid composites. *Journal of Reinforced Plastics and Composites, 10*(1), 91-101.

265. Mohan, R., Shridhar, M. K., & Rao, R. M. V. G. K. (1983). Compressive strength of jute-glass hybrid fibre composites. *Journal of Materials Science Letters, 2*(3), 99-102.

266. Patel, B. C., Acharya, S. K., & Mishra, D. (2011). Effect of stacking sequence on the erosive wear behavior of jute and juteglass fabric reinforced epoxy composite. *International Journal of Engineering, Science and Technology, 3*(1).

267. Raghavendra, G., Ojha, S., Acharya, S. K., Pal, S. K., & Ramu, I. (2014). Evaluation of mechanical behaviour of nanometer and micrometer fly ash

particle-filled woven bidirectional jute/glass hybrid nanocomposites. *Journal of Industrial Textiles*, 1528083714557058.

268. Gowda, T. M., Naidu, A. C. B., & Chhaya, R. (1999). Some mechanical properties of untreated jute fabric-reinforced polyester composites. *Composites Part A: applied science and manufacturing*, *30*(3), 277-284
269. Dalbehera, S., & Acharya, S. K. (2015). Effect of cenosphere addition on the mechanical properties of jute-glass fiber hybrid epoxy composites. *Journal of Industrial Textiles*, 1528083715577936.
270. Sabeel Ahmeda K. & Vijayarangan S. (2008). Tensile, flexural and interlaminar shear properties of woven jute and jute-glass fabric reinforced polyester composites. *Journal of materials processing technology, 207*,330–335.
271. Biswas, S., & Satapathy, A. (2010). A comparative study on erosion characteristics of red mud filled bamboo–epoxy and glass–epoxy composites. *Materials & Design, 31*(4), 1752-1767.

Mrs. NIHARIKA MOHANTA is a faculty member in the Department of Mechanical Engineering, Government Polytechnic, Balasore, and Odisha, India-756019. She has four years of research and five years of teaching experience in her field. She did M Tech in Mechanical Engineering from NIT Rourkela. This dissertation is being submitted for the fulfillment the Ph.D. degree.

The contact address is:

Address:-

Government polytechnic Balasore
Bidyadhar Pur
Remuna, Balasore
Odisha-756019
India
E mail: mohanta.niharika@gmail.com
Phone: 9439794382 (M)

Residence-

At/Po-Bhanjakia
Via-Jashipur
Dist-Mayurbhanj
Odisha-757091
India